INSTITUTO SUPERIOR TÉCNICO

ASSOCIATION EURATOM/IST

ASSOCIATED LABORATORY WITH FCT

Centro de Fusão Nuclear
Centro de Física dos Plasmas

2007 ANNUAL REPORT

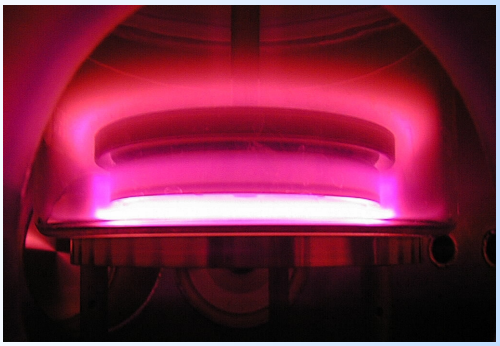
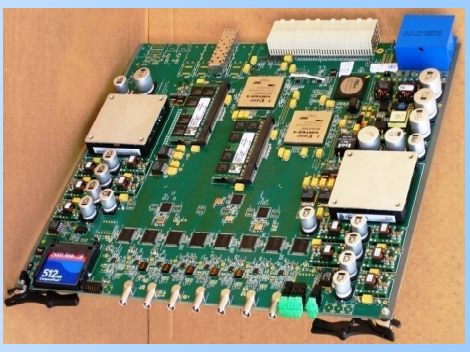
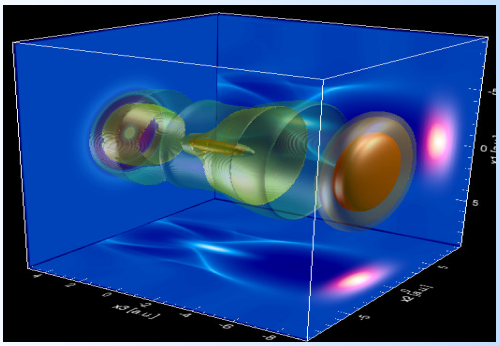
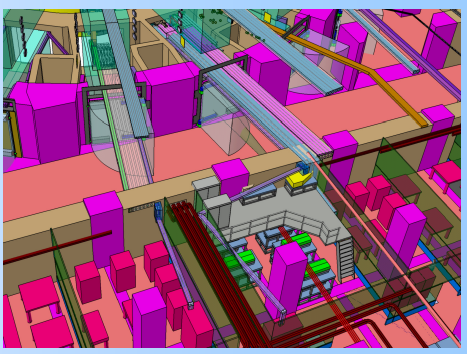
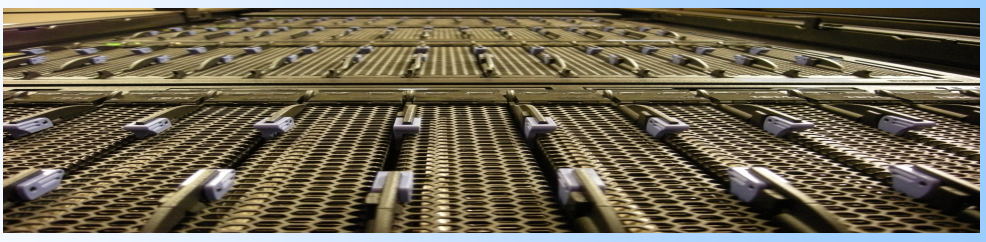

Figures on cover (from left to right, and top to bottom)

Capacitively coupled radio-frequency plasma reactor, running a discharge in N_2.
Prototype of a 400 MSPS, 14-bit, 8-channel transient recorder board for JET.
QuickPIC simulation showing a plasma wave and a laser entering the plasma.
Plasma position reflectometer with ITER: proposed ex-vessel waveguide routings for gaps 4, 5, and 6.
Front view of the IST Cluster.

Centro de Fusão Nuclear

INSTITUTO SUPERIOR TÉCNICO
CENTRO DE FUSÃO NUCLEAR
CENTRO DE FÍSICA DOS PLASMAS

Centro de Física dos Plasmas

2007 ANNUAL REPORT

Activities carried out in the frame of:

- **The Contract of Association EURATOM/IST on Plasma Fusion Research**
- **The Contract of Associated Laboratory with FCT on Plasma Physics and Engineering**

IST, July 2008

CONTENTS

[1] Activities carried out in the frame of the Contract of Association EURATOM/IST and the Contract of Associated Laboratory.

[2] Activities performed in the frame of the Contract of Associated Laboratory, out of the Contract of Association EURATOM/IST.

1. INTRODUCTION

F. Serra, C. Varandas, L.L. Alves (Editors)

1.1. FOREWORD

This document presents the main activities carried out in 2007 in the frame of the Contract of Association (CoA) signed in 1990 between the European Atomic Energy Community (EURATOM) and "Instituto Superior Técnico" (IST), hereinafter referred to as Association EURATOM/IST, and of the Contract of Associated Laboratory on Plasma Physics and Engineering signed in 2001 by "Fundação para a Ciência e a Tecnologia" (FCT) and IST, hereinafter referred to as Associated Laboratory (AL). The CoA activities are described in chapters 2 to 13, while the AL activities are presented in chapters 2 to 10 and 13 to 21. Chapter 22 contains the list of publications, laboratorial prototypes, prizes and awards.

The activities described in this document were mainly performed by "Centro de Fusão Nuclear" (CFN) and "Centro de Física de Plasmas" (CFP), two Research Units of IST (Figure 1.1). The other collaborating Institutions are presented in Figure 1.1 and Table 1.1.

1.2. FUSION-RELATED ACTIVITIES

1.2.1. Introduction

The research and development activities on controlled nuclear fusion have been carried out according to the Contract of Association EURATOM/IST, which frames the Portuguese participation in the EURATOM Specific Research and Training Programme in the Field of Nuclear Fusion Energy, hereinafter referred as Community Fusion Programme. This Programme has as its long-term objective the development of a prototype commercial fusion power plant. It is presently implemented through several Agreements, in particular: (i) Contracts of Association signed between EURATOM and Institutions of the Member States of the European Union and Switzerland (Associates); (ii) the European Fusion Development Agreement (EFDA); and (iii) the Mobility Agreement, both signed by EURATOM and its Associates.

The main European fusion-related event in 2007 was the approval by the Council, on March 27th, of the statutes of the "European Joint Undertaking for ITER and the Development of Fusion Energy" (Fusion for Energy). This enterprise is the EU Domestic Agency for ITER and it is also in charge with the project-oriented DEMO activities as well as with the EU contribution for the Broader Approach, a bilateral agreement signed between the European Union and Japan, aiming at speeding up the development of fusion energy. Fusion for Energy entered into force on April 19th and its first Director, Dr. Didier Gambier, started his functions on October 1st 2007.

In the meantime, the EURATOM Fusion Programme has started its re-organization taking into account the beginning of ITER construction and the enter into force

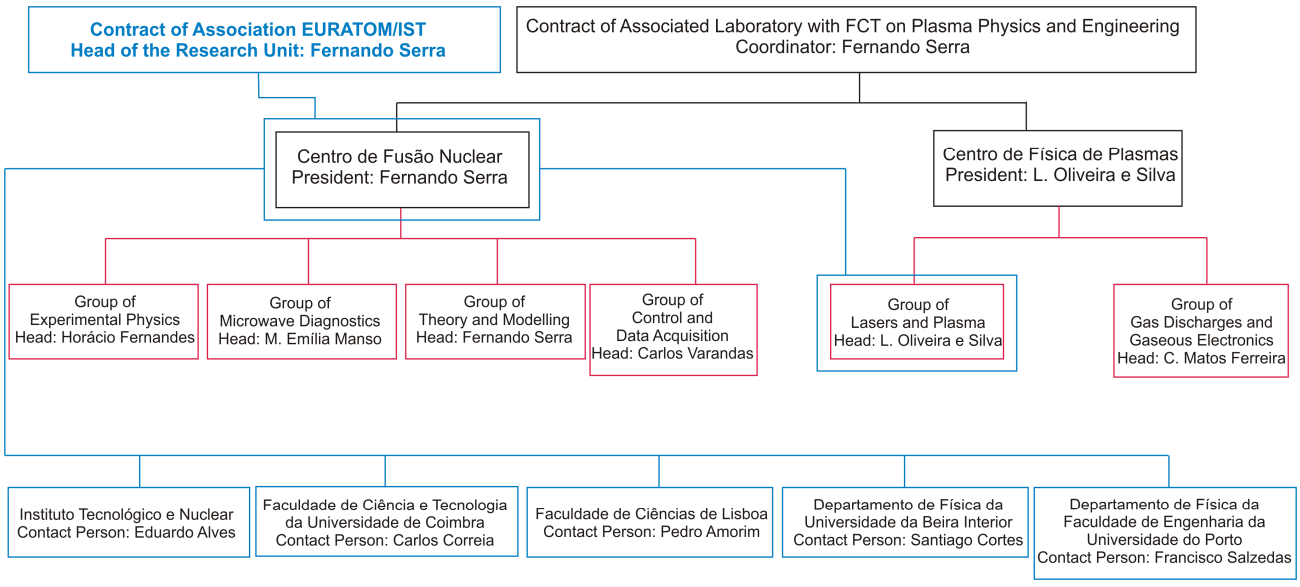

Figure 1.1 – Organization of the Associated Laboratory and Association EURATOM/IST

of Fusion for Energy. Particular relevant for our activity is the new European Fusion Development Agreement (EFDA) and the new Contract of Association, which entered into force on January 1st 2008.

1.2.2. Main projects of the Association EURATOM/IST

The work programme of the Association EURATOM/IST included activities carried out in Portugal (mainly related with the tokamak ISTTOK) and abroad related with the operation and scientific exploitation of large and medium-sized tokamaks and stellarator (JET, ASDEX-Upgrade, TCV, and TJ-II) as well as with the design of the next generation fusion devices (ITER and W7-X). Its main projects in 2007 were:

- Tokamak ISTTOK;
- Participation in the collective use of the JET facilities by the EFDA Associates;
- Participation in the ITER Project;
- Participation in the ASDEX-UPGRADE Programme;
- Participation in the TJ-II Programme;
- Participation in the TCV Programme;
- Collaboration with the Association EURATOM/CEA
- Other activities on theory and modelling;
- Other activities on control and data acquisition;
- Keep-in-touch activities on inertial fusion energy;
- Participation in the Fusion Technology Programme;
- Other fusion-related activities[1].

Table 1.1 presents information about the responsible person(s) and the Institutions involved in each project.

1.3. ASSOCIATED LABORATORY

The Associated Laboratory on Plasma Physics and Engineering has two thematic areas:

- Controlled Nuclear Fusion;
- Technologies of Plasmas and High-Power Lasers

The first area includes the activities carried out by CFN and CFP staff in the frame of the projects of the Association EURATOM/IST, while the area on "Technologies of Plasmas and High Power Lasers" had in 2007 the following projects:

- Plasma theory and simulations;
- High density laser plasma physics;
- Fundamental physics and quantum computing;
- Environmental engineering plasma laboratory;
- Nonequilibrium kinetics and simulation of plasmas and afterglow plasmas;
- Modelling of plasma reactors;
- Plasma and electromagnetic propulsion.

1.4. OTHER PROJECTS

CFN and CFP have also developed in 2007 activities in the frame of the following projects[1]

- Re-Equipment of the ISTTOK Laboratory (FCT[3], C. Varandas, 2005-2007);
- Re-Equipment of the CFN Microwave Laboratory (FCT, M.E. Manso, 2005-2007)
- Cosmic Concordance (FCT, O. Bertolami, 2005-2007);
- A Mission to Test the Pioneer Anomaly (FCT, O. Bertolami, 2006-2009);
- Estudos Teóricos de Ignição Rápida em Fusão Inercial (FCT, J. R. Davies, 2005 – 2007);
- Relativistic Harmonic Generation in Underdense Plasmas (FCT, João Mendanha Dias, 2004-2007)
- New Sub-cycle Rediation Sources in the Visible by Relativistic Mirror (FCT, João Mendanha Dias, 2005-2007);
- Tabletop Ultra-Intense XUV Sources for Femtobiology and Related Applications (TUIXS), (European Commission, M. Fajardo, 2005-2008);
- Advanced Plasma Accelerators: Beam Optimization, Diagnostics and Applications, (FCT, N. Lopes, 2006-2007);
- Dos Choques Relativistas aos Lasers Ultra Intensos: Ciência das Elevadas Densidades de Energia, (FCT, L. Silva, 2005-2007);
- European Laser Electron Controlled Acceleration in Plasmas to GeV Energy Range (European Commission L. Silva, 2006-2009);
- Laboratório de Engenharia de Plasmas para Aplicações Ecológicas (FCT, C.M. Ferreira, 2005-2007);
- Plasmas HF de Grandes Dimensões para Aplicações Ambientais" (FCT, C. M. Ferreira, 2006-2007);
- Electron Kinetics in Gas Mixtures Used for Analytical Glow Discharge Optical Emission Spectroscopy (GRICES[4]/OTKA[5], M.J. Pinheiro, 2006-2007)
- Mecanismos de Dissociação em Plasmas de H_2, O_2 e Misturas com Ar, Utilizados na Modificação e Depósito de Materiais, (GRICES/CSIC[6], L.L. Alves, 2006-2007);
- Desarrollo y Optimización de Métodos Basados en Plasmas de Microondas para la Destrucción de Compuesto BETX y Derivados (MEC[7] (Spain), L.L. Alves, 2004-2007).
- Sistema innovador de micro-ondas para a produção de mini-plasmas à pressão atmosférica (GRICES/CNRS[8], L.L. Alves, 2007-2008).

[1]Including the collaborations with the Associations EURATOM/IPP.CR and EURATOM/ENEA, IPP-Greisfwald and Brazilian Fusion Institutions.
[2]The funding institutions, the main investigator and the duration is indicated between brackets.
[3]FCT means "Fundação para a Ciência e a Tecnologia".
[4]GRICES means "Gabinete de Relações Internacionais da Ciência e do Ensino Superior".
[5]OTKA means "Hungarian Scientific Research Fund".
[6]CSIC means "Consejo Superior de Investigaciones Científicas".
[7]MEC means "Ministerio de Educación y Ciencia".
[8]CNRS means "Centro National pour la Recherche Scientifique".

Project	Responsible Person(s)	Collaborating Institutions	
		Portuguese	Other
Tokamak ISTTOK	Horácio Fernandes Carlos Silva	CFN[9] UBI[10] CEI[11], CFA[12]	CIEMAT[13], IPP-Kharkov[14], UI[15], IFUR[16], IFUSP[17]
Participation in the collective use of the JET Facilities by the EFDA Associates	Fernando Serra	CFN, CEI, UBI	EFDA[18] CSU[19] Culham UKAEA[20]
Participation in the ASDEX Upgrade programme	Maria Emília Manso Fernando Serra	CFN	IPP-Garching[21]
Participation in the ITER Project	Carlos Varandas Maria Emília Manso	CFN	EFDA CSU Garching
Participation in the TJ-II programme	Carlos Varandas Maria Emília Manso	CFN, CEI	CIEMAT
Participation in the TCV programme	Carlos Varandas	CFN	CRPP[22]
Collaboration with the Association EURATOM/CEA	J. Pedro Bizarro	CFN	
Other studies on theory and modelling	Fernando Serra J. Pedro Bizarro	CFN	IFP[23], PT[24], DFRC[25]
Keep-in-touch activities on inertial fusion energy	J.T. Mendonça	CFP[26]	
Participation in the Fusion Technology Programme	E. Alves	ITN[27], CFN	
Other fusion related activities			

Table 1.1 – Responsible person(s) and collaborating Institutions in the 2007 projects of the Association EURATOM/IST

[9] CFN means "Centro de Fusão Nuclear"
[10] UBI means "Universidade da Beira Interior"
[11] CEI means "Centro de Electrónica e Instrumentação da Faculdade de Ciências e Tecnologia da Universidade de Coimbra"
[12] CFA means "Centro de Física Atómica da Universidade de Lisboa"
[13] CIEMAT means "Centro de Investigaciones Energeticas Medioambientales y Tecnologicas"
[14] IPP- Kharkov means "Institute of Plasma Physics of the National Science Center" "Kharkov Institute of Physics & Technology".
[15] UI means "University of Innsbruck".
[16] IFUR means "Institute of Physics of the University of Riga"
[17] IFUSP means "Instituto de Física da Universidade de São Paulo"
[18] EFDA means "European Fusion Development Agreement"
[19] CSU means "Close Support Unit"
[20] UKAEA means "United Kingdon Atomic Energy Authority"
[21] IPP-Garching means "Max-Planck-Institut für PlasmaPhysik"
[22] CRPP means "entre de Recherches en Physique des Plasmas de École Polytechnique Fédérale de Lausanne"
[23] IFP means "Istituto di Física del Plasma"
[24] PT means "Politécnico di Turino"
[25] DFRC means "Department de Recherches sur la Fusion Controlée".
[26] CFP means "Centro de Física dos Plasmas"
[27] ITN means "Instituto Tecnológico e Nuclear"

2. TOKAMAK ISTTOK[1]

H. Fernandes (Head) C. Silva (Deputy Head), M.P. Alonso, B.B. Carvalho, P.A. Carvalho, R. Coelho, B. Gonçalves, I. Nedzelskij, V. Plyusnin, C.A.F. Varandas, I. Carvalho, P. Carvalho, A. Duarte, P. Duarte, H. Figueiredo, J. Figueiredo, J. Fortunato, R. Gomes, A. Neto, T. Pereira, A. Soares, Y. Tashchev, D. Valcárcel.

2.1. INTRODUCTION

This project has included, besides the normal tokamak maintenance activities, work in the following main research areas:

- Fusion-relevant materials;
- Diagnostics;
- Real time control and data acquisition;
- Plasma physics studies.

CFN organized in October 2007 the Joint Experiments in the framework of the IAEA Coordinated Research Project on "Joint Research Using Small Tokamaks". Remote experiments were also organized in November 2007.

2.2. FUSION-RELEVANT MATERIALS

2.2.1. Introduction

The activities in this area included the testing of the liquid metal limiter concept[2] and the development of nanostructured materials[3].

2.2.2. Testing of the liquid metal limiter concept

The following tasks were performed in 2007:

▪ *Testing of an infrared sensor (IR) intended to measure the temperature increase on the gallium jet surface during its interaction with ISTTOK plasmas.* The response of an IR sensor intended to perform the measurements of the gallium jet surface temperature was investigated. When absolutely calibrated, this diagnostic will provide an estimate on the power extraction capability of such a liquid metal jet in tokamaks. A HgCdTe (Mercury-Cadmium-Tellurium) sensor operated at cryogenic temperature (78 K) and specially designed to measure low temperature (>150 ºC), low emissivity materials like this kind of liquid metals has been tested. Since this sensor is sensitive in the infrared region of the spectra (peak efficiency from 6 to 7 μm) the chosen optics (viewing window and collection lens) has to be transparent in this range. From the analyses of the obtained data, it has been possible to clearly identify the heating of each individual droplet (at this position the jet is already in droplets from) and also a clear shift of the jet due to electromagnetic forces (Figure 2.1). It is possible to observe a wavy formation corresponding to the droplet signal passing in front of the detector. The disappearance of this signal (at about 160 ms) for the jet at r=68 mm can be related to the motion of the jet that partially leaves the field of view (FOV) of the sensor. The signal for the jet at r=58 mm appears only in the detector FOV when the discharge occurs due to the influence of the forces.

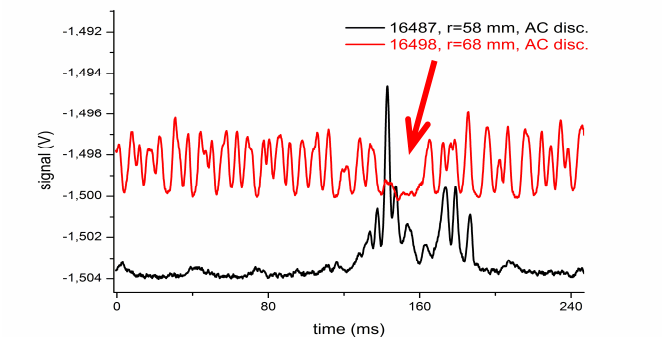

Figure 2.1 - Signal response of the IR sensor for two different radial positions of the of the gallium injector.

▪ *Estimation of the gallium jet surface temperature increase* The heat flux profiles at the ISTTOK edge plasma have been evaluated measuring the power deposited in a copper wire probe (30 mm height and 2.0 mm diameter) (Figure 2.2). The increase in the gallium jet surface temperature was obtained from the measured heat flux profile using the equation:

$$\Delta T(t) = \frac{1}{\sqrt{\pi \rho C_P \kappa}} \int_0^t \frac{q(t-t')}{\sqrt{t'}} dt' \qquad (2.1)$$

The jet temperature for several flow velocities and for each element of volume along the jet trajectory is shown in Figure 2.3. The maximum expected temperature on the jet surface was estimated to be ~173 ºC, at which gallium still has a very low vapour pressure.

▪ *Exhaustive operation of ISTTOK with the liquid Gallium jet interacting with plasmas at several radial positions.* No significant changes in the plasma parameters were observed for a wide variety of discharge conditions.

▪ *Analysis of discharges with respect to the plasma contamination by gallium.* No plasma or machine contamination by gallium has been observed after ~500 pulses with gallium.

[1] Activities carried out in the frame of the Contract of Association EURATOM/IST and the Contract of Associated Laboratory, by CFN staff of the Experimental Physics, Theory and Modelling and Control and Data Acquisition Groups.
[2] Work in collaboration with the Associations EURATOM/University of Latvia and EURATOM/ENEA.
[3] Work in collaboration with "Departamento de Materiais e Produção do Laboratório Nacional de Energia e Geologia".

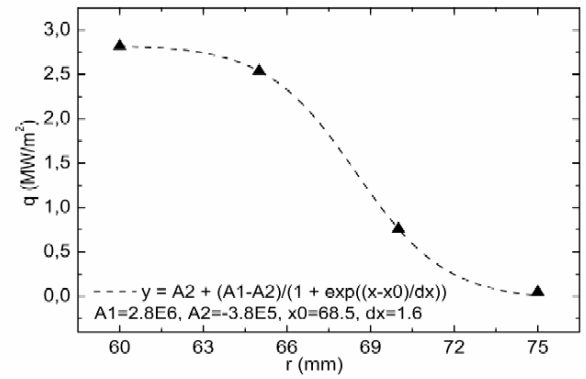

Figure 2.2 - Average heat flux profile for a 9 kW discharge.

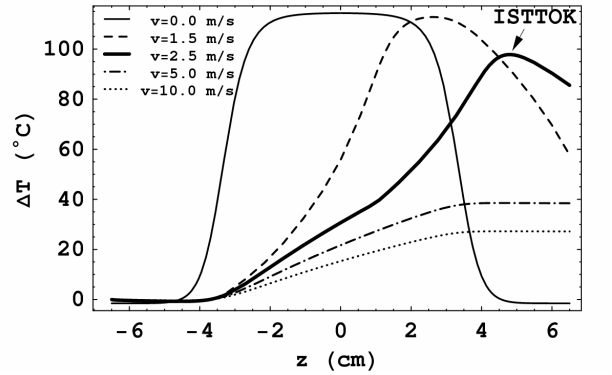

Figure 2.3 - Temperature increase for the element of volume in the gallium jet initially at $z=z_0$ and several flow velocities.

▪ *Design and construction of a multi-jet gallium system to increase its efficiency as a limiter*. A liquid gallium jet curtain with five jets (~1 cm width) is being developed with the aim of increasing the efficiency of the gallium system as a limiter. The test of a multi-jet system has been performed in Riga (Latvia). The installation on ISTTOK has been delayed since the produced limiter has not yet achieved the required stability and break-up length. The resistances in the gallium flow path have been identified has responsible for this result. Further tests have to be performed prior to the installation in ISTTOK.

▪ *Assessment of the possibility to implement a multi-jet liquid gallium limiter on FTU*[4] *based on the experience gained on ISTTOK*. The characterization of the required jet has been performed taking into account the specification of the FTU geometry and SOL plasma characteristics. The break-up length (BUL, continuous length of the jet before decomposing into droplets) has been estimated as a function of the magnetic field and flow velocity. To achieve the required BUL (0.4 m) a flow velocity of ~3.5 m/s will be required on FTU. The estimated temperature increase on the jet surface, taking into account the heat flux density profiles on FTU, is presented in Figure 2.4. It shows that a tolerable temperature increase is expected for flow velocities above 1 m/s.

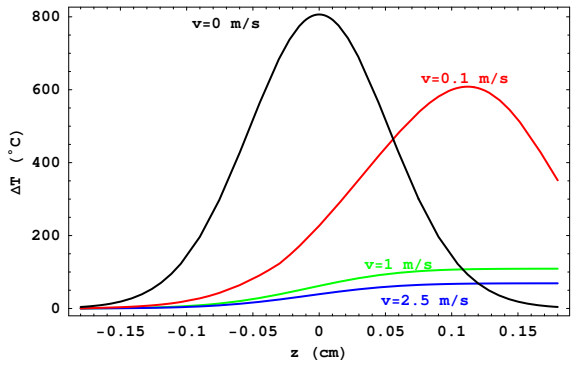

Figure 2.4 - Temperature increase for the element of volume in the gallium jet initially at $z=z_0$ and several flow velocities.

2.2.3. Development and study of nanostructured materials

The following activities were carried out in 2007:

▪ *Production of consolidate W-nD and Cu-nD nanocomposites*[5]. A novel material for nuclear fusion devices was proposed based on W-nDiamond nanostructured composites. Generally, a microstructure refined to the nanometer scale improves the mechanical strength due to modification of plasticity mechanisms. Moreover, highly specific grainboundary area raises the number of sites for annihilation of radiation induced defects. As a result, the concept of a composite is promising in the field of nanostructured materials. The hardness of diamond renders nanodiamond dispersions excellent reinforcing and stabilization candidates and, in addition, diamond has extremely high thermal conductivity. Consequently, W-nDiamond nanocomposites are promising candidates for thermally stable first-wall materials. Different mechanical alloying process and consolidation methods have been used to produce W-nDiamond composites. High density W-nD nanocomposites have been produced without the undesired carbide formation. The best results were achieved with high-energy milling at 200 rpm followed by Spark Plasma Sintering (SPS) at 800ºC;

▪ *Exposure to ISTTOK plasma of rolled W-nD nanocomposites.* Figure 2.5 presents the first results obtained with the W-nD material consolidated by hot-rolling at 800ºC and exposed to the ISTTOK edge plasma. Zone 1 shows signs of intense evaporation, and subsequently modification of structure. However, below 1 mm the nanoparticles of nanodiamond were essentially preserved;

▪ *Study of hydrogen diffusion in tungsten and copper probes* Commercial pure tungsten and copper used as Langmuir probes on ISTTOK have been investigated for long term hydrogen migration. The microstructure of both

[4] FTU is a tokamak of the Association EURATOM/ENEA, located in Frascati.
[5] Work performed by "Laboratório Nacional de Energia e Geologia".

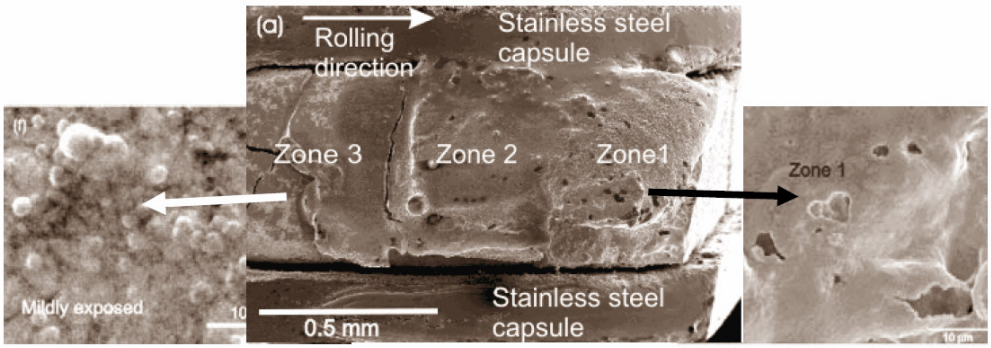

Figure 2.5 - W-nD subjected to mechanical alloy (4 h at 200 rpm) and rolling at 800ºC and exposed to the edge plasma.

materials revealed recrystallization and strong grain growth at the most severely exposed regions. A high density of small intergranular bubbles was found at the intermediate regions (Figure 2.6), whereas a low number of large intergranular bubbles (50 μm in tungsten and 0.5mm in copper) were present at the most severely exposed regions, as a result of a coalescence process. Hydrogen saturation was assessed through the lattice parameter and Young Modulus variations across longitudinal cross-sections of the probes. The results indicate that bubble formation in tungsten and copper first wall components can be expected to occur and strategies for minimization of the phenomenon need to be implemented.

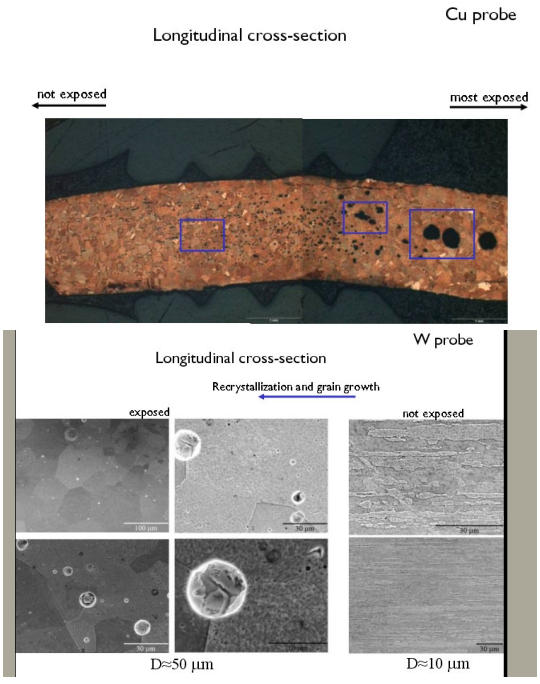

Figure 2.6 - (a) Optical microscopy images of the longitudinal cross-section of a Cu probe; (b) Scanning electron microscopy images of the longitudinal cross-section of a W probe.

2.3. DIAGNOSTICS

2.3.1. Main activities

The following main activities were made in 2007:

- *Test of channeltrons for the time-of-flight energy analyzer (TOFEA) diagnostic.*With the aim of improving the signal-to-noise ratio of the Heavy Ion Beam TOFEA diagnostic, two channeltrons have been installed on the "start" and "stop" detectors of the time-of-flight energy analyzer diagnostic. Although a gain of ~ 100 in the signal intensity was obtained, the SNR did not improve. The increase in the noise was attributed to the incomplete channeltrons shield from the plasma radiation. The use of the indirect detection with ion reflection or ion-electron conversion (Figure 2.7) has been proposed to shield radiation from the plasma and respective TOFEA modifications performed.

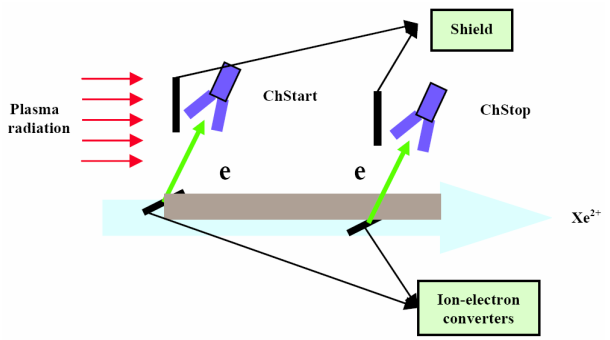

Figure 2.7 - TOFEA with indirect detection of secondary ions.

- *Development of fast tomographic reconstructions methods*. One of the main objectives of the bolometer tomography diagnostic on ISTTOK is to supply the required feedback to the plasma position control system. The Fourier-Bessel (FB) and Neural networks (NN) tomographic methods stand out due to their inherent speed necessary for real-time control. The performance and reliability of these methods have been compared. It has been found that although the FB based inversion proved to be faster, the NN reconstruction has fewer artifacts and is

more accurate (Figure 2.8). The real-time tomographic algorithm based on the FB method has been implemented and tested on the computer acquiring the tomographic data. This computer is running the Real-Time Application Interface (RTAI) layer in Linux, so as to ensure that the algorithm is always run with the maximum priority. Off-line tests showed that each tomographic reconstruction is generated in about 40 μs.

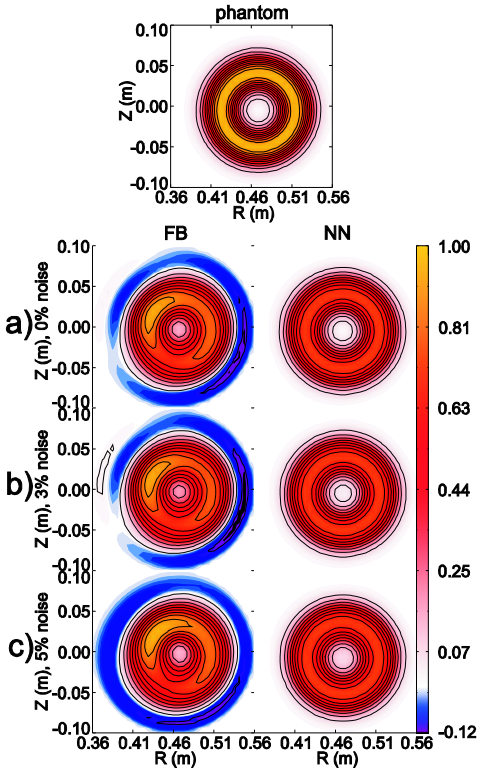

Figure 2.8 - Comparison of the reconstructions using Fourier-Bessel and Neural Networks algorithms for different ranges of measurement noise - a) has no noise, b) has 3% noise and c) has 5% noise. Clearly, the NN reconstructions are superior to the FB in any of the cases presented.

▪ *Development of a simple method for tomographic analysis*. A fast method for tomographic analysis has been developed to be used in real-time control and to quickly evaluate the data from the diagnostic. The method is based on the fact that a volume of plasma emits radiation isotropically and the relation between the total radiation emitted by two volumes and the sum of the signals in all the sensors viewing those volumes is similar. A grid representing the area covered by the sensors is build and the resulting image filtered to produce a realistic result. Although this method does not provide a solution to the tomographic problem, it is still a good approximation for the real radiation density profile. This method was used in plasma position calculations, demostratin that the plasma position obtained using the magnetic probes was biased and required corrections;

▪ *Development of a cantilever force probe (CFP) for plasma pressure measurements*. A compact cantilever force probe has been proposed for the plasma pressure measurements. It is based on the pull-in phenomena well known in micro-electro-mechanical-systems electrostatic actuators. The probe consists of a thin (25 μm) titanium foil cantilever and a fixed electrode separated by 0.75 mm gap. The probe is shielded by brass box enclosed into boron nitride housing with 9 mm diameter window for opening the cantilever surface to the plasma (Figure 2.9). When the voltage is applied between cantilever and electrode, an attractive electrostatic force is counter-balanced by the cantilever restoring spring force. At some threshold voltage the system becomes unstable and the cantilever abruptly pulls toward the fixed electrode until a breakdown occurs. The threshold voltage is sensitive to the additional externally applied force, being the resolution of the measurements $\pm 1.4 \times 10^{-5}$ N. The probe has been tested in the ISTTOK edge plasma, and a plasma pressure ~ 1.1 N/m^2 has been obtained near the leading edge of the limiter. This value is in good agreement with the estimations using local plasma parameters measured by electrical probes.

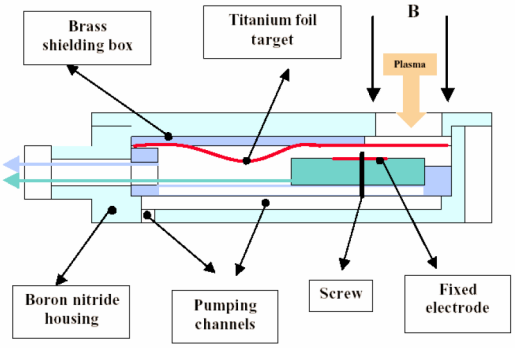

Figure 2.9 - Schematic illustration of the cantilever force probe.

▪ *Development of a five channels retarding field energy analyzer (RFEA)*. This diagnostic has been developed for edge ion temperature measurements in the TJ-II stellarator. Common grids for all channels have been used, allowing a simplification of the RFEA powering electronics. This innovative RFEA design has been implemented and successfully tested in the ISTTOK edge plasma;

▪ *Upgrade of the heavy ion beam diagnostic for fluctuations studies*. The use of a multi-cell array detector offers unique capabilities to the Heavy Ion Beam Diagnostic (HIBD) as it allows simultaneous measurements across the plasma column. New pre-amplifiers for the HIBD have been successfully tested with a bandwidth of 400 kHz, allowing the use of this

diagnostic for fluctuations studies. Broad band (<100 kHz) fluctuations at plasma periphery associated with turbulent transport as well as quasi-coherent fluctuations in bulk plasma at frequencies between 100-200 kHz have been identified. The localization and frequency of the latter fluctuations correlate well with the MHD activity of the plasma;

▪ *Installation of Cherenkov detectors for measurements of fast electrons*[6]. A movable Cherenkov detector measuring head, equipped with a 5 mm diameter input window, has been installed on ISTTOK. The detector consists of a small chamber containing a 10-micrometer-thick Ti-foil placed on an AlN crystal (used as a radiator) coupled with a light-pipe (a metal tube with the polished inner surface). Visible light, generated by the Cherenkov effect, was detected with a photomultiplier placed outside the tokamak chamber. The radial distribution of the fast electron fluence at different plasma densities, discharge currents and loop voltages was measured. It has been found that the radiation is larger for plasma with low colisionality due to the significant fraction of fast electrons observed in these conditions;

▪ *Installation of a seven channel photodiode array to measure the intensity of different radiation lines as the H_α and CIII.* This diagnostic records also radiation from spectral regions without line radiation with the aim of determining the Z_{eff}.

2.4. REAL TIME CONTROL AND DATA ACQUISITION

2.4.1. Main activities

The following main tasks were performed in 2007:

▪ *Validation of the plasma position determination.* A discrepancy between the plasma position given by the magnetic and tomography diagnostic was found. This difference, at some extent, can be explained by the magnetic equilibrium fields affecting magnetic measurements. A study was performed that consisted in measuring the magnetic field in two discharges: one with plasma and equilibrium fields; another with the same fields but no plasma. The plasma position was calculated using: (i) the raw data from the discharge with plasma (R and Z); (ii) data compensated by the expected magnetic fields (R_T and Z_T); data corrected with the measured fields in the discharge without plasma (R_E and Z_E); and (iii) with tomography data (R_{TOM} and Z_{TOM}). Figure 2.10 shows the results where it can be seen that the magnetic plasma position agrees with the tomographic position only when the correction based on the expected equilibrium field is used.

▪ *Development of video-conference tools to facilitate remote participation.* Fusiontalk, an open source project consisting of server and client software available to all nuclear fusion research institutes has been developed. Its main aim is to fill the gap between video-conferencing and data access. Fusiontalk has been used extensively during the ISTTOK Joint Experiments, where a remote room has been prepared to follow the experiments;

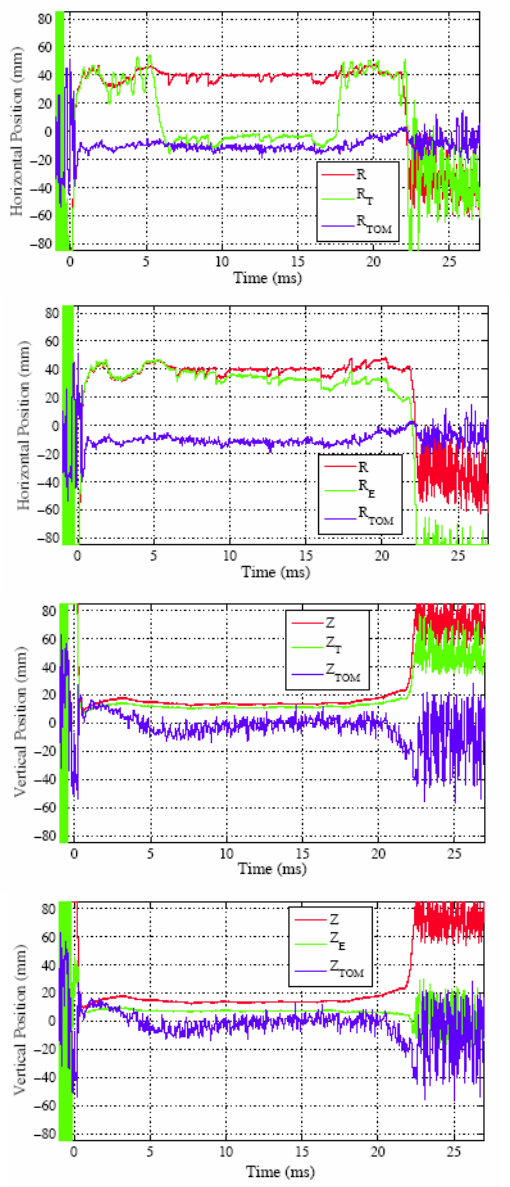

Figure 2.10 - Plasma position for discharge #16279 calculated from: (a) raw magnetic signals (R, Z), theoretically corrected magnetic signals (R_T , Z_T) and tomography (R_{TOM}, Z_{TOM}); (b) same as (a) except the corrected with measured signals (R_E, Z_E).

▪ *Installation of an ATCA crate* to test new concepts for the COMPASS control and data acquisition.

▪ *Conclusion of the data acquisition system migration from VME to PCI boards* (2 MS/s, galvanic isolated).

[6]Work in collaboration with Andrzej Soltan Institute for Nuclear Studies (IPJ), Poland.

▪ *Upgrade of the vertical field fast amplifier control*[7]. Alternate current plasma discharges require fast transitions in the vertical field fast amplifier. In order to reduce the time in a current inversion a new controller was developed for the vertical field fast amplifier, which allowed the current inversion from 100 A to -100 A within 1 ms (Figure 2.11), while the same power programmed with the old controller was achieved in 2 ms. The new algorithm is a hybrid controller based on the fast reacting on/off controller and on the robustness of a PID. The control algorithm switches between the two modes whenever stability or fast reaction is needed.

▪ *Development of new databases support for FireSignal and SDAS*. The amount of data generated in each pulse has grown rapidly due to extended AC discharge time and the improvement on the CODAC systems. A new solution using a combination of SQL and a high reliable and performance file system was developed. This system is also intended to be used in COMPASS and in the JET/GRS and JET/DNG-G projects.

▪ *Development of a FireSignal C++ generic node solutions*. FireSignal hardware controllers, also known as nodes, are now also available in C++. This allows a more transparent connection between the control system and the hardware itself. Most of the ISTTOK acquisition nodes are currently being migrated to work with this framework.

▪ *FireCalc a XML-based framework for distributed data analysis* Based on the principles of modularity and open-source, a framework for generic data analysis, named FireCalc, was developed. FireCalc makes use of tested data transfer and data analysis technologies to allow different computation language scripts to run on the same system. Moreover, supporting parallel computing capable languages, FireCalc can operate as a distributed computing calculus server. As for the data necessary for the calculation, its modular design allows for different communication protocols to access different data servers. The implementation of FireCalc in CFN uses the Scilab kernel for the computations, both server and client are programmed in Java and a graphical user interface is being developed, which will simplify the editing of the scripts and displaying the results.

▪ *Development of harmonic estimator based on Kalman filters* The time and frequency response of a lock-in amplifier scheme based on Kalman filter techniques was investigated and the potential application for the real time harmonic estimation embedded in fusion plasmas related signals highlighted. The frequency response of the filter reveals the proximity to an infinite response filter, with favorable balance between filtering response and time delay in the estimated amplitudes. The time delay never overcomes a quarter of the period of the signal under estimation. Although computationally more demanding the proposed filter method is much more powerful than a single-phase lock-in method that is more suited for offline analysis due to its Fourier nature. The latter is unable to cope with frequency jitter (Figure 2.12), to adequately filter out the noise and avoid contamination from neighboring frequencies (beating effect) when using a limited number of signal samples, owing to the frequency resolution of the box car window that needs to be used.

2.5. PLASMA PHYSICS STUDIES

Studies on MHD wavenumber analysis, poloidal structure of the ISTTOK edge fluctuations and alternating plasma current (AC) discharges have been carried out in 2007.

2.5.1 MHD wavenumber analysis in ISTTOK

The characterization of the spectra of unstable modes observed in ISTTOK plasma discharges has been addressed using a set of two poloidal arrays of magnetic coils (Mirnov coils). The poloidal and toroidal wavenumbers of the modes, with typical frequencies in the range 80-150 kHz, was determined by means of an integrated numerical tool that includes cross-spectrum, SVD and (θ,t) poloidal array signal contour analysis using all available coils. The dominant mode activity inferred from the data corresponds to an intermittent m=2,n=1, with occasional destabilization of m=1,3,4 harmonics.

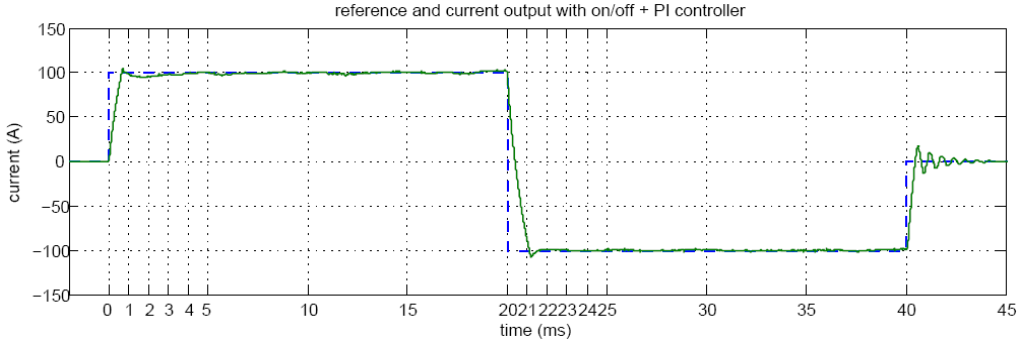

Figure 2.11 - Current inversion in the vertical field fast amplifier programmed with the hybrid controller.

[7]Work in collaboration with the Association EURATOM/ENEA.

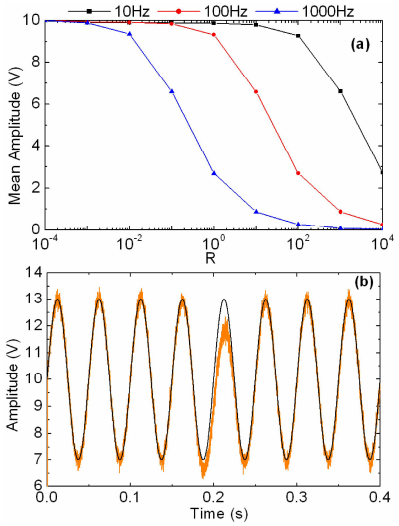

Figure 2.12 - Effect of a frequency mismatch on the estimated amplitude of an AM signal. Offset in the mean estimated amplitude increases with measurement covariance R and mismatch $\Delta\omega/2\pi$ (a). The time evolution of the estimated amplitude (in grey) for the case R=1 and 100Hz mismatch is shown (b).

Measurements of the modes' phase indicate that they propagate in the electron diamagnetic direction. The mode, in principle a resistive tearing mode (linear growth rate of the order 1-2 ms), appears in bursts of ~0.1-0.5 ms time duration. An example of a (2,1) mode, destabilized by negative electrode biasing is shown in Figure 2.13. Only mode numbers for which the calculated coherency is above 66% are shown.

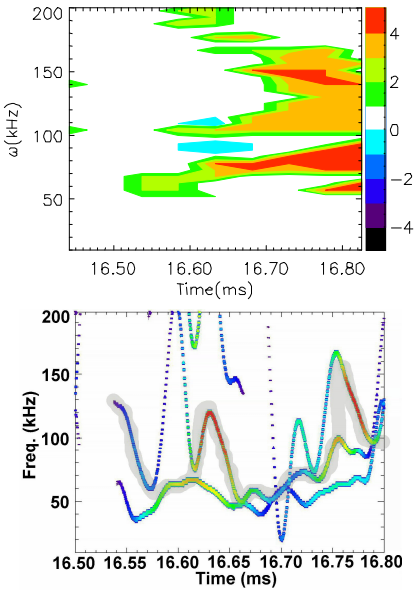

Figure 2.13 - Poloidal mode number of coherent rotating magnetic fluctuations and mode frequency evolution (highlighted in grey) using Hilbert Huang Transform.

2.5.2 Poloidal structure of the ISTTOK edge fluctuations

The poloidal structure of the fluctuations has been investigated using a poloidal array of Langmuir probes consisting of 7 pins poloidally separated by 1.5 mm. It has been observed that the ISTTOK edge plasma is characterized by low frequency (<100 kHz), small wavenumber (k_θ< 3 cm^{-1}) fluctuations. Large poloidal structures are clearly visible in the probe signal having a poloidal velocity around 1-2 km/s, a correlation length around 10 mm and a typical duration of 10 µs, resulting in an estimated structure poloidal size of 1-2 cm.

The cross-correlation between the signals from different pins has also been investigated as a function of the frequency. It was observed that the correlation length is very large for frequencies between 50 and 150 kHz (>10 mm), being the correlation roughly constant across the 7 pins in this range (Figure 2.14). This frequency range corresponds to time scales of ~10 µs, which is the typical time scale of the large events observed. On the contrary, the correlation length is small at high frequencies. These results show evidence of multi-scale structures with different properties. The high frequencies are dominated by small-scale structures while the intermediate frequencies are dominated by large structures with long correlation lengths.

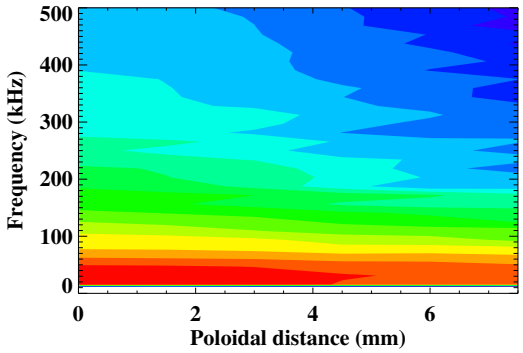

Figure 2.14 - Poloidal cross-spectrum of the edge floating potential fluctuations.

2.5.3. Study of AC discharges

The development of a new plasma position controller and digital controlled current amplifiers in 2006 has enabled to achieve regular AC discharges (end of 2007) with 250 ms, extending the plasma duration for almost one order of magnitude. The optimization of the machine space parameters allowed a successfully AC campaign during the IAEA Joint Experiment (see next section), generating a significant amount of relevant data to be analyzed during 2008.

2.6. ORGANIZATION OF THE ISTTOK JOINT EXPERIMENT

CFN has organized in October 2007 the Host Laboratory Experiment on the tokamak ISTTOK. The Joint Experiment (JE) was organized in cooperation with the IAEA in the framework of the IAEA Coordinated Research Project (CRP) on "Joint Research Using Small Tokamaks" with the participation of 24 scientists from 13 countries (Austria (1), Belgium (1), Brasil (3), Bulgaria (1), Canada (1), Czech Republic (1), Egypt (1), Iran (2), Kazakhstan (1), Mexico(4), Poland (1), Russia (5), UK (1)).

Taking into account the ISTTOK scientific programme and the feedback from the pre-registered participants the following areas were explored during the ISTTOK JE: (i) study of the poloidal structure of the edge fluctuations; (ii) tokamak operation in alternating current regimes; and (iii) testing of the liquid metal limiter concept. These activities were successfully carried out being distributed in five experimental sessions. Other areas related with plasma engineering and diagnostics were also investigated, although with no dedicated experimental sessions attributed. These areas, organized in small workshops, included: (i) plasma diagnostics; (ii) plasma control; (iii) data acquisition; and (iv) remote data access.

Remote experimental sessions in the following weeks were also organized to complement the experiments performed during the ISTTOK JE. The participants could run experiments using the ISTTOK remote participation tools. Working groups have been formed for data analysis and remote meeting regularly organized to plan experiments and discuss results.

Transverse areas to the ISTTOK JE were data acquisition, signal processing and remote access tools, where CFN has a long experience. These systems have been successfully used for data management on several tokamaks and they may serve as a platform for a unified environment for data exchange and processing in the framework of the activity on small tokamaks.

3. PARTICIPATION IN THE COLLECTIVE USE OF THE JET FACILITIES BY THE EFDA ASSOCIATES[1]

F. Serra (Head), J.P. Bizarro, D. Borba, R. Coelho, S. Cortes, L. Cupido, L. Fattorini, A. Figueiredo, A. Fonseca, B. Gonçalves, S. Hacquin, M.E. Manso, F. Nabais, M.F. Nave, I. Nedzelski, I. Nunes, V. Plyusnin, T. Ribeiro, F. Salzedas, C. Silva, J. Sousa, A. Vannucci, C. Varandas, P. Varela, D. Alves, P. Belo, N. Cruz, J. Ferreira, L. Meneses.

3.1. INTRODUCTION

The Association EURATOM/IST has continued its participation in the collective use of the JET facilities, in the frame of EFDA through the "JET Operation Contract" and the "JET Implementing Agreement".

The main activities in this project were related with:

- Operation;
- Scientific exploitation;
- Performance enhancements;
- Management.

3.2. OPERATION

Two members of the IST/CFN staff have been working in the JET Operation Team:

▪ One physicist has continued to work in the JET "Plasma Operation Group", as a session leader for the Campaigns, and has also been involved on JET-EP2 ITER-like wall project;

▪ One physicist has carried on his work in the Reflectometry and LIDAR Diagnostic Group, being responsible by: (i) maintenance of the X-mode correlation reflectometer (KG8b); (ii) the analysis and validation of the signals of the KG8b X-mode correlation reflectometer and the KG3 O-mode fluctuation reflectometer.

3.3. SCIENTIFIC EXPLOITATION

3.3.1. Introduction

IST has proceeded with an important contribution to the JET scientific exploitation mainly through an active participation of sixteen scientists in the experimental campaigns (C18-C19) and in analysis/interpretation and modelling of the experimental data, with emphasis in the integration of transport and MHD codes.

3.3.2. Controlling the ITB oscillations in advanced tokamak scenarios with a dominant fraction of bootstrap current[2]

Modelling of advanced tokamak scenarios with very large bootstrap current has continued, and a detailed understanding of the mechanism behind ITB oscillations, as well as of the means to control them, has been achieved. The analysis of truly steady-state tokamak discharges, meaning zero loop voltage, has also begun. Typical ITB oscillations in JET-like plasmas are shown in Figure 3.1.

It was shown that relaxation oscillations associated with repetitive ITB buildup and collapse, with ICRH, NBI and LHCD, and with a dominant fraction of bootstrap current, can be overcome if the LHCD power is sufficiently high. This result has been obtained using a bench marked, fully predictive transport model iterated with given ICRH profiles and self-consistently with NBI and LHCD modules, the stabilizing role of the E×B flow shear being combined with that of reversed magnetic shear in the simulation of ITB dynamics.

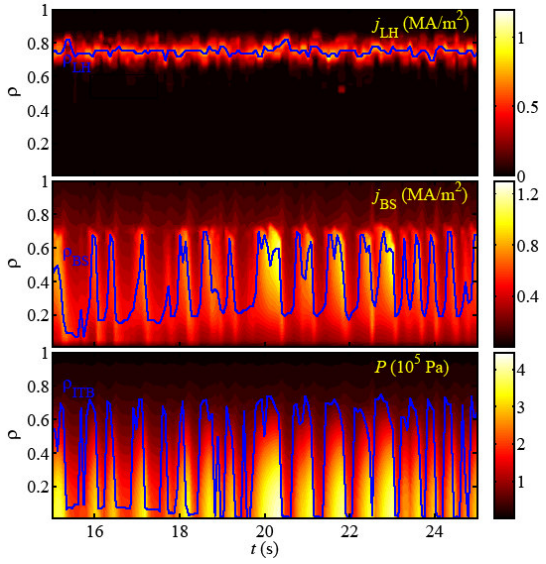

Figure 3.1 - Time evolution of the profiles for the Lower Hybrid (LH)- and Bootstrap (BS)-driven current densities, and for the plasma pressure. Also shown is the time evolution of the locations for the LH and BS current-density peaks and for the ITB foot.

3.3.3. Experiments on fast ion redistribution and losses

Fast ion losses are of concern for ITER since the first wall can only tolerate losses at a very low level before suffering damage. To explore the physics of fast ion loss, JET has installed new fast ion loss detectors[3] and is now able to undertake dedicated fast ion redistribution experiments which allow predictions for ITER to be made.

---

[1]Activities carried out in the frame of the Contract of Association EURATOM/IST and the Contract of Associated Laboratory, by CFN staff of the Experimental Physics, Microwave Diagnostics, Theory and Modelling and Control and Data Acquisition Groups.

[2]Work performed in collaboration with CEA and VTT.

[3]Particle loss signatures during sawtooth events at JET , M. Reich et al., 34th EPS Conf on Plasma Physics, Warsaw, Poland, 2007

A set of experiments on fast ions redistribution was planned and carried out in 2007 experimental campaign. Using a high ICRH power on a low density plasma, a large population of highly energetic ions was build up which constituted a strong drive for many instabilities responsible for the redistribution of fast ions. In particular, diamagnetic, hybrid and precessional drift fishbones were destabilised, as well as TAE and core-localised TAE (tornado modes).

Two types of fast ions were identified by the gamma-ray diagnostics[4]: fast protons with an energetic tail in excess of 4.5 MeV due to ICRH tuned to a fundamental H-resonance in the centre of the plasmas and D-ions accelerated with second harmonic heating whose energies exceeded 0.5 MeV. Aside of it, three types of losses were identified (Figure 3.2), one associated with sawtooth crashes, one associated with TAE and high frequency fishbones and a third group observed when tornado modes and low frequency fishbones are unstable.

An important result came out from these experiments: The type and number of lost ions change as soon as tornado modes are destabilized. This may support the possibility of sawtooth crashes being caused by fast ions redistribution due to tornado modes.

3.3.4. Momentum transport modelling[5]

Activities supporting interpretative and predictive transport modelling have been continued. Perturbative methods were used to complement the usual steady-state analysis with the aim of better understanding transport phenomena in fusion plasmas. Recently, in JET, experiments with modulation of the injected neutral beam power were accomplished, and, as believed, a modulated source of momentum was obtained[6]. Applying cross correlation methods to experimental data from the new improved Charge eXchange Recombination Spectroscopy (CXRS), particularly, toroidal rotation and ion temperature measurements every 10 ms, and to results from careful transport modelling with JETTO and TRANSP codes, interesting findings were obtained[7]. First results show that beam modulation technique can be useful for momentum transport studies and point to the existence of a "pinch" in the momentum transport, supporting on-going theoretical work done by collaborators[8].

3.3.5. Effect of the deuterium density profile on the impurity transport

Experiments at JET have found that impurity density profiles in the plasma core are dependent of the inclusion or not of ICRH. The impurity profile is hollow with ICRH and peaked when only NBI is in use. Two hypotheses were raised to explain these profiles: The impurity transport in the plasma core follows the neo-classical description or there is an anomalous contribution for the convective impurity velocity that is outward directed without the ICRH and inward directed otherwise[9].

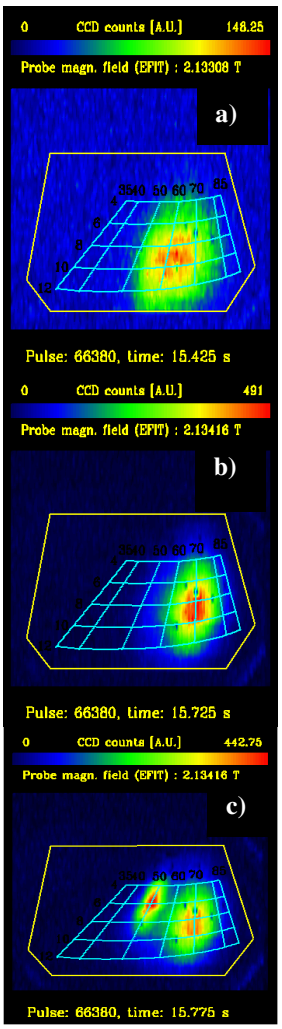

Figure 3.2 - The three types of measured fast ion losses as function of the pitch angle and gyro radius: before tornado modes are destabilized (top), after tornado modes are destabilized (middle) and during a giant sawtooth crash (bottom) (pulse #66380).

[4]V.G. Kiptily *et al*. Nucl. Fusion 42, 999, (2002).
[5]Work performed in collaboration with CNR, VTT, IPP, Univ.Warwick, VR and UKAEA.
[6]J.S. Ferreira, et al., Recent modeling of NBI modulation experiments, EFDA-JET Task Force T Meeting, Culham, UK, 29 March 2007.
[7]P. Mantica *et al*., Analysis and modelling of NBI modulation session, EFDA-JET Task Force T Meeting, Culham, UK, 16 October 2007.
[8]A. G. Peeters, *et al*., Toroidal Momentum Pinch Velocity due to the Coriolis Drift Effect on Small Scale Instabilities in a Toroidal Plasma, Physical Review Letters 98: 265003, June, 2007.
[9]L.Carraro, Proceedings of 34th EPS Conference, Warsaw July 2007.

Three sets of JETTO/SANCO simulations were done with the three different electron density profiles represented in Figure 3.3, with the same electron and ion temperature profiles. The electron density profiles changes are within the experimental error bar which is around 20%. The impurities were predictive in these simulations and an ad-hoc anomalous transport for $\rho > 0.4$ and completely neo-classical for $\rho < 0.4$, as represented in Figure 3.4, was used. This transport profile is very similar to the ones observed experimentally[10]. In steady state regime the impurity profile is observed to be hollow when a flat density profile is used in the simulations and peaked when a peaked density profile is used within the region where the transport is completely neoclassical. The neoclassical convective impurity velocity is inward for the peaked profile and outward for flat profile case. The neo-classical transport seems to explain the hollow profiles observed experimentally. However, further simulations using more theoretical driven impurity anomalous transport should be performed to confirm these results.

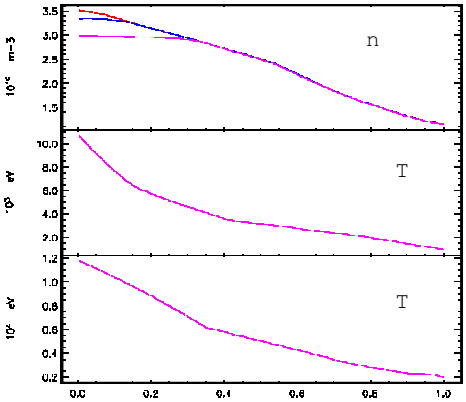

Figure 3.3 - Density and Temperature profiles used in JETTO/SANCO simulations.

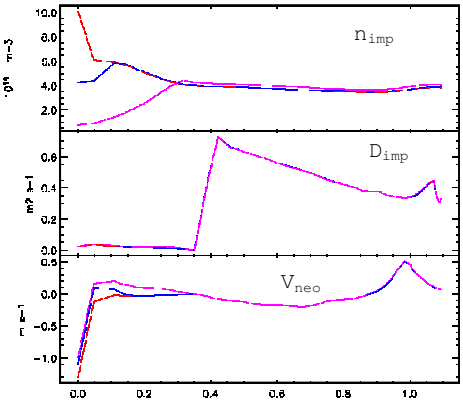

Figure 3.4 - Sum of all ionization stages density profiles, impurity diffusion and neo-classical convective velocity. The colour of the impurity profiles corresponds to the colour of the deuterium profiles in Figure 3.3.

[10]Giroud, C., et al, Proceedings of 34th EPS Conference, Warsaw July 2007.
[11]Fichtmuller, M., *et al, J. Nuclear Mat*., 266-269 (1999) 330.
[12]Monier-Garbet, P., *et al*, *Nuclear Fusion*, 38 (1998) 1839.

3.3.6. Synergetic effects on impurity transport with Deuterium SOL flows

JET impurity seeded plasma experiments have at least two impurities present. The introduced extrinsic impurity (normally Nitrogen, Neon and/or Argon) coexists with intrinsic Carbon which comes from the wall and divertor plates due to the chemical and physical sputtering. An increase of the friction force on the recycled impurity due to the presence of Carbon was observed in previous simulations with EDGE2D/NIMBUS[11].

The simulations using EDGE2D/NIMBUS allowed concluding that the addition of an intrinsic impurity (Carbon) does not qualitatively change the screening of the extrinsic impurity (Neon) by the main gas puffing (Figure 3.5). This means that friction force and thermal force still play dominant roles in establishing the Neon distribution. The introduction of a second impurity increases total radiated power resulting in a decrease in electron temperature, moving the conditions for plasma detachment to a lower density range.

A significant reduction of the C^{2+} spectral line intensity and Z_{eff} not increasing significantly was observed experimentally after the onset of extrinsic impurity puff in high density and triangularity JET H-mode plasma. These findings inferred a conclusion that Carbon was replaced by the extrinsic impurity in the plasma core[12]. Although simulations with EDGE2D/NIMBUS gave similar results for high density plasmas was not possible to draw the same conclusion, because Carbon was not substituted by Neon in the plasma core but in the divertor region. The increase of the Zeff is mainly due to an increase of the Carbon concentration in the core rather than the Neon concentration which was very low. The increase of the Carbon concentration was also observed in the reference JET pulses used in the EDGE2D/NIMBUS simulations, (Figure 3.6), after the onset of Argon puff: 53550 (Argon seeded plasma); while there was change in the pulse 53549, which was no seeded plasma. The reduction of the C^{2+} spectral line intensity was not due to a decrease of Carbon influx from the divertor plates but an increase of Carbon upstream flux, leading to a decrease of Carbon flux to the pump.

Overall the addition of an extrinsic impurity, or second impurity into the plasma, changes the parallel transport of the intrinsic impurity, or first impurity, by decreasing the friction force on it. As a result the second impurity does not allow the first impurity to be removed from the plasma through the pumps and even pushing it further into the plasma core, while the first impurity has exactly the opposite effect on the second impurity.

3.3.7. Effects of the magnetic configuration on the impurity transport and plasma detachment

The divertor configuration at JET was changed allowing more flexibility on the magnetic equilibrium configuration. Figure 3.7 shows the four possible

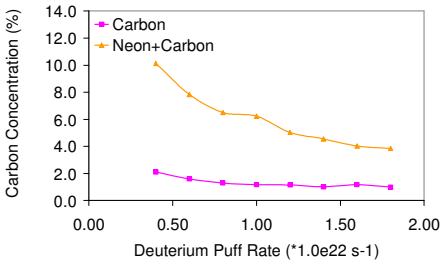

Figure 3.5 - Carbon concentration inside the last closed flux surface as a function of deuterium puff rate for the EDGE2D/NIMBUS simulations with Carbon only (pink line) and simulation with Neon (orange line).

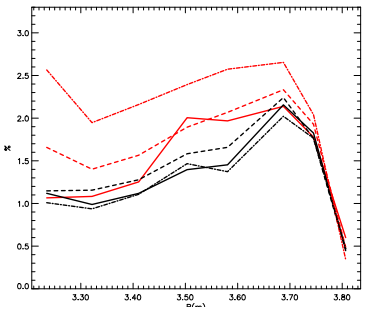

Figure 3.6 - Carbon concentration profiles for three different times at 59.5 s, half a second before the impurity puff onset, at 60.5 s, half second after the impurity puff onset and at 62.5 s, 1.5 s after the onset and half a second after the onset of the exponential rise of the impurity radiations. The profiles are from two the JET pulses one is the reference pulse without extrinsic impurity 53549 (black line) and with the extrinsic impurity 53550 (red line).

configurations used in the study of the effects of the magnetic configuration on the impurity transport and plasma detachment. An external source of momentum was also included.

The EDGE2D/NIMBUS simulations show that all configurations that have the strike point at tile 5 have higher deuterium densities at the separatrix at outer mid plane. In these configurations the plasma is detached at the inner target even for deuterium puff rates as low as 1×10^{20} particles/s due to lower pump efficiency (Figure 3.8). Nevertheless a lower concentration of impurities in the plasma core was observed.

3.3.8. Testing mechanisms to explain the parallel transport in the SOL

Simulations were done to compare JET plasmas with the new ITER like configuration (AT) with the external momentum force and the usual high triangularity magnetic equilibrium configuration (HT3). The relevant experimental values were used: inlet deuterium gas puff positioned at the outer mid plane separatrix varying from $3.5\text{x}10^{21}$ particles/s until the pressure at the targets was less than a half of the pressure at the outer mid plane; the power across the separatrix was P_{ions}=6.0 MW and $P_{elec.}$=6.0 MW; the impurity content was set to be constant, $5.0\text{x}10^{17}$ particles in the whole computational grid; and the perpendicular transport was determine using the JETTO/SANCO simulations for this pulse, 70286 in ELM free H-mode.

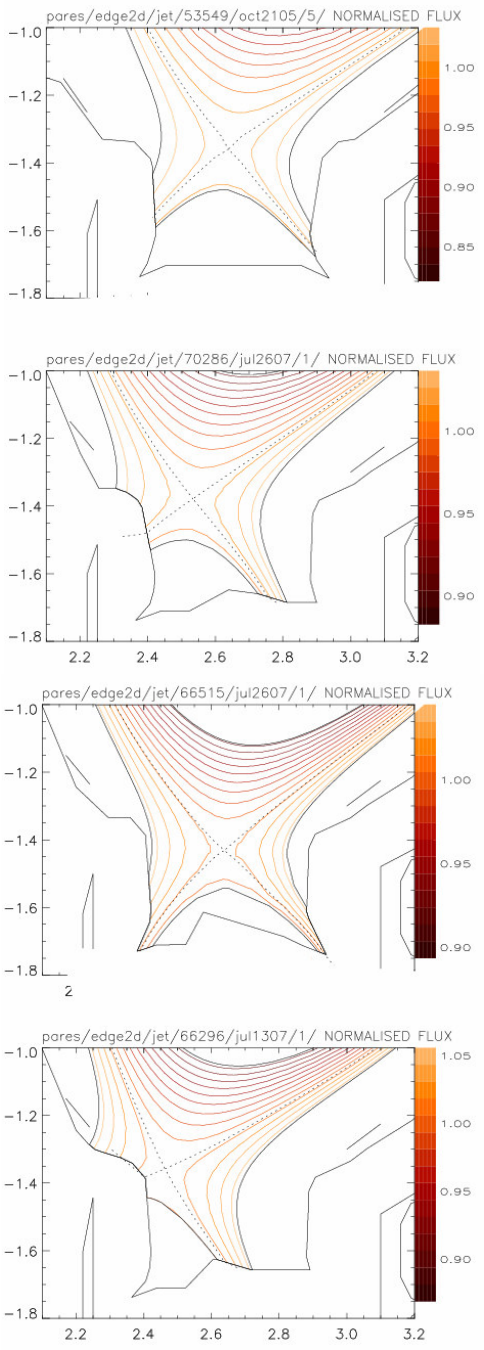

Figure 3.7 - Four possible magnetic equilibrium flux surfaces at the divertor region for the latest divertor configuration: a) low triangularity with the X point at the middle of the divertor region, the strike point at tile 7(66515); b) high triangularity with the X point at the middle of the divertor(53549); d) high triangularity with the strike point at tile 5 and the X point closer to the inner target (15 cm) (66296) and d) high triangularity with the X point closest to the inner target (5 cm) (70286).

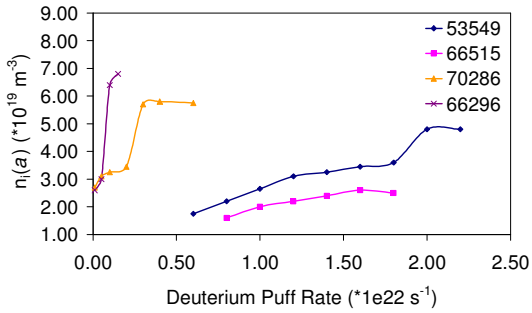

Figure 3.8 - Deuterium density at the separatrix increases as a function of the deuterium puff rate for the different magnetic configurations.

Figure 3.9 shows the simulation results for the normalised total pressure at the inner (a) and outer (b) targets to the outer mid plane total pressure of all possible combinations for the parallel transport. The plasma detachment occurs when the normalised pressure at the targets drops below 0.5. From the figure it is clear that the maximum gas puff rate possible is 7.5×10^{21} particles/s which is much lower than experimentally observed for this type of magnetic equilibrium. For some of the cases, mainly with the flux limiters, the plasma detachment occur first at the outer target like or even in both targets at the same time. This also occurs for the case with the ballooning transport and the external source of momentum.

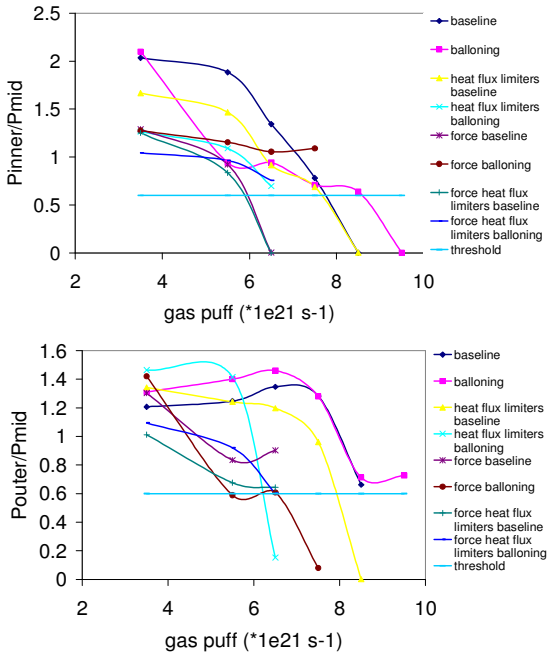

Figure 3.9 - Normalised total pressure at the outer (a) and inner (b) targets by the total pressure at the outer mid plane separatrix for all the possible combinations of the parallel transport in the plasma EDGE2D/NIMBUS.

[13]Belo, P. *et al*, Plasma Phys. Control. Fusion, 46 (2004) 1299.

Simulations with the external source of momentum predict a much higher deuterium density at the outer mid plane separatrix than for all the cases without the force the deuterium density. In latter cases the deuterium density are within the error bar of the experimental measurement. Besides all the simulations with the different parallel transport contributions predict a much higher increase of the deuterium density with the deuterium gas puff than it is experimentally observed.

3.3.9. Influence of the ELMs in the impurity transport

Figure 3.10 shows the time traces of the Neon concentration inside the separatrix for an ELMy H-mode plasma for the three different deuterium gas puff levels which are compared with the correspondent runs without the ELMs. The Neon concentration inside separatrix is lower for the simulations where ELMs were included. Qualitatively this result is independent on the deuterium puff rate. The reason for fewer impurities in the plasma core for the ELMy H-mode in COCONUT (when compared with results from stand-alone JETTO/SANCO code[13]) and possibly in real experiments, is the fact that ELMs not only removes deuterium particles and energy from the ELM perturbation region inside separatrix but also from the main SOL to the wall and divertor target plates. The high deuterium flux to the divertor during the ELM drags the Neon particles also to the divertor region through the parallel friction force. While the energy is deposited and lost at the walls and divertor target plates the ionised impurity particles in the divertor region are not lost and return back to the main SOL. The time scale for the Neon particles going upstream is longer than the time scale of the atomic processes. A great number of Neon particles become neutralised and removed from the system through the cryogenic pump. Consequently there are fewer impurities in the whole plasma than in the ELM free H-mode plasmas. It is important to note that although the ELMs have a positive effect on the impurity removal, it only delays the radiative collapse in H-mode plasma with low deuterium puff rate.

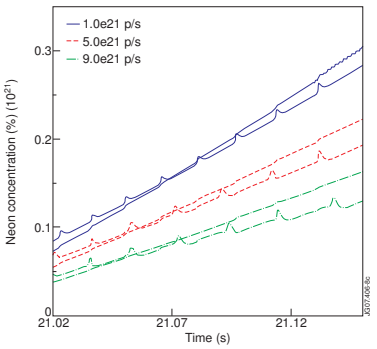

Figure 3.10 - Time evolution of the total Neon density inside the last closed flux surface for two deuterium puff rates of: a) 1×10^{21} p/s and b) 9×10^{21} p/s and with Neon puff rate of 6×10^{19} p/s.

3.3.10. Influence of the impurity concentration in the plasma core on the ELM frequency

It has been observed experimentally at JET that the ELM frequency decreases with the radiation levels for high triangularity and high density plasmas. To simulate this effect two sets of COCONUT simulations were done, using two different levels of impurity puff rate and for each set two runs with deuterium puff rates of 1×10^{21} particles/s and 9×10^{21} particles/s. The starting point of these COCONUT simulations was the end of the simulations previously described which were evolved for another 200 ms. In the first set the impurity puff rate was not changed while in the second set the Neon puff rate was increased from 6×10^{19} particles/s to 3×10^{20} particles/s. The deuterium flux across the last closed flux surface for these simulations are plotted in Figure 3.11a. This figure shows a clear decrease of the ELM frequency with the Neon puff rate. This figure also shows that the ELM frequency is the lowest for the highest deuterium and impurity puff rate, as observed in the experiment. Figure 3.11b shows clearly that the simulation with the highest radiated power within the ETB had the lowest ELM frequency. This simulation corresponds to the case with highest deuterium puff rate and the highest Neon puff rate.

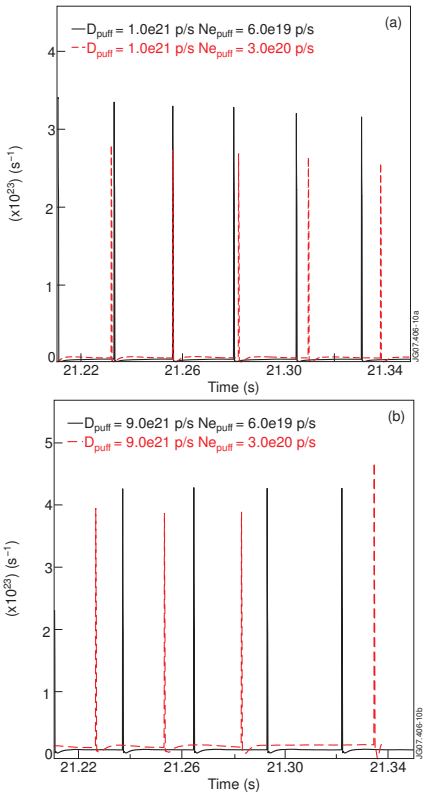

Figure 3.11 - Main ion flux through the last closed flux surface for two sets of runs with different Neon inlet level of 6×10^{19} p/s and 3×10^{20} p/s and with different deuterium puff rates of: a) 1×10^{21} p/s and b) 9×10^{21} p/s.

3.3.11. Fixed frequency and correlation reflectometer (KG8b) data analysis

Using the JET reflectometry fixed frequency systems coherent modes inside of the plasma column were detected. Figure 3.12 shows the identification of Alfvén Cascades (ACs) and Toroidal Alfvén Eigenmodes (TAEs) from the spectrograms of the phase perturbation in one of the fixed frequency channels (103 GHz) of KG8b reflectometer system.

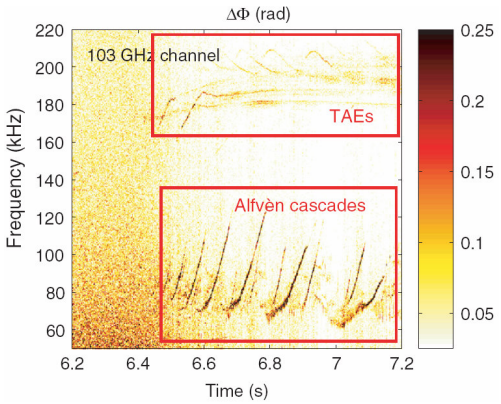

Figure 3.12 - Alfvén Cascades and Toroidal Alfvén Eigenmodes identified in the spectrogram of phase perturbation of the KG8b reflectometer[1] (channel 103 GHz).

Figure 3.13 permits to identify the Fishbone instability in the spectrogram of KG8b reflectometer (channel 85 GHz).

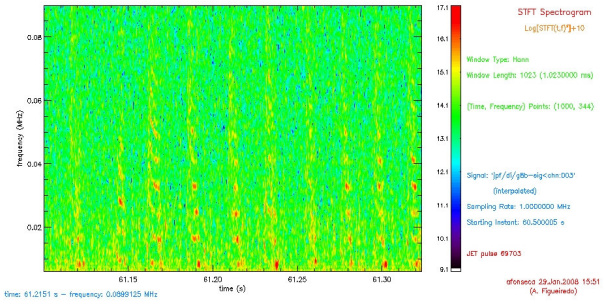

Figure 3.13 - Fishbone instability identified in the spectrogram of signal of the KG8b reflectometer (channel 103 GHz).

Figure 3.14 presents a spectrogram where is possible to identify the bi-TAEs from the signal of KG8b reflectometer (channel 62 GHz).

The Fishbone instability and Bi-directional TAEs have a lack of localization information and KG8b could give interesting information about that (like was recently obtained in the characterization of the ACs and TAEs).

The effect of the Lower hybrid Current Drive (LHCD) and low magnetic shear at large radii in transport barriers at high betaN of JET was observed in the KG8b reflectometry.

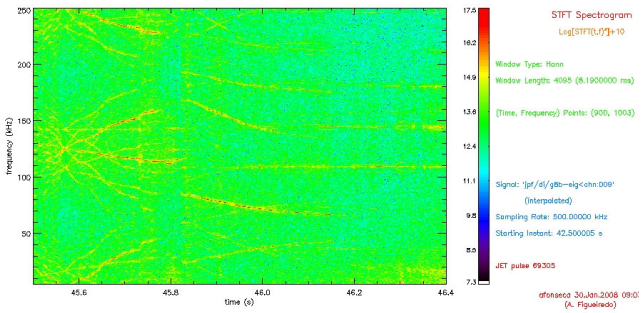

Figure 3.14 - Bi-directional TAEs identified in the spectrogram of signal of the KG8b reflectometer (channel 92 GHz).

3.3.12. Turbulence studies from radial correlation reflectometry in JET[14]

Radial correlation reflectometry can be used to estimate the radial scale of turbulence L from the variation of coherence with the radial separation between the cutoff positions of two distinct probing waves. JET correlation reflectometry diagnostic has four reflectometer systems, each one equipped with a fixed-frequency channel and a variable-frequency one, allowing measurements around four different radial positions. The formation of an ITB is accompanied by a reduction of the core turbulence, and a decrease of the turbulence correlation length in the region inside the ITB foot[15]. During JET pulse #69389, an ITB is formed between R = 3.49 m and R = 3.54 m. Figures 3.15 and 3.16 show the analysis of data collected by two reflectometer systems with fixed channels working at 103 GHz and 92 GHz, respectively, in two different measurements during this pulse. While the first measurement occurs before the ITB, the second one takes place during the ITB. For the 103 GHz system, which scans the region inside the ITB foot from R ≈ 3.42 m to R ≈ 3.535 m, a reduction from L = 1.14 cm to L = 0.43 cm can be observed between the two measurements, which might be associated with a reduction of the core turbulence. On the contrary, the cutoff positions of the 92 GHz system are located in the outboard region of the ITB from R ≈ 3.68 m to R ≈ 3.815 m, where no significant change occurs in the measured correlation length. In this case, the low L ≈ 1 mm values are consistent with higher turbulence levels, for which the coherent reflected power is low and the measured correlation length can be much smaller than the real one[16].

These results show a clear decrease of the radial correlation length in the region inside the ITB foot, which is compatible with a reduction of turbulence in the plasma core. The correlation length in the region outboard of the ITB remained unchanged by the ITB, which is consistent with the conclusion that turbulence in this region is unaffected by the formation of the ITB. These measurements point to correlation lengths with an order of magnitude of 1 cm in the plasma core of JET plasmas without ITBs, and half that value when ITBs are formed. More conclusive and quantitative results require theoretical and code modelling, which are essential to validate correlation reflectometry results.

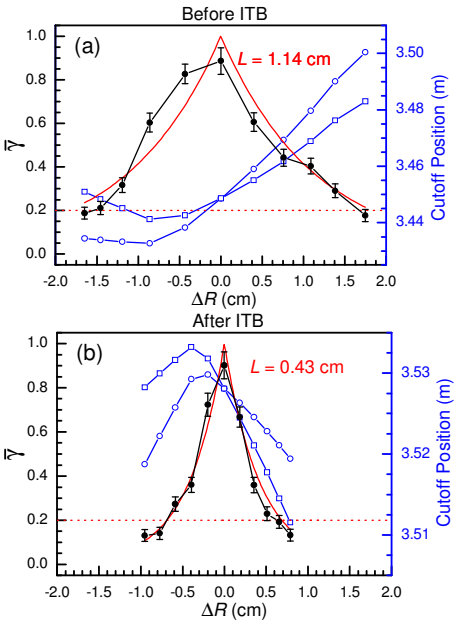

Figure 3.15 - Coherence analysis using reflectometer system 4 working at 103 GHz fixed frequency, showing a reduction of the correlation length L in the region inside the ITB foot. The first measurement (a) occurs before and the second (b) during the ITB.

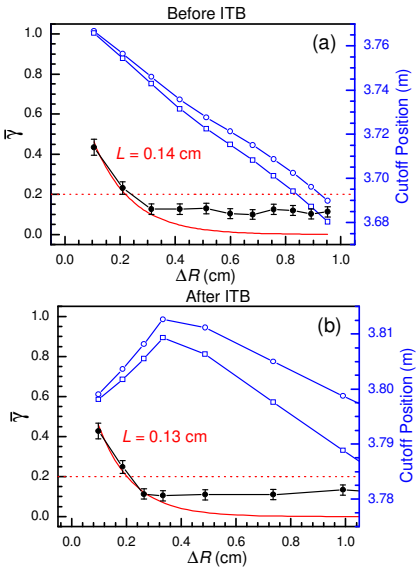

Figure 3.16 - Coherence analysis using reflectometer system 3 working at 92 GHz fixed frequency, showing no significant change in the correlation length L in the region outboard of the ITB. The first measurement (a) occurs before and the second (b) during the ITB.

[14]Work performed in collaboration with CEA, UKAEA and PPPL.
[15]G. D. Conway et al., Phys. Rev. Lett. 84, 1463 (2000).
[16]G. Leclert et al., Plasma Phys. Control. Fusion 48, 1389 (2006).

3.3.13. Sweeping frequency reflectometer (KG8a)

The KG8a reflectometry system is proof of principle diagnostic with one channel only aiming to demonstrate the capability of reflectometry to measure density profiles using complex and long transmission lines such as those implemented at the JET tokamak. After first experiments some problems of long propagation paths were revealed. Some modifications were made to ameliorate performance, including the installation of a new delay line and a new frequency calibration. The data evaluation program for profile inversion was also upgraded with optimized filtering and updated calibration. Figure 3.17 presents the schematic configuration of system.

During the last week of the 2007 campaign, high resolution density profiles from swept reflectometry were, for the first time, obtained at JET. In particular, the abrupt change of gradient due to ELMs could be detected. Figure 3.18 shows the edge density profiles from Reflectometry fitting the density data from Thomson scattering diagnostic in both L and H modes. After the promising results, JET decided to implement a swept reflectometry diagnostic with six channels.

3.3.14. Li Beam source characterization

The characterization of lithium beam after installation of a new emitter was performed. The lithium beam characteristics investigated after installation of new emitter showed the same double (Li-Na) structure of the beam, as it was with a previous emitter. This result confirmed a suggestion of not a proper procedure of the emitter preparation. HV tests and step-by-step training allowed increase of beam energy from 45 keV to 65 keV, thus sufficiently improving the diagnostic capabilities.

Analysis of the plasma density profiles de-convoluted with EFIT and EFTM equilibria showed approximately 1 cm inside shift of the profiles in high triangularity regimes in accordance with the shift of the magnetic surfaces.

A review of solid state and plasma ion sources used in lithium beam diagnostic has been completed and presented, pursuing the aim to analyze different concepts and possibilities to increase the intensity of lithium beam.

3.3.15. Motional Stark Effect signal processing

The Kalman filter has been proposed as an amplitude estimation method of known frequency components in quasi-periodic signals[17] (Figure 3.19). It was shown that it provides an improved filtering capability as well as the minimization of the Edge Localized Modes (ELMs) impact and 50 Hz power grid component when compared with the conventional lockin-amplifier signal processing for the Motional Stark Effect (MSE) diagnostic signals[18]. As a result, and aiming the implementation of an upgrade to the current real-time MSE system in JET, a C code has been developed for multi-component amplitude estimation of known frequencies in the MSE Avalanche Photo-Diode (APD) signals.

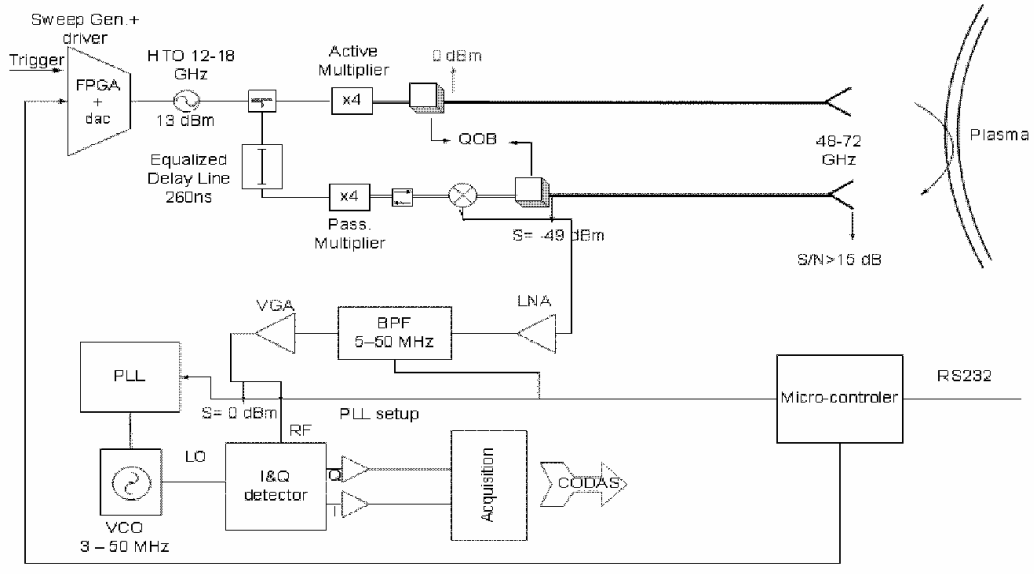

Figure 3.17 - Schematic implementation of the KG8a reflectometer after the implementation of the delay line.

[17]R. Coelho and D. Alves, "Real time Lock-in amplifier implementation using a Kalman filter for quasi-periodic signal processing in fusion plasma diagnostics", submitted to IEEE Transaction on Plasma Science (2008).
[18]R. Coelho, D. Alves and EFDA contributors, "Real-time Magnetic Field Pitch Angle Estimation with a Motional Stark Effect Diagnostic Using Kalman Filtering", International Conference on Burning Plasma Diagnostics, Varenna, Italy September 24 – 28, 2007, to appear in AIP Proceedings.

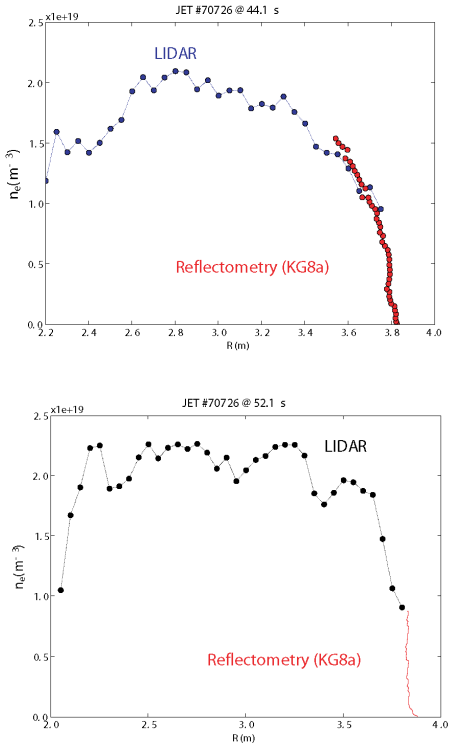

Figure 3.18 - Electronic density profiles by reflectometry and Thomson scattering both in L and H mode plasmas.

Predict measurement based on process model	Correct prediction with actual measurement
State variable: $\hat{x}_k^- = F\hat{x}_{k-1}$	$\hat{x}_k = \hat{x}_k^- + K_k\left(z_k - H\hat{x}_k^-\right)$ (Z_k = measurement at sample k)
Model: $F = \begin{bmatrix} F_1 & & & \\ & F_2 & & \\ & & \ddots & \\ & & & F_N \end{bmatrix}$, $F_i = \begin{bmatrix} \cos(\Delta\theta_i) & -\sin(\Delta\theta_i) \\ \sin(\Delta\theta_i) & \cos(\Delta\theta_i) \end{bmatrix}$, where: $\Delta\theta_i = 2\pi\omega_i / \omega_s$	The filter gain (K_k) minimizes: $\hat{P}_k = E\left[\left(x_k - \hat{x}_k\right)\left(x_k - \hat{x}_k\right)^T\right]$ in the least-square sense

Figure 3.19 – Predictor-Corrector Kalman estimator of known frequency components in a quasi-periodic signal.

The real-time amplitude estimation of selective harmonics from an Avalanche Photo Diode (APD) signal of a Motion Stark Effect diagnostic was addressed using the Kalman filter. The proposed technique was shown to be much more robust and provide less noisy estimates than a lock-in amplifier scheme. The negative impact of Edge Localised Modes (ELMs) on the data analysis is minimized, reducing significantly the biasing in the amplitude estimation and ultimately allowing for the pitch angle estimation in the vicinity of the ELM. The inherent biasing in the amplitude estimation due to the 50 Hz modulation in the NBI power grid is also easily circumvented with such a technique, rendering dispensable any further filtering of the data (Figure 3.20[19]). An extensive data validation/verification for the newly proposed Real-Time amplitude estimates was carried out at JET with other methods[20].

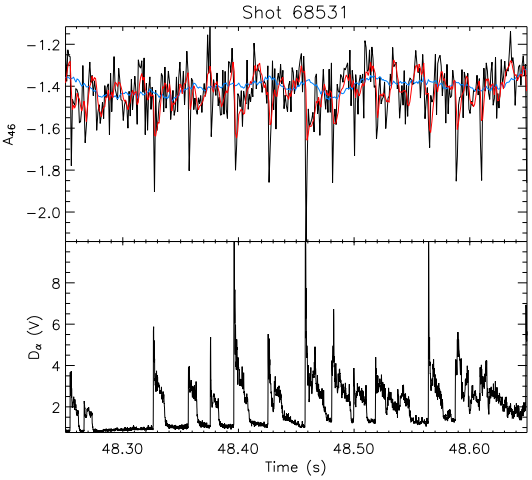

Figure 3.20 – Time evolution of the amplitude of the 46kHz harmonic of the APD signal from presently used RT system (black), using Kalman filter with no removal of ELM (red) and with joint removal of ELMs and 50Hz biasing (blue). The spikes in the D_α radiation signal (lower figure) provides a direct indication of the ELM onset. Shot 68531 and channel 18 were used.

3.3.16. ELM mitigation in JET H-alpha diagnostic signal using a Kalman filter

Preliminary attempts were done to mitigate the ELMs from the Bremsstrahlung signal in order for them not to disturb the Z-effective measurement. To achieve this goal, a Kalman filter DC estimator with peak detection and intelligent gain adjustment was implemented. Preliminary results are encouraging when comparing with another, routinely used, ELM removal code, Figure 3.21. Besides the dramatic improvement in the peak detection algorithm (notice how the conventional filter fails to detect some peaks), the Kalman filter approach provides a smoother, though still fast, convergence towards the original signals' baseline as the ELM vanishes. Furthermore, the latter scheme is inherently a real-time oriented method ready for providing, for example, a real-time ELM detector control signal.

3.3.17. Novel neural networks methods applied to the L-H transition

Two algorithms based on neural networks (NN) for the study of L-H transitions were developed. Both of the

[19]G. Leclert et al., Plasma Phys. Control. Fusion 48, 1389 (2006).
[20]A. C. A. Figueiredo, M. F. F. Nave, EFDA-JET Contributors, Nucl. Fusion 44, L17–L20 (2004).

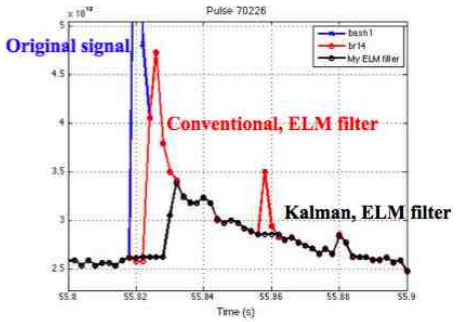

Figure 3.21 – Comparison of conventional and Kalman filter based ELM mitigation algorithm.

methods assume that some of the connections on a neural network are redundant ant their contribution to the overall result can be neglected. Once the NN has been trained, using one of the already well known methods, the algorithms are applied in order to try to simplify the network as much as possible. Using the simplified network one tries to extract an analytical expression which can describe the studied phenomena. This work was firstly tested in NN classic problems (like the XOR) and then applied to the L-H transition.

3.3.18. Real-time application interface applied to JET RT framework

The improvements and requirements to the existing real-time control libraries were addressed with the JET control group. A new working branch to the existing project was created allowing to integrate into the existing system, the support for a novel real-time operating system, named RTAI.

Extensive performance tests were performed on RTAI, mainly to assess if all the needed features were available, test the reliability of the system and confirm if the obtained latencies and jitters were acceptable. All results were extensively documented on the project Wiki page. A small conference with all the participating parties[21] was organized and this work was presented in two distinct oral presentations.

In order to allow the real time framework to be executed in kernel real-time mode, an high performance novel solution was developed, allowing to execute calculations in the kernel-space while having at the same time, access to all the user-space features, like networking and file system access (Figure 3.22).

Using the solution described before, the JET real-time control libraries were fully ported into RTAI. The system is still being commissioned, exploiting all the potentialities of the new multi-core computer technology, producing very encouraging results.

The system was also tested inside the new ATCA solution for the vertical stabilization and its performance is currently being commisioned with excellent results so far.

[21]UKAEA, IST and ENEA.

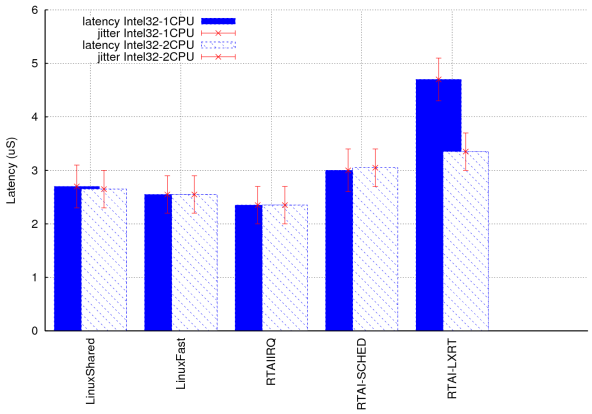

Figure 3.22 - Comparison between the Linux and RTAI schedulers, using one and two CPUs.

3.3.19. Rotation studies of JET discharges with low momentum input

3.3.19.1. Influence of toroidal field (TF) ripple in plasmas with ICRF heating

Parametric studies for discharges with 0% ripple confirmed that the core plasma rotation depends on the plasma current. Once the Ohmic intrinsic rotation was subtracted, we concluded that the ICRF induced rotation is mainly in the co-current direction. In the experiments to study rotation in ICRH plasmas with different levels of the TF ripple, charge exchange rotation data was not available. Information on rotation was therefore obtained from MHD mode analysis. In this case, NTMs indicated clear differences in the core rotation of plasma with 1.5% ripple, that was found to be counter rotating, while the reference plasmas without ripple were co-rotating (Figure 3.23).

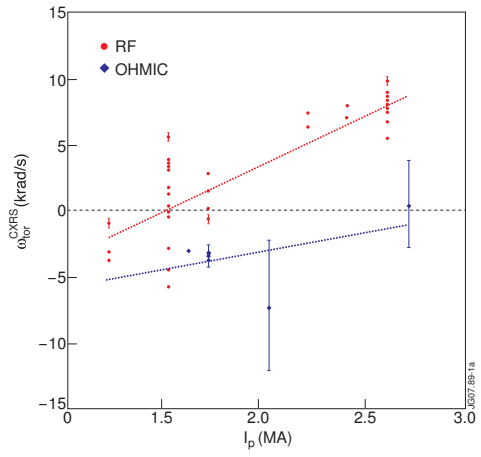

Figure 3.23 – Central Toroidal Angular Frequency from CXRS measurements vs Ip for ICRF (red) and Ohmic (blue) heated plasmas. Negative values indicate counter-rotation.

3.3.19.2. Study of sawtooth effects on core rotation of ICRF heated plasmas

JET experiments to investigate toroidal rotation in purely ICRF heated plasmas have shown both peaked and hollow rotation frequency profiles. The hollow profiles suggested that the core of some ICRH plasmas might be counter-rotating. These observed profile differences have been though to be associated to differences in MHD activity. At the low ICRH powers (P_{ICRH}<6 MW) used in these L-mode discharges the main MHD instability observed was sawtooth activity. In order to study the possible influence of core MHD instabilities on rotation profiles, discharges with and without sawtooth crashes (with q_0>1) were produced. These were either obtained by early X-point formation and RF heating applied before the plasma current was fully penetrated or in a few cases by application of 2 MW of Lower Hybrid Current Current Drive (LHCD). The range of central rotation frequency values (-6 krad/s to +10 krad/s) was found to be the same in discharges with or without sawtooth (Figure 3.24). In addition, no correlation was found between profile shape and sawtooth period.

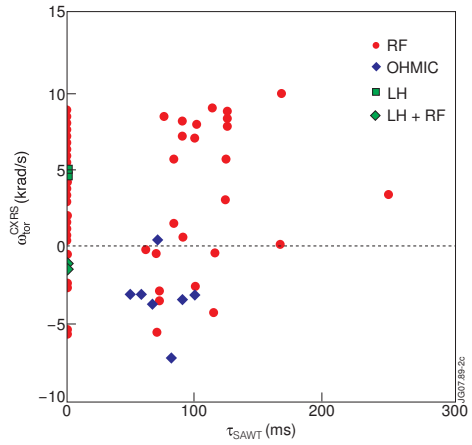

Figure 3.24 - Central rotation frequency as a function of sawtooth period. The range of central rotation frequency values (-6 krad/s to +10 krad/s) was the same in discharges with or without sawtooth.

3.3.20. Validation of EFIT equilibrium reconstruction using MHD mode analysis

MHD mode analysis and mode localization can be used to improve the accuracy of the reconstructed q-profile. In particular, AE cascades can be used to determine q_{min} in optimized shear discharges, while a variety of low frequency modes (such as sawteeth precursors, fishbones, NTMs and snakes) allow the determination of the radial position of q surfaces in monotonic and reversed shear q-profiles (Figure 3.25). In collaboration with the JET Core Spectroscopy Group, the q values determined from MHD analysis of a discharge with optimised shear were compared with EFIT q profiles obtained with different boundary conditions. Systematic runs of EFIT were done using magnetics, MSE, polarimeter and pressure data input in various combinations. Large discrepancies in the EFIT calculated q_{min} were found, depending on the choice of the EFIT input parameters. In particular, for EFIT runs with MSE data, the reconstructed q profiles depend strongly on how the data MSE data is fitted. Closely fitted MSE data delivers a significantly smaller qmin than what's indicated by the MHD events (Figure 3.26). The independent q measurements from mhd analysis indicated the best combination of input choices to run EFIT for this particular discharge. The best agreement with MHD data was obtained when EFIT was run with MSE, pressure and polarimeter data constrains. It is recommended to add q value constrains into the JET version of the EFIT code.

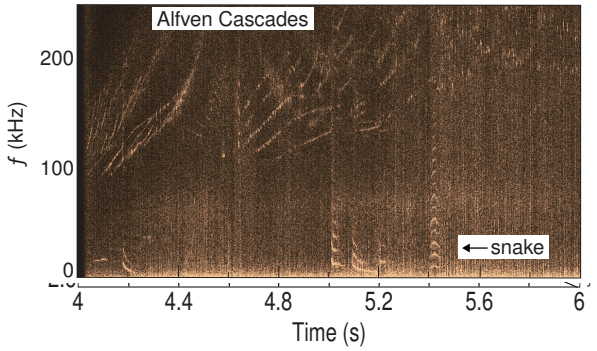

Figure 3.25 - Spectrogram from microwave interferometer signal showing Alfven cascades and snake-like modes that give information about the value of q_{min} and about the position of the q=3 surface respectively.

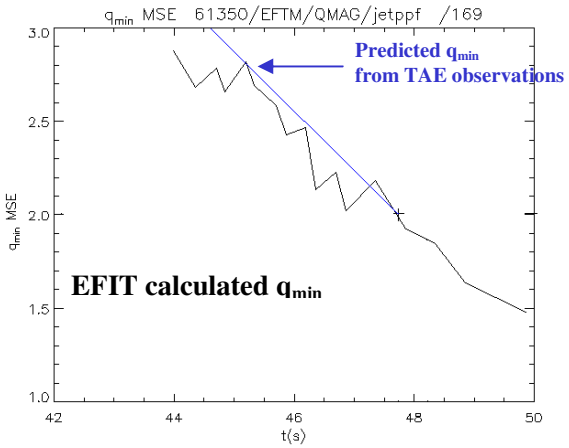

Figure 3.26 - Temporal evolution of q_{min} in agreement within 10% with estimated value from TAE cascades, obtained when EFIT was run with MSE, pressure and polarimeter data constrains.

3.3.21. Integration of MHD and transport codes

3.3.21.1.Implementation of sawtooth models into the transport code JETTO:

Two new features were implemented and tested in the transport code JETTO. First the sawtooth package has been extended to include Porcelli´s model of partial reconnection, second the reconnection models have been

linked to the code PION to provide redistribution of fast ions at a sawtooth crash. In the new JETTO version the effect of a sawtooth crash on the plasma profiles can be treated either as in Kadomtsev theory for magnetic flux reconnection or as in Porcelli's model for partial reconnection. Following a sawtooth crash, the q-profile and plasma profiles (density and temperature of H ions, density of impurities and toroidal momentum) and fast ion distribution profiles are modified inside a mixing radius, calculated by the code, depending on the model used. In the Kadomtsev reconnection model a nearly flat q profile is obtained within the mixing region. The q profile after the crash has $q(0)=1$ and $q'(x)>0$ with $q(x)>1$ for $0<x\le x_{mix}$. Partial reconnection is simulated using an empirical model. Profiles after a sawtooth crash are a weighted average of the profile immediately before the crash and the full reconnection profile after the crash, such that: $q(x)^{after\_crash} = fq(x)^{Kadomtsev} + (1+f)q(x)^{before\_crash}$ where the input parameter f=1-0 is the reconnection fraction. In the Porcelli's partial reconnection model, (Figure 3.27) plasma mixing occurs in two separate regions: an island around the q=1 surface, and an axial region enclosed by the island where a Taylor relation is assumed. The inner boundary of the island, x_{min}, is a free parameter specified by the user. The q profile after the sawtooth crash becomes a two-step function: In the island region, $q^{after\_crash}(x)=1$. While in the inner, axial, region, $q^{after\_crash}(x)=q^{before\_crash}(x_{min})$. In the Porcelli model, the mixing radius is determined by the condition $\psi(x_{mix})=\psi(x_{min})$, while in the Kadomtsev model, $\psi(x_{mix})=\psi(0)$.

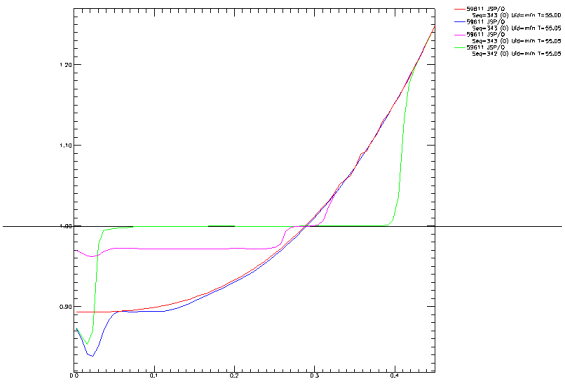

Figure 3.27 - q profiles before (red) and after a sawtooth crash using Porcelli's Partial Reconnection model. Plasma mixing occurs in two separate regions: an island around the q=1 surface, with the inner boundary of the island specified by the user as $x_{min} = (1-f)*x_{q_1}$ *and, an axial region enclosed by the island.*

3.3.21.2. Verification, validation and benchmark of ELM modules in the code JETTO

The ELM models coded in JETTO have continued to be tested for a wide range of input parameters. Several JETTO runs were performed scanning input options in the Simple ELM model and in the MHD Theory Based model. ELMs were assumed triggered by either pressure-driven ballooning modes or current driven peeling modes. The edge stability of H-modes with ELMs was tested in a wide range of pedestal current density values. Simulations were done for a typical high-density ELMy H-mode discharge, a low density quiescent H-mode discharge and an ITER-like plasma. JETTO ELM triggering calculations for the cases with large pedestal bootstrap currents were benchmarked with stability calculations for the n=1 peeling mode from the MHD code MISHKA.

3.4. PERFORMANCE ENHANCEMENTS

3.4.1. Introduction

The Association EURATOM/IST has been involved in several tasks carried out in the frame of the second stage of the JET Enhancement Projects (EP-2):

- Fast Wave Reflectometer (FWR) – Phase I: conceptual and pre-engineering designs;
- Plasma Control Upgrade – Vertical Stabilisation Controller project (PCU-VS);
- Data Acquisition for the Gamma Camera Diagnostics enhancements (DNG);
- Data Acquisition for the Gamma Ray Spectrometry (GRS);
- Real-Time Measurement (RTM) and Control Diagnostics and Infrastructure

IST has provided the project leader for the FWR, DNG and RTM Projects

3.4.2. Fast Wave Reflectometer[22]

IST finished in 2007 the pre-engineering of all in-vessel design. Following a successful conceptual design, detailed in-vessel and ex-vessel designs were made and simulations studies predicted a good diagnostic performance. The diagnostic proposal presented at CSU-Culham had a very positive assessment and the relevance of the diagnostic both for JET and ITER was recognized. However, it was considered the routine results were difficult to obtain in the short term, as they require input data from other diagnostics, namely the magnetic equilibrium and density profiles, and for that reason the diagnostic was not considered a priority for JET and project phase II was not approved.

3.4.3. Plasma Vertical Stabilization Controller project[23]

This project is a major enhancement of the JET-EFDA Vertical Stabilisation system with the objective of doubling the survivable ELM size in JET operation and also to validate the vertical stabilisation systems for

[22]Luis Cupido is the Project Leader.
[23]Jorge Sousa is the IST Main Researcher.

ITER. IST is involved on Task 2, which studies and will implement the new VS controller in terms of both software and hardware. The new VS controller will increase the processing power, decrease the control loop delay and allow the processor direct access to individual sensors.
The following tasks were performed in 2007:

- Design and implementation of prototype of a control card with 32 galvanic isolated ADC channels sampling at 2 MSPS@18-bit, 4 channel DAC and 8 channel I/O board dedicated to fast MIMO control;
- Implementation of a testbench for hardware emulation and code testing before the prototype availability. The code was developed for implementing/testing the PCIe interface, DMA transfer mode, and interrupt handling;
- Development of the prototype FPGA code and the host computer drivers/API;
- Production of the required boards including the ATCA controller and the PSU RTM board, assembling of the complete ATCA system and electronics tests in laboratory (Figure 3.28);
- Delivery to JET of an ATCA controller for evaluation and software development;
- Development at JET of the real-time framework interfaces, multi-processor support, and control library porting to Linux.

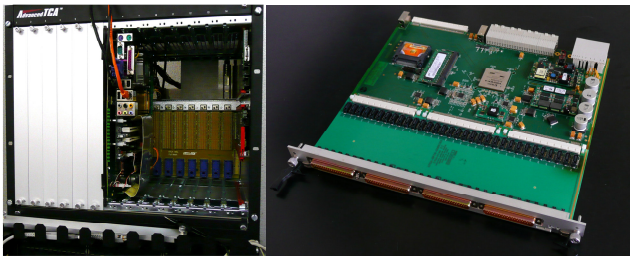

Figure 3.28 - Vertical Stabilization Controller prototypes.

3.4.4. DNG and GRS diagnostics

In the last years gamma ray spectrometry has provided new insight into the physics of fast ions in JET. Present count rate limitations at JET are due, in part, to the obsolete electronics modules used for signal processing and DAQ. A fully digitized DAQ is being designed by IST for the DNG and GRS projects, allowing count-rate improvement beyond 500 kHz (targeting 2 MHz) almost without pile-up losses and providing also on-system high-speed gamma-ray spectroscopy functions to reduce the amount of data to CODAS accepted levels while simultaneously extending the acquisition time.
The following tasks were performed in 2007:

- Design, implementation and test of a prototype of a 400 MSPS, 14-bit, 8-channel transient recorder board (Figure 3.29);

Figure 3.29 – Spectroscopy data acquisition prototypes.

- Started the production of the final prototype with the required corrections;
- Development of computer drivers/API and the CODAS interface;
- Development and test of the FPGA firmware code including: PCIe/DDR2 memory interface; acquisition block and data path to memory and PCIe host;
- Development of algorithms for Pulse Height Analysis (PHA) and Pulse Shape Discrimination (PSD) for FPGA[24] processors applied to digitized pulses.

3.4.5. Real-Time Measurement & Control Diagnostics & Infrastructure[25]

The essential aim of this project is to expand JET real-time diagnostics and control capabilities required to fulfill the programmed objectives of JET in the proposed FP7 phase of operation dedicated to the preparation of ITER. The following tasks were developed:

- Collaboration with JET/EFDA CSU plasma control Coordinators in the assessment of the requirements in real-time data interfaces, data rates and latencies in other JET EP2 Projects and to evaluate the actual limits of the present JET current RT Network (ATM);
- Identification, evaluation and selection of best candidates, among current fast switch fabric based interconnect communication technologies that can prove to enhance the performance of real-time plasma digital control systems;
- Identification of testing methodologies for evaluation and benchmarking of real-time network standards and protocols;
- Assessment, documentation and planning of other sub-stasks integrated in this EP2 Project (KG1 Interferometer Diagnostic Upgrade, KN1/KH1/KM7 Basic Neutron Diagnostics Upgrade, and EQUINOX upgrade).

[24] Field Programmable Gate Arrays.
[25] Bernardo Brotas de Carvalho is the Project Leader.

3.5. MANAGEMENT

The Association EURATOM-IST has collaborated on the management of the use of the JET Facilities by the EFDA Associates as follows: (i) one scientist at the Close Support Unit team, as Head of Office for the EFDA Associate Leader for JET[26] until 31st August 2007; (ii) one as deputy TFL for TFD since July 2007[27]; and (iii) two[28] have integrated the Remote Participation Users Group.

[26] Duarte Borba
[27] Bruno Gonçalves
[28] Horácio Fernandes and Paulo Varela

4. PARTICIPATION IN THE ITER PROJECT[1]

C.A.F. Varandas (Head), M.E. Manso (Deputy Head), L. Cupido, H. Fernandes, F. Serra, A. Silva, P. Varela, A. Ferreira, J. Santos

4.1. INTRODUCTION

This project included in 2007 scientific work on microwave reflectometry, control and data acquisition and quality assurance, as well as activities for the promotion of ITER to the Portuguese firms and research units.

4.2. MICROWAVE REFLECTOMETRY

4.2.1. Introduction

IST/CFN has carried out activities related with the conceptual study of the plasma position reflectometer and the development of a prototype of an advanced reflectometer.

4.2.2. Plasma position reflectometer

A first draft of the Project Plan was submitted on November and the Project Plan status was presented in December, during a Project Pleaders Meeting (PLM) organized by EFDA. Currently, the Draft Project Plan is being revised according to the suggestions that arise from the PLM so that a new version can be submitted early 2008. The full cost of the procurement package, including resources, is being evaluated.

The following sub- tasks were also performed by CFN in 2007:

- Study of three possible solutions for the diagnostic localization;
- Simulation of the routing of the oversized waveguides from the PIT cell to the diagnostic RF hall.

4.2.2.1. Electronics location

The ex-vessel waveguide routing is closely related with the location of the mm-wave front-end and associated electronics. Three different possibilities are currently being envisaged: (i) all equipment in the pit cell (PC); (ii) all equipment in the Diagnostic Hall (DH) and/or Assembly/RF Hall (RFH); and (iii) the mm-wave front-end in the PC and the associated electronics in the DH/RFH.

Each of the solutions for the mm-wave/electronics location discussed above presents advantages, disadvantages, and implementation problems. Therefore, we prefer to keep all options open deferring the choice of a particular solution to a later time when the designs are more advanced and/or more information about each location is available. Because it involves the largest number of interfaces with the tokamak building and its surroundings we started by routing the waveguides for the case where the mm-wave front-end and electronics are located away from the port cells, in the diagnostic hall and/or in the RF hall. To prevent and help to identify possible clashes with other diagnostics, the space occupied by the cubicles that would contain the mm-wave front-end and electronics has been modeled (by solid parallelepipeds) in CATIA. This has been done for all possible locations. Figure 4.1 shows the ex-vessel waveguide routing for gaps 4, 5 and 6.

4.2.2.2. Development of a solution for a frequency combiner/de-combiner

Independently of the final choice for the electronics location, it is foreseen the use of three frequency bands (K, Ka, and U) to cover the desired frequency range (15 – 60 GHz). These bands must be combined in a single waveguide before being tapered to rectangular or circular waveguide. On the receiver side, a de-combiner should be used to separate the three bands.

4.2.2.3. Directional coupler solution

Figures 4.2 and 4.3 show a three-band combiner that uses a multihole directional coupler and the corresponding de-combiner setup. Testing of a four port multihole power splitter to combine the K and Ka bands into a single WR51 waveguide has led to excellent results. The coupling to each output port is 4.8 dB down in respect to the output port. Directivity is greater than 40 dB. Tests must now be done in the upper band 40 to 60 GHz to fully validate this solution.

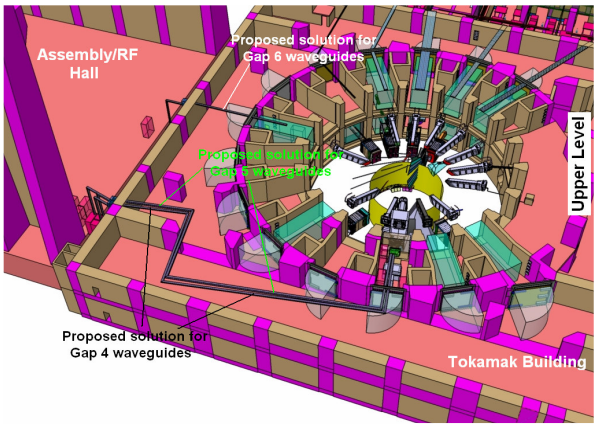

Figure 4.1 - Proposed ex-vessel waveguide routings for gaps 4, 5, and 6.

[1]Activities carried out in the frame of the Contract of Association EURATOM/IST and the Contract of Associated Laboratory, by CFN staff of the Experimental Physics, Microwave Diagnostics and Control and Data Acquisition Groups.

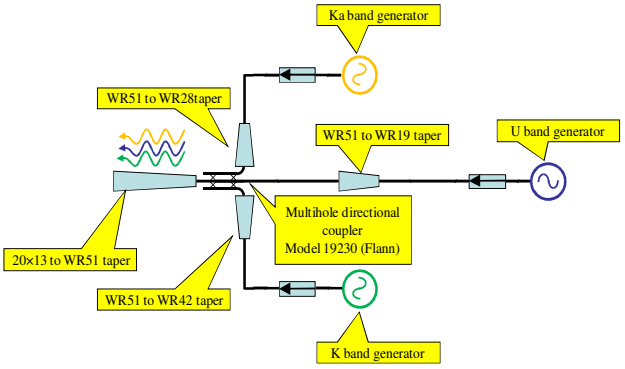

Figure 4.2 - Combiner setup using a multihole directional coupler model 19230 from FLANN.

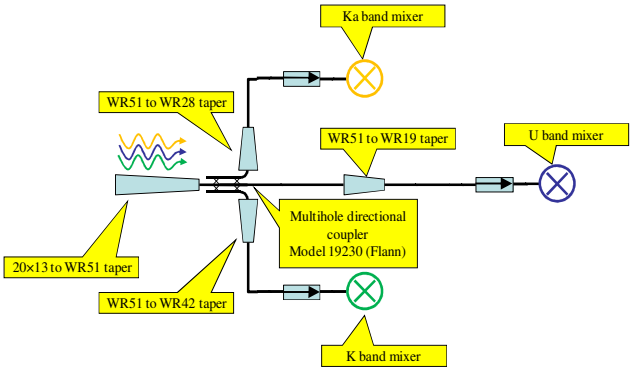

Figure 4.3 - De-combiner setup using the same multihole directional coupler.

4.2.2.4. Design of a taper to simulate the coupling of the standard WR51 waveguide to the 20x12 mm waveguide

The waves must be coupled to the non-standard waveguides installed inside the vessel by using a tapered transition from a standard waveguide band. Due to the minimal frequency of 15 GHz we propose to use the WR51 waveguide with internal dimensions of 6.48x13 mm. This almost matches the 12 mm of the in-vessel waveguide. Instead of designing a complicated taper with tapering in both dimensions we'll make a proposal to increase the dimension of the in-vessel waveguide from 20x12 mm to 20x13 mm. This should not have big implications in the overall design besides a small increase of the antennas gain.

Our approach was to design a linear taper with the size of 10 wavelengths for the minimal frequency. In the model used on HFSS (Figure 4.4.), two symmetry plans were used (perfect E and perfect H) to speed up the simulations by reducing the model size and consequently CPU and memory consumption.

The taper performance was evaluated using HFSS and the results are presented in Figure 4.5, showing insertion losses below 0.06 db and return losses smaller than -38dB in the frequency range 15 to 60 GHz. The increase of the oscillations at high frequencies in the return loss curve is linked to simulation "noise".

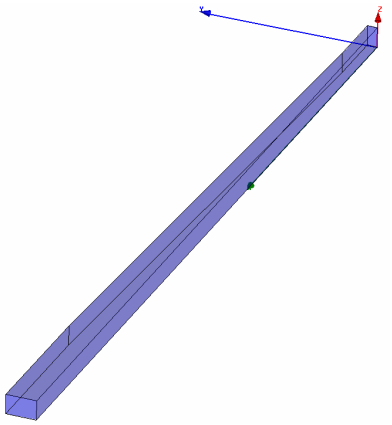

Figure 4.4 - HFSS model used to simulate the electromagnetic performance of the WR51 to 20x13 mm taper. Two symmetry plans were used (perfect E and perfect H) to speed up the simulations by reducing the model size and consequently CPU and memory consumption.

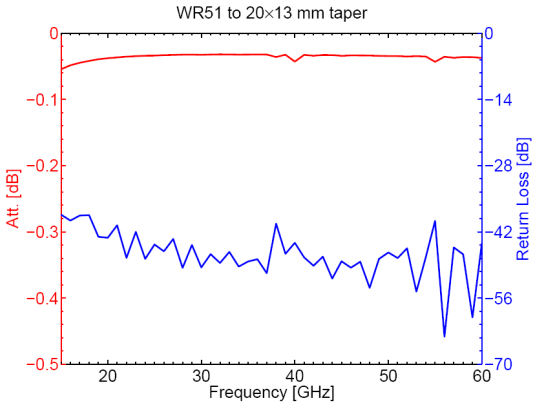

Figure 4.5 – Electromagnetic performance of the WR51 to 20x13 mm taper: attenuation (red trace) and return loss (blue trace).

4.2.2.5. Simulation of critical bends and their optimization using an electromagnetic code

HFSS has been used to evaluate the electromagnetic performance of critical components of the in-vessel transmission lines, namely the so-called first bends which connect the emission/reception antennas to the waveguides. Two types of bends have been simulated: constant radius bend and hyperbolic secant bend. For the later, simulations were performed for two different values of the equivalent radius: 72 and 120 mm. Results show that the hyperbolic secant bends have better performance than constant radius bends. Results also show that the performance is better for smoother curves.

4.2.2.6. Simulations of broad band swept reflectometry experiments

Reflectometry at ITER presents unusual challenges not faced in present day machines. Apart from the harsh environment surrounding the diagnostics, the need of oversized waveguides, which also has to act as antennas, their insertion within a gap in the blanket module and the proximity of the antennas to the very steep edge plasmas, create a strong potential for spurious mode excitation as well as for resonances and multi-reflections. In the case of GAP 5, the scenario is even more acute since the plasma will most likely not be probed perpendicularly to the iso-density surfaces. Those surfaces in addition exhibit a poloidal spatial divergence plus curvature, which are most adverse conditions for profile measurements. In a first approach simulations were performed not including the blanket, the curvature, MHD modes or turbulence. The results showed that the effect of the electronic density poloidal divergence can be tolerated except for extreme values of divergence that will seldom occur. First simulations including the blanket, however, indicate that that the blanket metallic structure induces a high level of multi-reflections. This study will be pursuit in 2008.

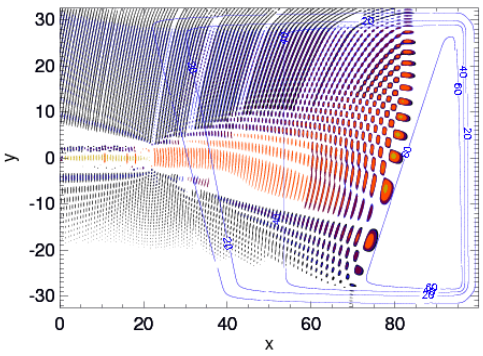

Figure 4.6 - Electromagnetic field snap-shot showing a plasma with electronic density poloidal divergence being probed at 60 GHz.

4.2.3. Prototype of an advanced reflectometer

The development of a new generation of swept reflectometers capable to cope with the long and complex transmission for JET and ITER was pursued. The studies and simulations for the generator section of a full coherent reflectometry system have been performed some laboratorial tests and partial prototypes were produced. The project underlying technique is now mature enough to be implemented in a diagnostic to be implemented at a large fusion machine.

4.3. CONTROL AND DATA ACQUISITION

4.3.1. Introduction

The activities on control and data acquisition were in 2007 related with the conceptual design of dedicated systems for two ITER diagnostics, the equatorial visible/infra-red wide angle viewing system and the core-plasma LIDAR Thomson scattering system, and the participation in the European Ad-Hoc Group that is following the ITER CODAC activities.

4.3.2. ITER Equatorial Visible / IR Wide Angle Viewing system[2]

The amount of data provided by the infra-red and visible cameras at ITER is expected to be considerably larger in respect to other diagnostics. ITER will have twelve infra-red cameras plus twelve visible cameras in four different equatorial port plugs. One of the key functions of these cameras will be the protection of the first wall, thereby is considered a particular diagnostic where direct connections to the Central Interlock System are required.

In 2007 CFN developed a full specification following the ITER CODAC guidelines.

This specification, presented in three reports, covered the camera specifications, data collection and compression, image processing, internal state machine, communication with CODAC and a proposal for a prototype (Figure 4.7).

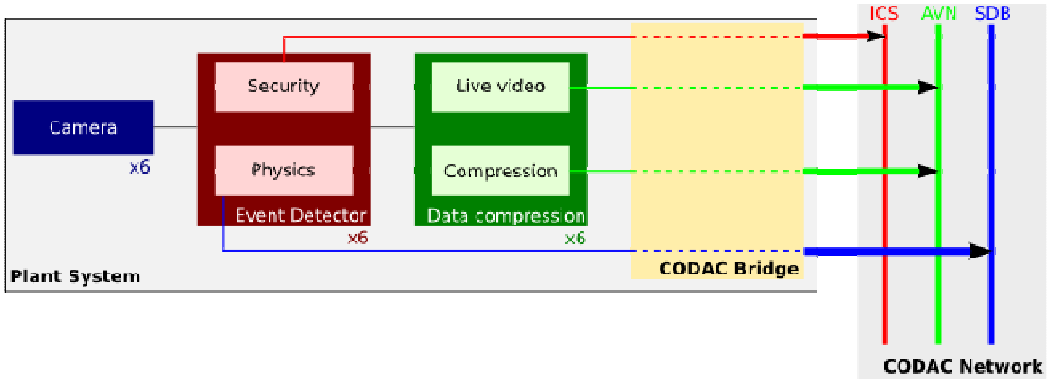

Figure 4.7 - Block diagram of the PP11 CODAC sub-system.

[2]Task TW6-TPDS-DIADES-PP11.

4.3.3. Core-plasma LIDAR

The following tasks were performed in 2007 regarding the local CODAC sub-system design for the core-plasma LIDAR (Figure 4.8):

- Contribution to the project plan of the data acquisition CODAC interfacing and local control systems for the ITER core-plasma LIDAR Thomson scattering diagnostic;
- Elaboration of the Intermediate Report on the Interfaces and Control system of the ITER core-plasma LIDAR.

4.4. QUALITY ASSURANCE[3,4]

IST is participating in the development of the (QA) system for the ITER EU domestic agency and implementation of a Quality Assurance Programme in the European Fusion Associations for ITER-relevant activities (contract FU06-CT-2006-00405)[5]. The main responsibilities of IST in this task were:

- *Report on the level 3 documentation.* The initial set of Level 3 documents (typically standards and rules) have been identified, which can be used for the initial procurements. To facilitate the access, the documents were compiled in a MS Access database that is part of this deliverable;
- *Report on the implementation of quality provisions showing the practical application of the proposed principles of QA and the analysis of the problems encountered during the implementation.* A draft quality management system for F4E has been prepared in order to comply with the ITER Quality Programme. CEA and IST have implemented quality provisions in two on going R&D EFDA tasks.

In parallel, CFN has started the preliminary studies for the implementation of QA procedures in our own activities.

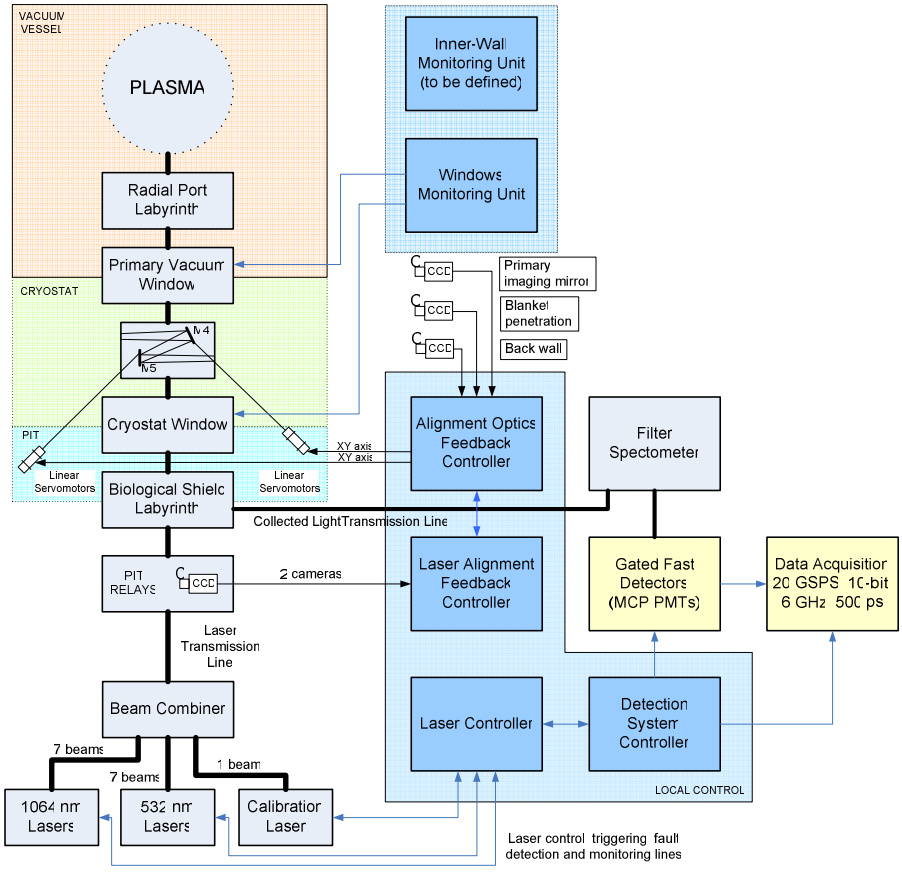

Figure 4.8 - Interfaces and Control system of the ITER core-plasma LIDAR.

[3]Task TW6-TDS-QA2.
[4]Work in collaboration with "Instituto de Soldadura e Qualidade".
[5]Work in collaboration with the Association EURATOM/CEA.

5. PARTICIPATION IN THE ASDEX UPGRADE PROGRAMME[1]

M.E. Manso (Head), F. Serra (Deputy Head), D. Borba, R. Coelho, L. Cupido, L. Fattorini, S. Hacquin, I. Nunes, T. Ribeiro, F. Salzedas, A. Silva, F. Silva, P. Varela, A. Combo, A. Ferreira, S. Graça, L. Guimarães, L. Meneses, J. Santos.

5.1. INTRODUCTION

This project included in 2007 activities related with the development, modelling and scientific exploitation of microwave reflectometry system as well as plasma physics studies on transport and MHD.

5.2. MICROWAVE REFLECTOMETRY

5.2.1. Introduction

The two hopping systems developed by CFN with improved sensitivity and enlarged measuring capability due to the frequency hopping set-up for each plasma discharge were fully operational in 2007.

The swept FMCW profile reflectometer system, however, was not in operation during the 2007 campaign due to renovation of waveguides and the installation of isolation shutters for protection against ECHR radiation after the recent upgrades and modifications in the ECRH system. An alternative bistatic transmission line for the broadband reflectometry system has been investigated and design studies are in progress. A proposal for a new system has been performed and will be presented in 2008. In order to increase the capability of profiles from FM-CW systems, a new PCI data acquisition system is being developed.

5.2.2. Hardware developments

5.2.2.1. Microwave circuits and systems

Protection switches for the electronics of the FM-CW diagnostic were installed except for the two channels Q and V bands operating in X mode. However, the critical in-vessel directional couplers cannot be protected and a new system must be considered to measure density profiles from swept reflectometry on ASDEX Upgrade.

The outer and in vessel access for the implementation of a microwave broadband transmission line at a different location for a possible new FM CW reflectometry system using a bi-static arrangement (avoiding critical in-vessel components) was investigated. It was found that no possibility exist to implement a new system neither at the HFS or LFS.

It was studied an inboard launch at the High Field Side at the same location of the present system that would permit to probe the plasma from the edge to the core operating in lower cutoff – X mode. This would in addition be an ITER relevant demonstration not possible to test in any other fusion device. The study of electromagnetic access is presented in Figure 5.1.

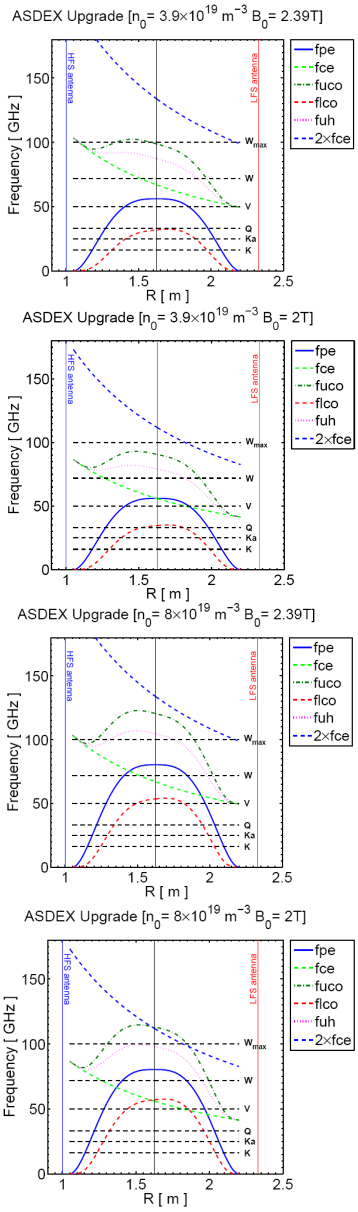

Figure 5.1 - Study of the electromagnetic access of probing microwaves to the ASDEX Upgrade plasma using O and X mode waves from both the HFS and LFS.

[1]Activities carried out in the frame of the Contract of Association EURATOM/IST and the Contract of Associated Laboratory, by CFN staff of the Microwave Diagnostics, Theory and Modelling and Control and Data Acquisition Groups, in collaboration with the ASDEX-Upgrade Team. Contact Person: G. Conway

5.2.2.2. Control and data acquisition

A new PCI data acquisition system able to increase significantly the density profile measuring capability of the FM-CW system is being developed. A 2-channel Transient Recorder prototype was developed, constructed and tested. The control software structure and development tools were assessed and specified. The development of the DSP software, PCI Waveform Generator and its firmware were initiated.

5.2.3. Data analysis

5.2.3.1. Density profiles

Software development has proceeded with new algorithms for the automatic analysis of the edge pedestal characteristics directly from the group delay. An investigation of magnetic ripple effects on the inversion of X-mode data will be used to improve the density profile reconstruction accuracy, in particular at the plasma outer edge and SOL. It was initiated the study of a new density profile inversion technique using algorithms based on Bayesian analysis[2].

5.2.3.2 Real time density profiles

Validation studies of the real-time reconstruction procedure for fast plasma position monitoring using neural networks were completed. Using a highly optimized code on a dual core 2 GHz Intel CPU the separatrix position in ELMy H-mode discharges could be tracked with a <1 cm resolution and a 10 ms repetition, thus meeting the ITER requirements. A demonstration of a real-time radial position control system is planned for the 2008 campaign using a fast dedicated acquisition system. At the moment several configurations using in-house available/developed technologies (both at IPP and CFN) are under consideration.

An highly optimized multithreaded calculation code was implemented to reconstruct the profiles from the binary acquired samples up to the final profile. This code was benchmarked in a dual core 2 GHz Intel CPU. The inversion of a density profile (up to n_e=3x10^{19} m^{-3}) using data from bands K, Ka and Q, acquired in a burst of four sweeps taken every 35 us, took < 400 µs (Figure 5.2). With the use of faster quad-core processors ~200-250 µs profile reconstruction cycles are expected to be achieved using the four probing bands K, Ka, Q and V (profiles up to ne=6x10^{19} m^{-3}) and 4 sweep/burst measurements. This code was tested using AUG experimental data showing good separatrix position tracking capabilities, as had been achieved and demonstrated in the referred studies using the standard supervised methods.

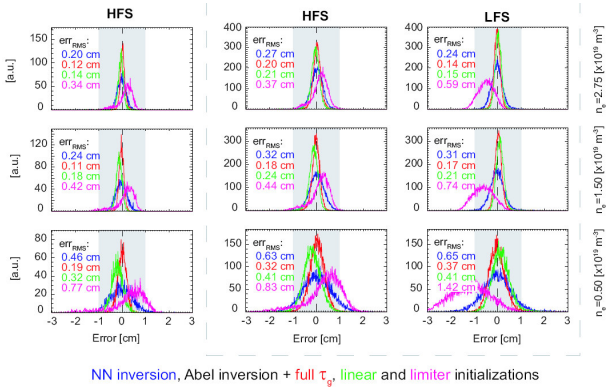

Figure 5.2 - Positions error histograms of the reconstruction of a test dataset perturbed by an high amplitude level of density fluctuations (9% of n_{e_sep}) with a NN and the Abel inversion with various initializations (limiter = standard / experimental initialization).

5.2.3.3. Upgrade of the reflectometer acquisition system to real-time capability

The demonstration of the application of reflectometry for control purposes in AUG requires the adaptation of the existing diagnostic. This upgrade will make the system compatible with an integration in the real-time (RT) AUG diagnostic network. At the same time, it must have a minimal impact in the present diagnostic operation and configuration. Since dedicated acquisition systems are required to achieve real-time compatible on-line data transfer rates to the data processing host, a new such system needs to be built. At the moment several configurations using in-house available/developed technologies (at IPP and CFN) are under consideration. A fast data acquisition front-end needs to be developed to be connected to the processing host using an optical link connection based either on Hot-Link/cPCIe (IPP), depicted in Figure 5.3, or RocketIO/ATCA (CFN) technologies. In any case, the data collecting board should provide very fast data transfer speeds to the main memory of the data processing host. A standard dual quad-core workstation/server, featuring PCIe slots (4x, 8x) and running a RT Linux variant, is thought to be adequate to produce the target measurements in a theoretical 1 ms cycle. The ultimate goal is to produce HFS and LFS edge density profiles in the fastest AUG RT cycle (1.6 ms[3], possibly 1 ms[4]), which would make the measurements compatible with the plasma performance feedback control timing, and would allow multiple profile measurements to be made on the timescale of the magnetic feedback control for plasma vertical and radial position (10 ms) and plasma shape (100 ms)[5].

[2]Work in collaboration with Dr. Rainer Fisher (IPP).
[3]G. Raupp *et al*., Fusion Eng. Design 81, 1747 (2006).
[4]W. Treutterer, 6th IAEA TM on Control Data Acquisition and Remote Participation on Fusion Research, 2007, Japan.
[5]G. Raupp *et al*., Fusion Eng. Design 74, 697 (2005).

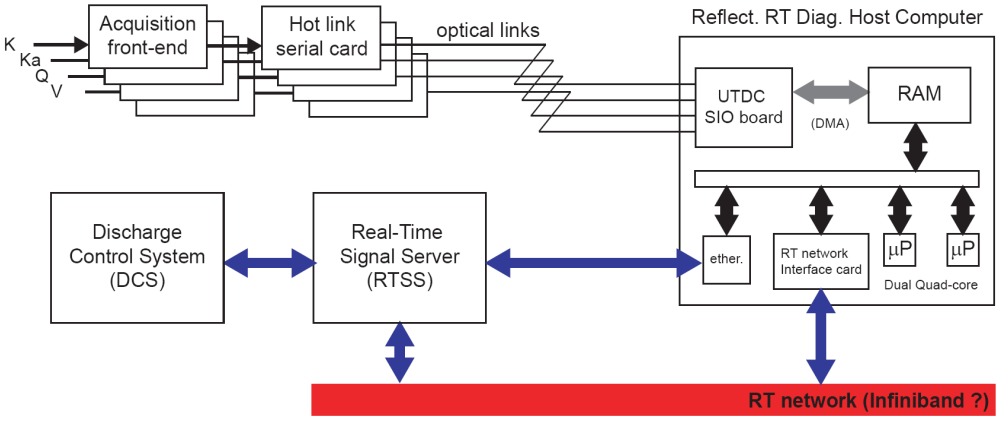

Figure 5.3 - Simplified schematic of the proposed solution (IPP tech. variant).

5.3. PLASMA PHYSICS STUDIES

5.3.1.Density Fluctuation/mode analysis

The fast hopping reflectometers were fully operational during the complete 2007 campaign. However, due to the break of EZ4 generator the campaign was postponed to May 2007 and the plasma scenarios were limited. The full tungsten machine program without boronization that was in place during the all campaign was not adequate for fast particle experiments and the relevant scenario was difficult to achieve. Nevertheless, discharges from earlier campaigns were analyzed.

Further progress has been made in the study of fast particle and MHD modes. The radial eigenfunction of an n = 4 TAE (Toroidal Alfvén Eigenmode) was measured using the fast frequency hopping reflectometers. A phase and coherence analysis was used to estimate the radial displacement and density fluctuation level profiles from which the amplitude and sign of the radial eigenfunction are deduced. A comparison with CASTOR and LIGKA simulation codes shows excellent agreement. MHD modes (Washboard type) at the L to H-mode transition have been investigated. Parameter dependence and radial structure studies are currently in progress.

5.3.1.1. Alfvén eigenmodes

Figure 5.4a shows the phase spectrum and the radial profile of δφ(f) for the n=4 TAE mode (solid line) for the shot #21007. The horizontal error bars indicate the uncertainty in the measurement of density profile obtained from Thomson scattering and Lithium Beam over the 165 ms time interval considered. The maximum peak in δφ(f) is around $\rho_{pol} \approx 0.6 \pm 0.05$ with a less pronounced secondary peak at the edge.

Figure 5.4b presents simulated radial eigenfunction obtained with CASTOR code. It was concluded that both the phase and coherence techniques are important and complementary. Figure 5.4a gives information on density fluctuation level Figure 5.4b provides the relative strength between different peaks plus the sign of the radial eigenfunction.

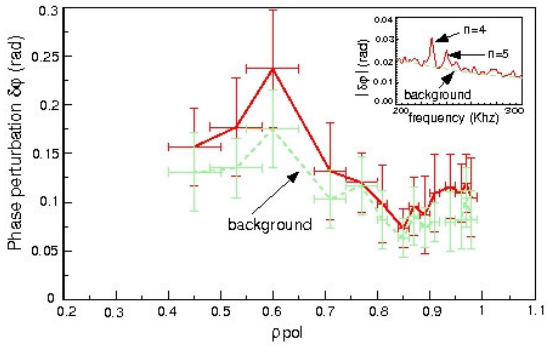

Figure 5.4a - Reflectometer phase perturbation profile for the n=4 TAE mode, background profile and phase spectra (inset) for shot # 21007.

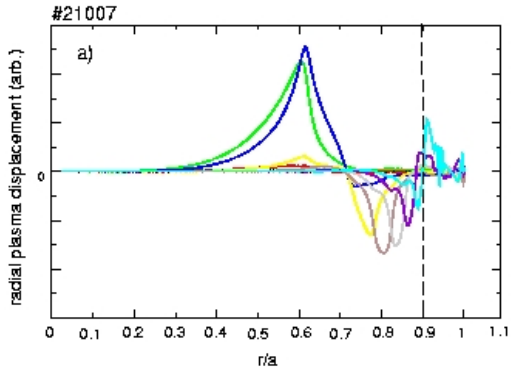

Figure 5.4b - Simulated radial eigenfunction of radial plasma displacement for n=4 TAE mode from CASTOR code.

Figure 5.5 depicts spectrograms from both the magnetics and reflectometry signals showing modes with upward frequency sweeping observed in the early phase of some discharges with ICRH power ramp-up and

identified as possible Alfvén cascades (ACs). The differences in mode frequency are due to some aliasing effects on reflectometry signals caused by the hardware analog filters. The radial extent of the TAEs derived from reflectometry is in good agreement with the results from the CASTOR code. Combining, the two hopping Q and V reflectometers, the chirping modes are core localized with $\rho_{pol} \approx 0.2\text{-}0.4$ ($\pm$ 0.05).

Further investigation aims at obtaining the radial eigen function of the ACs and compare it with LIGKA and CASTOR predictions.

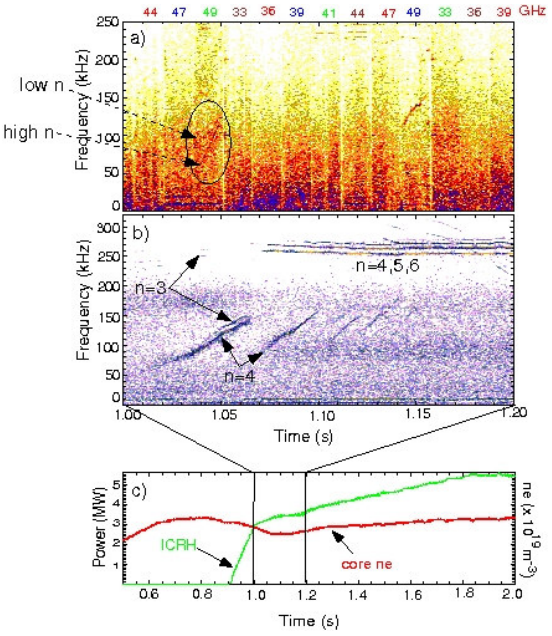

Figure 5.5 - Shot #20398: (a) FLQ-I spectrogram, (b) magnetic spectrogram and (c) time traces of ICRH and n_e.

5.3.1.2. Edge MHD modes

Figure 5.6 shows time traces of: (a) edge temperature, with time spectrograms of (b) FLV-I fixed frequency reflectometer and (c) Mirnov coil for ASDEX Upgrade shot #20393. Observed modes in H mode regimes can be either Wash board modes or Quasi-coherent modes. Both possibilities are being investigated.

5.3.2. ELM control studies

The detailed characterization of the ELM dynamics has been pursuit using new data analysis technique applied to the broadband signals aiming at investigation the ELM triggering mechanism produced by the pellets (Figure 5.7). The evaluation of the ELM onset time with simultaneous plasma probing at both HFS/LFS has been done is in good agreement with MHD findings.

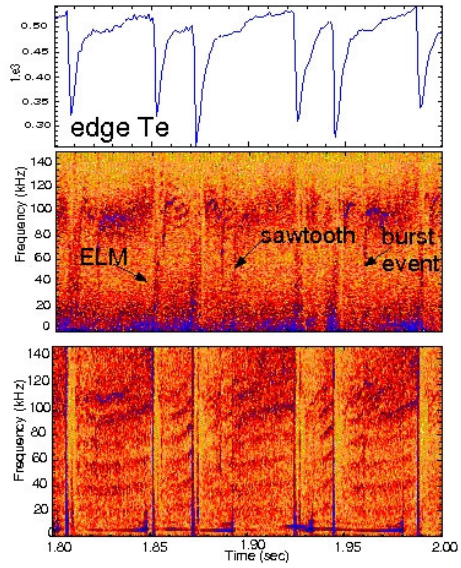

Figure 5.6 - Time trace of (a) edge temperature, with time spectrograms of (b) FLV-I fixed frequency reflectometer and (c) Mirnov coil for ASDEX Upgrade shot #20393.

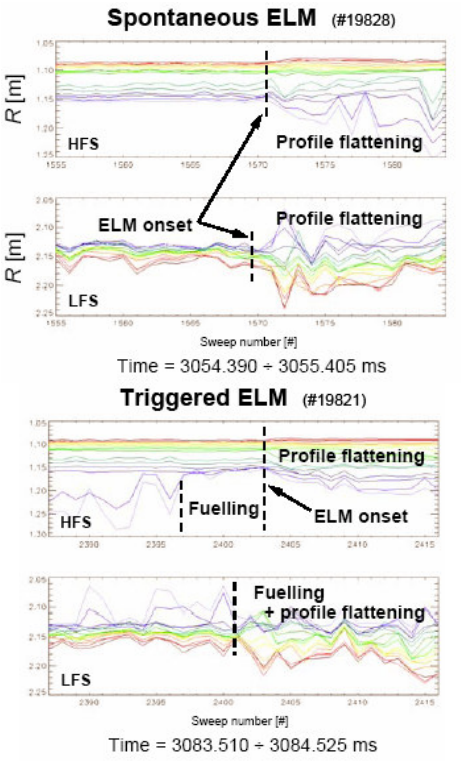

Figure 5.7 - Density Layer method example for spontaneous and triggered ELM. Up to sixteen density layer radial displacements are plotted (density increases from red to violet). ELM onset time and pellet ablation time are indicated by dashed vertical lines.

5.3.3. Electromagnetic gyrofluid turbulence in the boundary region of tokamak plasmas

The effect of the poloidal position of an axisymmetric Debye sheath (limiter cut) was studied computationally in the edge/SOL region[6] using the gyrofluid turbulence model GEM[7]. Furthermore, a geometrical model including an X-point-like singularity was developed specifically for the purpose of checking its effect (e.g., via its enhanced local magnetic shear) on egde turbulence. Initial results were obtained[8]. Complementary activities included the participation in the "EFDA Task Force on Integrated Tokamak Modelling" within the turbulence project (IMP4), and in the European DEISA project in collaboration with the Max-Planck-Gesellschaft Computer Centre (RZG).

5.3.3.1. Gyrofluid turbulence studies of the effect of the poloidal position of an axisymmetric Debye sheath

This study was originally motivated by the results of the old ASDEX on single (one X-point) vs. double (two X-points) null configurations[9]. In line with those, the disconnection between the low field (LHS) and high field sides (HFS) of the SOL region, yield by using two limiter cuts in our computations (top and bottom of the torus – DN), led to a much more quiescent HFS (where the curvature is stabilising for interchange modes) than what was observed for the single limiter cut case (SN). In the latter, in contrast to the former, the fast Alfvenic dynamics was able to connect both sides of the SOL and govern the propagation of the "blobs" along the field lines. Such pronounced differences between the HFS and LFS are in principle also accessible experimentally on the ASDEX Upgrade tokamak, which can one or two X-points, and further allows for density fluctuations probing on both HFS and LFS simultaneously, via microwave reflectometry[10]. Qualitative experimental comparisons are foreseen for 2008.

Independently of the limiter configuration, it was further observed that the turbulence measured in the SOL region was not being generated there, but rather in the edge region, which serves as a source. This is illustrated by Figure 5.8. However, due to the abrupt change in the parallel boundary condition upon entering the SOL, the turbulence changes character from the drift wave/ITG type in the edge to interchange in the SOL[11], with the transition occurring over about 10-20ρ_s (sound gyroradius), which corresponds to roughly 1cm for the plasma parameters used.

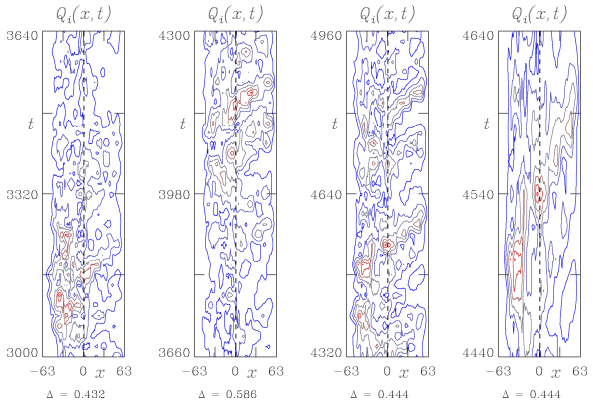

Figure 5.8 - Edge/SOL causality. Contours of as a function of radial coordinate (units of ρ_s) and time (in units of the sound speed c_s over the background profile scale length $L_\perp$), averaged over the magnetic flux surface. The vertical dashed line at (x=0) represents the last closed flux surface. The orientation of the contours towards the upper right indicates turbulence propagation from the edge into the SOL, but not the opposite. The rightmost plot corresponds to an expanded time slice of the plot to its left, showing the time scale of a single event (about \$40 $L_\perp$ c_s, too short to be accountable to any linear instability local to the SOL

5.3.3.2. Self consistent MHD equilibrium in turbulence simulations

This work was motivated by the necessity to treat self consistently the temporal evolution of the MHD equilibrium and turbulence together, on more realistic geometries that can impact the turbulence behaviour. The edge region plasma parameters are such that the equilibrium and turbulence interact strongly, and evolve together. The magnetic vector potential is a dynamical quantity evolved by an electromagnetic model (like GEM), which takes part in the MHD equilibrium (defined by the balances describing the Pfirsch-Schlueter currents, via the Ampere's law) as its axisymmetric component yields changes to the q-profile (field pitch), as well as the Shafranov shift. To study of the effect of the tokamak geometry, an increase in the sophistication involved in advancing the self-consistent equilibrium together the changing background profiles (pressure, electrostatic potential, etc.) was achieved. Starting from the earlier, simpler models[12], involving two control parameters (S-alpha geometry[13]), another more general model was introduced, involving circular magnetic flux surfaces, together with an analytical description for the X-point.

[6]T.T. Ribeiro and B. Scott, Plasma Phys. Control Fusion 50: (accepted) 2008.
[7]B. Scott, Phys. Plamsas, 12: 102307, 2005.
[8]T.T. Ribeiro, 34th EPS Conference on Plasma Physics, ECA Vol.31F, P-4.055, 2007.
[9]M. Endler, Nucl. Fusion 35: 1307, 1995.
[10]A. Silva, Rev. Sci. Instrum 67: 4138, 1996.
[11]T.T. Ribeiro, Plasma Phys. Control. Fusion 47: 1657, 2005.
[12]B. Scott, Contrib. Plasma Phys. 46: 714, 2006.
[13]J.W. Connor, Phys. Rev. Let. 40: 396, 1978.

Such model was applied to gyrofluid turbulence computations including self consistent MHD equilibrium on local geometries by means of coupling the turbulence code GEM and the geometrical code METRICS[14]. Initial results were obtained (Figure 5.9), and the continuation of the work is planned.

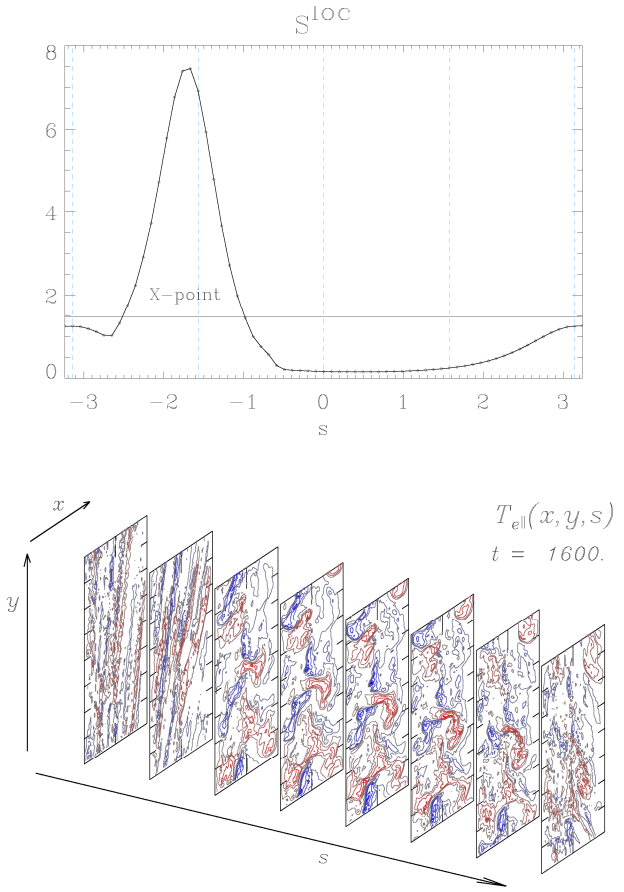

Figure 5.9 - (top) The local magnetic shear function along the magnetic field (s-coordinate) for both the S-alpha (constant line) and the circular model with an analytical description for the X-point that shows a the sharp spike. (bottom) The (spatial) three dimensional morphology o the electron temperature for the latter geometry model. There one sees the effect of the enhanced local shear caused by the X-point on twisting the turbulent structures as they extend along the field lines. This important effect is not included in the simpler S-alpha model.

5.3.3.3. EFDA Task Force on Integrated Tokamak Modelling activities

Under the project IMP4 (Microinstability and turbulence), an effort was done to agree upoon standards for the input/output files in the HDF5 format, with the purpose of sharing data across different turbulence codes, a necessary step within the ongoing benchmarking activities. The implementation of the preliminary standard agreed upon in the local version of the GEM code has been done.

[14]T.T. Ribeiro, 30th EPS Conference on Controlled Fusion and Plasma Physics, ECA Vol. 27A, P-2.152, 2003.

6. PARTICIPATION IN THE TJ-II PROGRAMME[1]

C. Varandas (Head), M. Manso (Deputy Head), L. Cupido, H. Fernandes, I. Nedzelskij, A. Silva, C. Silva, P. Carvalho, A. Duarte, L. Guimarãis, A. Neto, F. Oliveira.

6.1. INTRODUCTION

This project had in 2007 activities related with microwave reflectometry and edge physics

6.2. MICROWAVE REFLECTOMETRY[2]

A second hopping reflectometry system operating in the Q band (33-50 GHz) developed by CFN was installed at TJ-II. A study was performed based on data from the reflectometer hopping systems to investigate the parameters that control the radial electric field in the TJ-II stellarator (Figure 6.1).

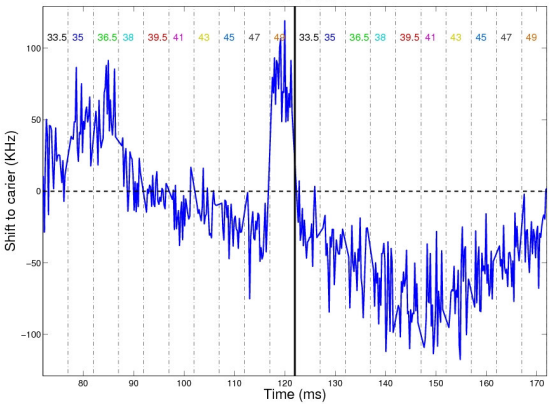

Figure 6.1 - The plasma poloidal velocity direction can be inferred by the frequency shift of the returning wave to the carrier of the Reflectometry Hopping System. A positive shift corresponds to a positive radial electric and a negative shift to a negative field. Each point in the graph corresponds to the abcissa of the first momentum of a spectrum. Each spectrum is taken from 2048 points from the reflectometry signal.

In TJ-II ECH plasmas, a perpendicular velocity shear layer develops spontaneously at the plasma edge, above a certain line-averaged density. The transition for the shear layer formation has been characterized using Langmuir probes, Ultra Fast Speed cameras and microwave reflectometry. It has been studied the dependence of the critical line-density on the ECH heating power and on the magnetic configuration: rotational transform and plasma volume. To further investigate the physics behind it, the behaviour of local plasma parameters: density, temperature and pressure and their radial gradients was analysed. It was found that the inversion in the perpendicular rotation velocity occurs when the line-averaged density reaches a certain critical value that depends on plasma conditions. The parametric dependence of the critical density on ECH power level and magnetic configuration characteristics shows a positive exponential dependence on EC heating power and a negative one on plasma radius; the dependence on rotational transform is weak and has low statistical meaning. Analysis of local plasma parameters points to plasma collisionality as the parameter that controls the inversion of the perpendicular rotation velocity of the turbulence.

6.3. EDGE PHYSICS[3]

The edge physics studies concerned the identification of zonal flows in TJ-II. This stellarator is an ideal laboratory to study the development of edge sheared flows as they can be easily driven and damped at the plasma edge changing the plasma density or during biasing experiments. Cross-correlation between edge magnitudes (density and potential) simultaneously measured with Langmuir probes located at two different positions approximately 160º toroidally apart, has been obtained in TJ-II. Results show a long distance correlation between floating potential signals that increases when probes are approximately at the same radial location, whereas there is no correlation between ion saturation current signals.

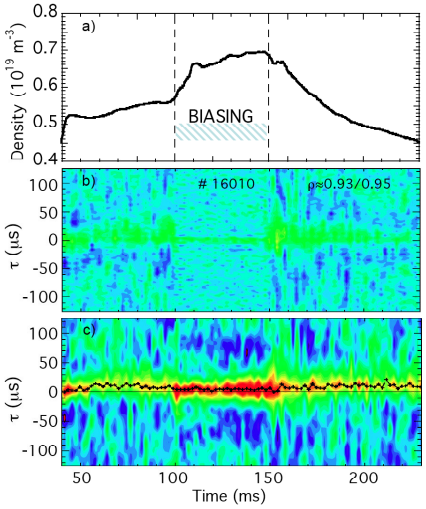

Figure 6.2 - a) Line averaged density for the same shot; Cross-correlation function between b) ion saturation current and c) floating potential signals measured toroidally apart and at the plasma edge as a function of time for one shot with electrode biasing. The over-plotted solid line in c) represents the evolution of the time delay where the correlation is maxima.

[1]Activities carried out in the frame of the Contract of Association EURATOM/IST and the Contract of Associated Laboratory, by CFN staff of the Experimental Physics and Microwave Diagnostics Groups, in collaboration with the TJ-II Team. Contact Person: Joaquin Sanchez
[2]Contact Person: Teresa Estrada.
[3]Contact Person: Carlos Hidalgo.

Cross-correlation shows a maximum value when plasma density is close to the threshold for the development of spontaneous edge sheared flows with cross-phase close to zero. Furthermore, correlation between potential signals increases in the presence of externally applied electric fields. These findings show for the first time that the development of fluctuating perpendicular flows (with zonal flow-like structure) can be considered the first step in the transition to improved confinement regimes.

7. PARTICIPATION IN THE TCV PROGRAMME[1,2]

C. Varandas (Head), P. Amorim, A.P. Rodrigues, N. Cruz, T.I. Madeira, B. Santos.

7.1. INTRODUCTION

This project has two main research lines: X-ray diagnostics and advanced plasma control system (APCS).

7.2. X-RAY DIAGNOSTICS

7.2.1. Introduction

This research line included the commissioning and scientific exploitation of the Vertical Pulse Height Analysis (PHA) Diagnostic and the development of a Rotating Crystal Spectrometer.

7.2.2. Vertical PHA diagnostic

7.2.2.1. Main activities

The following main activities were carried out in 2007:

- Commissioning and scientific exploitation of the vertical pulse height analysis (PHA) diagnostic;
- Demonstration of the throughput limit of the diagnostic;
- Calibration of the feedback system parameters;
- Increase of the temporal resolution (50 ms maximum, hardware and software limited);
- Participation in some TCV scientific campaigns.

7.2.2.2. Aperture feedback control

The tests to the hardware and the software of the aperture feedback control (Figure 7.1) have been continued. The feed-back control performance and parameters have been determined/calibrated by analysing the response of the system to moderate heating operation scenarios and then during extreme situations of very high, variable radiation fluxes during the same plasma discharge, caused by intense ECH and ECCD heating; dedicated experiments took place in order to demonstrate that the throughput limit of the system was a signal processing constraint of the electronic chain and not an imposition of the feedback circuit regulation. The plateau achieved (~200 kHz), which represents an increase of a factor of 2.5 in what concerns previous PHA system and of known present day single line signal processing chain PHA diagnostics, has permitted the improvement of the temporal resolution down to 50 ms (hardware and software limited), which has permitted increase the diagnostic sensitivity to plasma phenomena occurring in shorter time intervals.

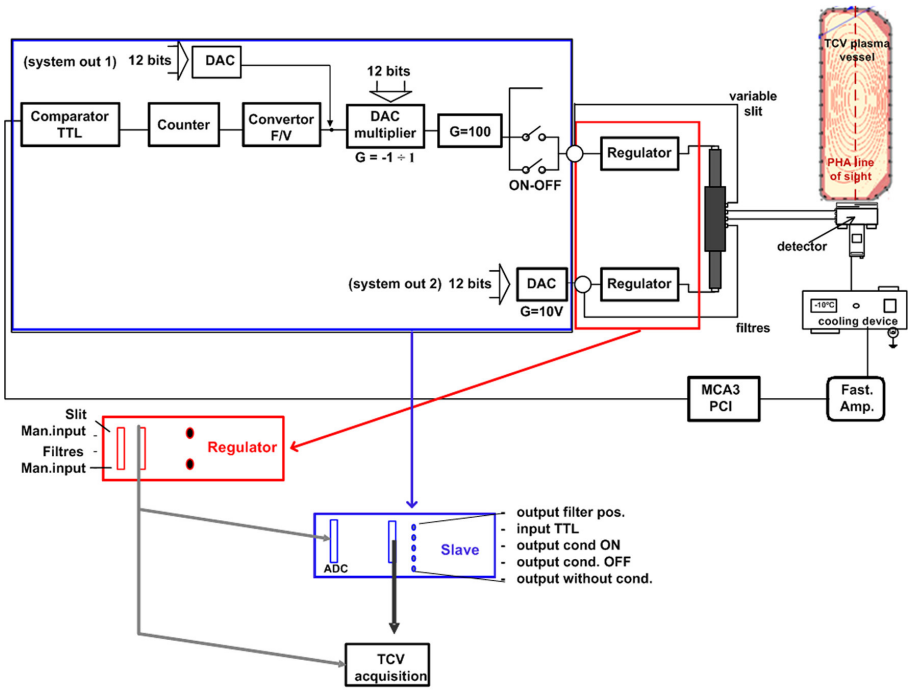

Figure 7.1 - Block diagram of the experimental arrangement showing the feedback loop that acts upon the variable input aperture

[1]Activities carried out in the frame of the Contract of Association EURATOM/IST and the Contract of Associated Laboratory, by CFN staff of the Experimental Physics and Control and Data Acquisition Groups.
[2]Work in collaboration with the Association EURATOM/Confederation Suisse. Contact Person: Basil Duval.

7.2.2.3. Participation in TCV scientific campaigns

7.2.2.3.1. Introduction

The vertical PHA diagnostic has been used in the following TCV experimental campaigns: (i) studies on electron temperature fluctuations by means of correlation electron cyclotron emission (ECE); (ii) analysis of MHD activity in low-density electron cyclotron current drive plasmas with oscillations of the electron temperature; (iii) study of the physics of suprathermal electrons; (iv) study of the non-thermal high field side/low field side ECE study of X2/X3 heated plasma; (v) analysis of suprathermal transport in electron internal transport barriers (eITB); (vi) study of particle transport in eITBs and (vi) analysis of particle transport in additionally heated H-mode plasma.

In particular, this diagnostic provided important contributions for the electron temperature fluctuation studies and complemented the study of the physics of suprathermal electrons.

7.2.2.3.2. Analysis of electron temperature oscillations

Due to the technical achievements it was possible to use the PHA to observe the electron temperature oscillations in different heating regimes (Ohmic, ECRH, and moderate ECCD) and related to the MHD activity in low-density ECCD plasmas. As already known, in the cases of strong non-Maxwellian response to ECRH, the data fitting method employed, based on the Maxwellian approximation, never provides values with physical meaning; during these measurements only the qualitative behavior could be quoted together with the physical process behind it (Figure 7.2). In fact, these were the first results obtained in the line of the research program proposed last year:

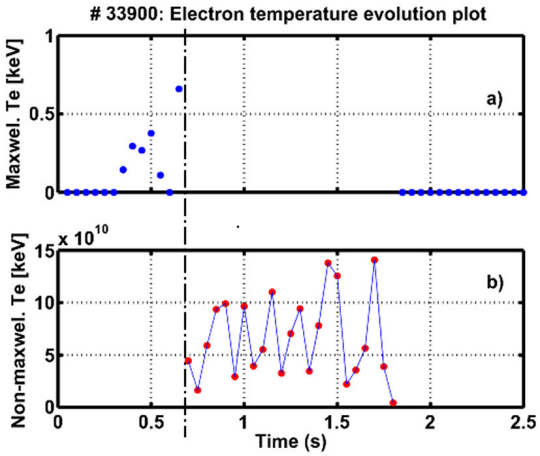

Figure 7.2 - Measurement of the electron temperature evolution (50 ms temporal resolution) for TCV # 33900. After 0.7 s, the PHA traces indicate a non-maxwellian energy distribution from which a reliable temperature can no longer be deduced only the evolution behavior could be quoted: Te oscillations during the settle down of the O-regime.

- access physical process in short time intervals;
- determination of the physical processes behind the non-maxwellian behaviour in order to provide a qualitative interpretation of the experimental results.

Although the feasibility of the above points have been verified, the possibility of providing/obtaining quantitative results was not neglected and is under investigation. The following lines of research have been followed:

- Analysis of the domain of applicability of the Maxwellian function;
- Verification of validity of the approximations usually employed;
- Fitting the data with the Maxwellian function but employing a different fitting philosophy to obtain the Te results (promising); in order to validate this new procedure, simulations were performed and demonstrated the correctness of the reasoning;
- Fitting data with generic functions whose output parameters provided the Te values;
- Investigation of alternatives to the pure Maxwellian approximation (two hypothesis in queue);

7.2.3. Rotating crystal spectrometer

The development of the high-resolution X-ray rotating crystal spectrometer has proceeded. The following tasks were carried out:

- Testing of the pre-amplifier both in the differential and integral mode (with some problems to be corrected in the integral mode, which is the final set-up when operating in the tokamak);
- Assembly and re-testing of the diagnostic with a radioactive source;
- Development of the software that will produce the spectra from the acquired data;

7.3. ADVANCED PLASMA CONTROL SYSTEM

The following activities were performed in 2007:

- Finalization of the laboratorial tests at IST/Coimbra and delivery of the equipment to Lausanne;
- Installation of the advanced plasma control system (APCS) on the TCV tokamak and integration into the plant control software;
- Implementation of corrections and upgrades on the APCS including the change of the anti-aliasing filter by a new one with a different cut-off frequency;
- Realization of off-line tests;
- Preliminary operation of TCV using APCS in parallel with the old analog system;

An effective TCV plasma control using the new APCS was achieved in February 2007, in shot 34313. Figure 7.3 presents a comparison of the output (voltage vs. time) using the APCS system (red) and the PID controllers (blue). The ripple in the APCS signals when compared to the PID controller signals is due to the APCS signals

having much bigger time resolution than the PID controller signals.

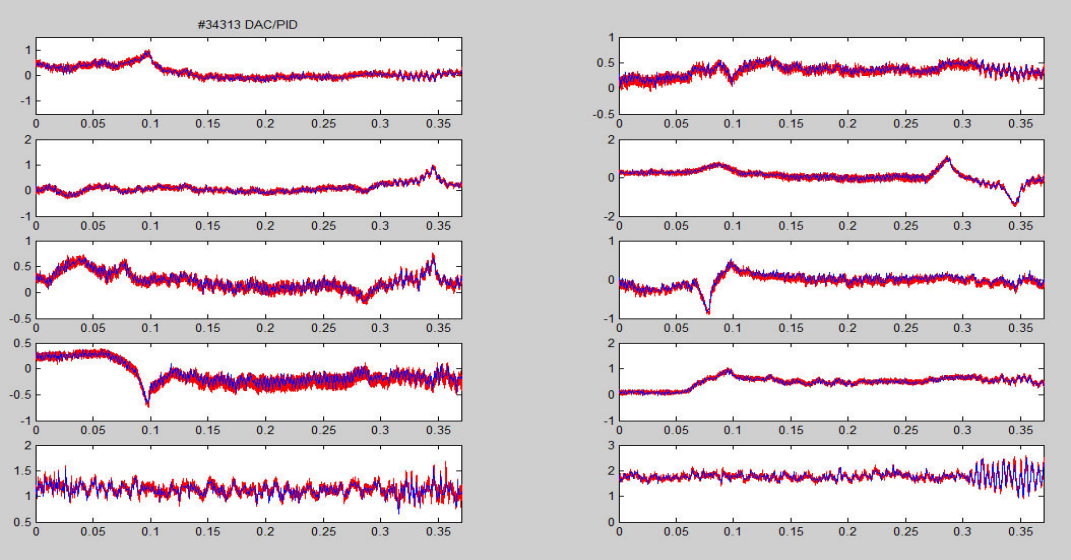

Figure 7.3 - The APCS signals (red) and the PID controllers signals (blue) in TCV shot 34313 controlled by the new system.

8. COLLABORATION WITH THE ASSOCIATION EURATOM/CEA[1]

J.P. Bizarro (Head), M. Manso and R.V. Mendes (Deputy Heads), J.H. Belo, F. Cipriano, F. Silva, J. Ferreira, P. Rodrigues.

8.1. INTRODUCTION

This project had three research lines:

- Modelling of reflectometry experiments;
- Basic theory on plasma turbulence;
- Lower hybrid current drive.

8.2. MODELLING OF REFLECTOMETRY EXPERIMENTS

The following tasks have been performed:

▪ Study using a FDTD code of the contribution of the forward scattering to Doppler reflectometry. Simulations were performed illustrating in a very clear way the mechanisms which intervene in both Bragg backscattering and forward scattering;

▪ Beginning of simulation studies using narrow band Kolmogorov and Gaussian spectra with identical correlation lengths, to pursuit the comparisons with a forward scattering theoretical model proposed by E. Gusakov.

8.3. BASIC THEORY ON PLASMA TURBULENCE[2]

8.3.1. Fluctuations and control in the Vlasov equation

The fluctuation spectrum of a linearized Vlasov-Poisson equation in the presence of a small external electric field was studied. The solution generalizes to the controlled equation an Hilbert-transform technique previously used by Ph. Morrison. Conditions for the control of the fluctuations around steady-state solutions were established as well as the functional form of the required electrical field.

8.3.2. Gyrokinetics as an exact reduction

The gyrokinetics formulation of plasmas in strong magnetic fields aims at the elimination of the degree of freedom associated with the Larmor rotation of charged particles around the magnetic field lines. In a perturbative treatment or as a time-averaging procedure, gyrokinetics is an approximation to the true dynamics. An invariant, exact to all orders, has been obtained through a Borel convergent series for the dynamics of charged particles in external electromagnetic fields. This allows for the construction of the gyrokinetics formulation as an exact reduction in the framework of systems with symmetry.

8.3.3. Stochastic solutions of nonlinear kinetic equations

Figure 8.1 represent the branching processes that, given an initial condition of a very general class, construct the solutions of both the Fourier transformed and the configuration-space Poisson-Vlasov equation.

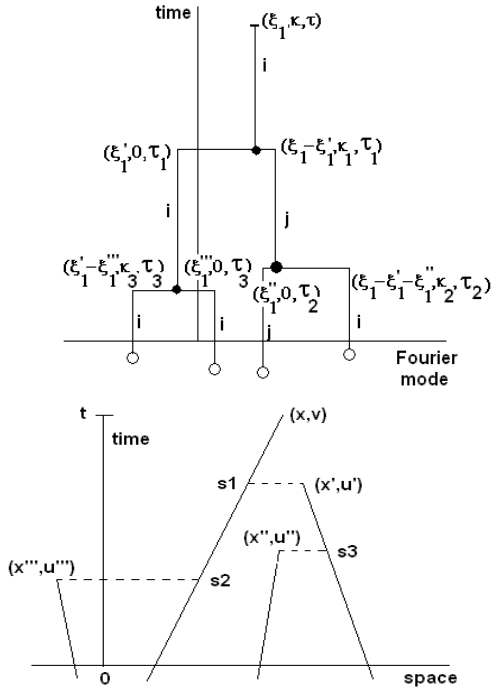

Figure 8.1 - Branching processes that, given an initial condition of a very general class, construct the solutions of both the Fourier transformed and the configuration-space Poisson-Vlasov equation.

8.4. LOWER HYBRID CURRENT DRIVE

8.4.1. Introduction

The following tasks have been performed:

▪ Participation in the pre-project (conceptual design) of a LH system for ITER having at its core a launcher based on the PAM principle: "A Day-1 LHCD system on ITER";

▪ Support to the validation procedures throughout the prototyping-manufacture process of Tore-Supra's ITER-like LHCD PAM antenna, via theoretical modelling of its components, addressing the impacts of issues resulting from this process.

8.4.1. A 'day-one' LHCD system for ITER

Contributions to the international (EU, USA, Japan, Korea) project "A 'day-one' LHCD system for ITER" in which a proposal that a reduced LHCD system (1/4 the

[1]Activities carried out in the frame of the Contract of Association EURATOM/IST and the Contract of Associated Laboratory, by CFN staff of the Microwave Diagnostic and Theory and Modelling Groups.

[2]Collaboration with the Centre de Physique Théorique (CPT) (CNRS-Marseille) and Département de Recherche sur la Fusion Contrôlée (DRFC) (Cadarache).

full power) be installed from day-1 on ITER was advocated as the first part of a two-step modular approach to the LHCD system needed for the second phase of ITER (20 MW) – where it would then be reused. It aims at reducing the risks on a full system being introduced only at the 2020-2025 horizon of the second phase and guaranteeing that competences would not be lost in this important and fully fusion specific field.

8.4.2. Stability studies for Tore Supra's PAM

Investigations have been started or resumed for Tore Supra's PAM on the stability of its power splitting (at the output ports) as well as of its total reflection coefficient (at the input port) against changes in plasma loading conditions – translated to reflection coefficients on its output ports, ρ_i. Figure 8.3 shows a simulation of the power splitting stability for the single module in Figure 8.2 at one of its 6 output ports (left) and on all 6 output ports (right), whereas Figure 8.4 portrays for the same module a simulation of the stability of the total reflection coefficient at its input port.

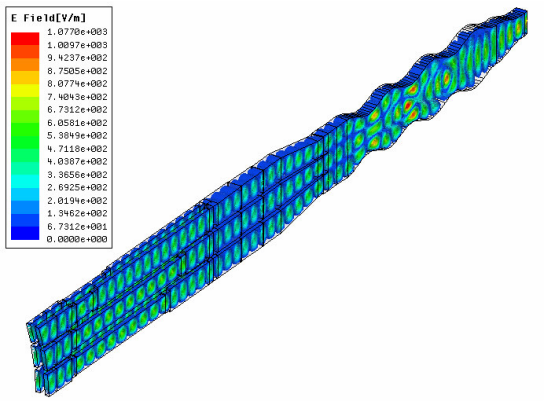

Figure 8.2 - Electric field of the TE wave determined inside the waveguides of Tore Supra's LH PAM launcher(prototype) module showing how the TE mode transmogrifies along this structure (the TE_{10}-TE_{30} mode converter is the undulating section on the right).

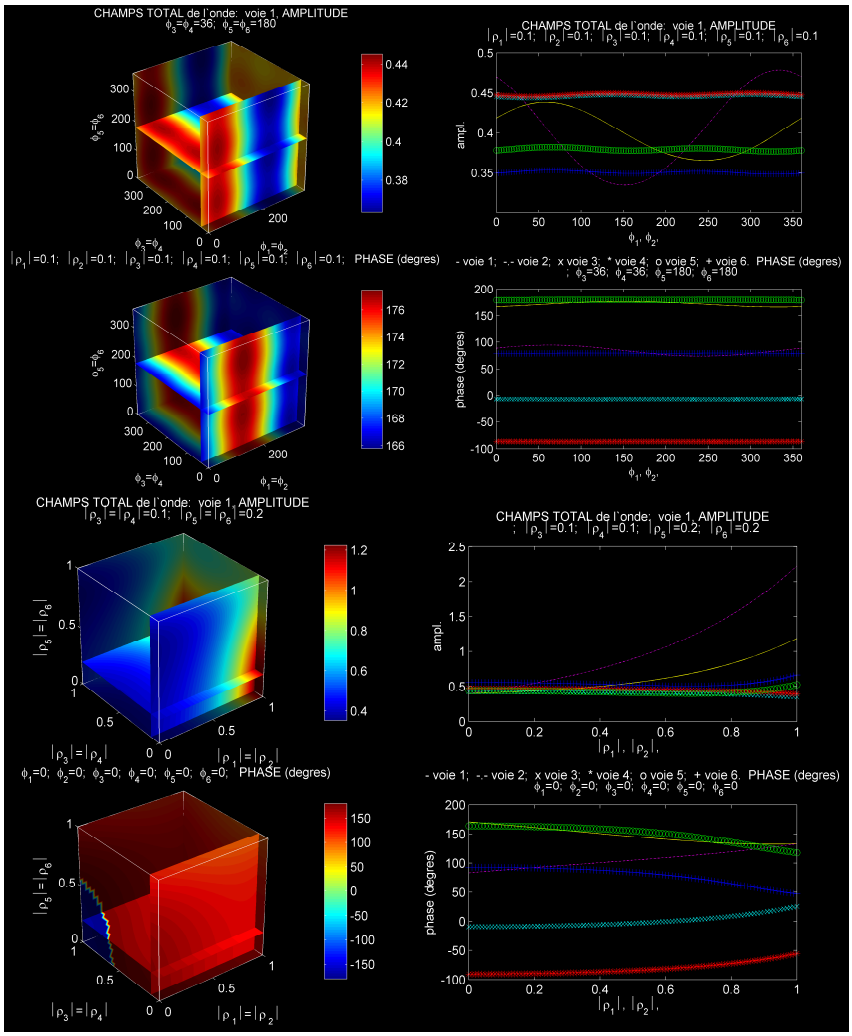

Figure 8.3 - Power splitting stability of Tore Supra's PAM+MC LH launcher module (in Fig. 1) as a function of the reflection coefficients at the output ports, ρ_i: total electric field in amplitude and phase for port 1 (left) and in all 6 port (right).

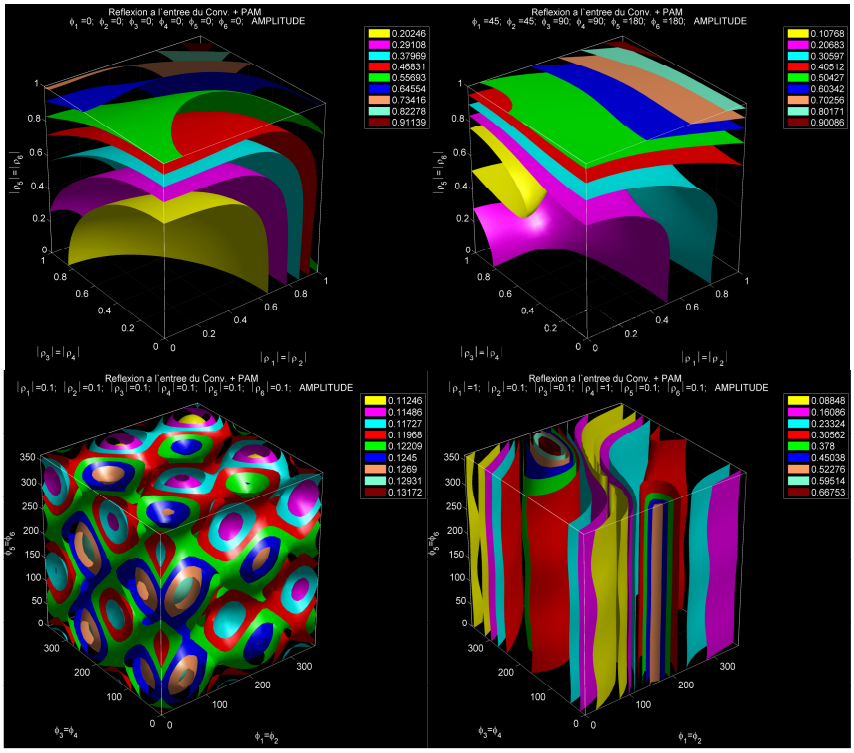

Figure 8.4 - Stability of the (total) reflection coefficient at the input port of one of Tore Supra's LH PAM+MC launcher modules as a function of the reflection coefficients at its 6 output port , ρ_i (in amplitude and phase).

9. OTHER THEORY AND MODELLING STUDIES[1]

F. Serra (Head), J.P. Bizarro (Deputy Head), R. Coelho, F. Nave, J. Ferreira and P. Rodrigues.

9.1. INTRODUCTION

This project included in 2007 two research lines:

- MHD stability studies;
- Tokamak equilibria with toroidal current reversal.

9.2. MHD STABILITY STUDIES

A non-linear MHD code, written in C-language, was developed to study the physics and strategies for the controlled feedback stabilization of neoclassical tearing modes in tokamak plasmas, a detrimental instability that degrades significantly the plasma confinement[2,3]. The numerical code, developed for a cylindrical geometry that replicates a large aspect ratio Tokamak, incorporates, besides pressure driven bootstrap current effects, the effects of plasma rotation and anomalous perpendicular viscosity. Code benchmarking was carried out for a wide variety of q-profiles in order to confirm typical linear growth rate scalings with magnetic Reynolds ($S = \tau_R / \tau_A$) and Prandtl ($\Gamma = \tau_R / \tau_V$) numbers at zero plasma beta (Figure. 9.1). Extension to the non-linear regime and finite beta is currently being addressed.

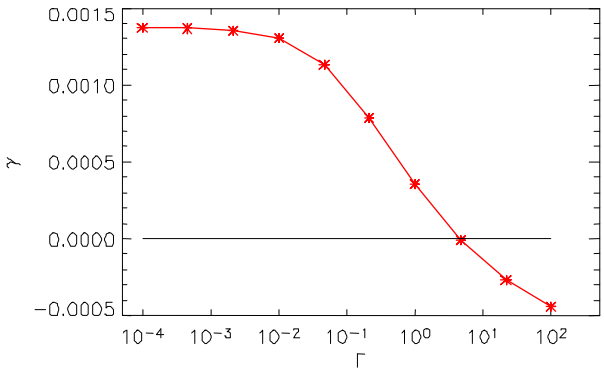

Figure 9.1 – Scaling of the linear growth rate of a (2,1) resistive tearing instability in cylindrical geometry with magnetic Prandtl number for S=10[5]. A large plasma viscosity is shown to stabilize the mode.

9.3. MODELLING OF TOKAMAK EQUILIBRIA WITH TOROIDAL CURRENT REVERSAL

It has been found that solutions of the Grad-Shafranov equation displaying toroidal current reversal are not limited to small negative-current fractions nor to hollow pressure profiles. The equilibrium reconstruction tools developed previously[4,5] have been tested in a case where the ratio between negative and positive current-density peaks is about 0.4 and the plasma pressure has its maximum value on axis (Figure 9.2). In the first place, this shows that equilibrium reconstruction can robustly tackle large negative-current fractions, which may become an asset in future studies of AC-operated tokamaks. Secondly, it shows also that early predictions of hollow pressure profiles in the presence of toroidal current reversal[6,7] hold only if the flux-surface topology is nested, stressing the relevance of the axisymmetric island system when dealing with toroidal current reversal configurations. This relevance is further enhanced if the toroidal current density and the poloidal flux distributions are displayed simultaneously, as in Figure 9.3. There, two strong and positive current channels are clearly seen flowing through the high and low-field side islands, which may help to stabilize the negative one against small displacements.

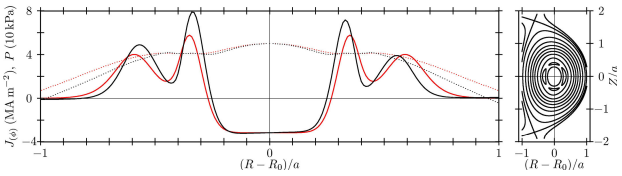

Figure 9.2 - Toroidal current density (left panel, solid lines) and plasma pressure (left panel, dotted lines) along the midplane, with the zeroth-order input profiles drawn in red and the computed distributions in black, together with the flux surfaces in the poloidal section (right panel, solid lines).

[1]Activities carried out in the frame of the Contract of Association EURATOM/IST and the Contract of Associated Laboratory, by CFN staff of the Theory and Modelling Group.

[2]Coelho, R. "Nonlinear growth of marginally unstable tearing modes", Phys. Plasmas 14, 052302 (2007).
[3]Coelho, R. and E. Lazzaro, "Effect of sheared equilibrium plasma rotation on the classical tearing mode in a cylindrical geometry", Phys. Plasmas 14, 012101 (2007).
[4]Rodrigues, P and JPS Bizarro, Phys. Rev. Lett. 95, 015001 (2005).
[5]Rodrigues, P and JPS Bizarro, Phys. Rev. Lett. 99, 125001 (2007).
[6]Chu, MS and PB Parks, Phys. Plasmas 9, 5036 (2002).
[7]Hammett, GW, SC Jardin, and BC Stratton, Phys. Plasmas 10, 4048 (2003).

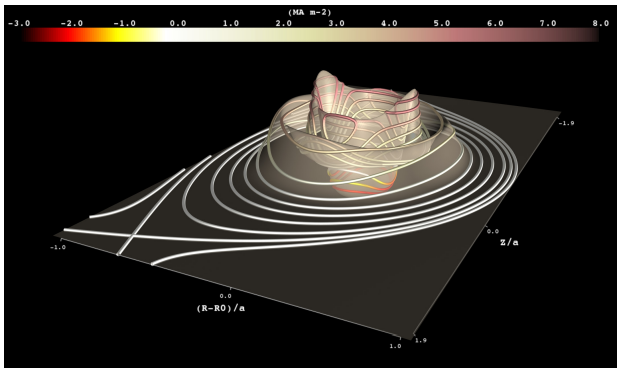

Figure 9.3 - Toroidal current density distribution Jf(R,Z) throughout the poloidal section (shaded surface). The lines of constant poloidal flux are first vertically deformed and then colored according to the value of Jf(R,Z), appearing as paths sloping up and downhill on the toroidal current density landscape.

10. OTHER ACTIVITIES ON CONTROL AND DATA ACQUISITION[1]

J. Sousa (Head), C. Correia, A. Batista, M. Correia, N. Cruz, A. Duarte, J. Fortunato, R. Pereira, T. Pereira, D. Valcárcel.

In parallel with the project-driven tasks, other research activities occur aiming to support present and future developments on the areas of control, data acquisition and signal processing. The following activities have been carried out in 2007:

- Development and test of a high performance control and data acquisition platform based on the ATCA and PCIe standards.
- Development of high-speed parallelized spectroscopy algorithms based on the trapezoidal filter method (Figure 10.1 shows the simulation results where 95% of total pulses were resolved in a scenario with 75% of pile-up events, at max. pulse rate, 20 ns pulses, using the HPD+DTS algorithms).
- Development of a real-time Application Interface framework and debug/testing programs for the PCI Express bus under Linux real-time extensions (RTAI), focusing speed/throughput optimization.
- Production of a fast timing and event management board for the PCI bus (EPN-PCI).
- Development of an ATCA digitizer board with 12-bit resolution, 1 GSPS, 4 channels.

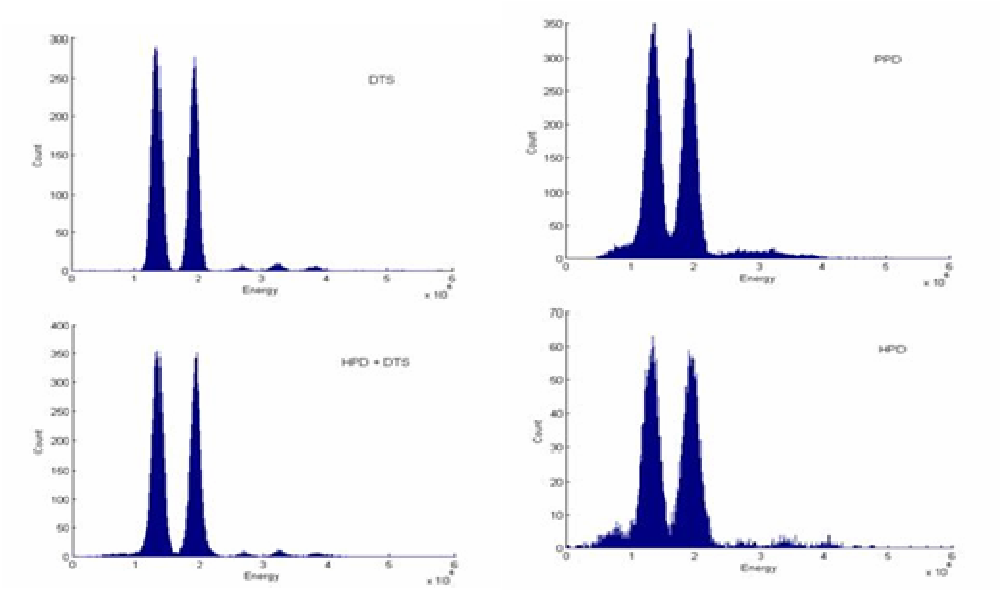

Figure 10.1 - Spectra obtained by the simulation of 1000000 pulses with two energy amplitudes with periodic noise to cause spectral degradation (increases peak width), base line shift and 75% of pile-up events. PPD (peak pulse discriminator) - the amplitudes were directly measured from the sampled data; DTS - the energy of pulses with and without pile-up; HPD - all the energy of pile-up pulses that couldn't be resolved by DTS; HPD+DTS - the sum of the p1(n) with p2(n) outputs.

[1]Activities carried out in the frame of the Contract of Association EURATOM/IST and the Contract of Associated Laboratory, by CFN staff of the Control and Data Acquisition Group.

11. KEEP-IN-TOUCH ACTIVITIES IN INERTIAL FUSION ENERGY[1]

J. T. Mendonça, (Head), J. Davies, J. M. Dias, M. Fajardo, G. Figueira, R. Fonseca, A. Guerreiro, C. Leitão, N. Lopes, A.M. Martins, D. Resendes, J.A. Rodrigues, L.O. Silva.

11.1. INTRODUCTION

The main results obtained in 2007 on keep in touch activities on inertial fusion energy during 2007 have been obtained along three different lines in ICF research:

- Fast ignition and ICF theory;
- High intensity photonics;
- Plasma accelerators and intense radiation sources.

11.2. FAST IGNITION

Keep in touch activities in IFE, with an emphasis on fast ignition of fusion targets, have covered (i) experiments conducted at the VULCAN Petawatt facility to understand the effects of laser intensity on the main features of the fast electron beam (e.g. divergence, energy), (ii) experiments on warm dense matter conducted at PALS (iii) theory on magnetic field generation due to plasma expansion in laser-solid interactions, (iv) transition from the collisionless to the collisional regimes in the electromagnetic filamentation instability in fast ignition, and (v) theory and numerical work on the temporal growth rates of Stimulated Raman Scattering in the presence of light with statistics typical of ICF scenarios.

11.3. HIGH INTENSITY PHOTONICS

Several ytterbium-doped laser media were tested and characterized in a diode-pumped, mJ-level regenerative amplifier as a possible independent medium-energy beam for experiments and to assess their features for a diode based beam line. Additionally, a high performance diode stack for high energy and high intensity pumping, able to deliver 4 kW, 3 ms pulses at 10 Hz, was acquired. This will allow an increase from the mJ pulse energy from the current regenerative amplifier to the 100 mJ level. Together with the developed full modelling of the temperature, pump and amplification (Figure 11.1), we are now ready to test new and promising ytterbium-doped laser materials, as well as to provide a medium-energy pump pulse for optical parametric chirped-pulse amplification (OPCPA) setups.

With regard to this technique, we are able to demonstrate experimentally the advantages of the dispersed-signal geometry for generating ultra-broadband (>500 nm), high-energy pulses, capable of leading to ultrahigh intensities in the few-cycle pulse regime.

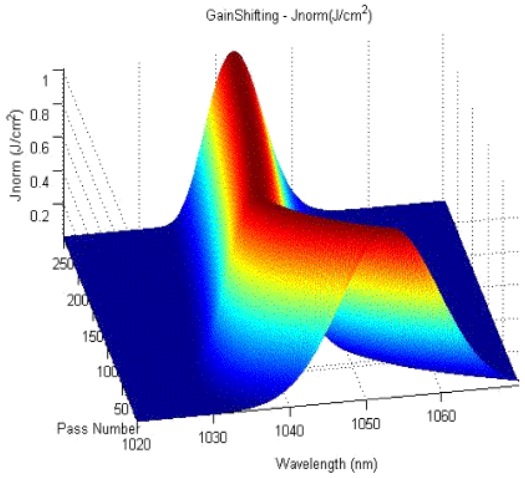

Figure 11.1 - Calculated spectral shift and narrowing of a laser pulse initially centered at 1053 nm as a function of the number of passes in a diode-pumped Yb:glass regenerative amplifier. The numerical code takes into account the full pump and seed pulse parameters, and the optical, material and thermal properties of the gain medium.

At the level of diagnostics development, a new wavefront sensing diagnostic and a novel patented deformable mirror were installed, for optimizing the focal spot of the high power multi-terawatt laser system at IST, leading to intensities on target in the range of 10^{19} W/cm2 A permanent suite of diagnostics was installed before and after final pulse compression. These include a calibrated photodiode for energy measurement, a near-field CCD camera for monitoring the beam profile before compression, a far-field CCD after the compressor, a radial shearing interferometer and a second-order single-shot autocorrelator.

11.4. PLASMA ACCELERATORS AND INTENSE RADIATION SOURCES

The activities on this topic have covered the following aspects: (i) experiments on plasma waveguiding, including full characterization of the devices at low power, and demonstration of guiding at high intensity, and (ii) implementation, experimental demonstration, and implementation of a high harmonics source from laser-gas interaction at IST, with the existing laser parameters, with single shot harmonic generation up to the 47th harmonic.

[1]Activities carried out in the frame of the Contract of Association EURATOM/IST and the Contract of Associated Laboratory, by "Grupo de Lasers e Plasmas" (Golp) of "Centro de Física dos Plasmas".

12. PARTICIPATION IN THE FUSION TECHNOLOGY PROGRAMME[1]

C. Varandas (Head), E. Alves, L.C. Alves, N.P. Barradas, M.R. da Silva.

12.1. INTRODUCTION

This project included in 2007 activities in the frame of Underlying Technology and of the Tasks referred to in Table 12.1. The work carried out in ITER-specific tasks is described in chapter IV.

Task	Area	Beginning
TW5-TPDS-DIARFA	ITER diagnostics	07.09.2005
TW5-TTMS-006	Structural Materials	09.03.2005
TW6-TPP-ERDEP	Plasma-Wall Interaction	12.10.2006
TW6-TDS-QA2	Quality Assurance	08.12.2006
TW6-TPDS-DIADES	ITER diagnostics	08.12.2006
TW6-TVR-WHMAN2	Remote Handling	01.09.2007
TW6-TTFF-VP75-2	Fuel Cycle	01.09.2007

Table 12.1 – IST tasks in the Fusion Technology Programme

12.2. MATERIAL CHARACTERIZATION USING NUCLEAR TECHNIQUES: TITANIUM BERYLLIDE OXIDATION STUDIES

Be alloys are under intense research due to its potential to replace pure Be as functional material on Fusion reactors. However allowing Be with transition metals is difficult and there is a lack of knowledge about its behavior. In this work we continued the study of the structural properties of these intermetallic compounds with emphasis on the oxidation behavior. The samples were characterized with Electron microscopy (SEM), X-ray diffraction and Ion beam analyses (IBA). The thermal stability and oxidation behaviour at high temperatures under air annealing was studied with emphasis on the oxidation kinetics aiming at understanding the physical mechanisms underlying the oxidation process. The surface of each of the samples was polished and the oxidation was accomplished by annealing at 800º C in air atmosphere. The RBS results. (Figure 12.1) reveal for the 5at%Ti sample, not only that the oxidation occurs preferentially at the Ti depleted (Be rich) zones but also that the oxide layer formed in the time step annealing is smaller than the one formed in single step annealing, even if we reach the same annealing time.

The elemental distribution map of Ti, (Figure 12.2) shows that topography changes are noticeable for the single 8 h annealing procedure, indicating that the Be diffusion continues even if the oxide layer doesn't seem to change that much, as shown in the spectra of Figure 12.2. Our results clearly indicate that oxidation of Beryllides occurs preferentially along the Be richch zones and seems to be a continuous process.

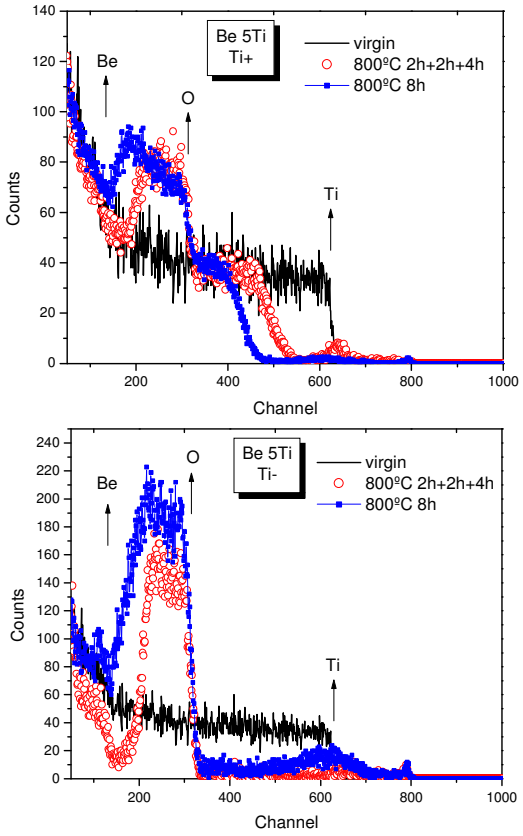

Figure 12.1 – RBS point spectra from the Be 5at%T_i sample before and after annealing procedures, obtained in the T_i rich region (top) and in the T_i depleted (bottom) zones.

12.3. TASK TW6-TPP-ERDEP - STUDIES OF MATERIAL EROSION AND REDEPOSITION IN ITER-RELEVANT DIVERTOR TARGET TEMPERATURES, PLASMA IMPACT ENERGIES AND DIVERTOR CHAMBER GEOMETRIES.

Delivery D3-Report on the effect of ITER-relevant material mixing on fuel retention and material characteristics

Previous studies have shown W to have favorable H/D/T retention characteristics. However, the ion flux densities in these experiments were well below the levels expected in the ITER divertor. Furthermore the behaviour of H/D/T retention as a function of fluence is critical in determining the retention saturation level for a W PFC in ITER.

[1]Activities carried out in the frame of the Contract of Association EURATOM/IST, by staff of "Instituto Tecnológico e Nuclear".

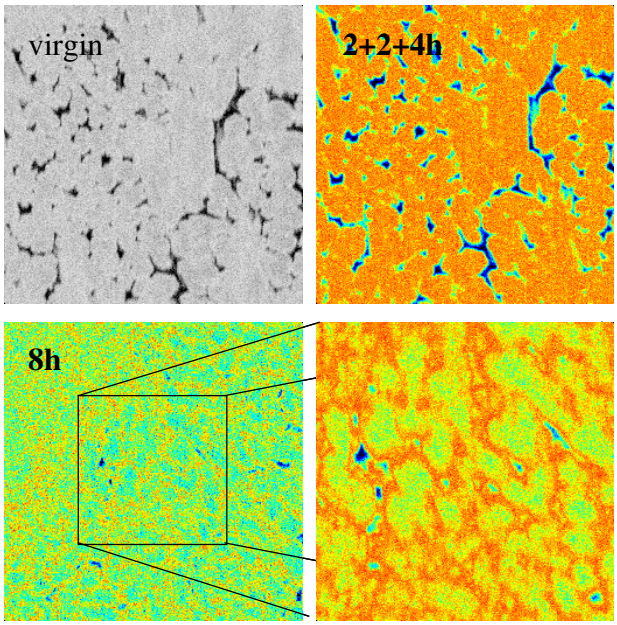

Figure 12.2 – T_i elemental distribution maps from the Be 5at%T_i sample obtained before and after annealing procedures, showing complete modification of surface structure after 8h annealing in air. The maps have dimensions of 530×530 μm^2 except for the bottom-right that is a zoom of the bottom-left map and presents dimensions of 264×264 μm^2.

The major goal of the study was the full characterisation of the surface composition and morphology and fuel retention of W targets exposed to plasma fluxes similar to the ones expected in the ITER divertor (>10^{23} $m^{-2}s^{-1}$). Tungsten samples were exposed to plasma fluxes in PSI-2 and studied with ion beam techniques and atomic force and electron microscopy. Fuel retention in the samples and its depth distribution was quantified with Elastic Recoil Detection Analysis (ERDA) and Nuclear Reaction Analyses (NRA).

W targets with 1mm thick, 20 mm diameter discs in thermal contact with a water-cooled copper heat sink and electrically grounded were exposed to deuterium plasma in the Pilot-PSI. This linear plasma generator produces plasma conditions that are expected to be typical at a detached ITER divertor strike point (n_e ~ 10^{20} D^+ m^{-3}, T_e < 5 eV, Γ_{D+} ~ 10^{24} D^+ $m^{-2}s^{-1}$).

Deuterium retention in W was measured as a function of incident plasma fluence at a plasma flux density in the ITER divertor range (Γ_{D+} ~ 10^{24} D^+ $m^{-2}s^{-1}$). The W targets exposed in Pilot-PSI were analysed ex-situ with ^{3}He(d,p)α nuclear reaction analysis (NRA) and thermal desorption spectroscopy (TDS). While NRA provides D depth profiles and concentrations over the first ~3 μm TDS gives information on global/bulk retention and trap mechanisms and energies. Initial NRA data, Figure 12.3 shows a D depth profile that is peaked at the surface and significant D retention (0.01 at. %) at a depth of ~3 μm after only 40 s (10 discharges) of total plasma exposure time. This demonstrates the trapping of D that has diffused away from the ion implantation zone towards the bulk.

The effects of surface polishing/roughness and pre-annealing targets before plasma exposure are investigated through the comparison of D retention as determined by NRA and TDS analysis. The results show that a W target with a surface roughness of <1 μm has nearly 6 times more D retention in the first 3 μm of the surface than an "as received" W target.

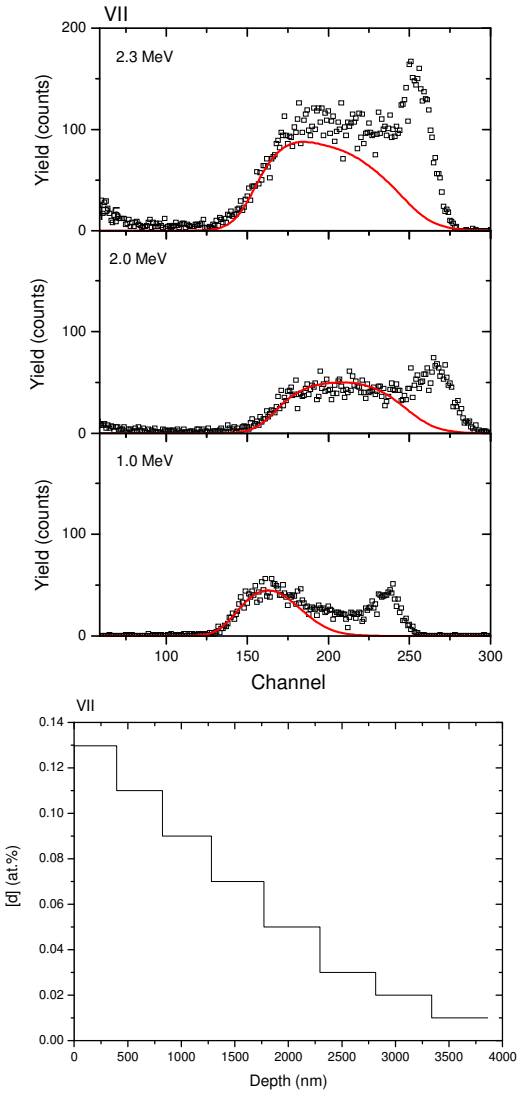

Figure 12.3 - Alfa spectra from the ^{3}He(d,p)α nuclear reaction for the energies indicated in the panels (top). The solid line is the simulation obtained with the NDF code and the peak observed at higher channels is due to the pile-up effect at the end of the depletion layer of the Si detector. The D depth profile extracted from the experimental spectra is shown on the bottom.

13. OTHER FUSION-RELATED ACTIVITIES[1]

C. Varandas (Head), H. Fernandes, M.E. Manso, A. Silva, J. Sousa, I. Carvalho, J. Fortunato, S. Magalhães, L. Meneses, A, Neto, T. Pereira, J. Santos, A. Soares, D. Valcárcel.

13.1. INTRODUCTION

This project included activities related with the collaboration of IST/CFN with IPP.CZ, IPP-Greisfwald, Brazilian Institutions and ENEA-Frascati as well as activities on socio-economics, education and training, organization of scientific meetings and management of the EURATOM Fusion Programme.

13.2. COLLABORATION WITH IPP.CZ

13.2.1. Introduction

This research line included in 2007 work on microwave reflectometry and control and data acquisition.

13.2.2. Microwave reflectometry

The following activities were carried out:

- Elaboration in June 2007 of a first conceptual design of a FM-CW reflectometer system for the Compass tokamak, using in-vessel antennas and separate waveguides for each of the four frequency bands;
- Elaboration in October/November 2007 of a new design using ex-vessel antennas and two complex transmission lines to launch and receive all the frequency bands, including combiners and decombiners, to be compatible with the reduced access available at Compass-D, which was only known after the tokamak drawings were received at IPP.CR;
- Design of the combiners/decombiners and lenses (Figure 13.1);
- Beginning of the assessment of the system proposal (Figure 13.2) in terms of cost and time schedule.

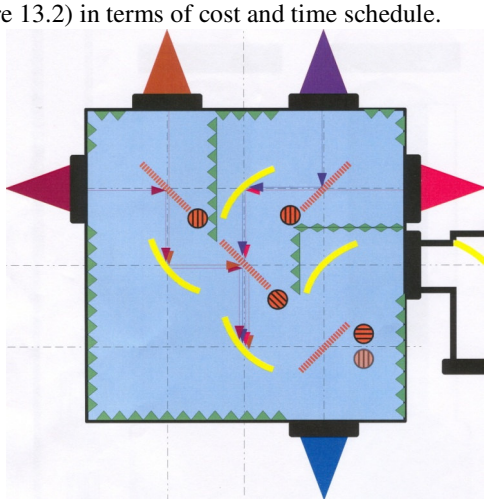

Figure 13.1 - Arrangement of the quasi-optical band-combiner

13.2.3. Control and data acquisition

The following tasks were performed:

- Development of the control and data acquisition system for COMPASS including hardware prototypes and software programs;
- Assessment and overall design of the CODAC system and some of related sub-systems (Figure 13.3);
- Preliminary instrumentation and operation software tests on ISTTOK an JET-EFDA.

13.3. COLLABORATION WITH IPP-GREISFWALD

13.3.1. Introduction

This collaboration started in 2007, with work on tomography diagnostics and control and data acquisition.

13.3.2. Tomography diagnostics

- Beginning of the development of a neural-network for tomography systems. The neural-networks algorithm[2] required training with artificial data (phantoms), for W7-X that has been processed to generate the neural network. These phantoms were rings placed at different positions and with different radii; 'zero' radius was included, yielding a gaussian emissivity profile. Tests with noisy artificial data suggest it to be robust and accurate;
- Implementation for W7-X, with good results for artificial data, minimum Fisher regularisation algorithm. Due to generalization of the code, it can easily be adapted for other machines such as W7-AS.

13.3.3. Control and data acquisition

It was agreed to install an ATCA system to show the feasibility of real time processing for some diagnostics of W7-X, namely the magnetics and tomography

13.4. COLLABORATION WITH BRAZILIAN INSTITUTIONS

13.4.1. Introduction

IST has maintained the collaborations with the TCA/Br[3] and ETE[4] programmes in the areas of microwave reflectometry, control and data acquisition and Thomson scattering.

13.4.2. Microwave reflectometry

The following tasks were performed:

- Selection and placement of orders for the millimetre-wave components of the broadband reflectometer of TCA/Br;

[1]Activities carried out in the frame of the Contract of Association EURATOM/IST and the Contract of Associated Laboratory.
[2]Supplied by S.Gori and U. Toussaint, from IPP-Garching
[3]TCA/Br is a tokamak of the "Laboratório de Plasmas, do Instituto de Física, da Universidade de São Paulo.
[4]ETE is a tokamak of the "Laboratório Associado de Plasmas, do Instituto Nacional de Pesquisas Espaciais, de São José dos Campos".

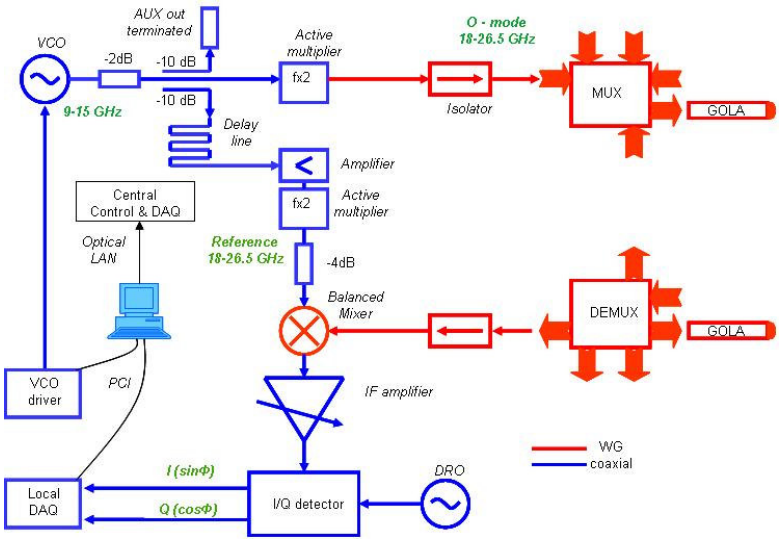

Figure 13.2 - Block scheme of O-mode 18-26.5 GHz transmitter and receiver

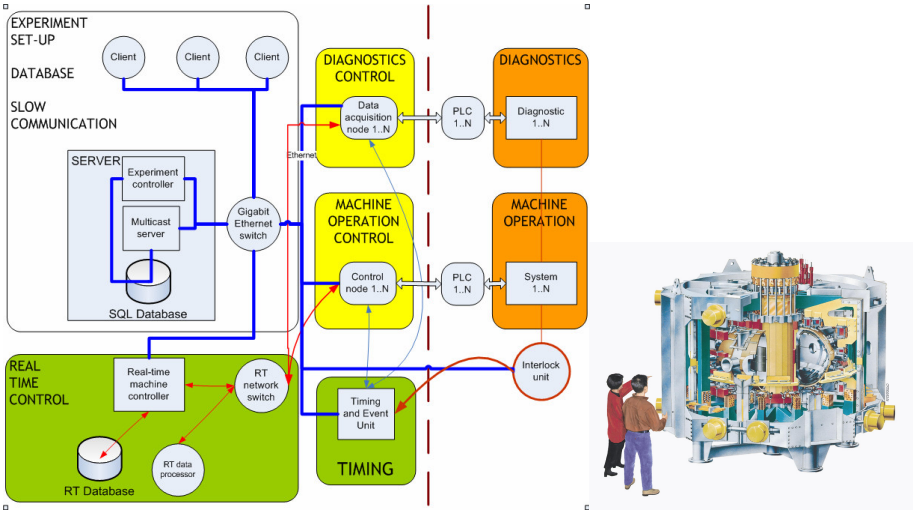

Figure 13.3 - Global diagram of the COMPASS CODAC system.

- Building ant testing of the tuning ramp generators, HTO drivers and the controller board;
- Design and starting of the fabrication of the IF detection amplifiers.

13.4.3. Control and data acquisition

The following activities were made:

- Remote support of the operation of the ETE data acquisition system;
- Elaboration of a proposal for the development of a set of VME transient recorders for TCA/Br.

13.4.4. Thomson scattering

The following tasks were carried out:

- Testing at the University of São Paulo of the ISTTOK Nd:YAG laser;
- Design and construction of part of the system to deliver the laser beam to the TCA/Br tokamak.

13.5. COLLABORATION WITH ENEA-FRASCATI

This collaboration included work related with liquid metal limiter plasma interaction and control and data acquisition. The following activities were carried out in 2007:

- Participation in FTU experiments for plasma liquid lithium limiter interaction studies. Analysis of the achieved results have shown a significant improvement of the plasma discharge, with lower plasma contamination by impurities, lower radiated power and higher plasma densities.

13.6. SOCIO-ECONOMIC STUDIES

TIMES was installed at IST by experts of EFDA-TIMES. A group (1 pos-doc and 3 PhD students) was created at IST to develop energy models with emphasis on the analysis of the sustainability of the energy systems at different scales.

13.7. EDUCATION AND TRAINING

The following activities were performed:

- Setting up of the European Doctorate on "Fusion Science and Engineering", organized jointly by University of Padova, Instituto Superior Técnico and Maxmilian University of Munich;
- Elaboration of a proposal (in collaboration with ENEA and CEA) on Data Acquisition and Plasma Control for a call of the EFDA Training Programme;
- Project MDEI - Training on Microwave Diagnostics;
- Launching of the recruitment process for all the partners of the MDEI-Training on Microwave Diagnostics project. This process was completed by December 2007 and it is expected that all the training positions can be filed in January 2008;
- Updating of the training plans of the MDEI project taking into account the time schedule of the present microwave diagnostics developments and experiments.

13.8. ORGANIZATION OF THE 17TH IAEA TECHNICAL MEETING ON "RESEARCH USING SMALL FUSION DEVICES"

The 17th IAEA TM on "Research Using Small Fusion Devices" was held in Lisbon, hosted by the Government of Portugal through the Centro de Fusão Nuclear of the Association EURATOM/Instituto Superior Técnico (EURATOM/IST) with the participation of 76 scientists from 24 countries most of them outside Europe (Argentina (5), Brazil (3), Canada (2), Chile (1), China (1), Egypt (2), India (2), Islamic Republic of Iran (2), Japan (1), Kazakhstan (1), Malaysia (1), Mexico (3), Pakistan (3), Russian Federation (8), Thailand (1), Turkey (1), Uzbekistan (1)). The objective of the meeting was to provide a forum for discussion of approaches to fusion research based on small and medium scale devices, such as small tokamaks, compact tori, dense plasma focus, reversed field pinches (RFP), helical devices, linear/discharge machines, etc. The meeting also covered other devices such as non-magnetic confinement devices, devices using beams or lasers and new trends or innovation concepts for fusion research.

The meeting provided an opportunity for scientists working in different fusion topics and different devices to exchange and discuss results of their research, compare methodologies and promote possible collaborations. The meeting provided discussion sessions to highlight where new contributions and new collaborations could be established among the small fusion devices community that will align their work with relevant fusion research topics for the future.

The International Advisory Committee, chaired by Prof. Carlos Varandas (CFN) selected a total of 54 submissions distributed over 6 invited, 21 contributed orals and 27 poster contributions. The list of topics was chosen taking into account those areas where small fusion devices can contribute to the main stream research. The IAC considered experimental and theoretical contributions reporting on: (i) Toroidal Systems; (ii) Dense Magnetised Plasma Systems; (iii) Theory and Numerical Modelling; (iv) Materials Research; (v) Diagnostic Systems and Components; (vi) Innovative Technologies and Applications; and (vii) Control and Data Acquisition Systems and Remote Participation Tools. After a referring process, the contributions will be published in the AIP conference proceedings series.

13.9. PARTICIPATION IN THE MANAGEMENT OF THE EURATOM FUSION PROGRAMME

Several members of the Association EURATOM/IST have been involved in the management of the EURATOM Fusion Programme as well as on Ad-Hoc Groups and Scientific Committees of the EFP and other Fusion Programmes.

- Carlos Varandas was Chairman of the EFDA Steering Committee (SC) (until June), is Chairman of the F4E Governing Board (since July) and member of the Consultative Committee for the Research and Training Programme on Nuclear Energy-Fusion (CCE-FU), Group of Chairman (GoC), Scientific and Technical Committee and EFDA Steering Committee.
- Maria Emília Manso was member of CCE-FU, EFDA SC and EFDA Public Information Sub-Committee.
- Fernando Serra was member of the EFDA Scientific and Technical Advisory Committee (STAC) and is Member of the F4E GB (since June).
- João Pedro Bizarro was member of the EFDA STAC.
- Carlos Silva was member of the EFDA Administrative and Financial Advisory Committee.
- José Tito Mendonça is member of the Inertial Fusion Energy Coordinating Committee.

13.10. OTHER MANAGEMENT ACTIVITIES

- Prof. Carlos Varandas is/was: chairman of the Ad-Hoc Group on the new European Fusion Development Agreement and the Contracts of Association; member of the EURATOM Delegation to the ITER Council and member of the EURATOM Delegation to the Steering Committee of the Broader Approach.
- Prof. Fernando Serra is/was member of: the Ad-Hoc Group from STAC for the Monitoring of W7-X Project; the ITPA (International Tokamak Physics Activity) Topical Group on Diagnostics; the Ad-Hoc Group from STAC for the COMPASS-D Project and the International Board of Advisories of the COMPASS-D Project.
- Profª Maria Emília Manso was: member of the Programme Committee of the ASDEX-Upgrade Project Chairperson of the International Advisory Board on Reflectometry, and coordinator of the Cluster of EURATOM Associations for the development of the Plasma Position Reflectometer for ITER.

14. PLASMA THEORY AND SIMULATION[1]

L. O. Silva (Head), J.R. Davies, R.A. Fonseca, F. Peano, G. Sorasio, P. Abreu, M. Fiore, F. Fiúza, L. Gargaté, J.L. Martins, S.F. Martins, M. Marti, J. Vieira, B. Brandão.

14.1. INTRODUCTION

The work on plasma theory and simulation covered the following topics:

- White light parametric instabilities;
- Laser-plasma accelerators;
- Fast ignition and laser solid interactions;
- Astro and space physics;
- High performance computing and development of massively parallel techniques in plasma physics;
- Computational physics;
- Radiation generation.

14.2. WHITE LIGHT PARAMETRIC INSTABILITIES

14.2.1. Coupling with longitudinal electron dynamics[2]

Parametric instabilities driven by partially coherent radiation in plasmas have been described using the generalized statistical Wigner-Moyal set of equations[3], formally equivalent to the full wave equation, coupled to the plasma fluid equations. A generalized dispersion relation for stimulated Raman scattering driven by a partially coherent pump field was derived, valid for all angles and all intensities. The one-dimensional longitudinal analysis has revealed a growth rate dependence, with the coherence width $\int$ of the radiation field, scaling with $1/\int$ for backscattering (three-wave process), and with $1/\int^{1/2}$ for direct forward scattering (four-wave process).

Furthermore, the exploration of the generalized dispersion relation allowed us to show that: (i) Raman forward scattering (and the relativistic modulation instability) are less sensitive to white light (Figure 14.1), and (ii) the range of unstable wavenumbers increases with increasing bandwidth for Raman backward scattering, being almost unchanged for the other Raman instability regimes. Our results demonstrate the possibility to control the growth rates of these instabilities by properly using broadband pump radiation fields[4].

14.2.2. Transverse modulation instability[5]

In order to understand the role of white light in the transverse modulation instability, we have initiated the analysis of the generalized dispersion relation for purely transverse wavenumbers. The preliminary steps undertaken include: (i) numerical solution of the monochromatic dispersion relation for Raman for all angles (based on previous works by Antonsen and Mora, and McKinstrie and Bingham), (ii) a detailed comparison of the results from McKinstrie and Bingham, with the classic paper of C. Max *et al*, and (iii) preliminary numerical exploration of the transverse modulation instability in the presence of white light. Further work will include a detailed exploration of the numerical solutions of the generalized dispersion relation and analytical solutions for the growth rate for simplified photon distribution functions.

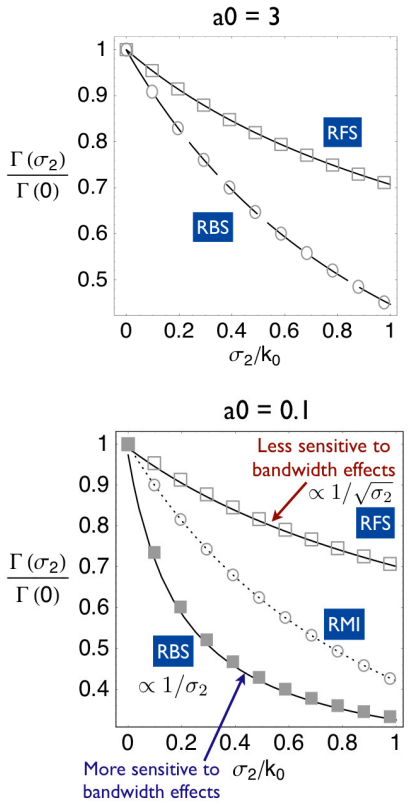

Figure 14.1 - Growth rate dependence with bandwidth for an asymmetric waterbag with k_0/k_p=80, and $\int_1$= 16 k_p c, in the relativistic regime (a_0=3, top panel), and in the weakly relativistic regime (a_0 = 0.1, bottom panel).

[1]Activities performed in the frame of the Contract of Associated Laboratory, out of the Contract of Association EURATOM/IST, by CFP staff of the "Grupo de Lasers e Plasmas".
[2]Work developed in collaboration with R. Bingham, Rutherford Appleton Laboratory, UK, and J.E. Santos, University of Cambridge, UK.
[3]Santos JE and Silva LO, J. Math. Phys. 46, 102901 (2005).
[4]Santos JE, Silva LO and Bingham R, Phys. Rev. Lett. 98, 235001 (2007).
[5]Work developed in collaboration with R. Bingham, Rutherford Appleton Laboratory, UK.

14.2.3. Derivation of a general dispersion relation for Stimulated Brillouin Scattering[6]

The increasing attention dedicated to nonlinear and collective effects such as solitons, vortices, self-organization and spontaneous ordering have turned parametric instabilities into a mandatory concern, reaching many fields of science. An approach to parametric instabilities based on a coherent wave description is clearly insufficient: most systems only achieve partial coherence and, in many others, incoherence is induced by fluctuations or external passive systems (such is the case of inertial confinement fusion, for example).

The Wigner-Moyal formalism of quantum mechanics provides a natural treatment of radiation in terms of its statistic description but, in its standard form, this theoretical framework is only valid for Schrödinger-like equations, allowing only the description of direct forward stimulated scattering. J. E. Santos *et al*[3,4], have recently developed a generalized Wigner-Moyal statistical theory of radiation, or generalized photon kinetics (GPK), formally equivalent to the full wave equation. This GPK could readily be employed to obtain a general dispersion relation for Stimulated Raman Scattering (SRS) driven by a spatially stationary radiation field with arbitrary statistics, which is valid for all ranges of coherence of the pump field.

In 2007, the properties of another white light parametric instability occurring in a plasma, the Stimulated Brillouin Scattering (SBS), were studied in detail. The monochromatic limit could be recovered from the general result, providing the correct values for maximum growth rates, as well as all the long studied features[7] of this instability. The general dispersion relation was numerically further explored, allowing a study of the growth rate of the instability as a simultaneous function of the bandwidth of the pump wave and the wavenumber of the scattered wave.

One particular case, that of the stimulated backscattering, was studied in more detail, as it is the one known to provide the highest growth rates. As expected, the results confirmed a strong dependence of the instability on the bandwidth of the radiation used as a driver. For a bandwidth of just 10% in terms of the pump wavenumber, the instability is already reduced to 1% of the plane wave limit (Figures 14.2 and 14.3), which justifies the use of bandwidth as a mean of significantly reducing the strength of this potentially deleterious instability.

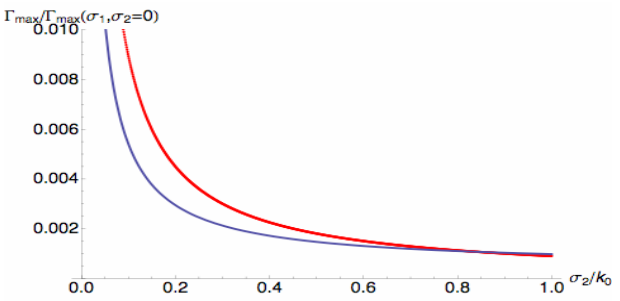

Figure 14.2 - Maximum growth rate of SBS as a function of the bandwidth of the pump wave (red – theory, blue – numerical).

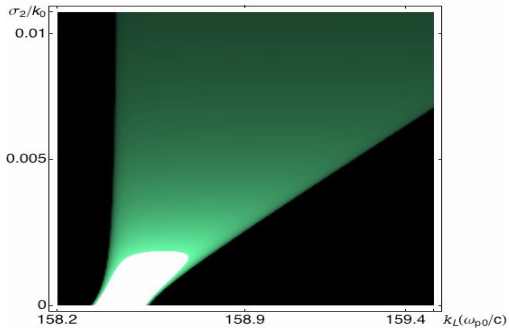

Figure 14.3 - Growth rate of SBS as a function of the bandwidth of the pump wave and the wavenumber of the scattered wave.

14.3. LASERS-PLASMA ACCELERATORS

14.3.1. All-optical trapping and acceleration of heavy particles[8]

Ultraintense lasers opened the way to compact acceleration of charged particles. Acceleration can be obtained either directly or indirectly, i.e., mediated by the interaction with a gaseous or solid target.

A novel method for direct acceleration of heavy particles has been developed, wherein the superposition of two lasers generates a beat-wave structure with slow phase velocity, which is capable of trapping and accelerating heavy particles (Figure 14.4). The phase velocity of the beat wave is regulated by varying the frequency of one of the lasers, allowing for optimal control of the particle beam features (e.g., final energy, energy spread, and total charge). The technique could find applications in the treatment of cancer with hadron beams, or in the ultrafast accelerations of muons in future neutrino factory and muon collider machines.

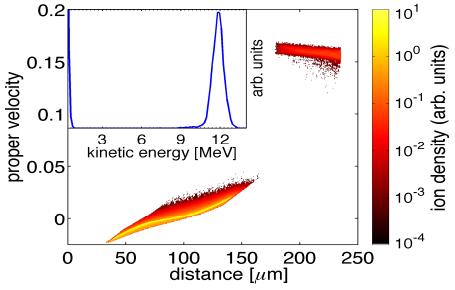

Figure 14.4 - Phase-space and energy spectrum after 6 ps using a fixed-frequency laser and a linearly chirped laser, and considering a hydrogen gas as a source of protons (results from two-dimensional particle-in-cell simulations with Osiris 2.0).

[6]Work developed in collaboration with J.E. Santos, University of Cambridge, UK.
[7]Kruer WL, in "The Physics of Laser Plasma Interactions", Addison-Wesley (1988).
[8]Work developed in collaboration with R. Mulas and G. Coppa, Politecnico di Torino, Italy, and R. Bingham, Rutherford Appleton Laboratory, UK.

14.3.2. Controlled injection of electrons in laser-driven plasma waves

Laser-wakefield accelerators (LWFAs) allows for the production of GeV electron beams on the cm scale[9]. A central problem in LWFAs is controlling the injection of electrons into the plasma wave (the wakefield) driven by the laser, e.g. by employing a counterpropagating laser pulse to suddenly heat part of the electrons promoting them to region of phase space where trapping by the wakefield is possible.

The dynamics of the colliding-pulse electron injection and the corresponding full-length acceleration has been simulated with one-dimensional simulations using Osiris 2.0, finding an excellent agreement with experimental data in terms of final electron energy. The simulation results revealed the central role of stochastic heating in the injection process and the importance of the drive-pulse evolution before collision (Figure 14.5). The analysis also suggested possible alternative injection techniques, based on localized plasma heating.

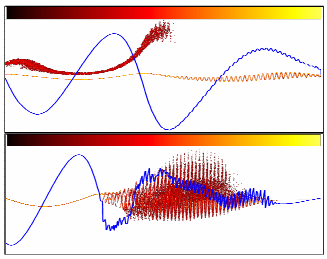

Figure 14.5 - Electron phase space (color scale) and electric field (blue line) during (top panel) and after (bottom panel) the pulse collision.

14.3.3. Nanoplasma expansions and dimensional collapse in Coulomb explosions[10]

A detailed understanding of the dynamics of the laser-driven expansion of nanoplasmas is important for applications ranging from the ultralocalized production of nuclear particles to the single-shot imaging of biomolecular samples via x-ray diffraction.

Ion acceleration in the expansion of spherical plasma has been analyzed with reduced kinetic models both in the presence and in the absence of hot electrons (pure Coulomb explosion of a bare ion sphere). In the latter case, a new shock solution has been found wherein all ions starting within a given three-dimensional region overtake each other at the same radial position at a given time (an occurrence named dimensional collapse), leading to high compression factors and to the possibility of time-resolved production of nuclear particles.

14.3.4. Self-steepening and self-guiding of intense laser pulses in underdense plasmas

The self-consistent evolution of laser pulses in underdense plasmas plays a major role in state-of-the-art Laser Wake Field Acceleration (LWFA) experiments. In these experiments, the plasma wave created at the entrance of the plasma does yet not satisfy the criteria for electron self-trapping. However, as the laser propagates, it self-modulates both in the transverse (self-focusing) and longitudinal (self-compression and self-steepening) directions. These self-modulations lead to the excitation of large amplitude plasma waves, thus leading to the self-injection of plasma electrons.

The early dynamics of a laser pulse in underdense plasmas was investigated with the photon-kinetic equations. The early motion of a single photon was primary determined, solving the ray-tracing equations for a general plasma refractive index. The early dynamics of the laser pulse was then obtained by inserting these results in the photon distribution associated with the laser. Using the one-dimensional plasma response to determine the plasma refractive index, threshold conditions for the on-set of the self-steepening of the laser pulse were retrieved (Figure 14.6). In addition, estimates for the ponderomotive force enhancement via pulse compression and amplification were obtained.

A similar analysis was employed to investigate the transverse dynamics of the laser pulse. By constructing an analytical model for the transverse plasma response in the long-pulse regime, self-guiding conditions in strongly relativistic regimes were determined.

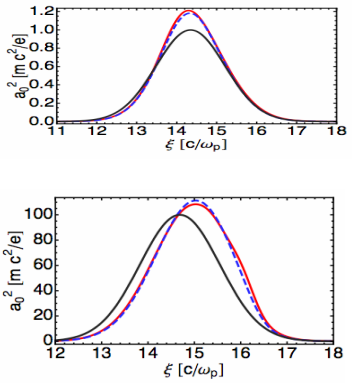

Figure 14.6 - Comparison between 1D Osiris 2.0 simulations (red curves) and the analytical model (blue) for the longitudinal propagation of a Gaussian laser pulse, for two different intensities and propagation distances. The black curves show the initial laser profile.

14.3.5. Ten-centimeter scale LWFA simulations with QuickPIC[11]

QuickPIC[12] is a reduced particle in cell (PIC) code, which

[9]Leemans W *et al*, Nature Phys. 2, 696 (2006).
[10]Work developed in collaboration with G. Coppa. Politecnico di Torino, Italy.
[11]Work developed in collaboration with C. Huang, W. Lu, M. Tzoufras and W.B. Mori, University of California-Los Angeles, US; J. Cooley and T. Antonsen Jr., University of Maryland, US.
[12]Huang C *et al*, J. Comp. Phys. 217, 658-679 (2006).

works under the quasi-static approximation, specially designed for the study of Laser Wake Field Acceleration (LWFA). This code can be two-three orders of magnitude faster when compared with a full PIC code like Osiris 2.0 and can thus be used to investigate the LWFA in longer propagation distances. Numerous full-scale simulations of LWFA were conducted, using laser and plasma parameters that will be available for the next LWFA experiments. The simulation parameters were chosen according to the scaling laws of Ref[13]. These scalings provide the most stable acceleration regime, in either uniform plasmas or plasma channels.

In the simulations, the stable self-guided propagation of a ~10 J laser pulses was observed (Figure 14.7). Since QuickPIC cannot model self-injection, the dynamics of an externally injected beam, placed at the end of the first plasma oscillation, was studied. The simulations showed stable acceleration of the externally injected electron beam, which accelerated to 1.7 GeV in a 2.3-centimeter uniform plasma, and to 4 GeV in a 20-centimeter plasma channel.

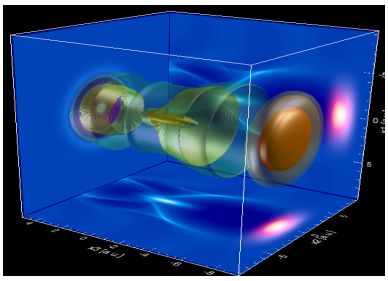

Figure 14.7 - QuickPIC simulation showing the plasma wave and laser, immediately after it entered the plasma. An externally injected electron beam is placed at the end of the first plasma wave.

14.4. FAST IGNITION AND LASER-SOLID INTERACTIONS

14.4.1. Proton acceleration above 300 MeV

Recent experiments and numerical simulations have shown that the interaction of high intensity ($I > 10^{21}$ W/cm^2) short laser pulses (~100 fs) with solid targets lead to the formation of collimated beams of ions with energies in the MeV range. The acceleration is either due to space charge effects in the back of the target, at low laser intensities ($I < 10^{19}$ W/cm^2), to collisionless shocks[14], at moderate intensities, and to laser-piston acceleration, for very intense laser pulses ($I > 10^{21}$ W/cm^2).

We explored the physics of the interaction of high intensity ($I > 10^{19}$ W/cm^2), long laser pulses (1 ps) with thin solid targets (~5 µm) with a pre-plasma layer, by means of particle in cell (PIC) simulations with Osiris 2.0 in one and two dimensions[14].

The simulations showed that, when the pre-plasma density scale length is comparable with the laser wavelength, the laser pulse accelerate a large fraction of the target protons to high energies, in the MeV range. The ions beams generated in such a process are neutralized by the cloud of high temperature electrons heated by the laser. In the simulations, all the targets had bulk densities well above the critical density ($n > 10^{21}$ cm^{-3}).

The simulations have also shown that, at very high laser intensities $I > 10^{21}$ W/cm^2, the laser pulse not only accelerates a large fraction of the target protons to very high energies, in the 100 MeV (Figure 14.8), but also that a fraction of the long pulse actually gets through the main target (Figure 14.9) and continuously accelerates the fastest ions to energies well above 300 MeV.

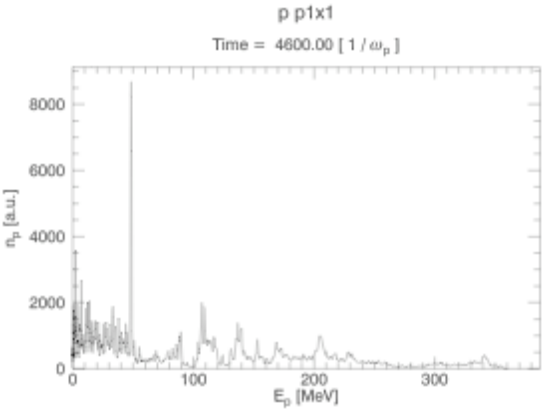

Figure 14.8 - Ion Energy Spectrum resulting from 1 ps, 10^{19}W/cm^2 laser pulse over a 5 µm thin solid target (results from 2D PIC simulations with Osiris 2.0).

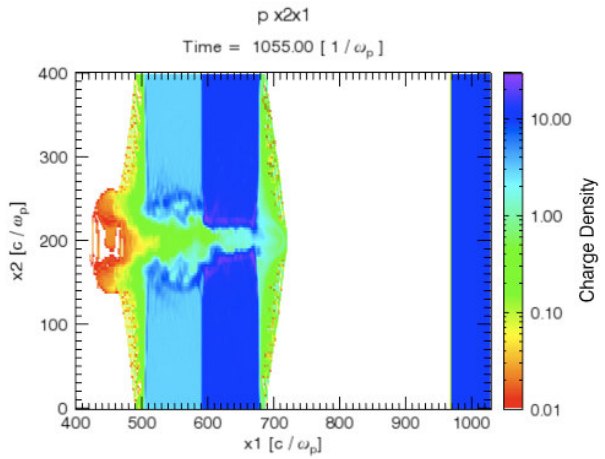

Figure 14.9 - Ion phase space during the interaction of a short laser pulse over a multiple layer target (results from two-dimensional particle-in-cell simulations with Osiris 2.0).

[13]Lu W *et al*, Phys. Rev. St Accel. Beams 10, 061301 (2007).
[14]Sorasio G, Marti M, Fonseca RA, and Silva LO, Phys. Rev. Lett. 96, 045005 (2006).

14.4.2. Hiper adventure

In the present analysis, we explored the physics of the interaction of high intensity, short laser pulses with multi-layer targets of various densities, by means of particle in cell (PIC) simulations with Osiris 2.0[15] in one and two dimensions. The targets were composed of two or three layers of fully ionized hydrogen slabs, with different sizes and different number densities.

The results have shown that, when the layer thicknesses are appropriate, multiple shock structures are formed, which develop in the transition regions between the layers. The shocks, that have different velocities, accelerate the ions inside the target creating a series of energetic ion beams. When the layer density decreases, the shocks move in the same direction. When the layer density does not vary monotonically, the shocks move one toward the others, creating region of interactions where the final ion temperature can reach values above 100 keV.

14.4.3. Enhancement of the filamentation instability due to collisions

In recent years, the filamentation or Weibel Instability (WI)[16] has been widely invoked in different scenarios, as a mechanism to generate magnetic fields in astrophysical events (e.g., Gamma Ray Bursters (GRBs)[17]), as well as a mechanism to enhance the coupling between the PW-laser driven electron beam and the ions in fast ignition (FI)[18].

Collisions can become important in the inner zones of the FI fuel pellet, while in the coronal regions of the target the plasma is collisionless. Thus, the transition from the collisionless to the collisional WI is crucial in FI scenarios, being the literature very poor on this subject. A non-relativistic analytical study[19] showed that the collisional WI always occurs, regardless of the transverse temperature. Since collisions tend to isotropize a system, one would expect the instability to be weaker when collisional effects are included. This apparently counterintuitive result has to be deeply examined to better understand the collisionless-collisional transition.

In order to check the predictions of a theoretical relativistic kinetic model including warm species, space charge effects and collisions through the particle number-conserving Bhatnagar, Gross, and Krook (BGK) model, large scale particle-in-cell (PIC) simulations have been carried out with Osiris 2.0[20] including binary relativistic collisions. Very high resolution one-dimensional simulations guaranteed that the numerical collision frequency was negligible. This simulation set-up led to a strong numerical noise reduction, allowing for a direct comparison between the theoretical and the numerical growth rate of the WI. The theoretical predictions are confirmed by the simulations, showing both the enhancement of the growth rate of the WI and the formation of filaments due to collisions larger than in the collisionless regime, consequence of the k_{max} shifting (wavenumber corresponding to the larger growth rate) towards smaller wavelengths (i.e., larger wavenumbers) (Figure 14.10).

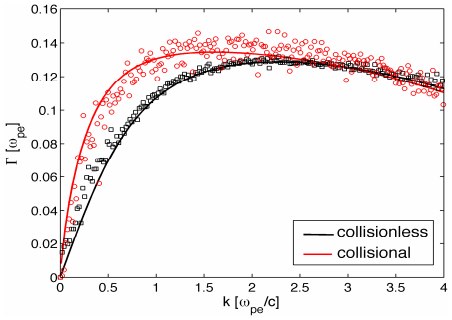

Figure 14.10 - Growth rate of the WI in the collisionless and collisional (ν_{ei}=0.57 ω_{pe}) regimes: theory (solid lines) vs simulations (markers).

14.4.4. Long-time evolution of the collisional filamentation instability

In order to study the long-time evolution of the transverse filamentary structure for time scales and length scales in the hybrid code range (time~ps, length~10's μm), one-dimensional long (t_{max} = 2000 ω_{pe}^{-1}) particle in cell (PIC) simulations, including binary relativistic collisions have been carried out with very high resolution. Filament generation, due to the linear phase of the Weibel Instability (WI), and filament coalescence after saturation have been numerically explored through simulations carried out with Osiris 2.0[20]. A preliminary study of the importance of the transverse filament coalescence dynamics, in different scenarios relevant for fast ignition, has been performed, by focusing the attention on the mean kinetic energy temporal evolution of the species. Beam electrons lose their kinetic energy by heating up plasma electrons and ions and feeding the magnetic field generated by the WI. Each filament coalescence dissipates a sizable fraction of the beam kinetic energy into the background species and magnetic field (14.11). Longer simulations are in progress to analyze the energy transfer from plasma electrons to ions through collisions.

14.4.5. PIC modeling of laser-plasma interactions for fast ignition scenarios

The study of the interaction of ultra-intense lasers with overdense targets (densities above the critical density n_c) is important for fast ignition scenarios[18]. In particular, to understand the coupling of the ignition laser and the transport of the accelerated electrons in the mildly dense

[15]Fonseca RA, Silva LO, Tonge J *et al*, IEEE Trans. Plasma Sci. 30, 28 (2002).
[16]Weibel ES, Phys. Rev. Lett. 2, 83 (1959).
[17]Medvedev MV and Loeb A, Astrophysics. J. 526, 697 (1999); Fiore M *et al*, MNRAS 372, 1851 (2006).
[18]Tabak M *et al*, Phys. Plasmas 1, 1626 (1994); Silva LO et al, Phys. Plasmas 9, 2458 (2002).
[19]Molvig K, Phys. Rev. Lett. 22, 1504 (1975).
[20]Fonseca RA *et al*, Lect. Not. Comp. Sci. 2331, 342 (2002).

region of the target. For such highly non-linear phenomena there is no theory and particle in cell (PIC) modeling appears as the main tool for its study.

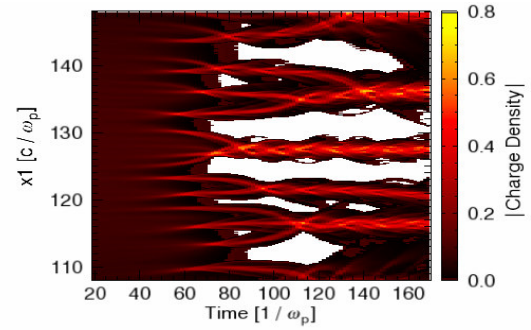

14.11 - Beam electron density temporal evolution: onset of the WI and filament coalescence.

The interaction of a PW laser pulse with a pre-ionized target has been studied resorting to two-dimensional PIC simulations that have been performed with Osiris 2.0[20]. A parametric scan of the target density and thickness has been carried out in order to understand the importance of these parameters for the laser energy absorption and for the electron filamentation in the target. The angular distribution of the relativistic electrons generated through the interaction of the PW laser with the preformed plasma has been studied. Preliminary results from PIC simulations show that the divergence angle of the filaments ranges from 20º to 30º for target densities ranging from 30 n_c to 10 n_c, respectively (Figure 14.12). For target densities of 10 n_c, laser filamentation has been observed along with electron filamentation in the target. At 30 times the critical density, laser filamentation does not occur, though electron filamentation has been observed.

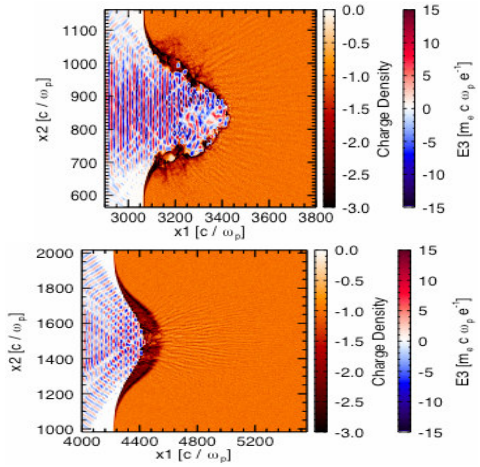

Figure 14.12 - Results from PIC simulations for the electron density (shaded) and laser electric field (contours) at the peak of the PW laser pulse using a 10 n_c 50 µm thick target (top) and a 30 n_c 50 µm thick target (bottom).

14.5. ASTRO AND SPACE PHYSICS

14.5.1. Solar energetic particle production in coronal mass ejection shocks[21]

Acceleration mechanisms of solar energetic particles are usually associated with Coronal Mass Ejections (CME) in the solar corona environment. CME structures propagate at speeds up to 2000 km/s, interacting with the slower solar wind and creating a shock. As the CME structures have a frozen-in magnetic field, both parallel and perpendicular shocks are formed with the solar wind.

Two simulation setups, mimicking the corona environment, were used to capture the physics of the accelerating particles. In the first scenario the solar wind flows quasi-parallel to the background magnetic field and a slab of plasma is shocked against the solar wind plasma. In the second more realistic scenario, the frozen-in magnetic field in the CME zone is also included. Simulations show the formation of Alfvèn-like waves upstream of the shock, in the solar wind, due to the quasi-parallel flow (Figure 14.13). These waves interact with the coronal mass ejection particles through wave-particle interaction, accelerating them mainly in the perpendicular directions through a surfatron like mechanism, but also in the shock direction.

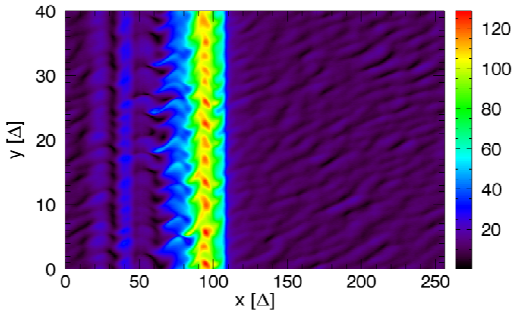

Figure 14.13 - Electric field intensity of a CME quasi-parallel shock showing wave formation in the solar wind. Quantities are expressed in normalized simulation units.

14.5.2. Energetic ion interaction with mini magnetospheres[22]

Solar energetic ions, originating from Coronal Mass Ejections and Solar Flares, have energies up to several GeV and are a known hazard to both spacecraft electronics and to manned space flights, particularly in space missions that extend over a long period of time like interplanetary missions. Laboratory experiments and simulations were performed to assess the feasibility of using a dipole like magnetic field, in conjunction with a plasma source, to provide effective means of protecting a spacecraft against solar energetic ions.

Preliminary experimental results show a plasma beam being deflected by a dipole like magnetic field generated by a permanent magnet, and a mini magnetosphere being generated (Figure 14.14). A simple theoretical model,

[21]Work developed in collaboration with R. Bingham, Rutherford Appleton Laboratory, UK.
[22]Work developed in collaboration with R. Bamford and R. Bingham, Rutherford Appleton Laboratory, UK.

balancing plasma dynamic pressure with the magnetic pressure from the dipole field, provides means of calculating the plasma standoff distance from the center of the dipole field. In the simulations performed with dHybrid[23], results show the plasma deflection distance increasing with the density and magnetic field intensity, and decreasing with the plasma flow velocity, as expected from theory.

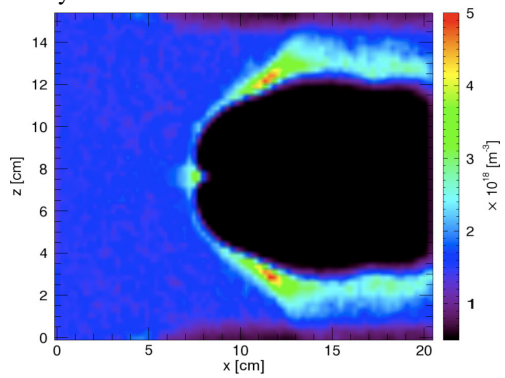

Figure 14.14 - Plasma density cut of the simulation of the laboratory experiment showing the plasma being pushed out of the dipole field region. Plasma is flowing from the left, and the magnetic moment of the dipole magnetic field is oriented in the +z direction.

14.5.3. Ultra-relativistic flows and particle acceleration in astrophysics

Ultra-relativistic flows are pervasive in astrophysics, leading to the formation of relativistic shocks, particle acceleration to extreme energies, and generation of intense radiation. Due to the strong nonlinear and kinetic effects, a self-consistent description of relativistic shocks and of particle acceleration in these nonlinear structures is still missing as one of the unsolved problems in astrophysics[24].

Leveraging on the new diagnostic tools for particle tracking available in Osiris 2.0, a detailed numerical study of these shocks was performed, identifying the critical regions of particle acceleration both in the precursor and shock-front regions (Figure 14.15).

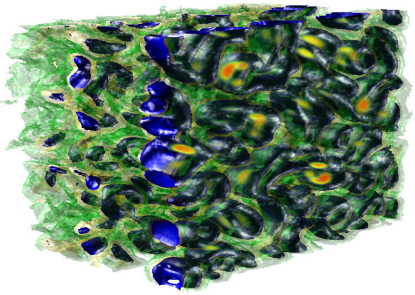

Figure 14.15 - Magnetic field energy for two electron-ion plasmas flowing through each other; current filaments and magnetic fields are generated by the Weibel instability.

14.6. HIGH PERFORMANCE COMPUTING

14.6.1. Particle tracking diagnostics in PIC codes

The field of laser plasma acceleration has witnessed significant development over recent years, with experimental demonstrations of the production of quasi mono-energetic electron bunches, with charges of ~ 50 pC and energies of up to 1 GeV[9]. These accelerators require no external injectors, and recently it has also been shown experimentally that the self-injection mechanism can be controlled[25]. Given the highly nonlinear and kinetic processes involved during high-intensity laser beam-plasma interactions, fully relativistic particle-in-cell (PIC) codes, such as Osiris 2.0[20] are the best tools for modeling of these physical problems. However, PIC codes *per se* are not enough and sophisticated visualization and data analysis routines[26] are required to extract physical meaning from the large volumes of data being produced.

A complete and detailed understanding of self-injection mechanisms in the Laser Wakefield Accelerator (LWFA) is yet to be achieved and to that end a detailed knowledge of single particle evolution in the accelerator is critical (Figure 14.16). To this end a particle tracking diagnostic was developed for Osiris 2.0[20], but that can be easily ported to work with other codes. Generally the simulation needs to be run twice; once to determine which are the particles worth tracking and a second time to save the actual tracking information. If only low temporal resolution is required these tracks can also be extracted from standard particle dumps.

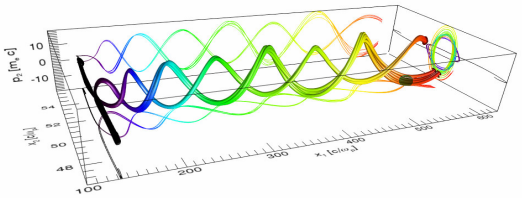

Figure 14.16 - Braided Trajectories in 3D phase space of injected particles in the LWFA.

Given that we are searching for groups of several hundreds of particles in a set of tens of millions, the main obstacle to this diagnostic was performance. Searching for the particles being tracked at every time step would represent an immense computational cost, especially when parallel issues are considered. To overcome this issue a novel technique was devised that effectively eliminates the overhead of particle tracking.

14.6.2. Data visualization environment

The present visualization and data analysis tools[26], available for use with our suite of codes, have been successfully applied to datasets ranging up to a Terabyte in size. However, despite representing a major leap in

[23]Gargaté L, Bingham R, Fonseca RA, Silva LO, Comput. Phys. Comm. 176, 419 (2007).
[24]Piran T, in "Unsolved Problems in Astrophysics", (eds. J. N. Bahcall and J. P Ostrker), Princeton: Princeton University Press, p. 343 (1997).
[25]Faure J *et al*, Nature 444, 738 (2006).
[26]Fonseca RA, Proceedings of ISSS-7 (2005).

scientific visualization for particle in cell (PIC) codes, these routines have some limitation in terms of interactivity and simultaneous representation of multiple datasets.

The new Data Visualization Environment being developed, while maintaining the previous ease of use and quick presentation quality plots, is being developed from scratch to address these issues (Figure 14.17). The visualization space can hold an unlimited number of data sources, and an unlimited number of visualization objects that represent them. As before, all annotations, including labels and units, are automatically generated from the metadata available in the input files, and the plot dimensions are set to better display all information. This new visualization environment also allows for interactive data analysis, such as Fourier transforms of grid data or data mining of particles, and for time navigation. Movie generation as also been improved, with all options being available interactively.

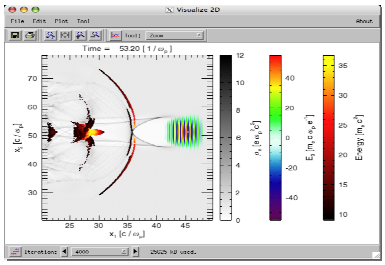

Figure 14.17 - New visualization toolkit, presenting multiple simultaneous datasets (density, laser field, and particles) and time navigation

14.6.3. IT infrastructure

A wide range of information technology (IT) infrastructure is installed and maintained by the our team. The current infrastructure ranges from computer and office networks over web-servers up to high performance computing (HPC) clusters. Services embedded into this infrastructures include desktop computing, web-hosting for the IPFN, GoLP, and epp web-pages, hosting and maintenance of code repositories, availability and access of HPC resources, storage and accessibility of simulation data, online diagnosis and management of the HPC infrastructure, and online visualization of intermediate simulation results.

14.6.4. IST Cluster

The IST Cluster is an IBM Cluster 1350 computing system consisting of seventy dual-CPU, dual-core Power5 JS21 blades with 2 GByte of memory per core, running the AIX 5.3 operating system, interconnected by dual gigabit Ethernet (Figures 14.18 and 14.19).

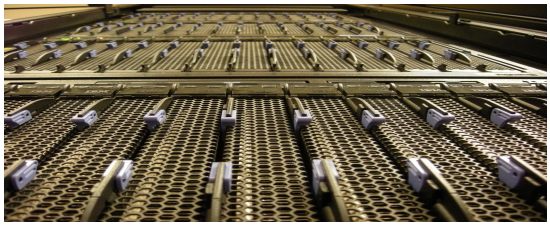

Figure 14.18 - Front view of the IST Cluster (picture: Michael Marti).

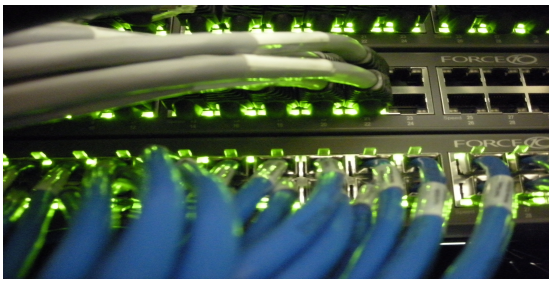

Figure 14.19 - Interconnect: one of the core components of a distributed memory machine (picture: Michael Marti).

Ever since the very beginning of the IST Cluster, members of our team showed a strong interest in this project. It is for this reason that our team provided and still provides a major part of the manpower and effort necessary for the installation, deployment and maintenance of the IST Cluster. Amongst the tasks done by our team during the installation and deployment phase are: basic hardware and software installation, setup and maintenance of a set of administrative scripts allowing for a decentralized user administration, preparation, test and deployment of the HPC core services (compilers, parallel libraries, performance libraries), configuration of the resource manager, definition and implementation of the policy structure for the job scheduler, and others. Ongoing tasks include: periodic hardware maintenance, software updates, fine tuning of user environments and policy settings, and naturally supporting the several users in the usage of the available infrastructure.

14.6.5. Exposing stream processors as Grid services with a GPGPU example[27]

Recent graphics processing units (GPUs) with single instruction, multiple data (SIMD) and multiple instruction, multiple data (MIMD) capabilities have shown to provide good performance not only on streaming applications as well as on applications that have sufficient parallelism and computational intensity to hide memory latency. Another SIMD/MIMD processor that has recently been introduced is the Cell Broadband Engine Architecture (Cell processor), from Sony, Toshiba and IBM (STI), which has shown tremendous potencial for the scientific community, in terms of performance and power efficiency[28]. Integrating such fine-grained stream resources in a Grid

[27]Work developed in collaboration with J.M. Pereira, IST/INESC-ID, Portugal.

system as a general computational resource or service is an important way to significantly increase a Grid's performance and computing power at very little cost.

As an integration example, we used the already tested simplified Boris particle pusher, which was previously adapted to general purpose computation on GPU (GPGPU) code[29]. This time, this GPGPU algorithm was implemented on commodity hardware that is normally used as part of a Grid node for plasma physics simulation. On one processor, we achieved 4–5 frames per second (fps), which is comparable to the performance on the CPU. Simulations run on a system with two Worker Nodes showed a very good performance gain, since this simplified Boris pusher requires a minimal node communication Figure 14.20). With 4 particles per cell (ppc) we achieved 8–9 fps with two GPUs and with 8 ppc the system kept a steady 4 fps. These results showed that it is very useful to expose the SIMD capabilities of GPUs on a Grid.

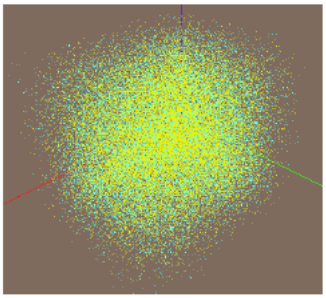

Figure 14.20 - Real-time visualization of the results of the GPGPU implementation of the simplified Boris pusher.

From a down-up approach, the first place to expose these capabilities is at the schema used to announce the Computing Element (CE) to the rest of the Grid. As specified in the GLUE schema specification[30], a processor type is described in the SubCluster entity, with specific attributes divided in two sub-entities: Software and Host. The host entity has attributes such as ProcessorModel, ProcessorInstructionSet and ArchitecturePlatformType, that can be used to uniquely define a SubCluster of GPU's (or other commodity stream processors). The attributes of the Software entity can further clarify the capabilities supported by the processor, giving extra granularity in selecting a correct software version or environment.

A SubCluster of this kind could have a dedicated queue, which means it would be visible to the outside as a set of job slots belonging to a certain CE. Another possibility is to assign this kind of SubCluster to a whole CE, which means that all the jobs slots of this CE would be for stream processing, thus defining a CE specific for streaming computation.

Acting at the schema level allows all the relevant parts possibility is to assign this kind of SubCluster to a whole which means that all the jobs of Grid middleware to have access to this information. Both the push model (where jobs are pushed to a CE and the pull model (where the CE asks the Workload Management Service for jobs) would work, and high-level application tools (such as P-GRADE or GENIUS) can easily be made aware of this kind of processors. Since the GLUE schema is widely used in Grids (e.g., in EGEE's gLite or in Globus), this approach is valid for different Grid middleware.

14.6.6. Remote visualization on the IST Cluster

A software system for remote visualization on the IST Cluster was implemented based on VisIt (Figure 14.21), an interactive tool for parallel visualization and analysis of scientific data from Lawrence Livermore National Laboratory, USA.

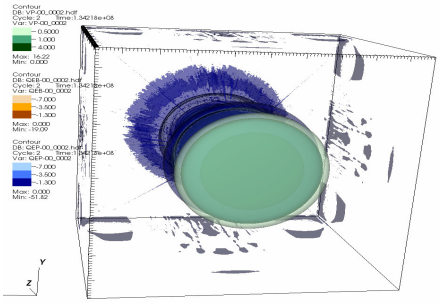

Figure 14.21 - Visit running on IST Cluster.

14.6.7. Hybrid code development for massively parallel applications[31]

Hybrid codes, using kinetic ions and a neutralizing electron fluid, are useful in space plasma scenarios, where the ion time scale needs to be properly resolved and the high frequency modes on the electron time/length scales are not thought to play a significant role. In dHybrid[23] we implement a space and time centered explicit hybrid algorithm, using massless electrons, neglecting the electron pressure term and neglecting the displacement current in Ampère's law. The algorithm is fully parallelized using spatial domain decomposition and employing the MPI libraries for inter process communication.

Space plasma simulation scenarios often lead to situations where there is a large particle imbalance between different volumes of the simulation space; the particle imbalance leads to severe loss of performance, some nodes finishing their calculations much sooner than other nodes. To boost performance, dynamic load balancing was added to dHybrid: parallel spatial partitions computational charge. Performance boosts up to 40% are achieved, depending on the problem in hand.

[28]Williams S, Shalf J, Oliker L, Kamil S, Husbands P, and Yelick K, "The potential of the cell processor for scientific computing", in CF '06: Proceedings of the 3rd Conference on Computing Frontiers, pages 9–20, New York, NY, USA, 2006, ACM Press.

[29]Abreu P, Pereira JM and Silva LO, "A Distributed Memory GPU Implementation of the Boris Particle Pusher Algorithm", in "Eurographics Symposium on Parallel Graphics and Visualization" 2006, Braga, Portugal.

[30]Andreozzi S, Burke S, Donno F, Field L and Fisher S, in "Glue Schema Specification", 2007, http://glueschema.forge.cnaf.infn.it/Spec/V13.

[31]Work developed in collaboration with R. Bingham, Rutherford Appleton Laboratory, UK.

14.7. COMPUTATIONAL PHYSICS

14.7.1. Monte Carlo simulations of relativistic collisions in plasmas[32]

The statistical analysis of many-particle systems in the relativistic domain is a fundamental research topic still lacking conclusive results. Even in the simple case of a dilute gas, describable by Boltzmann's equation, conflicting results on fundamental issues, such as the validity of the standard Jüttner distribution function (the "relativistic Maxwellian") repeatedly appear in the literature (cf.[33]).

The Monte Carlo simulation techniques developed at GoLP revealed the source of the conflicting results in the literature and provided a general recipe to simulate relativistic collisions in a way that is consistent with special relativity, thus always obtaining the Jüttner distribution function. Simulations with Osiris 2.0 confirmed the validity of the Jüttner distribution in ultrarelativistic scenarios.

14.7.2. Numerical studies with particle-in-cell codes in boosted frames[34]

A recent work by J.-L. Vay[35] demonstrated the possibility of reducing numerical simulation times by orders of magnitude, by performing the simulation in a Lorentz boosted frame. This scheme completely changes computational resources required for long simulations in several topics of state-of-the-art research, such as laser/plasma interaction, astrophysics relativistic outflows and undulator/wiggler modeling.

The necessary numerical algorithms for Lorentz transformation between relativistic frames and the specific diagnostics needed for data analysis were implemented in Osiris 2.0, for direct application in Laser Wakefield Plasma Accelerators (LWPA) and relativistic outflows simulations (Figure 14.22). The necessary time for processing was typically reduced by factors above one hundred.

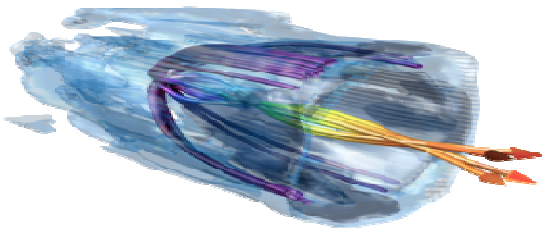

Figure 14.22 - Example of plasma "bubble" and particle injection in a boosted frame.

14.8. RADIATION GENERATION

14.8.1. Phase-matched even-harmonic generation in relativistic ionization fronts

In underdense plasmas, phase-matched second-harmonic generation is possible in the presence of a modulated magnetic field[36]. However, the required conditions for the magnetic field are demanding due to the short wavelength of the B-field modulation and the high B-fields required.

A novel scheme to generate even harmonics in uniform transparent plasmas has been studied. This scheme uses the magnetic mode[37] generated in the collision of electromagnetic radiation with a relativistic ionization front, driven by an intense laser pulse propagating in a gas target, to provide the magnetic field required for phase-matching.

A theoretical model has been developed, predicting the phase-matching conditions, describing the evolution of the amplitude of the second harmonic, and determining the features of the ionization front and of the colliding pulse required to generate a magnetic mode appropriate for relativistic even-harmonic generation.

In order to check the validity of the model, detailed one-dimensional and two-dimensional particle-in-cell (PIC) simulations have been performed with Osiris 2.0.

The analysis reveals a good agreement between the theoretical model and the simulation results. The magnetic mode has been observed to provide the required B-field for even-harmonic generation. The conversion efficiency of the process has also been studied, indicating the possibility of achieving controlled, short and intense, even-harmonic generation (Figure 14.23).

14.8.2. Radiation generation in the interaction of intense pulses with nanowires

Clusters, nanowires and other nano-structures represent an interesting medium to produce radiation by the irradiation of dense nanoplasmas with intense laser pulses. When small clusters or nanowires are hit by ultra-short laser pulses, their electrons can be completely removed or oscillate in the ion core potential, depending on the intensity of the laser field. This oscillatory motion of the electrons can lead to the generation of harmonic radiation[38,39]. The radiation emitted when a nanowire is hit by an ultra-short ultra-intense laser pulse (with 800 nm wavelength, pulse duration of ~3 cycles at FWHM and peak intensity 5×10^{19} W/cm^2) was studied using two-dimensional particle in cell (PIC) simulations performed with Osiris 2.0 and a power spectrum diagnostic[40,41].

---

[32] Work developed in collaboration with G. Coppa, Politecnico di Torino, Italy.
[33] D. Cubero et al, Phys. Rev. Lett. 99, 170601 (2007).
[34] Work developed in collaboration with W. Lu and W.B. Mori, University of California – Los Angeles (UCLA), US.
[35] Vay J-L, Phys. Rev. Lett. 98, 130405 (2007).
[36] Rax JM *et al*, Phys. Plasmas 7, 1026 (2000).
[37] Lampe M *et al*, Phys. Fluids 10, 42 (1978).
[38] Antonsen TM Jr. *et al*, Phys. Plasmas 12, 056703 (2005).
[39] Fomyts'kyi MV *et al*, Phys. Plasmas 11, 3349 (2004).
[40] Kazeminejad F, PhD thesis, UCLA (1986).
[41] Dawson JM, Rev. Mod. Phys. 55, 403 (1983).

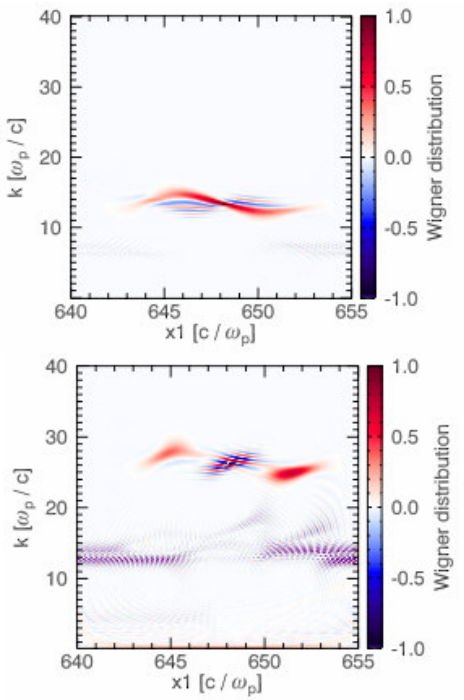

14.23 - Wigner distribution of the laser driver (top) and Wigner distribution of the second-harmonic (bottom) after a propagation distance of 767 μm.

It was found that in the case of thin nanowires (30 nm radius) the electrons are completely removed from the ion core by the laser pulse, generating a short-duration radiation burst as they leave. At these intensities, the ponderomotive displacement is so strong that it prevents the electron cloud from returning to the ion core and less than one oscillatory cycle is executed. The amplitude of the radiation generated is stronger in the direction of the velocity of the electron cloud as expected for relativistic electrons (Figure 14.24).

A parameter scan was performed to understand the influence of the electron density and the nanowire radius on the spectrum of the radiation, in particular as the diameter approaches the scale of the laser wavelength. Experiments performed with ethanol droplets hit by intense laser pulses have shown that submicron-scale targets interact differently from nanometer-scale clusters[42,43]. In the scenarios studied here, nanowires of 30, 100 and 300 nm radius and densities of ~2 n_{cr} and ~5 n_{cr} were irradiated by an ultra-intense ultra-short laser pulse (same parameters as above). In the cases of small or intermediate radius, results were similar. The electrons were removed from the cluster either in a single or multiple bunches, each of these generating a burst of radiation as they left the ion core. As for the larger nanowires, while in the 2 n_{cr} scenario the larger radius only resulted in more bunches being extracted, in the 5 n_{cr} case the laser was not able to remove bunches of electrons.

[42]Gumbrell ET *et al*, Phys Plasmas 8, 1329 (2001).
[43]Symes DR *et al*, Phys. Rev. Lett. 93, 145004 (2004).

Instead, a high electron density region was formed in the area first hit by the laser. The electrons from this region were transported along the nanowire surface accelerating to high energies (up to few MeV), radiating along this motion. Sub-wavelength electron density perturbations were also observed inside the nanowire as well as surface rippling.

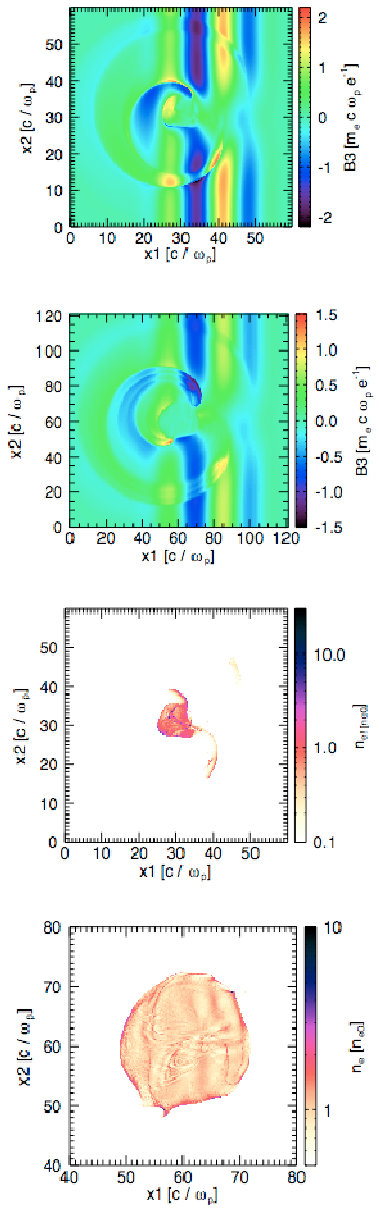

Figure 14.24 - Magnetic field in x3 direction (upper figures) and electron density (bottom figures) of clusters irradiated by an 800 nm wavelength 3-cycle laser pulse with peak intensity of 5×10^{19} W/cm^2; the targets are deuterium nanowires with a radius of 300 nm and electron densities of 1×10^{22} cm^{-3} and 4.6×10^{22} cm^{-3}.

The power spectrum of the radiation emitted following the irradiation of an array of periodically aligned thin (30 nm radius) nanowires by an ultra-short ultra-intense laser pulse was also studied (Figure 14.25). It showed an increase in the signal of the emitted radiation at multiples of the spatial frequency of distribution of the nanowires. This should be due to constructive interference of the radiation emitted by the different nanowires.

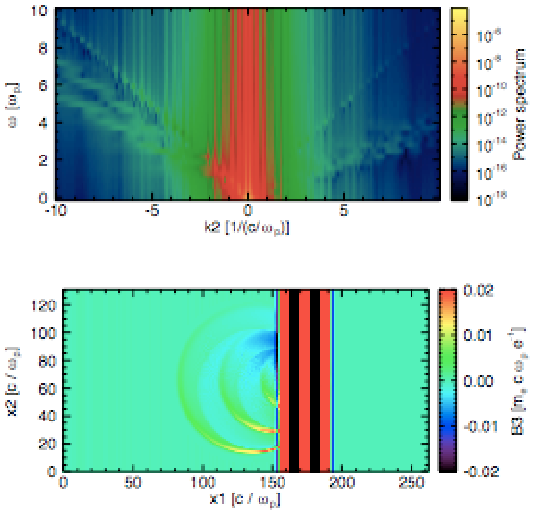

Figure 14.25 - On the upper, the magnetic field in x3 direction exhibits the radiation bursts generated as the laser hits successive nanowires. On the bottom, the power spectrum of the electromagnetic waves propagating perpendicularly to the laser pulse shows higher amplitude components at multiples of the spatial periodicity of the nanowires in the array.

15. HIGH DENSITY LASER PLASMA PHYSICS[1]

L.O. Silva (Head), J.R. Davies (Deputy Head) , M. Fajardo, F. Fiúza and J. Valente.

15.1. INTRODUCTION

The work on High Density Laser Plasma Physics was focused on:

- Design work for HiPER;
- Analysis of Results from Laser-Solid Experiments on the Vulcan PW;
- Filamentation in laser ablation of solids;
- Integrated numerical design of laser-plasma experiments.

15.2. DESIGN WORK FOR HiPER[2]

In collaboration with groups from Italy, Spain, the UK, France and Poland we prepared the "Fusion Science Case and Design" section of the "HiPER Technical Background and Conceptual Design Report", available in print and electronic versions at hiperlaser.org. This work was presented at the IFSA and APS conferences and will be published in a refereed journal in 2008. We also contributed to the successful preparatory phase proposal for the HiPER project (Figure 15.1). This 3 year preparatory phase should start in April 2008. We will lead the fast electron transport part of the fusion science work package.

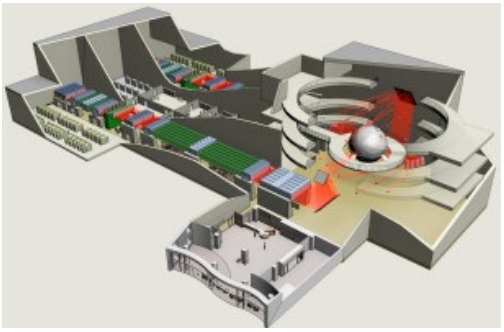

Figure 15.1 - Artists impression of the HiPER building.

15.3. ANALYSIS OF RESULTS FROM LASER-SOLID EXPERIMENTS ON THE VULCAN PW[3]

Analysis and numerical modeling of the HISAC results from 2005/6 was completed and an article has been prepared, which will be submitted at the beginning of 2008. Analysis of the results obtained from our Nov/Dec 2006 experiment is now well underway. Results from the K alpha imaging and the transverse probing have allowed us to infer the cone angle of the electrons accelerated into the target. Combined with previous results this clearly indicates that the cone angle increases with intensity and is unexpected result. This work has been accepted for independent of the spot diameter, a new and somewhat publication in Physical Review Letters. We have made a preliminary analysis of the results from the XUV imaging (Figure 15.2). The emission from all large area, plane solids is well characterized by a Gaussian, but the emission from 300×300 μm^2 plane solids has the same shape as the target and the result from the one successful shot with a 50 mg cm^{-3} silica aerogel target shows multiple, Gaussian peaks. This last result is particularly interesting, because it has been predicted that an electron beam in such low-density plasma should filament, but more detailed analysis and further experimental results are required.

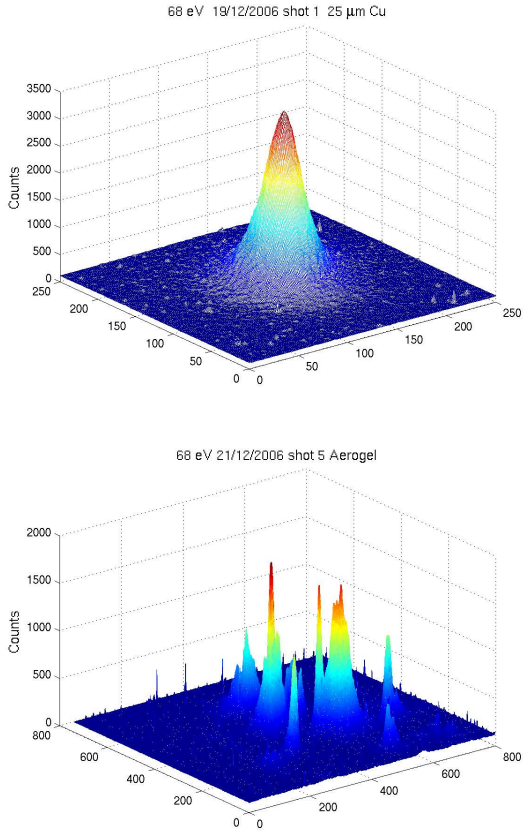

Figure 15.2 - A typical XUV image for a large area, plane solid target (top) and the XUV image for the aerogel target (bottom).

[1]Activities performed in the frame of the Contract of Associated Laboratory, out of the Contract of Association EURATOM/IST, by CFP staff of the "Grupo de Lasers e Plasmas".

[2]Work developed in collaboration with S. Atzeni and A. Schiavi, Italy; J. J. Honrubia, Spain; X. Ribeyre, G. Schurtz, Ph. Nicolai and M. Olazabal-Loumé, France; C. Bellei and R. G. Evans, UK; J. Badziak, Poland.

[3]Work developed in collaboration with M. Nakatsutsumi, Japan; J. S. Green and P. A. Norreys, Rutherford Appleton Laboratory, UK; T. Ma and F.N. Beg, University of California-San Diego, US.

We have analyzed the correlation of the size of the XUV spot in large area, plane solids with laser intensity, energy, pulse duration and spot diameter and with target thickness and areal density (thickness times density). This has shown that only the laser intensity and the areal density are determining factors. The spot size increases with increasing intensity and decreases with increasing areal density. The increase with intensity is consistent with an increase in cone angle with intensity, reinforcing our previous result. We are now investigating the physical mechanisms behind these correlations.

15.4. FILAMENTATION IN LASER ABLATION OF SOLIDS[4]

As part of our program on X-ray lasers, an experiment to characterize plasma production by a line focused, 80 J, 300 ps iodine laser was carried out at the "Prague Asterix Laser System" (PALS). This revealed filamentary structures at densities well below critical, but a uniform plasma at higher densities. This suggested to us the presence of magnetic fields, so we modeled the experiments using a two-dimensional MHD code. This accurately reproduced the experimental observations, as a result of the magnetic field diffusing from the critical surface, where it is generated, into the lower density plasma where the thermal pressure was lower than the magnetic pressure, leading to instability, as illustrated in Figure 15.3.

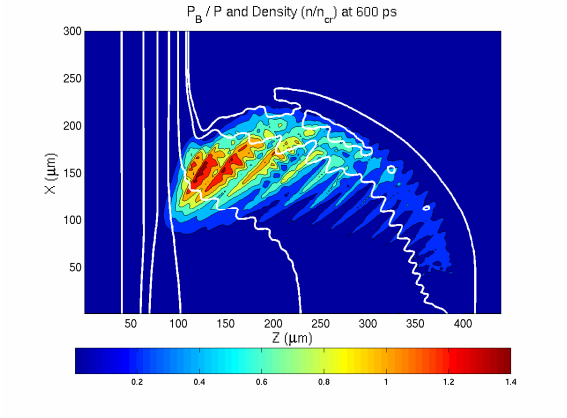

Figure 15.3 - The ratio of the magnetic pressure to the thermal pressure (shaded) and density contours at, from left to right, 1000, 100, 10, 1, 0.1, 0.01 and 0.005 times the critical density, after the laser interaction.

We have derived a dispersion relation for density perturbations perpendicular to a temperature gradient and an existing magnetic field that reproduces the essential features of the numerical results. This would appear to explain a large number of experimental observations of density filaments in laser-solid experiments. It is also of importance to fast ignition inertial fusion, because it has been proposed to use a ~ 100 ps laser pulse roughly a ns before the main compression pulse to achieve a low adiabat compression. This work is being prepared for publication. A proposal for an experiment on PALS to measure the magnetic field has been accepted.

15.5. INTEGRATED NUMERICAL DESIGN OF LASER-PLASMA EXPERIMENTS[5]

The high-power chirped pulse amplification (CPA) lasers, at Vulcan PW and at the "Laboratoire pour l'Utilisation des Lasers Intenses" (LULI) 2000, now have additional nanosecond beams, making it possible to carryout laser-*plasma* rather than laser-*solid* experiments by pre-heating targets. This will greatly facilitate a direct comparison with theory, avoiding the complications of ionization, degenerate electrons and strongly coupled ions, which are irrelevant for many applications. Not only that, it will also be possible to obtain plasma targets with densities between those of a gas and a solid by pre-heating and homogenizing aerogel or foam targets, which are basically porous solids. The homogenization time of such targets has been found to be almost a nanosecond, so the results of experiments such as that shown in Figure 15.2 maybe significantly affected by the target structure. With these developments in mind we have started a numerical study of laser-plasma experiments, modeling the target pre-heating using a hydrocode, the PW interaction with the pre-heated target using a particle in cell (PIC) code and the transport of the electrons accelerated deep into the dense plasma by the PW laser using a hybrid code. Some preliminary results are given in Figures 15.4 and 15.5. Such experiments should be able to demonstrate the theoretically predicted transition from filamented to stable electron beam propagation with increasing plasma density and would provide an excellent test of our modeling capabilities.

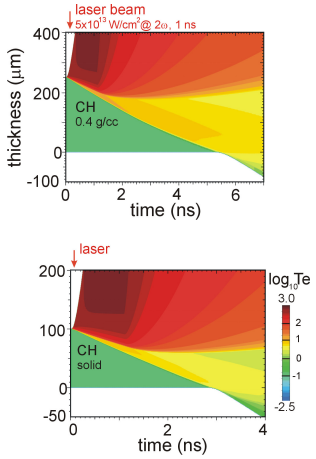

Figure 15.4 - 1D hydrocode results giving the target temperature as a function of space and time for (left) a 0.4 g cm^{-3}, 250 μm wide CH target and (right) a 1 g cm^{-3}, 100 μm wide CH target irradiated by a box pulse, with a rise time of 0.1 ns, a duration of 1 ns and an intensity of 5x10^{13} W cm^{-2}.

[4]Work developed in collaboration with B. Rus, Prague Asterix Laser System, Czech Republic.
[5]Work developed in collaboration with J. J. Honrubia, Spain

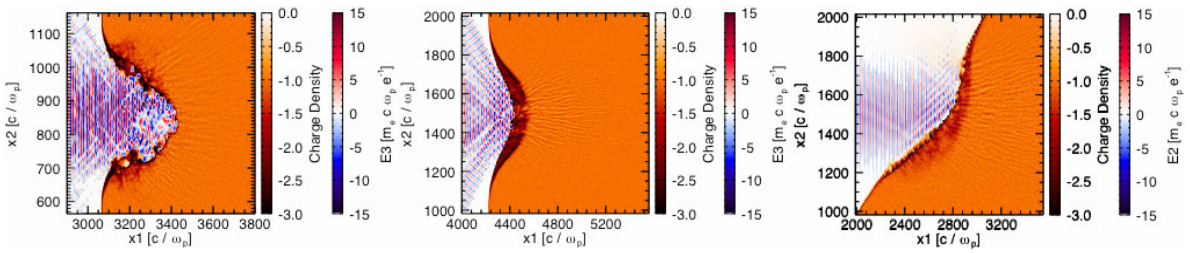

Figure 15.5 - PIC code results for the electron density (shaded) and laser electric field (contours) at the peak of the PW laser pulse. Left; 10 n_{cr}, 50 μm thick; Centre, 30 n_{cr}, 50 μm thick, Right; 30 n_{cr}, 100 μm thick, 45° angle of incidence.

16. HIGH INTENSITY PHOTONICS AND EXPERIMENTAL LASER-PLASMA INTERACTIONS[1]

L.O.Silva (Head), N.C. Lopes (Deputy Head), J.M. Dias, M. Fajardo, G. Figueira, D. Whittaker, E. Abreu, R.A. Bendoyro, L. Cardoso, F. Fiúza, N. Lemos, R.I. Onofrei, J. Wemans, J. Berardo, N. Cornet.

16.1. INTRODUCTION

The work in this field was developed along the following main topics:

- High-power laser research and development;
- Laser-plasma accelerator;
- Coherent x-ray sources;
- Laser-plasma interactions;
- Diagnostics;
- High-voltage pulse generator.

16.2. HIGH-POWER LASER RESEARCH AND DEVELOPMENT

16.2.1. Setup and optimization of diode-pumped Yb: glass and Yb:CaF_2 regenerative amplifiers[2]

The diode-pumped ytterbium project at the "Laboratório de Lasers Intensos" (L2I) was the subject of several improvements campaigns and modelling efforts in order to raise pump the intensity and overall performance. These included the ordering of the best performing diode stack available on the market for high energy and high intensity pumping, able to deliver 4 kW, 3 ms pulses at 10 Hz. This will allow an increase from the millijoule pulse energy from the current regenerative amplifier to the 100 mJ energy output. Together with the developed full modelling of the temperature, pump and amplification (Figure 16.1), we are now ready to push the experimental limits of some new and promising ytterbium-doped laser materials.

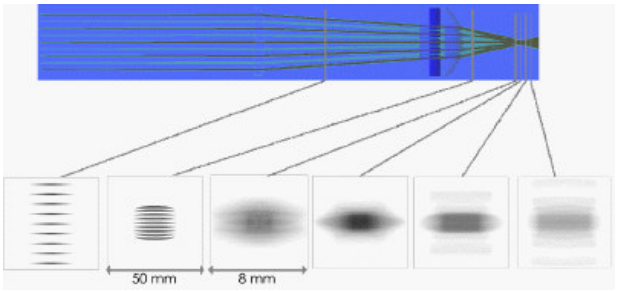

Figure 16.1 - Simulation of focusing light from a stack of diode bar. Above: use of two cylindrical lens and a spherical one. Below: beam profile at different planes.

Ray-tracing of the focusing of the high-divergence light from the diodes led to the optimisation of the focal spot and confirmation of the experimental evidence that spot diameters below 2 mm are not feasible with our diode stack and using only imaging optics.

Parallel to this work, we started investigating an innovative and promising technique for more efficient diode pumping schemes[3] in collaboration with researchers from "Universidade Nova de Lisboa (UNL), which allows for simpler, alignment and microlens-free diode pumping, and is scalable to high energies. The plan for experimental confirmation was defined and will be applied at L2I with the existing diode stack and a new ytterbium laser rod.

16.2.2. Optical parametric chirped pulse amplification

We obtained the first experimental confirmation of the validity and effectiveness of the concept of optical parametric chirped pulse amplification (OPCPA) of a signal pulse with angular dispersion, proposed earlier by ourselves[4]. This approach enables gain bandwidths up to 700 nm, extending even further the broadband nature of OPCPA. The experiment built on a previous attempt, which was limited by the finite reflectivity of the optical coatings used and the spectral response of the CCD camera. The signal pulses are generated by sending 4 nJ, 100 fs pulses at 1053 nm, produced by the L2I oscillator through a length of photonic crystal fibre (Crystal Fibre SC-5.0-1040), resulting in the output spectrum shown on top of Figure 16.2.

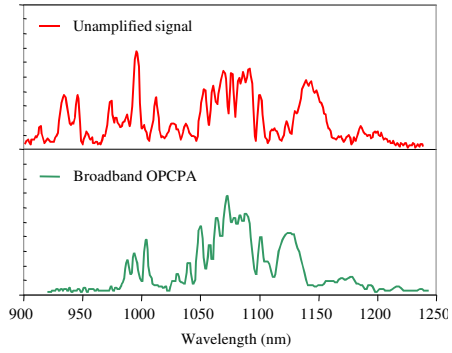

Figure 16.2 - Spectra for OPCPA of signal pulses with angular dispersion. Top: input pulse, bottom: broadband amplified pulse.

This pulse was angularly dispersed by using a single-pass, 150 l/mm grating pair to provide a beam lateral chirp, which was then focused at the entrance surface of a 5 mm long BBO crystal. The pump pulse was generated from a synchronized Ti:sapphire regenerative amplifier, seeded by a fraction of the original oscillator pulse. The 2 mJ pulses at 10 Hz were frequency doubled in another BBO crystal,

[1]Activities performed in the frame of the Contract of Associated Laboratory, out of the Contract of Association EURATOM/IST, by CFP staff of the "Grupo de Lasers e Plasmas"
[2]Work developed in collaboration with M. Siebold, Institute for Optics and Quantum Electronics (Jena), Germany
[3]Liang D and Pereira R, Opt. Comm. 275, 104 (2007).

spatially filtered and relayed to the crystal surface. We compared the amplified spectra with (bottom of Figure 16.2) and without angular dispersion, obtaining evidence that the gain bandwidth in the latter case is clearly larger than the 150 nm conventionally possible. Even broader bandwidths are possible by using a higher pump power, while keeping the gain on the order of 10^4 per pass.

16.3. LASER-PLASMA ACCELERATORS

16.3.1. Pre-formed plasma channel devices[5]

A laser-plasma electron accelerator uses an intense ultra-short pulse laser to produce relativistic acceleration structures in plasma targets[6]. These structures can sustain electric fields in the GeV/cm range and are created in the laser beam focal zone where the laser is intense. The acceleration length can be increased from a few mm to longer than a few cm, by using pre-formed plasma channels[7-11]. In this way, it is possible to increase the electron bunch energy from about 100 MeV to the GeV range and above[12]. A pre-formed plasma channel consists in cylindrically symmetric plasma with a parabolic profile and a minimum density on axis. Such plasma can be seen as a graded-index optical fiber for intense lasers. It can be produced by the hydrodynamic expansion of a plasma line produced by a laser pulse in a gas background or by a high-voltage discharge.

Our team aims the development of pre-formed plasma channels to be used in GeV and above electron accelerators. We intended to generate reproducible plasmas with the adequate radial geometry and a length in the range 1-20 cm, close to the maximum acceleration length (depending of the plasma density). Moreover, they should be compatible with the accelerator operation in high vacuum; allow optical access to the plasma for diagnostics or high-power beams; allow interesting repetition rate and device lifetime; be compatible with future applications. This development program was initiated, at IST, in 2006. In 2007 we have characterized the plasma generated inside the devices and demonstrate guiding of low power laser beams.

A schematic of the device used in these experiments is shown in Figure 16.3. The length between the conic electrode apexes is 17 mm, the thickness of the dielectric plates is 250 micron, and the diameter of the apertures in the electrodes and dielectric plates is 300 micron. The gas (hydrogen) is injected from the bottom through individual gas ducts for each cell. The gas injection conductance is much higher than the gas leak through the electrode apertures, limiting the amount of non-ionized gas in the laser path. The electrodes are cooper made and the device keeps working after more than 20000 discharges. The tungsten electrodes. The device is connected to the high-voltage pulser by a 125 Ohm home-made coaxial cable.

The interface between this cable and the device is made by 20 cm leads. Optical windows on both sides provide the optical access to the plasma channel and seal the device cells that will be connected by the apertures or by a much longer path through the gas injection ducts. The pulsed gas injection uses a fast gas valve that opens about 20 ms before the discharge. The initial plasma line is produced by applying a negative ns-rise-time high-voltage pulse at one of the electrodes. The dielectric apertures constrain the position and size of the initial plasma line. The pulse current heats the plasma that expands evolving to the required density profile.

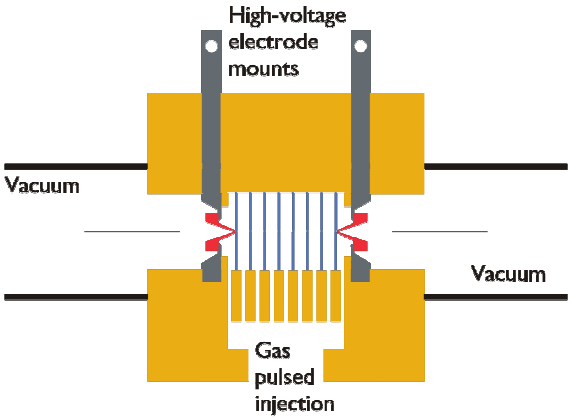

Figure 16.3 - Schematic of the plasma channel device.

16.3.2. Plasma channel density measurement and guiding demonstration[5]

The feasibility of the guiding scheme under investigation was experimentally demonstrated by measuring the plasma density evolution by interferometry and by measuring the guided focused beam spot radius at the channel exit, for a set of experimental parameters.

The experimental setup can be seen on Figure 16.4. In this experiment we have used the "Laboratório de Lasers Intensos" (L2I) laser system at IST. We have used the 10 Hz laser beam produced by the system front end with an approximate energy of 1 mJ/pulse. The wavelength is 1.053 μm and the pulse duration 300 fs. The laser beam is divided in a main beam (red) for beam propagation measurements and into another probe beam (orange) used for plasma density measurement by transverse Mach-Zehnder interferometry through the device transparent windows. Fresh gas (H_2) is injected every new shot into the

[5]Work developed in collaboration with C. Clayton and F. Fang, University of California-Los Angels – Electrical Engineering, US.
[6]Tajima T and Dawson JM, Phys. Rev. Lett. 43, 267 (1979).
[7]Lopes NC, Figueira G, Silva LO *et al*, Physical Review E 68, 035402 (2003).
[8]Durfee CG and Milchberg HM, Physical Review Letters 71, 2409 (1993).
[9]Buttler A, Spence DJ, and Hooker S, Physical Review Letters 89, 185003 (2002).
[10]Volfbeyn P, Esarey E, and Lemmans WP, Physics of Plasmas 6, 2269 (1999).
[11]Fang F, Clayton CE, Lopes NC *et al*, Proc. Advanced Accelerator Concepts: 12th workshop, AIP 721 (2006).
[12]Leemans WP, Nagler BA, Gonçalves J *et al*, Nature Physics 2, 696 (2006).

device by a fast valve. The synchronization of the discharge and the laser is made by a custom made electronic system with sub-ns accuracy, using a low jitter scheme. For each shot we grab images of the transmitted beam and the interferometry beam taken by CCD cameras. We also acquire scope traces of the discharge current and voltage signals as well as of the gas pressure measured by a fast sensor placed in the gas feeding tube.

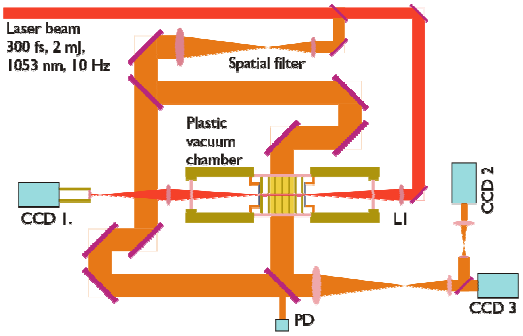

Figure 16.4 - Experimental setup for interferometric plasma density measurement and channel laser guiding at moderate intensities.

In Figure 16.5 we can see two low magnification pictures of the plasma lines taken at two different times, 25 ns (a) and 42 ns (b), after current start. These are interferometry pictures, but due to the low magnification only the shadowgraphy effect of the plasma in the probe beam can be seen. These pictures were obtained using high-voltage pulses with ~77 kV and ~ 614 A, as well as a maximum background gas cell pressure of ~ 120 mbar.

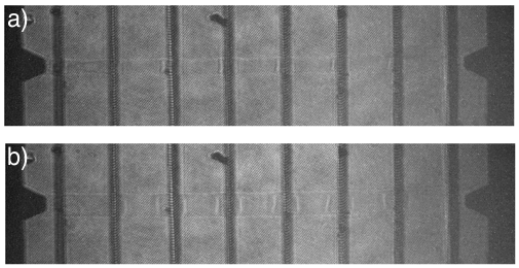

Figure 16.5 - Low magnification interferometry images showing the shadowgraphy of the plasma line created by the discharge, with delays of 25 ns (a) and 42 ns (b).

In Figure 16.6 we can see the interferometry detail of one of the cells obtained by optical magnification of the images shown in Figure 16.5. It is possible to extract the plasma density from an area inside the cell, using an automatic phase retrieval technique followed by Abel inversion.

In Figure 16.7 we present a lineout of the plasma density obtained by treatment of the interferogram shown in Figure 16.6. This image was obtained with a low pass filter on Fourier Space so non-physical oscillations are eliminated.

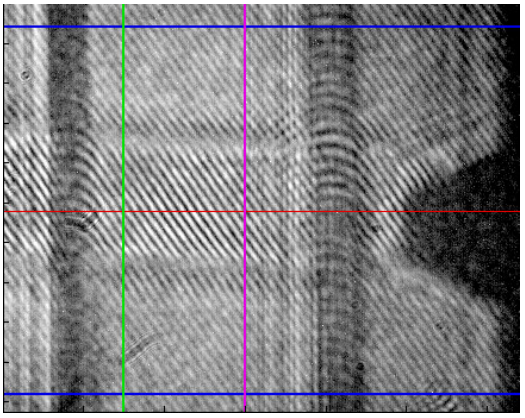

Figure 16.6 - Interferogram obtained for a plasma with a delay of 75 ns after the start of the current rise.

The retrieved density shows a close fit to parabolic profile with a density on axis of about 3×10^{17} cm^{-3}, a diameter of about 500 micron and a channel depth of about 1×10^{18} cm^{-3}. The density on the axis is compatible with a dephasing length of about 12 cm and a maximum energy gain of about 8 GeV for an acceleration length matching the dephasing length.

Preliminary guiding experiments were performed using plasmas with parameters similar to the ones of Figures 16.6 and 16.7. In Figure 16.8.a) we can see an image of the laser beam taken at channel exit when there is no plasma. We can see that the beam suffers multiple reflections inside the device structure. In Figure 16.8.b) we present an image taken in the same conditions as 16.8.a) but this time we have produced a plasma channel inside the device. The plasma used was very similar to the one presented in Figure 16.6 obtained with 80 ns plasma expansion. The focal spot diameter at capillary entrance was ~52 µm. The spot diameter obtained after guiding in Figure 16.8.b) is ~46 µm. The transmission beam data as well as the plasma density data are consistent with a transmission close to matching guiding. However, this needs to be confirmed by more extensive guiding data or by transverse Thomson scattering using high-energy pulses.

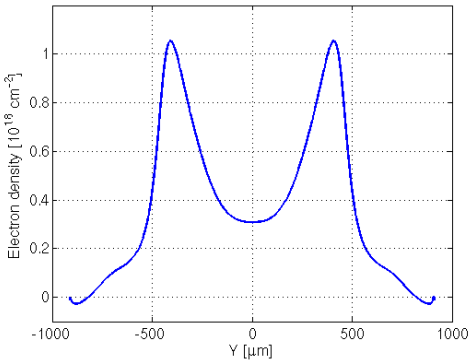

Figure 16.7 - Line-out of the plasma density obtained from the interferogram of Figure 16.6.

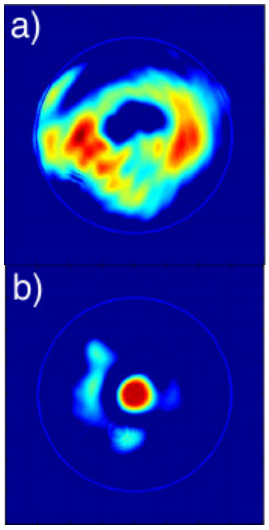

Figure 16.8 - Images of the transmitted beam at device exit (cathode aperture) with a) no plasma and b) a plasma channel produced by a discharge with a 80 ns delay. A circle on the aperture position was drawn over the image. The exit spot diameter on b) is 46 μm.

16.4. COHERENT X-RAY SOURCES

16.4.1. High harmonic generation at L2I[13]

High Harmonic Generation is a nonlinear process in laser-gas interaction that produces coherent radiation up to the XUV range[14]. This low-power, laser-like radiation source, with a broadband, frequency comb spectrum, has produced the shortest pulse durations – attosecond – on record. In 2007 we have produced and detected High Harmonic Generation at "Laboratório de Lasers Intensos" (L2I) for the first time.

In an experimental campaign in June 2007, the L2I Nd:YAG IR laser, amplified to around 50 mJ, with a pulse duration of 300 fs, was focused by a 500 mm achromat onto an 8 mm Ar gas jet at 20-50 torr pressure. An XUV spectrometer consisting in a 1000 lines/mm gold transmission grating, a grazing incidence, platinum coated, spherical mirror of 10 m radius, and an 1024×1024 pixel XUV back-thinned CCD, imaged the XUV source at a 1:2 magnification. Differential pressure was used to separate the XUV spectrometer housing from the main interaction chamber, to protect the components from oil contamination (Figure 16.9). The IR beam was filtered by a 1500 Å aluminum foil, which has an overall 50% transmission in the 17-70 nm window.

XUV spectra were obtained in two configurations. Using the non-apertured IR beam, with a total energy of 35 mJ and an intensity on target of 10^{15} W/cm^2, Ar XUV emission spectrum resulting from ionization up to Z=2, in the 17-50 nm range, was recorded. A clear cutoff from the Al L-edge filter is present on the right side of the spectrum in Figure 16.10.

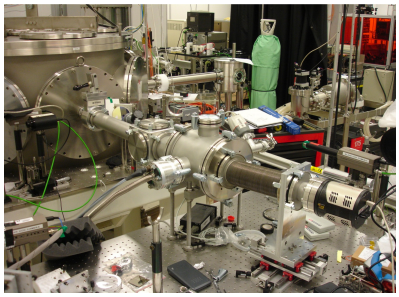

Figure 16.9 - XUV spectrometer and main interaction chamber at L2I.

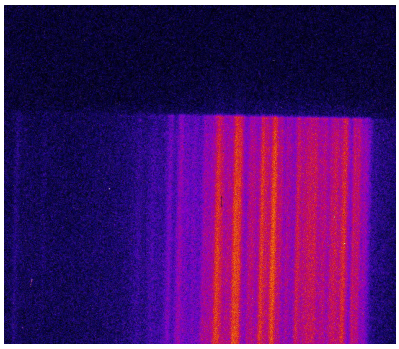

Figure 16.10 - XUV emission spectrum of Ar at 10^{15} W/cm^2 irradiation.

An aperture of variable diameter was placed on the IR beam path for an optimal control of the interaction, limiting the incident energy and increasing the spot size up to 50 μm, producing an intensity around the threshold of 10^{14} W/cm^2, below ionization, where high harmonics are generated. Optimization of the total high-harmonic output was made in the 0-order, imaging configuration of the spectrometer, by varying the aperture diameter and the position of the lens. Harmonics up to the order 51 (20.6 nm for our 1.053 μm laser) were observed (Figure 16.11).

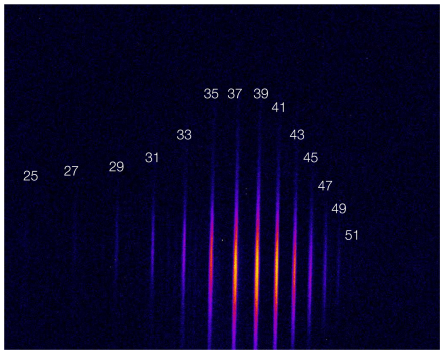

Figure 16.11 - High harmonic generation spectrum at L2I on an 8 mm Ar gas jet, with identification of harmonic order.

[13]Work developed in collaboration with D. Douillet and G. Rey, Laboratoire d'Optique Appliquée, France; M. Kozlova, Prague Asterix Laser System, Czech Republic.

[14]Gibson EA, "Quasi-Phase Matching of Soft X-ray Light from High-Order Harmonic Generation using Waveguide Structures", PhD Thesis, University of Colorado (2004).

16.4.2. Design of quasi-phase matching in high harmonic generation

High harmonic generation up to harmonic order 51 has been achieved at "Laboratório de Lasers Intensos" (L2I) in June 2007. The final aim is to generate harmonics of higher order, which requires a better phase matching between the fundamental and the harmonic beam. Higher harmonic generation requires higher ionization of the plasma, which leads to an enhanced plasma dispersion effect, making phase matching techniques impossible. Harmonics generation can nonetheless be enhanced, for higher orders, by quasi-phase matching techniques, which periodically turn harmonic generation on and off.

When harmonics are generated in a waveguide, quasi-phase matching can be done in several ways: varying the radius of the waveguide, to cause a periodic change in the intensity of the fundamental laser[15]; counter-propagating a less intense beam, which interferes with the harmonics generating beam, to periodically vary the laser intensity on the gas[16]; uncoupling the incident laser and the waveguide entrance, to excite several waveguide modes and thus modulate the laser intensity[17]. When no waveguide is present, quasi-phase matching can be achieved by varying the gas or electron plasma density, to make the laser propagate in a periodically modulated medium[18].

At L2I, an electron density variation will be implemented in the high harmonic generating setup. Two lasers will be made to interfere, which gives rise to an interference pattern (Figure 16.12), where the spatial period of the fringes, Λ, is set by the angle between the lasers, as shown in Figure 16.13. Both arms are focused into a line focus by a pair of cylindrical lenses. For L = 10 cm and D = 1 m, a 0.24º angle leads to a fringe spacing of Λ = 250 μm; increasing the angle to 1.21º makes the spacing as small as Λ = 50 μm. For comparison, quasi-phase matching in waveguides is limited to Λ_{min} = 250 μm.

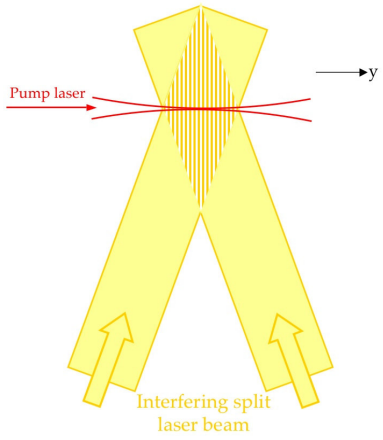

Figure 16.12 - Interference of two laser beams, which gives rise to an electron density modulation in the gas.

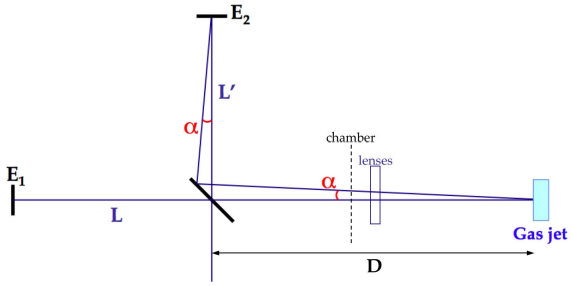

Figure 16.13 - Experimental setup for modulated irradiance with controlled interference period on a gas jet.

16.4.3. Population kinetics of laser-produced plasmas[19]

The first experiment, described above, is designed to enhance a particular harmonic order. The final aim is to achieve harmonic generation from ions, along with the modulated density quasi-phase matching technique, in order to extend the harmonics energy cutoff.

For plasma-based x-ray lasers, simulation work is crucial to optimize conditions for lasing with high gain and short pulse durations. In 2007 we initiated a program to incorporate time-dependent routines to predict quantum state populations into the Arwen two-dimensional hydrodynamic code. The rationale for doing so is to determine plasma conditions suitable for producing ultra-short pulses of EUV / X-ray radiation during experiments scheduled for autumn of this year. It is important to assess (i) the degree of accuracy required and (ii) approximations that can be made without undermining this significantly. Many of the routines have been or are in the process of being written, and it will simply remain to incorporate them into the program itself. In the meantime, other options are available to assist in the design of the experiment.

High intensity pulses in the XUV are defined as those greater than 10^{16} $Wcm^{-2}s^{-1}$ and ultra-short is defined by timescales of less than 100 fs (the current record for a plasma-amplified pulse being ~ 2 ps). Analysis already performed suggests that these should, indeed, be deliverable using a seeded plasma amplifier with 'engineered' plasma conditions to maximize collisional line broadening. This reliance on collisional broadening constitutes a major change in strategy to maximize pulse bandwidth. It is motivated by the conclusion that saturation re-broadening will almost certainly not be observed due to a combination of (i) a high Lorentzian component (because of collisional broadening) dominating the wings of the profile and (ii) homogenization of the Gaussian component of linewidth (the form attributable to Doppler broadening) due to frequent velocity-changing collisions over the timescale of interest.

[15]Christov IP *et al*, Optics Express 7, 362-367 (2000).
[16]Voronov SL *et a*l, Physical Review Letters 87, 133902 (2001).
[17]Zepf M *et al*, Physical Review Letters 99, 143901 (2001).
[18]Shkolnikov PL *et al*, Physical Review A 50, R4461 (1994).
[19]Work developed in collaboration with P. Velarde, Universidad Politécnica de Madrid, Spain, and P. Zeitoun, Laboratoire d'Optique Appliquée, France.

It is crucial, though, that conditions do not render gain insignificant – this places an upper limit on electron density of ~ 10^{21} cm^{-3} – beyond which collisional de-excitation depletes the upper lasing level too strongly. Simple estimates to predict the extent of collisional broadening have already been made and, despite their simplicity, predictions are in very good agreement with experiment[20]. Figures 16.14 and 16.15 show the predicted linewidth and intensity, both with and without seeding, as a function of distance into a Ne-like Se plasma amplifier for (i) the experimental conditions of Koch *et al*. and (ii) a lower temperature and higher electron density, for which the gain and linewidth having been recalculated accordingly. Bearing in mind that the gain obtained today is typically much greater than that of the neon-like laser used by Koch *et al*., results are promising.

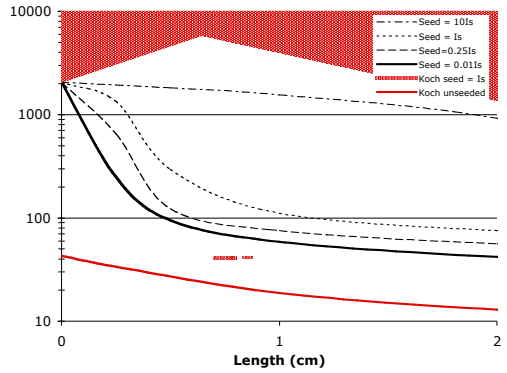

Figure 16.14 - FWHM as a function of plasma length for T_e = 450 eV and $N_e = 8x10^{20}$ cm^{-3} and 'Koch conditions'.

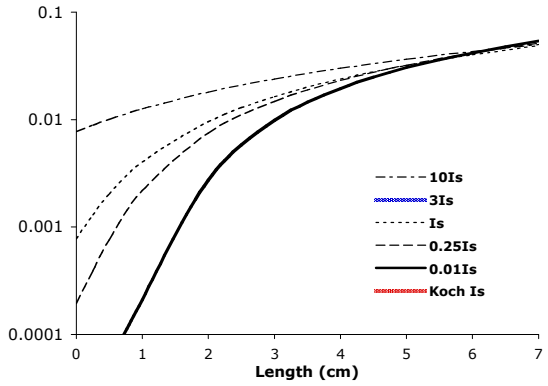

Figure 16.15 - Peak intensity as a function of plasma length for T_e = 450 eV and $N_e = 8x10^{20}$ cm^{-3} and 'Koch conditions'.

16.5. LASER-PLASMA INTERACTIONS

16.5.1. Formation of plasma channels by ultra-short laser pulses

Many laser-plasma experiments benefit from a longer interaction length, which can be achieved by guiding the laser pulse in pre-formed plasma channels. Several schemes have been proposed and tested but one of the most promising schemes is the thermally driven laser-induced plasma expansion. In this scheme, a laser pulse creates a plasma column, which heats and expands, creating an on-axis depletion of the density. This plasma profile can be used to guide a second laser pulse, behaving as a plasma optical fiber.

Until recently it was thought that short intense pulses were inefficient at heating plasmas, since the collision frequency is reduced for large quiver velocities. Recent preliminary results[21] show that, due to stochastic heating and the Weibel instability, tunnelled ionized gases can heat the plasma enough to create a good plasma channel[22].

In order to study plasma channels created by ultra-short laser pulses an experimental setup was prepared at the "Laboratório de Lasers Intensos" (L2I). A high power laser propagated across an 8 mm supersonic gas jet, produced by a Laval nozzle. To characterize the generated plasma channel, we used a diagnostic that could provide both interferometric and shadowgraphic measurements at the same time. Using an automatic fringe-pattern analysis code, it was possible to calculate the density profiles of the acquired interferograms. By making use of a long delay line it was possible to make a temporal study of the channel evolution. As shown in Figure 16.16, an 8 mm plasma channel was created, which expanded 55 μm after 8.67 ns. This was corroborated through one-dimensional simulations using the Osiris 2.0 code in the *epp* cluster. With a short laser pulse such as the one used in the experiments, we were able to demonstrate that through the ionization process the plasma can be heated long enough to allow channel formation. From the experimental data of the parabolic profile of the channel, the calculated matched laser spot size was 36 μm, suitable for guiding very intense laser beams.

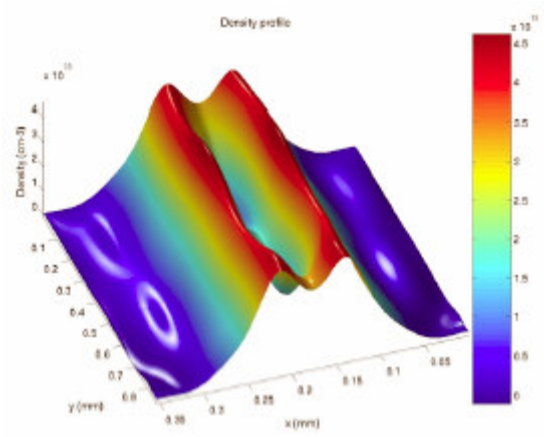

Figure 16.16 - Density plot of a Mach 6 nozzle with P_0=20 bar.

[20]Koch JA *et al*, Phys. Rev. A, 50, 1877 (1994).
[21]Dias JM. *et al*, Laser and Plasma Accelerators Workshop 2007, Azores, (2007)
[22]Leemans WP *et al*, Phys. Rev. Lett. 68, 321, (1992)

16.5.2. THz characterization and generation[23]

The search for relativistic mirrors in the optical domain is one of the challenges in new tunable and ultra-short coherent radiation sources from laser-plasma interactions. In order to create these relativistic mirrors we can interact electromagnetic waves with a relativistic ionization front. Focusing in vacuum an intense, short laser pulse on a high-density gas jet will generate a relativistic front by optical field ionization along its propagation through the background gas. However, the difficulty of producing a total reflection relativistic mirror by the ionization front is the low cutoff frequency given by the relativistic factor of $1/r^2_{mirror}$, for the typical plasma densities.

The current possibility of generating low frequency THz radiation sources produced by femtosecond laser pulses opens up the possibility of achieving the reflection conditions needed to obtain a relativistic mirror using ionization fronts. In order to investigate this approach, we assembled an experimental setup for producing and characterizing THz pulses at the laboratory "Terahertz to Optical Pulse Source" (TOPS) at the University of Strathclyde (Glasgow). The THz radiation was created using a photoantenna of GaAs. Applying a high-voltage and irradiating the surface of the semiconductor (GaAs) with the fs laser pulse makes it become conductive, accelerating the electrons and producing photons in the THz frequency region. The generation of these single-cycle THz pulses, triggered by the same laser driving the ionization front, allows us to fully collide the THz pulse with the counter-propagating ionization front.

For the detection and characterization of the THz pulse two electro-optic techniques were used: spectral encoding and cross-correlation[25]. In both techniques, a THz and a chirped laser pulse are passed through an electro-optic crystal (ZnTe). The electric field of the THz pulse will change the refractive index of the crystal on one axis, inducing birefringence and changing the polarization of the chirped laser pulse. This way, the THz electric field leaves a "fingerprint" on the chirped laser pulse. The detection of this "fingerprint" is what differs in the two detection methods used. With the first one we obtain a time-to-frequency conversion, by impressing the temporal evolution onto the spectrum of the chirped beam, which is then measured by a spectrometer. The second one is a higher temporal resolution, single-shot method, which directly measures the amplitude of the encoded chirped pulse, by using a cross-correlation measurement technique upon a β-barium borate (BBO) crystal. The results of both methods reveal that the pulse duration is 500 fs and the central frequency is 0.2 THz (Figure 16.17).

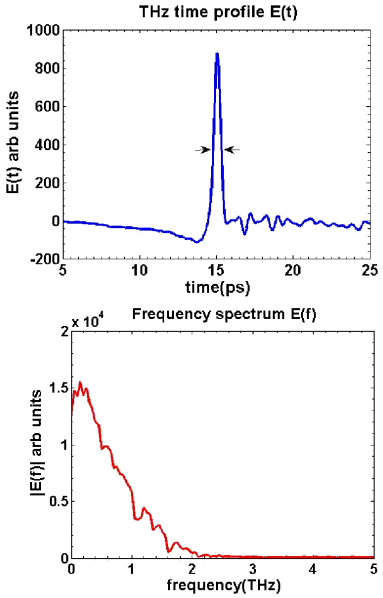

Figure 16.17 - THz time and frequency characterization.

16.6. DIAGNOSTICS

16.6.1. Single-beam interferometer and shadow diagnostic for laser-plasma interactions

Two of the most common diagnostics in laser-plasma interactions are interferometry and shadowgraphy. With the interferograms one can calculate the density of the plasma, and shadowgrams allow us to obtain the precise shape of the plasma. Apart from the interferograms, common interferometric setups also allow one to obtain the shadowgrams produced by the plasmas. The problem with this kind of setups is that they normally rely upon two independent arms (one through the plasma and another as a reference) and it is only possible to use one diagnostic at a time. With this in mind, we developed a new compact single-beam interferometer that uses just one beam passing through the plasma, and thus was able to retrieve both interferometry and shadowgraphy simultaneously. As shown in Figure 16.18 the resulting images only show interference in half the beam aperture, allowing the remaining half, in one of the beams, to be used for obtaining the shadowgraphy.

In order to obtain faster and better results in the laboratory, a program for acquiring data using digital or analog CCD cameras, with different interfaces, was developed (Figure 16.19). Several cameras are used for different types of diagnostic, such as interferometry and shadowgraphy. The objective of this program is to enable the use of several parallel cameras at the same time, in just one experimental setup, and this system has already been tested with success. To complement this program, a calculus platform was created to obtain important conclusions in real time.

[23]Work developed in collaboration with G. Gallacher, J. Sun, C. Issac and A. Jaroszynski, University of Strathclyde (Glasgow), Scotland.
[24]Jiang Z *et al*, Appl. Optics, 37, 8145-8146, (1998).
[25]Jamison SP, Opt. Lett., 28, 1710-1712, (2003).

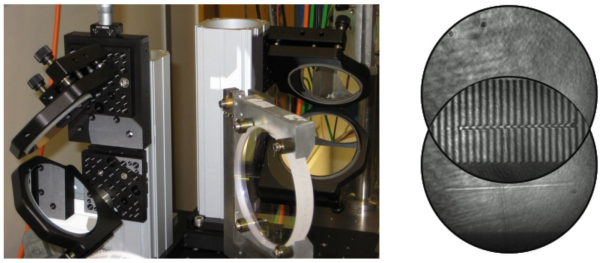

Figure 16.18 - Interferometer that delivers interferometry and shadowgraphy at the same time.

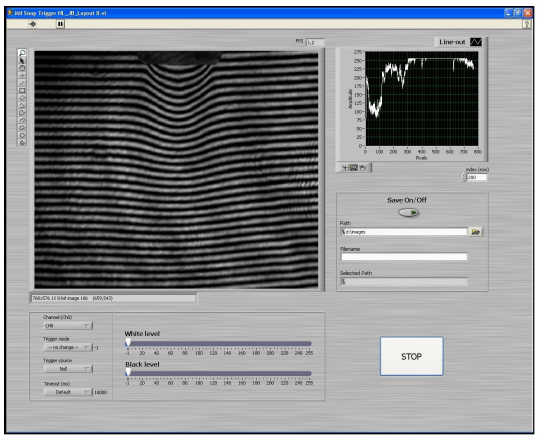

Figure 16.19 - Data acquisition and calculus program developed.

16.6.2. Plasma refraction[26]

The information that one can usually retrieve from a shadowgraphy diagnostic is limited to the plasma shape. Considering the refractive effects in the shadow image, a detailed analysis of the image formation can also enable us to obtain more information, such as an estimate of the plasma density and structure.

A study of laser propagation through a plasma with a refractive index gradient has been performed, using a ray-tracing simulation program and mathematical software. A Gaussian density profile was simulated to understand physical phenomena. With careful analysis it can be concluded that the plasma acts as either a convergent or a divergent lens, depending on its density profile (Figure 16.20). Simulation results were compared with theoretical values[27] to pinpoint the focusing distance of the optical system, enabling the density profile of the plasma to be deduced.

16.6.3. Suite of diagnostics for high power laser pulses

Owing to the need expressed by researchers performing high intensity laser-plasma experiments using the "Laboratório de Lasers Intensos" (L2I) laser to obtain systematic data about each laser shot, a permanent suite of diagnostics was installed before and after final pulse compression.

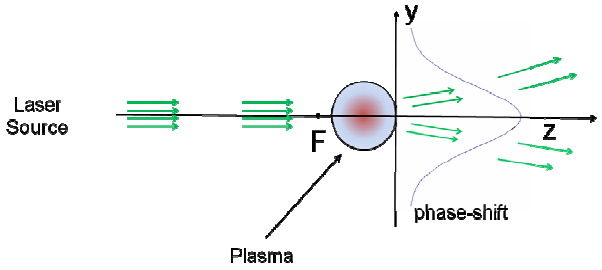

Figure 16.20 - Plasma acting like divergent lens when crossed by coherent light source.

The diagnostics include a calibrated photodiode for energy measurement, a near-field CCD camera for monitoring the beam profile before compression, a far-field CCD after the compressor for alignment stability and monitoring of focused beam profile, a radial shearing interferometer, and a second-order single-shot autocorrelator. The CCD images are obtained by imaging a leak through high-reflectivity mirrors. For the compressed pulse diagnostics, a tuneable fraction of the compressed beam is leaked through the turning mirror after the second grating and sent through a vacuum window and a removable beam elevator. The effects of compressed pulse propagation through this window and the subsequent air path were calculated in order to minimise the nonlinear distortions upon the probed pulse (Figure 16.21).

Additionally, a 6-channel video switch and a LabView-based image acquisition program developed in-house allow fast recording of any image, without the need for synchronised triggering. These additions, together with a set of new alignment references and monitoring, have allowed a considerable improvement in the efficiency of both the laser maintenance and the experiments.

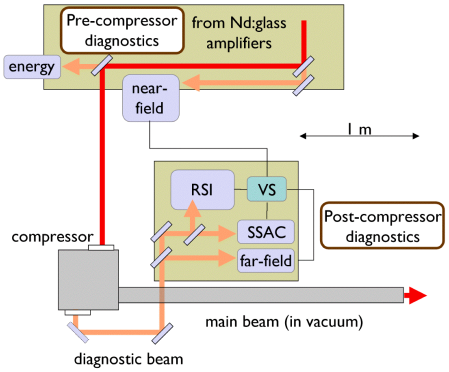

Figure 16.21 - Schematic view of diagnostics setup. RSI: radial shearing interferometer; VS: video switch; SSAC: single-shot autocorrelator.

[26]Work developed in collaboration with C. Clayton, University of California – Los Angeles, US.
[27]Behjar A *et al*, J. Phys. D: Appl. Phys. 30, 2872-2879 (1997).

16.7. HIGH-VOLTAGE PULSE GENERATOR[28]

The previous experiments on plasma channel generation by high-voltage discharges, performed in 2006, allowed us to conclude that we could produce good quality plasma channels, but not with the required sub-ns jitter for precise laser pulse injection. This jitter was due to the non-reproducible way the plasma was initiated. In order to overcome this problem we decided to add a magnetic compressor to the system in order to provide a reproducible voltage in the device gap in the moment the discharge was initiated. This consists of a new section of coaxial transmission line added to the existent cable. The new schematic of the whole pulse generator can be seen on Figure 16.22. The pulse compressor is a 40 cm section of coaxial cable with ferrite toroidal cores (Ferroxcube ref. BD3/1/4S2), displaced around the inner conductor substituting part of the PTFE dielectric. This magnetic material needs to be biased with a DC current (37-80 A depending of the pulse voltage) before each shot. A robotic arm is used to apply this current safely between shots.

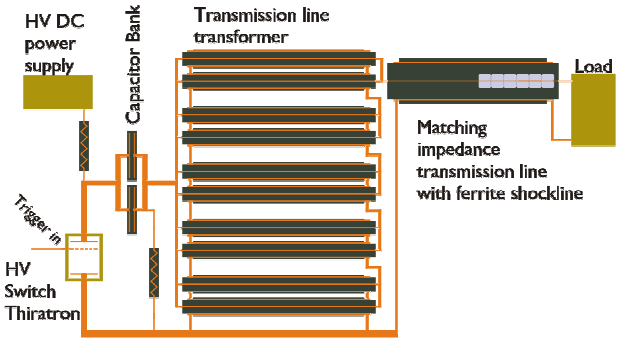

Figure 16.22 - Scheme of the high-voltage pulse generator including the new magnetic compressor added to the 125 Ω transmission line.

In Figure 16.23 we can see the oscilloscope traces produced in a typical shot with magnetic bias. The current rise-time (red) doesn't follow the voltage rise (blue) due to the device inductance. The voltage rise-time shown in Figure 16.23 is ~ 5 ns, close to the limit of the oscilloscope bandwidth. Shorter rise-times can be achieved by extending the length of the magnetic compressor. However, the introduction of this compression section reduced the jitter to less than 1 ns our initial goal.

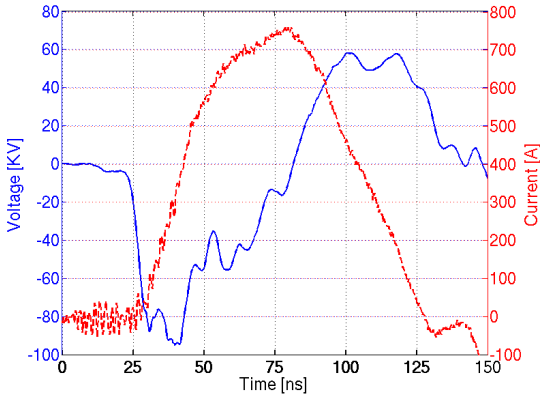

Figure 16.23 - Voltage obtained by ddot signal integration (solid blue), and current measured using a pulse transformer (dashed red).

[28]Work developed in collaboration with C. Clayton, University of California – Los Angeles – Electrical Engineering, US.

17. FUNDAMENTAL PHYSICS AND QUANTUM COMPUTING[1]

L.O. Silva (Head), O. Bertolami (Deputy Head), T. Barreiro, C. Carvalho, A.M. Martins, J. Paramos, C. Bastos.

17.1. INTRODUCTION

The work in this field has covered several topics, namely:

- Pioneer anomalous acceleration;
- Alternative models of gravity;
- Dark energy and dark matter;
- Putative violations of fundamental symmetries of nature;
- Quantum computing.

17.2. PIONEER ANOMALOUS ACCELERATION

The unexpected Doppler shift detected in the telemetry data of the Pioneer 10 and 11 spacecraft can be interpreted as an anomalous acceleration of the order of 8×10^{-10} m/s^2. The study of the potential systematic effects is being carried out by several groups throughout the world, but so far no concrete evidence has been found. This suggests that the anomalous acceleration might be a new physical effect; in this respect, many proposals have been advanced, from new gravity models to a new scalar field[2].

In 2007, our group participated in two proposals submitted in the context of the Cosmic Vision 2015 - 2025 call for missions of the European Space Agency (ESA), whose aim was to confirm and characterize the Pioneer anomaly. The main feature of the first proposal, Odyssey mission (Figures 17.1 and 17.2), is to incorporate in its payload a state of the art accelerometer to directly measure accelerations and contrast with Doppler shift readings. Beyond Jupiter, the main body of Odyssey launches a radio beacon experiment to carry on acceleration measurements and to extend the life of the mission.

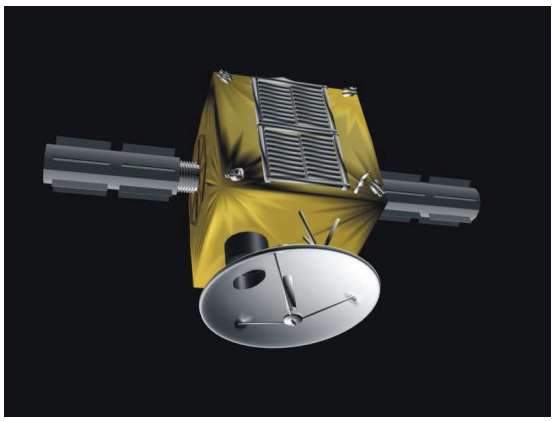

Figure 17.1 – Artistic impression of Odissey

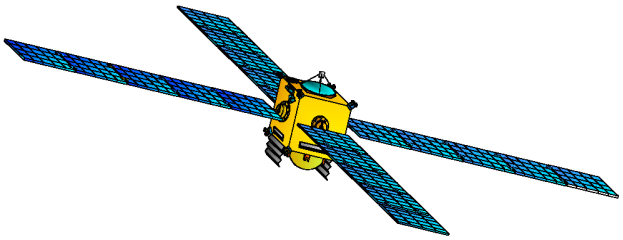

Figure 17.2 – View of Odissey

The second proposal search for anomalous gravitation using atomic sensors (SAGAS), is based on measurements of gravitational fields, by comparison of the frequencies of a clock on board with clocks on Earth and on the International Space Station. The sensitivity and the expected life span of the mission would allow it to make relevant measurements of the gravitational field of the Kuiper belt, which in turn could help to sort out the nature of its structure[3].

In 2007, we have also carried out a study of the systematic effects affecting a hypothetic mission where accelerations would be measured through laser ranging of spheres launched by the mother spacecraft.

17.3. ALTERNATIVE MODELS OF GRAVITY

Our study of alternative models for gravity has taken a new turn, by considering the possibility of directly coupling a function of the scalar curvature with the matter Lagrangian. This new coupling implies that the motion of a test particle is not geodesic, and opens the possibility of addressing the dark matter and Pioneer anomaly problems in the context of this new class of gravity theories.

It is particularly interesting that our model presents features that are similar to some well discussed, but somewhat *ad hoc* and problematic, alternative gravity models, such as Modified Newtonian Dynamics (MOND)[4].

In the context of alternative gravity models, we have also considered the possibility of testing extensions of general relativity through the Galileo satellite constellation.

17.4. DARK ENERGY AND DARK MATTER

In 2007, our work on dark energy and dark matter has focused on the detection of their interaction. We found that this interaction would affect the virial equilibrium of stationary clusters. The Abell cluster A586 (Figure 17.3),

[1]Activities performed in the frame of the Contract of Associated Laboratory, out of the Contract of Association EURATOM/IST, by CFP staff of the "Grupo de Lasers e Plasmas".

[2]Bertolami O and Páramos J, Class. Quant. Grav. 21, 3309-3321 (2004).

[3]Bertolami O and Vieira P, Class. Quant. Grav. 23, 4625-4635 (2006).

[4]Bertolami O and Páramos J, "Current tests of alternative gravity Theories: The Modified Newtonian Dynamics case", Nov 2006. 12pp., Presented at 36th COSPAR Scientific Assembly, Beijing, China, 16-23 Jul (2006), e-Print: gr-qc/0611025.

composed by thousands of millions of years.

Actually via the so-called Layzer-Irvine equation, that accounts for the interaction of dark matter and dark energy, we have found that the ratio between kinetic to potential energy densities is away from the expected -1/2 value at 1-sigma level. Furthermore, we found evidence that this interaction does affect the fall of dark matter into dark matter so that it differs, on cosmological scales, from the fall of baryons into baryons. This evidences a violation of the Equivalence Principle.

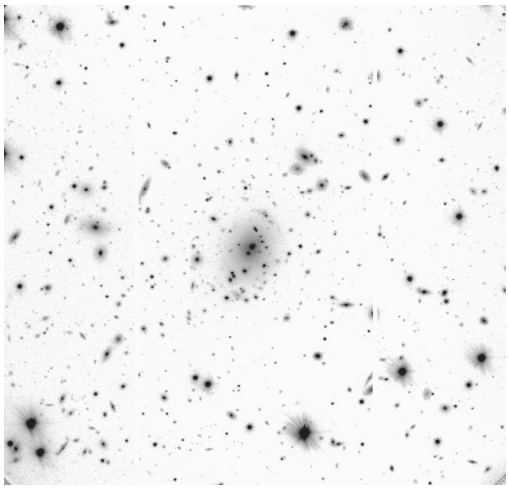

Figure 15.3 – The massive strong-lensing cluster Abell586

In 2007, we have also considered models of dark energy and dark matter at a fundamental, quantum field theory level, in opposition to the fluid description considered in most of our work so far. We have studied, in particular, models where the dark energy field is a Standard Model singlet field and couples to the Higgs sector and to the neutrino sector. In the former case, we found that this coupling opens the possibility of indirect detection of the dark sector via its effect on the decay width of the Higgs field. This is particularly relevant as the detection of the Higgs field and the study of its decay modes is a top priority of LHC at CERN, which will start operating in a few months time. In what concerns the coupling with neutrinos, we have devised a perturbative approach that allows us to consistently treat the coupling of neutrinos with a large class of dark energy models. Our analysis shows that many of these models are free from instabilities, which were diagnosed due to an unsatisfactory treatment of the problem.

17.5. PUTATIVE VIOLATIONS OF FUNDAMENTAL SYMMETRIES OF NATURE

In 2007, we have continued our work on the connection between the physics in the bulk 5-dimensional space and the one on our 4-dimensional brane. We have considered the question of spontaneous breaking of gauge symmetry and the issue of mass generation and localization on the brane. For that we considered a Higgs-like scalar field in the bulk, minimally coupled with a U(1) gauge vector field. Our results indicate that the process of spontaneous breaking of the gauge symmetry cannot account for the Standard Model symmetry breaking, as the bulk-brane mechanism we proposed is essentially gravitational. Nevertheless, we have shown that our mechanism is fairly interesting and effective in what concerns the localization of fields on the brane.

Another line of research that we have opened up in 2007, was the suggestion that, in the context of string/M-theory vacua landscape, the various associate multi-universes could actually interact among themselves. We have shown, in the context of a simplified model with two interacting universes, that the cosmological constant of one of the universes could be altered by the dynamics of the other universe. To account for the interaction between universes, we have advanced a new curvature principle. Interestingly, this curvature principle can also account for a suitable interpretation of the Generalized Second Law of Thermodynamics at a cosmological level.

Finally, we have continued our study of noncommutative geometry phase space models. We have considered this more general noncommutativity in the cosmological context and studied the most likely initial conditions for a universe governed by this noncommutativity. This was achieved through the Wheeler-DeWitt equation for a Kantowski-Sachs geometry. We have shown, in opposition to the case of configuration space noncommutativity, that the wave function of the universe exhibits damping. This feature suggests that the choice of initial conditions in noncommutative phase space models can be done without any other additional principle.

17.6. QUANTUM COMPUTING

In order to understand computation in a quantum context, it might be useful to introduce as many concepts as possible from the classical computation theory to the quantum case. One of these basic concepts concerns the functioning of finite quantum automata (QA)[5,6].

In this work we proposed a new model for a quantum automaton working with n-qubits and we addressed the question of minimizing it. The minimization of a QA is an important question not only because qubits are an expensive resource, but also because a deeper comprehension of any automaton starts always with its minimal-state equivalent automaton.

[5] Kondacs A and Watrous J, Proceedings of the 38th Annual Symposium on Foundations of Computer Science, 66-75 (1997).
[6] Moore C and Crutchfield J, Theoretical Computer Science 237, 275-306 (2000).

The traditional approach to QA only considers pure states and represents them as unit vectors of a finite Hilbert space. In this work we generalized the usual description to mixed states, which are represented by density operators[7]. The problem of minimizing the dimension of the underlying Hilbert space was addressed using the partial trace operator.

The two main results of this paper are: (i) The proof of a theorem for the existence of an equivalent QA. This theorem establishes a set of necessary and sufficient conditions in order that the dimension of the QA be reduced; (ii) an algorithm to find out the QA working with the least number of qubits.

[7] Ahronov D, Kitaev A, and Nisan N, "Quantum circuits with mixed states", arXiV:quantph/9806029.

18. ENVIRONMENTAL ENGINEERING PLASMA LABORATORY[1]

C.M. Ferreira (Head), E. Tatarova (Principal Investigator), F.M. Dias, V. Guerra, J. Henriques, M. Pinheiro, E. Felizardo.

18.1. INTRODUCTION

The research work in the Environmental Engineering Plasma Laboratory covered the following topics:

- Plasma torches for environmental issues;
- Extraordinary phenomena in hydrogen plasmas;
- Improvement of plasma diagnostic techniques.

18.2. PLASMA TORCHES FOR ENVIRONMENTAL ISSUES[2]

Having in view environmental issues, i.e. plasma sterilization and hazardous gases abatement, the main activity of the "Environmental Engineering Plasma Laboratory" (EEPL) during 2007 was focused on complex, experimental and theoretical investigations of microwave molecular plasmas over a large domain of operating conditions.

Atmospheric pressure discharges are receiving growing interest due to their easy and low-cost operation for applications in a variety of plasma processing and manufacturing techniques that are currently performed in vacuum conditions. Many of the problems related with conventional plasma torches induced by DC or RF electric fields can be eliminated if a waveguide-based, atmospheric plasma torch driven by a surface-wave (SW) is used instead. One of the main advantages of such microwave discharges at atmospheric pressure is that they make it possible to inject large power densities into the plasma and thus achieve high population densities of active species. The complex work on microwave plasma torches and its applications for bacteria sterilization falls into the following main fields of investigation: (i) further improvement of the surfaguide based experimental set up (Figure 18.1); (ii) development of new experimental techniques for spectral and radio-physics diagnostics of molecular plasmas; (iii) development of a detailed theoretical model for the air plasma torch as a tool for optimization of the plasma source operation; (iv) microwave plasma based system for bacteria "killing".

The waveguide-surfatron based experimental setup has been further improved in order to ensure stable operation of the torch. The up grated experimental set-up is shown in Figure 18.1. Air and water are used as a working media. A new system for plasma dilution with water has been created and incorporated in the principal gas flow system. The new system provides gas flow rates from 100 to 2000 sccm under laminar gas flow conditions.

The air plasma emission in the 250 – 850 nm range has been investigated. Emission spectroscopy has been used to detect the following emission lines: the 777.4 nm, 844.6 nm and 630 nm atomic oxygen lines, corresponding to the transitions $O(3p^5P \rightarrow 3s^5S)$, $O(3p^3P \rightarrow 3s^3S)$ and $O(2p^1D \rightarrow 2p^3P)$, respectively, and the NO(γ) band in the range 230–260 nm (0–1, 0–2 and 0–3 vibrational transitions). The relative emission intensities of the Q1-branch of the OH[$A2\,\Sigma^+ \rightarrow X2\,\Pi$] rotational band within the (0–0) vibrational transition (in the range 306–315 nm) have been used to determine the gas temperature. The experimental spectra have been compared with calculated ones to obtain the background gas temperature. Infrared sensitive measurements using an optical thermometer provided data about the wall temperature.

The radio-physics methods have been applied to measure the wave number and SW attenuation coefficient. Amplitude and phase sensitive recording using electrical antennas provided axially resolved measurements of the wave dispersion characteristics. The so called "interferogram method", based on the mixing of the traveling wave signal with a constant reference signal, has been further developed in order to be applied to the case of short plasma column lengths.

A detailed self-consistent model for a microwave plasma torch, using air mixed with water as a working media, was developed. The system under analysis is a plasma source comprising a discharge sustained by an azimuthally symmetric SW mode and a post-discharge (see Figure 18.2). The system of equations considered to describe the plasma source includes: (i) Maxwell's equations; (ii) the dispersion equation for the azimuthally symmetric TM surface mode; (iii) the rate balance equations for vibrationally excited states of electronic ground state molecules $N_2(X^1\Sigma^+_g, v)$; (iv) the rate balance equations for the excited states of molecules and atoms $N_2(A)$, $N_2(B)$, $N_2(a')$, $N_2(a)$, $N_2(C)$, $N_2(a'')$, $N(^2D)$, $N(^2P)$, $O_2(a)$, $O_2(b)$, $O(^1D)$, $O(^1S)$; the rate balance equations for ions and electrons N_2^+, N_4^+, O^+, O_2^+, O_4^+, NO^+, NO_2^+, H_2O^+, H_3O^+, H_2^+, H_3^+, HN_2^+, NH_3^+, NH_4^+, O^-, O_2^-, O_3^-, H^-, OH^-, $NO2^-$, $NO3^-$; the rate balance equations for ground-state molecules and atoms N, O, O_3, NO, N_2O, NO_2, NO_3, N_2O_5, H_2O, H, H_2, OH, HO_2, H_2O_2, NH_3, NH_2, NH, HNO, HNO_2, HNO_3; the gas thermal balance equation; the equation of mass conservation for the fluid as a whole.

A big number of chemical and physical processes were taken into account. Those processes are: excitation and deactivation of electronically excited states of N, O, and H atoms, N_2 and O_2 molecules (88 processes); 211 chemical reactions of neutrals in electronic ground state; 63

[1]Activities performed in the frame of the Contract of Associated Laboratory, out of the Contract of Association EURATOM/IST, by CFP staff of the "Grupo de Electrónica e Descargas em Gases".
[2]Work performed in collaboration with the Lebedev Physical Institute of Russian Academy of Sciences, Russia, the University of Sofia, Bulgaria, the Scientific Department of Shibaura Mechatronics Corp., Japan, and the Instituto Tecnológico de Aeronáutica, Brazil.

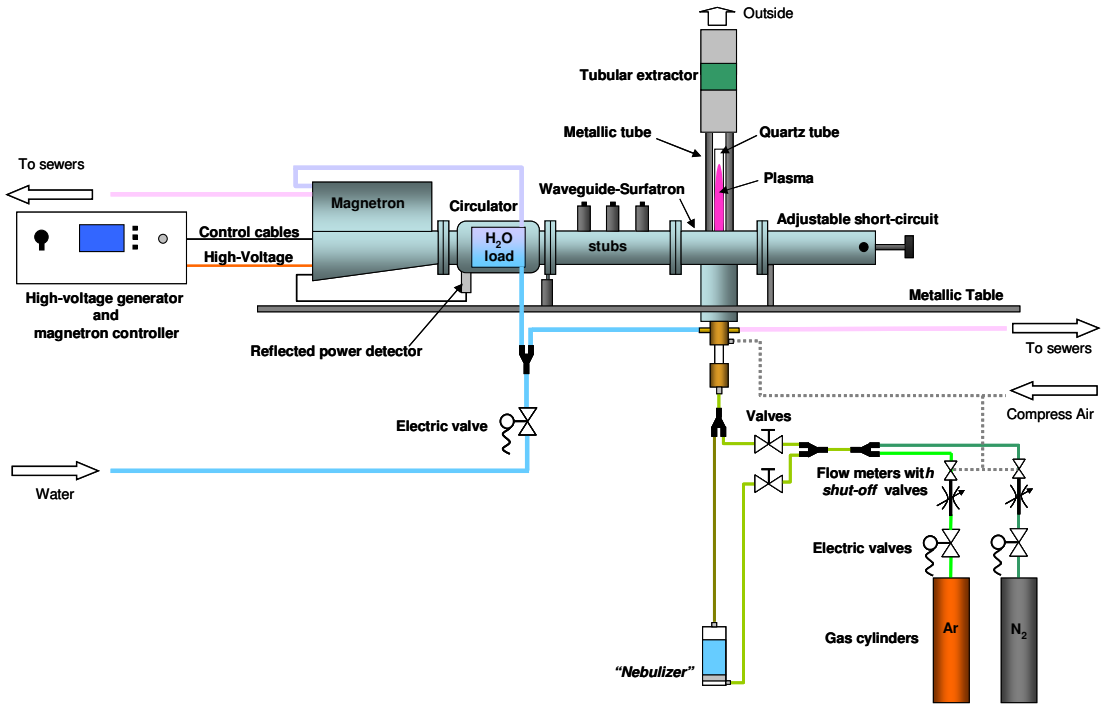

Figure 18.1 - Schematics of the experimental setup with the EEPL.

reactions of neutrals with negative ions; 25 reactions between charged particles. The developed model provides a complex and detailed description of the entire plasma source, i.e. discharge and post-discharge zone. We have also calculated the relative intensities of O(777.4 nm) and O(844.6 nm) lines, and NO(γ) band due to excitation of $O(3p^5P)$, $O(3p^3P)$, and NO(A) states respectively. Model predictions have been experimentally validated. The present model constitutes an instrumental tool for optimization of plasma source operation.

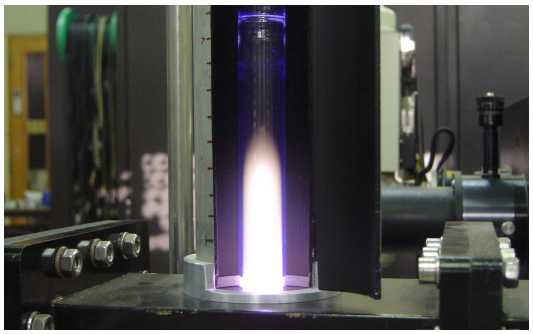

Figure 18.2 - Air plasma torch.

The measured and calculated gas temperatures demonstrate a quite good agreement as shown in Figure 18.3. The gas temperature T_g slightly varies around 3500 K along the main part of the plasma column, but it sharply drops to about 1000 K in the post-discharge zone (z > 3 cm). The length of the generated plasma torch is about 5 cm. There exists a significant radial gas temperature gradient since the difference between the axial gas temperature and the wall temperature is quite large (of about 3000 K). Thus, a strong radial variation of the collision rates and, consequently, of the species population densities is to be expected.

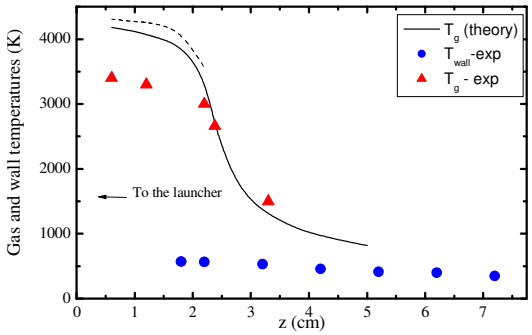

Figure 18.3 - Air plasma torch: gas and wall temperatures.

The results for integrated intensities of the NO(γ) band, corresponding to (0–1, 0–2 and 0–3) vibrational transitions, as a function of the microwave power delivered to the launcher are presented in Figure 18.4. As it can be seen, the initial increasing in the line intensity is followed by a nonlinear saturation at microwave power greater than 350 W. The good agreement between theory and experiment confirms the hypothesis that the main channels for pumping of upper NO(A) state can be the E-E energy exchange in collisions involving NO(X) molecules and N2(A) metastables, according to the reaction $N_2(A) + NO(X) \rightarrow N_2(X) + NO(A)$. The results clearly demonstrate that at higher temperatures the production of NO increases.

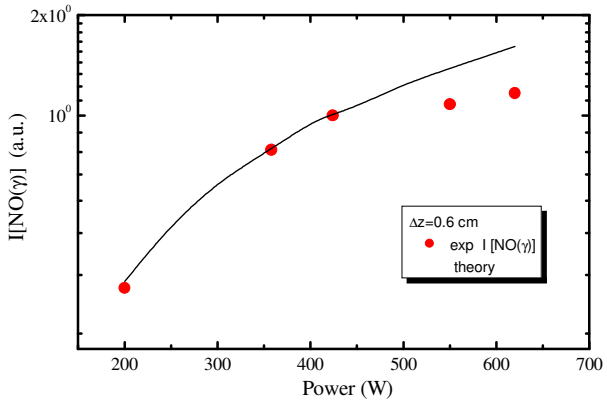

Figure 18.4 - Air plasma torch: integrated intensities of the NO(γ) band.

Generation of "super hot" oxygen atoms in the air plasma torch has been detected. The measured fine structure profiles of the O(777.4 nm) line indicate that the $O(3p^5P)$ atoms generated in the air plasma torch are "super hot", with a temperature of nearly 20000 K (Figure 18.5). This result can be readily explained keeping in mind that energies ΔE ~ 12.2 eV , 13.2 eV and 11.2 eV are available as a result of the ion-ion and electron-ion recombination processes $O^+ + O^- \rightarrow O(3p^5P) + O$, $O^+ + O_2^- \rightarrow O(3p^5P) + O_2$ and $N_2O^+ + e \rightarrow O(3p^5P) + N_2$, respectively. The increase in the microwave power delivered to the plasma torch from 200 to 600 W leads to an increase in the kinetic temperature of the oxygen atoms, from about 15000 to 24000 K, as demonstrated by results obtained. Having in mind that oxygen atoms appear to be the main precursors for many decontamination processes, this air plasma torch can be regarded as an attractive source for plasma based environmental technologies. The results indicate that this torch produces an abundance of reactive atomic oxygen that could effectively oxidize biological agents and destroy hazardous molecules.

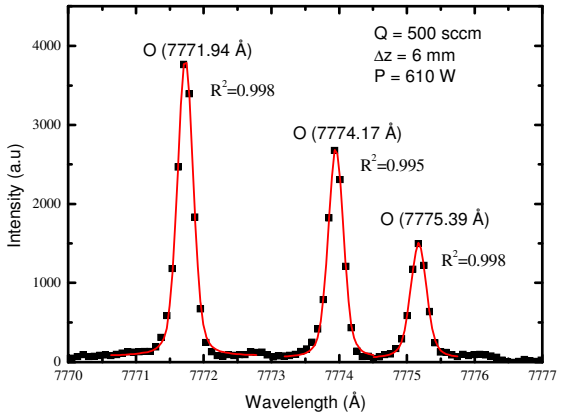

Figure 18.5 - Fine structure line profiles of the $O(3p^5P \rightarrow 3s^5S)$ transition fitted with a Voigth function.

A new experimental system has been created and applied for decontamination of biological agents. Figure 18.6 shows our first plasma sterilizer.

Figure 18.6 - Plasma sterilizer.

The active species come from a 2.45 GHz plasma torch operated within a 12 mm i.d. quartz tube. The microwave torch is situated on the top of the afterglow chamber made of Pyrex, as seen in the picture. The bacteria and its spores have been exposed in the post-discharge zone of the torch. A vertical lift platform directly below the plasma torch is used for the positioning of the sample placed inside a petri dish. The plasma effluent is directed downward towards the sample. *Bacillus subtilis* were chosen as the test biological agent to verify the efficacy of the created sterilizer. The preliminary experiments demonstrate high efficiency of air and water plasma torches to decontaminate the biological agents.

18.3. EXTRAORDINARY PHENOMENA IN HYDROGEN PLASMAS[3]

Recently, puzzling observations have been made in hydrogen containing plasmas. For example, excessive broadening of the Balmer lines of atomic hydrogen has been observed in different types of discharges, which has been explained in terms of Doppler shift and broadening due to the acceleration of charges. However, many questions about the mechanism of "hot" hydrogen atom generation leading to large Balmer-lines broadening are presently open. The purpose of our investigation was to address these problems.

Emission spectroscopy was used for the diagnostic of a large-scale, slot-antenna excited microwave plasma source operating in water vapor at low-pressure conditions. The Doppler temperatures corresponding to the broadening of the H_β line at 486.1 nm (~3000 K) are higher than the

[3]Work performed in collaboration with the Eindhoven University of Technology, The Netherlands.

rotational temperatures (~700 K) determined from the Q-branch of the Fulcher-α band [$d^3\Pi_u$ (v=0) → $a^3\Sigma_g^+$ (v=0)]. The Doppler broadening of the O(777.4 nm) triplet line also indicates generation of "hot" oxygen atoms. Kinetic considerations demonstrate that electron-ion [$H_3O^+ + e \rightarrow H_2O + H_{hot}$*] and ion-ion [$H_3O^+ + OH^- \rightarrow H_2O + H_2^+ O_{hot}$*] recombination processes can be important sources of "hot" atoms in the far remote plasma zone, as can be seen from the results shown in Figure 18.7.

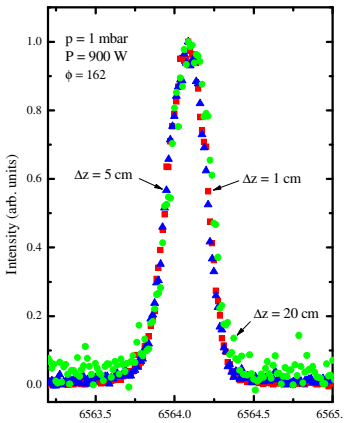

Figure 18.7 - H_α line profiles recorded at different axial distances in the remote plasma.

An experimental study on the spectral broadening of the Balmer lines of atomic hydrogen has been performed in a He-H_2, Ar-H_2, H_2 and water microwave plasmas at low pressure conditions (p = 0.3 mbar). A conventional SW sustained microwave (2.45 GHz) discharge (cylindrical plasma column) has been used as a plasma source. The spectral profiles of H_α, H_β, H_γ, H_δ, H_ε, H_ζ, and H_η lines, corresponding to the transitions H[(n=3–9)→(n=2)] have been measured. The measured line profiles have been fitted by a Voigt function, which results from the convolution of a Gaussian profile (Doppler, instrumental and fine structure broadening) with a Lorentzian one (Stark broadening). A deconvolution procedure has been applied to determine the Doppler broadening and the corresponding temperature. The fine structure and instrumental broadening have been taken into consideration. As seen in Figure 18.8, an amazing result is observed. The temperature of hydrogen atoms increases with the increase in the upper level quantum number, i.e. the atoms at highest electronic levels are hotter. For example, the kinetic temperature of excited H(n = 8) atoms is about 5 times higher than for H(n=4) atoms. This weird behavior is observed in pure hydrogen, He-H_2 and water vapor plasma. To the best of our believe, this effect is definitely outside the framework of standard physics.

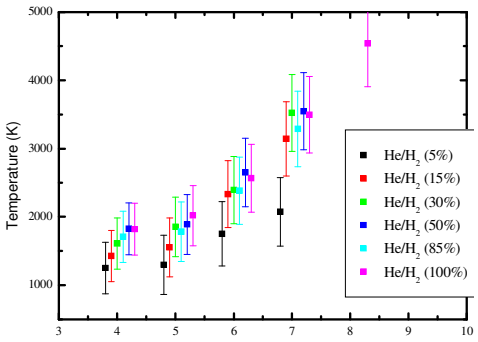

Figure 18.8 - Dependence of the temperature on the upper level quantum number.

18.4. IMPROVEMENT OF PLASMA DIAGNOSTIC TECHNIQUES

18.4.1. Optical emission diagnostics[4]

In order to improve analysis and processing of the measured emission lines, a new procedure to determine kinetic temperature of hydrogen atoms has been developed (Figure 18.9).

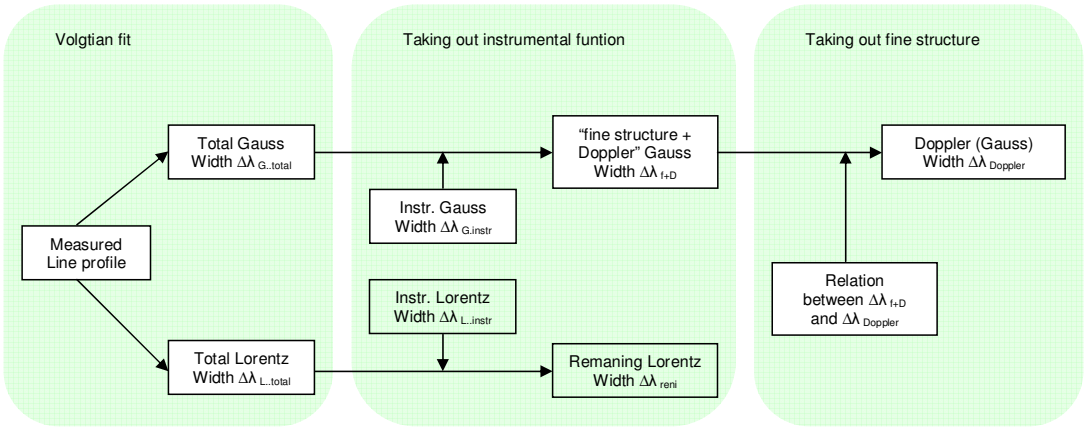

Figure 18.9 - The procedure for temperature determination.

[4]Work performed in collaboration with the Eindhoven University of Technology, The Netherlands.

This new procedure take into account the fine structure influence for H_α, H_β, H_γ, H_δ, H_ε, H_ζ, H_η lines of atomic hydrogen. As can be seen in Figure 18.10, where the synthetic spectrum of H_γ line is shown, at gas temperatures lower than about 1500 K the fine structure splitting must be taken into account by deconvolution.

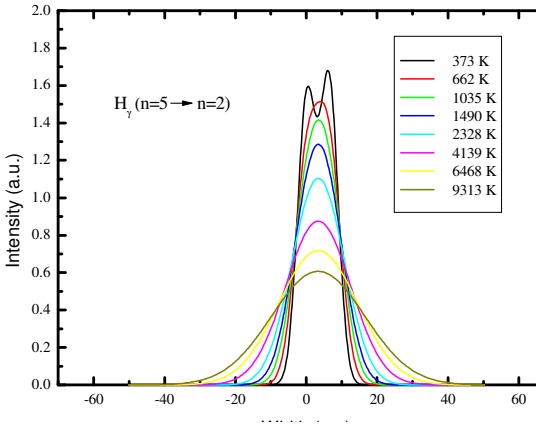

Figure 18.10 - Synthetic spectrum of H_γ line for different kinetic temperatures.

18.4.2. Langmuir probe diagnostics[5]

Differentiating electrical probe characteristics is still the unbeatable method for electron energy distribution function (EEDF) evaluation, under a wide range of experimental conditions. Yet, the differentiation procedure is often the first source of unreliable results. This work was devoted to a new differentiation procedure based on a combined harmonic-numerical scheme, which is able to provide acquisition-speeds typically 6000 times faster than those achievable while using standard differentiation techniques.Typical results are presented in Figure 18.11, where the achievable increased speed ratio is presented as a function of the noise level normalized to 1% electron density fluctuations.

We also developed numerical procedures intended to make EEDF evaluation possible in the experimental conditions when the presence of close-to-coherent noise cannot be avoided. Although magnetized plasmas, e.g. TOKAMAKs, are good examples, the above situation happens in a very wide range of situations, namely due to mains noise because data acquisition systems are seldom correctly synchronized. Results from a model test are shown in Figure 18.12, where the achieved noise reduction is about 40 dB.

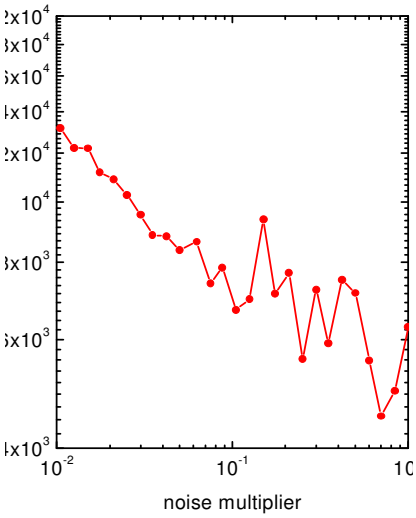

Figure 18.11 - Speed improvement achievable by the new differentiation scheme as a function of the noise level.

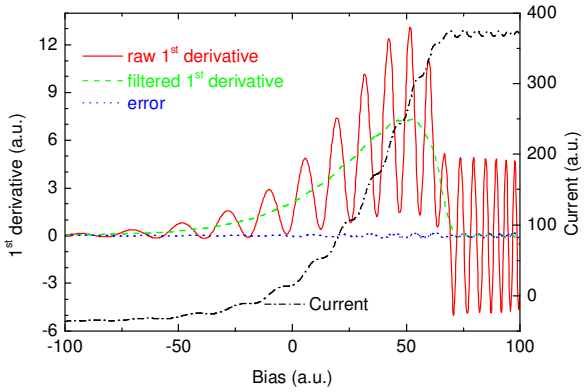

Figure 18.12 - Model test: 1st derivatives raw (solid) and after filtering (dash); error (dot), and I(V) data (dash-dot).

[5]Work performed by F.M. Dias in collaboration with Sofia University, Bulgaria.

19. NON-EQUILIBRIUM KINETICS AND SIMULATIONS OF PLASMAS AND AFTERGLOW PLASMAS [1]

C.M. Ferreira (Head), J. Loureiro (Principal Investigator), V. Guerra, K. Kutasi, M. Lino da Silva, C.D. Pintassilgo, P.A. Sá.

19.1. INTRODUCTION

The research work carried out in 2007 falls into the following main lines of investigation:

- Kinetic study of the nitrogen afterglow;
- Modeling of N_2-O_2 afterglow plasmas for plasma sterilization and insight in elementary processes;
- Modeling of N_2-CH_4 discharges and afterglow plasmas for planetary atmospheric studies and surface treatments;
- Theoretical modeling of heterogeneous atomic recombination;
- Modeling of kinetics and radiative processes in low-pressure, high-temperature plasmas.

19.2. KINETIC STUDY OF THE NITROGEN AFTERGLOW

Our previous analysis of the nitrogen pink afterglow was extended[2], by comparing model predictions with recently reported measurements of metastable $N(^2P)$ atoms and $N_2(a\ ^1\Pi_g)$ molecules[3]. It was shown that both species reveal the presence of a characteristic maximum on their populations, occurring downstream from the discharge after an initial stage of decrease. Such behavior is a consequence of the vibration-vibration (V-V) pumping-up mechanism taking place during the relaxation in the afterglow, which is followed by vibration to electronic (V-E) transfers that create locally $N_2(A\ ^3\Sigma_u^+)$ and $N_2(a'\ ^1\Sigma_u^-)$ metastables.

The very good agreement obtained for the concentration of $N(^2P)$ atoms supports the correctness of the present description of the atomic, vibrational and triplet kinetics and confirms the strong coupling between the kinetics of $N(^4S)$ and $N(^2P)$ atoms and $N_2(A\ ^3\Sigma_u^+)$ molecules. However, model predictions significantly overestimate the density of the $N_2(a\ ^1\Pi_g)$ state, which can be a consequence of an overestimation of the efficiency of the V-E transfer, leading to the formation of singlet $N_2(a'\ ^1\Sigma_u^-)$ metastables. As singlet $N_2(a'^1\Sigma_u^-)$ metastables play a crucial role in nitrogen ionization, the new results imply that the ionization mechanisms in the afterglow may have to be reviewed.

Another advance on this topic was a more accurate calculation of the vibrational level energies of the electronic ground-state $N_2(X\ ^1\Sigma_g^+)$, through the reconstruction of the potential curve according to Rydberg–Klein–Rees (RKR), followed by the resolution of the radial Schrödinger equation for this potential curve[4]. The number of 60 bound vibrational levels (above v=0) so predicted is clearly above the value of 45 levels obtained from the two-term polynomial expansion using spectroscopic data. The behavior of nitrogen discharges and post-discharges is strongly affected by the vibrational kinetics, such as in the case of (i) electron-superelastic collisions on $N_2(X, v>0)$ levels; (ii) excitation of electronic states of N_2 with an indirect role in the Penning ionization reactions; (iii) vibrational dissociation; (iv) afterglow light emissions. Therefore, the modifications resulting from the increase of the number of levels must be investigated. In particular, the effects of considering a higher number of levels on the vibrational ladder were analyzed and compared with previous results obtained using a smaller vibrational manifold. The comparison essentially focused on the changes of the rate coefficients for V-V energy-exchange processes, the vibrational distribution function of $N_2(X\ ^1\Sigma_g^+)$ molecules in microwave discharge conditions, the relaxation of this distribution in the afterglow, and the time-evolution of the most populated nitrogen electronic states $N_2(A\ ^3\Sigma_u^+, B\ ^3\Pi_g, C\ ^3\Pi_u, a'\ ^1\Sigma_u^-, a\ ^1\Pi_g)$.

19.3. MODELING OF N_2-O_2 AFTERGLOW PLASMAS FOR PLASMA STERILIZATION AND INSIGHT IN ELEMENTARY PROCESSES

The possibility of utilizing low temperature plasmas to sterilize medical devices has triggered numerous experimental studies with the aim of finding the optimal discharge conditions for sterilization. Our modeling investigations aim to contribute to this optimization.

Investigations performed by the group of Plasma Physics in the Physics Department of the University of Montreal (Canada) have shown that total inactivation of *Bacillus Subtilis* spores can be achieved in the afterglow of a low-pressure flowing N_2-O_2 microwave discharge, as a result of a synergistic effect between UV photons emitted by excited NO molecules and O-atoms[5,6]. Some

[1]Activities performed in the frame of the Contract of Associated Laboratory, out of the Contract of Association EURATOM/IST, by CFP staff of the "Grupo de Electrónica e Descargas em Gases".

[2]Sá PA, Guerra V, Loureiro J, and Sadeghi N, J. Phys. D: Appl. Phys. 37, 221 (2004).

[3]Eslami E, Foissac C, Supiot P, and Sadeghi N, 17th Europhysics Conference on Atomic and Molecular Physics of Ionized Gases (ESCAMPIG), Constanta - Romania, September 2004.

[4]Silva ML da, Guerra V, Loureiro J, and Sá PA, Chem. Phys., submitted.

[5]Moreau S, Moisan M, Tabrizian M, Barbeau J, Pelletier J, Ricard A, and Yahia L'H, J. Appl. Phys. 88, 1166 (2000).

[6]Philip N, Saoudi B, Crevier M-Ch, Moisan M, Barbeau J, and Pelletier J, IEEE Trans. Plasma Sci. 30, 1429 (2002).

experimental works have reported the existence of a significant erosion of the spores and of a variety of polymers in the afterglow chamber, mainly when the samples were located in the vicinity of the discharge tube axis. The erosion has been attributed to the action of the metastable states $N_2(A\ ^3\Sigma_u^+)$ and $N_2(a'\ ^1\Sigma_u^-)$, and of the molecular ions N_2^+ and N_4^+. Besides their supposed erosion effect, the metastables also contribute to ion formation and have no significant effect on the species densities relevant for sterilization. These facts draw two necessary conditions to be satisfied for an efficient sterilization in a large reactor: (i) to achieve large and homogeneous distributions for the densities of sterilizing species, which is determined, besides the discharge parameters, by the gas flow rate and gas pressure; and (ii) the reduction or elimination from the reactor of the species able to induce erosion, with the exception of O and N atoms, which can be achieved by controlling the gas flow rate and/or the distance between the discharge and reactor.

Our investigations have been performed for the post-discharge system presented on Figure 19.1 The density distributions in the post-discharge reactor have been calculated with a 3-D hydrodynamic model, while the species densities at the reactor entrance have been determined with the kinetic models developed for the discharge and early-afterglow regions, respectively, based on the homogeneous Boltzmann equation for electrons and the rate balance equations for different species. Based on our calculations some guide-lines can be drawn for an optimum sterilizer system.

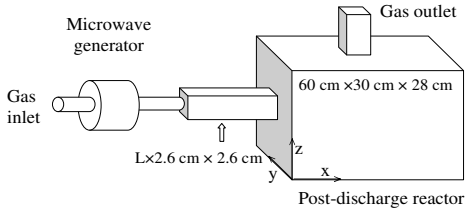

Figure 19.1 - The post-discharge system used in our investigations. Active species created in the N_2-O_2 flowing microwave discharge are carried by the flow into the reactor. The inlet and outlet are situated in the middle of the planes, giving symmetry to the chamber.

The time evolution of the species relative densities in the early-afterglow, presented in Figure 19.2 at 2 Torr, shows that if metastables and ions want to be avoided in the reactor, then species flight-times of about 1 ms, or even larger, should be obtained in the connecting region between the discharge and the reactor. This can be achieved by choosing an intermediate tube with 36 cm length at 2 Torr or with 96 cm at 0.6 Torr, when using a gas flow of 2000 sccm. The advantage of a longer tube, besides increasing the species flight-time, is also because it ensures a much more homogeneous velocity distribution at the reactor's entrance.

By investigating the species density distributions in the reactor, at different discharge tube radii (0.3, 0.6 and 1 cm), it has been found that the highest O-atoms, N-atoms and NO(B) molecules densities can be achieved when using the 0.3 cm radius tube. Comparing the species densities in the reactor in the case of a 0.3 cm tube radius for different microwave field frequencies (200 MHz, 915 MHz and 2450 MHz), we have found that the higher densities are achieved at the higher excitation field frequencies.

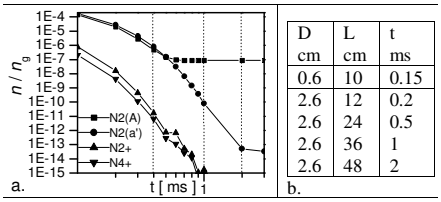

D cm	L cm	t ms
0.6	10	0.15
2.6	12	0.2
2.6	24	0.5
2.6	36	1
2.6	48	2

Figure 19.2 - Species relative densities as a function of time, and species flight-time in the connecting tube at 2 Torr.

Finally, it has been shown that the NO(B) density distribution becomes more homogeneous in the reactor with increasing gas flow rate (hence increasing UV radiation), as can be seen in Figure 19.3. However, the higher gas flow rate results also in higher gas temperature at the reactor entrance, as it is shown by the lower absolute densities obtained around the reactor's entrance.

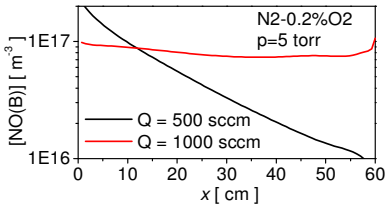

Figure 19.3 - NO(B) molecules density distribution as a function of x, at the discharge tube axis.

N_2-O_2 post-discharges have been also studied in a specific case where oxygen is added downstream from a pure nitrogen microwave discharge[7]. The aim of this research is to give insight to the knowledge of volume and surface elementary processes. The concentration of atomic nitrogen was measured by electron paramagnetic resonance. It was observed that the N-atom density increases when very small amounts of oxygen are added into the post-discharge. With the aim to fully understand this behavior, work is in progress to adapt our previous model[8] to the situation where oxygen is added into the afterglow[9,10].

[7]Work performed in collaboration with the Masaryk University, Brno, Czech Republic.
[8]Pintassilgo CD, Loureiro J, and Guerra V, J. Phys. D: Appl. Phys. 38, 417 (2005).
[9]Vašina P, Mrázková M, Pintassilgo CD, Guerra V, Kudrle V, and Tálský A, 16th Symposium on Applications of Plasma Processes (SAPP), Podbanské-Slovakia, January 2007.
[10]Mrázková M, Vašina P, Pintassilgo CD, Kudrle V, Guerra V, and Tálský A, 28th International Conference on Phenomena in Ionized Gases (ICPIG), Prague-Czech Republic, July 2007.

19.4. MODELING OF N_2-CH_4 DISCHARGES AND AFTERGLOW PLASMAS FOR PLANETARY ATMOSPHERIC STUDIES AND SURFACE TREATMENTS

With the purpose of simulating Titan's atmosphere, we have developed a kinetic model to describe the N_2-CH_4 mixture in a post-discharge in which methane is introduced either in the discharge or downstream in the afterglow region. The advantage of the latter approach is twofold. On one hand, the contribution of electron processes is negligibly small, which is the case of Titan's stratosphere and troposphere; on the other hand, the temperature conditions can be also similar to those observed in Titan, which range between 70 K and 180 K, since the post-discharge temperature is close to room temperature or even lower if specific care is taken (e.g. using liquid nitrogen).

In order to simulate Titan's atmosphere, we have determined the concentrations of the most populated species originating from methane dissociation[11], such as C_2H_2, C_2H_4, C_2H_6, C_3H_4, and C_3H_8, as well as other species produced in reactions with N_2, namely HCN, H_2CN, C_2N_2 , and HC_3N. Our calculations show that HCN and C_2N_2 are the most abundant nitriles, whereas the methane decomposition produces mainly C_2H_2, C_2H_4, C_2H_6, and C_3H_4, as also obtained in other Titan's atmosphere models[12], and in measurements from Voyager[13] and, more recently, from Cassini spacecraft[14].

The research work carried out for studying N_2-CH_4 mixtures in order to reproduce Titan's atmosphere has been also extended to low pressure capacitively coupled RF discharges, since they have been used with success in laboratory simulations[15] of the analogues of Titan's aerosols-*tholins*[16] In these experiments, the production of solid particles occurs only in the gas phase, without any wall effect. Our first calculations, realized for the case of pure N_2, have been presented in[17]. The work is now pursued by considering the modeling of an RF plasma reactor by means of a fluid model coupled to the Poisson's equation[18]. This approach is described elsewhere in this report.

Discharges and post-discharges in N_2-CH_4 mixtures are also used for metal nitrocarburising treatments, involving the diffusion of N and C atoms in metallic surfaces[19,20].

Accordingly, we have studied the afterglow of a low pressure pure nitrogen microwave discharge (at 2.45 GHz), in which methane is added in the post-discharge[21]. With this purpose, we developed a kinetic model and compared our predicted calculations with measured results for the populations of N and C atoms (Figure 19.4). An overall good agreement has been obtained[22].

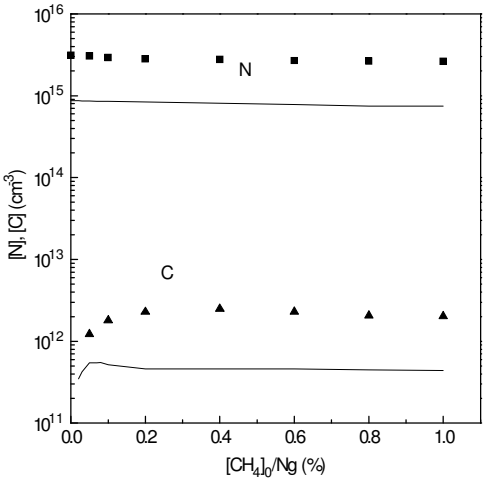

Figure 19.4 - Measured and predicted concentrations of N and C atoms.

19.5. THEORETICAL MODELING OF HETERO-GENEOUS ATOMIC RECOMBINATION

An analytic model to describe the heterogeneous recombination of a single atomic species on silica-like surfaces was developed. The theoretical formulation closely follows a popular approach corresponding to the use of a mesoscopic description in terms of the average fractional coverage of adsorption sites, which is ruled by a set of differential equations describing elementary reactions occurring with defined rates[23,24]. However, instead of numerically solving the system of equations leading to the determination of the heterogeneous atomic recombination probability, asymptotic analytical solutions were obtained, providing ready-to-use expressions for the surface atomic recombination probability, γ, given as a function of surface characteristics such as the densities of adsorption sites and the activation energies for the different elementary surface processes.

[11]Pintassilgo CD and Loureiro J, 2nd European Planetary Science Congress (EPSC), Postdam-Germany, August 2007.
[12]Lebonnois S, Toublanc D, Hourdin F, and Rannou P, Icarus 152, 384 (2001).
[13]Coustenis A, Bézard B, Gautier D, Marten A, and Samuelson R, Icarus 89, 54 (1991).
[14]Teanby NA, Irwin PGJ, de Kok R, Vinatier S, Bézard B, Nixon CA, Flasar FM, Calcutt SB, Bowles NE, Fletcher L *et al*, Icarus 186, 364 (2007).
[15]Szopa C, Cernogora G, Boufendi L, Correia JJ, and Coll P, Planet. Space Sci. 54, 394 (2006).
[16]Work performed in collaboration with the Service d'Aéronomie, Verrières le Buisson, France.
[17]Pintassilgo CD, Alcouffe G, Cernogora G and Loureiro J, 28th International Conference on Phenomena in Ionized Gases (ICPIG), Prague-Czech Republic, July 2007.
[18]Salabas A, Marques L, Jolly J, Gousset G, and Alves LL, J. Appl. Phys. 95, 4605 (2004).
[19]Jaoul C, Belmonte T, Czrwiezec T, Ablitzer D, Ricard A, and Michel H, Thin Solid Films 506, 163 (2006).
[20]Jaoul C, Belmonte T, Czrwiezec T, and David N, Appl.Surf. Sci. 252, 8360 (2006).
[21]Work performed in collaboration with the Laboratoire de Science et Génie de Surfaces, Nancy, France.
[22]Pintassilgo CD, Jaoul C, Loureiro J, Belmonte T, and Czerwiec T, J. Phys. D: Appl. Phys. 40, 3620 (2007).
[23]Kim YC and Boudart M, Langmuir 7, 2999 (1991).
[24]Gordiets BF, Ferreira CM, Nahorny J, Pagnon D, Touzeau M, and Vialle M, J. Phys. D: Appl. Phys. 29, 1021 (1996).

The model takes into account physisorption, chemisorption, thermal desorption, surface diffusion, and both Eley-Rideal (E-R) and Langmuir-Hinshelwood (L-H) recombination mechanisms. The results are applied to the cases of nitrogen and oxygen recombination on silica and to oxygen recombination on Pyrex. However, since the derivation is kept in a very general form, it allows the exploration of several distinct limit cases and provides a deeper understanding of the underlying surface kinetics.

The dependence of the recombination probability with the wall temperature and with the gas pressure was studied in detail. It was found that γ can have a complex non-monotonic behavior with the wall temperature, as a result of the competition between E-R and L-H recombination processes (Figure 19.5). E-R recombination is dominant at high temperatures, as the physisorbed atoms quickly desorb back to the gas phase and cannot reach the active chemisorption sites. As the temperature decreases, the collection zones – *i.e.*, regions around the chemisorption sites where a physisorbed atom stays long enough to be able to reach the active site by diffusion before it desorbs – start to increase and the L-H recombination probability may increase. When the collection zones start to overlap the L-H mechanism cannot improve its efficiency anymore and the L-H recombination probability goes down quickly, until the E-R process becomes again dominant.

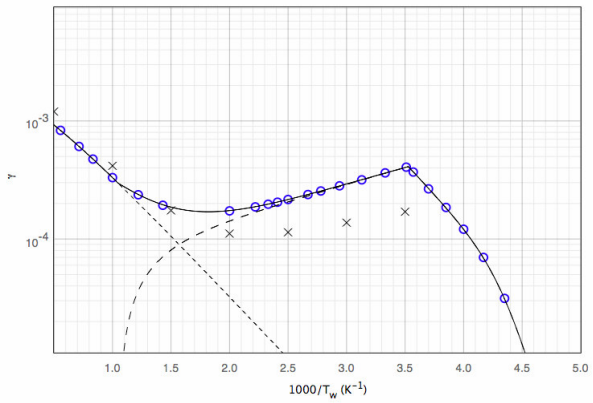

Figure 19.5 - Nitrogen recombination on silica. Asymptotic analytical solutions for (- - -) $\gamma_{E\text{-}R}$, (– –)$\gamma_{L\text{-}H}$, and (—)γ_{total}; (o) numerical solution; (×) theoretical results from other authors.

The transition from first to second order recombination (and vice-versa) with pressure was also studied and debated. The E-R mechanism is always first order, whereas the L-H one has a transition from first to second order when the pressure increases. Therefore, γ is first order at low pressures. In the model investigated, γ is first order as well at very high pressures, since L-H recombination stops to work then and, consequently, the E-R process becomes dominant.

19.6. MODELING OF KINETIC AND RADIATIVE PROCESSES IN LOW-PRESSURE, HIGH-TEMPERATURE PLASMAS

19.6.1. Fundamental kinetic and radiative processes

Physical-chemical processes such as energy transfer between species translational and internal modes, dissociation, ionization, recombination and radiative processes, are nowadays routinely modeled using the state-to-state approach. Numerical approaches utilized by different research teams have typically relied on first-order, perturbative models (FOPT - e.g., SSH theory) which only achieve accurate results for a restricted temperature range (typically low translational temperatures).

Our research group has been trying to use more unrestricted and improved theoretical approaches. Over the last year, we have concluded an investigation on the vibrational-translational processes in diatom-diatom, and atom-diatom collisions featuring the following improvements: (i) application of the Forced Harmonic Oscillator (FHO) theory to yield multi-quantum transition rates valid for higher collision velocities, unlike FOPT models, which only yield mono-quantum rates valid at lower temperatures[25,26]; (ii) a more accurate calculation of the manifold of the internal levels of a diatomic molecule, utilizing an extrapolated RKR method for the calculation of vibrational level energies and maximum vibrational number, instead of the less precise procedure of extrapolated polynomial expansions.

This has allowed us to build a complete and accurate database of vibration-translation (V-T) and vibration-dissociation (V-D) rates for N_2-N_2 collisions. A similar work has been carried by the Bari group for atom-diatom N_2-N collisions. A collaboration has been carried with this group, and these complementary approaches have been examined. An accurate and complete database of state-resolved coefficients for the modeling of nitrogen dissociation processes has been obtained.

A first application of such a database was carried, to model high-speed shock waves which evidenced a transition from a "ladder-climbing" dissociation path, typical of low temperature applications such as gas discharges processes, to an Arhenius-like dissociation path at higher temperatures, where multi-quantum transitions enhance dissociation processes up to the point where dissociation from any given vibrational level becomes equiprobable[25,26].

A second application utilizing such a set as a benchmark, involved the validation of popular two-temperature (T, T_v) dissociation models such as the Park, Hansen, Marrone–Treanor, Hammerling, Losev–Shatalov, Gordiets, Kuznetsov, and Macheret–Fridman models[27].

[25]Silva M Lino da, Guerra V, and Loureiro J, J. Thermophys. Heat Transfer 21, 303 (2007).
[26]Silva M Lino da, Guerra V, and Loureiro J, J. Thermophys. Heat Transfer 21, 40 (2007).
[27]Silva M Lino da, Guerra V, and Loureiro J, Chem. Phys. 342, 275 (2007).

Two dissociation regimes are predicted: preferential dissociation from the lower vibrational levels for $T>>T_v$, and preferential dissociation from the near-dissociation levels for $T<<T_v$, with an abrupt change of regime (Figure 19.6).

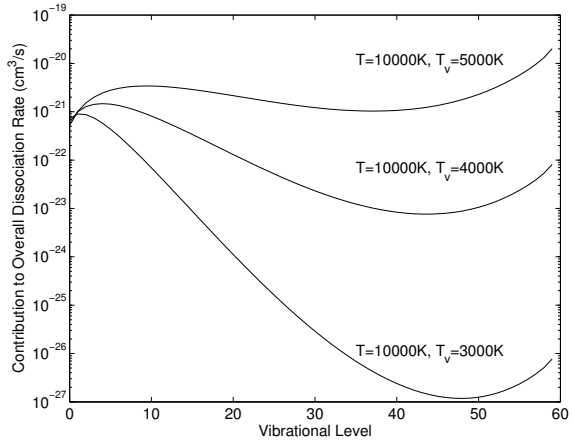

Figure 19.6 - Contribution of each vibrational level to the overall dissociation rate, for N_2–N_2 collisions at different translational and vibrational temperatures.

Investigations on radiative processes have proceeded through the permanent update of the "line-by-line" code SPARTAN (http://cfp.ist.utl.pt/radiation/SPARTAN/) and it's associated Gas and Plasma Radiation Database (GPRD, http://cfp.ist.utl.pt/radiation/GPRD/). The main research achievements for 2007 included (i) presentation and validation of the non-standard adaptive wavelength model for general radiative transfer applications[28]; (ii) update of the radiative database of the SPARTAN code, for the inclusion of additional radiative transitions from CO species; (iii) full line-by-line simulation of the emission from a Inductively Coupled Plasma of Martian-type composition (97% CO_2-3% N_2), at room pressure[29] (Figure 19.7).

19.6.2. Investigation of non-equilibrium collisional-radiative processes in support of Mars exploration[30]

Our group has participated in several research activities focused on the exploration of planet Mars, which requires detailed knowledge on atmospheric entry processes in a CO_2 environment (Mars atmosphere) and in high-speed Earth re-entries (inbound from Mars).

Dissociation processes behind high-speed shock-waves (12 km/s) have been modeled utilizing the state-to-state rates database. Dissociation behavior behind a shock wave might differ significantly in high speed entries (up to 12 km/s) or low speed entries (around 5 km/s)[25,26].

Investigations on Martian-type atmospheric entries have been carried in the scope of the EXOMARS preparatory program, which plans for an exploration vehicle to be launched towards Mars surface no latter than 2013, in order to search for any ground-level biologic activity.

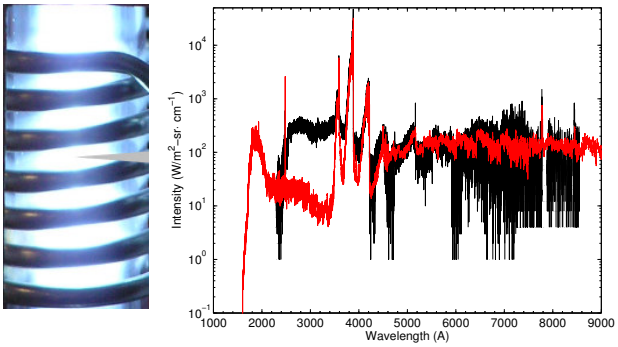

Figure 19.7 - Picture of the measured atmospheric pressure Martian-type plasma and comparison of the synthetic spectrum predicted by the SPARTAN code (in red) with the measured and calibrated spectrum (in black).

Our research group has participated or is participating in the following support activities for the EXOMARS mission. (i) A shock-tube campaign in the Moscow Institute of Physics and Technology, to evaluate the physical-chemical properties of pure CO_2 shock-heated flows[31]. Emission spectroscopy, absorption spectroscopy, and interferometry measurements have been carried out for shock velocities ranging from 3 to 6 km/s. Time-dependent emission spectra issued from a streak (Figure 19.8) have been numerically reconstructed using the "line-by-line"

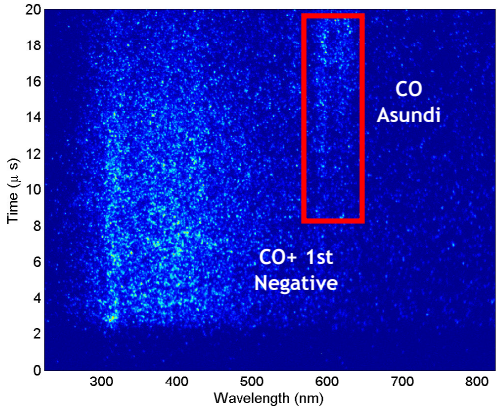

Figure 19.8 - Radiation behind a pure CO_2 shockwave measured at 5.6 km/s. Radiation from the CO^+ 1^{st} negative system is occurring in the shock-front, whereas in the relaxation zone recombination of CO^+ and e^- leads to the radiative emission of the CO Asundi bands.

[28]Silva M Lino da, J. Quantitative Spectrosc. Radiative Transfer 108, 106 (2007).
[29]Work performed in collaboration with the Université Blaise Pascal, Clermont-Ferrand, France.
[30]Work financed by the European Space Agency (ESA) in the frame of the AURORA program.
[31]Work performed in the frame of Fluid Gravity Eng./ESA Contract "CFD Validation in CO_2 Environment".

code SPARTAN for the identification of the main radiative species in the flow. A numerical rebuilding of the shock-heated flows has also been carried out (Figure 19.9), which showed an adequate agreement with experimental results. (ii) A full reconstruction of the radiative flowfield around the EXOMARS entry vehicle will be carried using the SPARTAN code, following the method described in [28][32]. This will allow predicting the values of the radiative heat fluxes impinging on the spacecraft heatshield, allowing a proper sizing of thermal protections. (iii) The NASA probe PHOENIX is scheduled to enter Mars atmosphere the 25th May 2008. ESA plans to observe the entry phase of such a spacecraft utilizing the MARS EXPRESS spacecraft, currently in orbit around Mars. We are providing support to such a mission. Our task is to evaluate the radiative field that is likely to be observed during the entry phase of PHOENIX, and to advise on which will be the appropriate instrumentation of the MARS EXPRESS probe for properly measuring the atmospheric entry radiation of the PHOENIX probe[33].

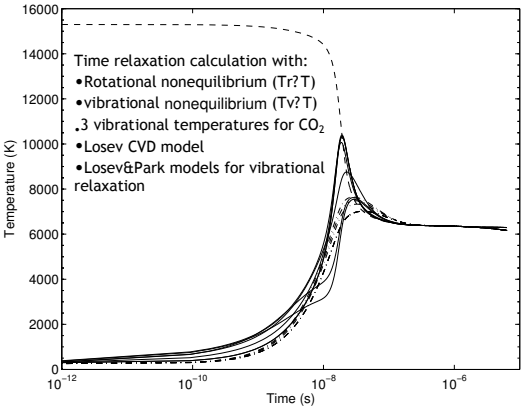

Figure 19.9 - Numerical rebuilding of the time-dependent relaxation processes behind a pure CO_2 shock-heated flow. We observe the quick equilibration of translational (dashed lines) and rotational (dashed-dotted lines) temperatures, followed by the equilibration with the CO_2 and O_2 vibrational temperatures (full lines) and finally the CO and C_2 temperatures.

[32]Work performed in the frame of Fluid Gravity Eng./ESA Contract "Rebuilding of the radiative flowfield around EXOMARS".
[33]Work performed in the frame of ESA project "MARS EXPRESS support to the PHOENIX mission".

20. MODELING OF PLASMA REACTORS [1]

C.M. Ferreira (Head), L.L. Alves (Principal Investigator), R. Alvarez, L. Marques, C. Pintassilgo, S. Letout, J. Cruz, J. Gregório, J.S. Sousa.

20. 1. INTRODUCTION

This project was focused on the modeling of different plasma sources, used in various applications (mainly with material processing and environmental control). The general goal was the development of sophisticated simulation tools describing the operation of these sources, in view of their optimization. The research work in this field studied the following devices:

- Microwave-driven plasma reactor operated by an axial injection torch;
- Micro-plasma reactors;
- Capacitively coupled plasma reactors;
- Inductively coupled plasma reactor;
- Surface-wave plasma reactors.

20.2. MICROWAVE-DRIVEN PLASMA REACTOR OPERATED BY AN AXIAL INJECTION TORCH[2]

We have continued the study of a microwave-driven (2.45 GHz) plasma reactor (cylindrical chamber with 55 mm radius and 150 mm height), operated by an Axial Injection Torch[3] (Figure 20.1), used for the destruction of industrial sub-products (VOC's and BEXT aromatic hydrocarbons). The torch (connected to a coaxial waveguide with 5.3 mm and 14.5 mm inner and outer radii, respectively) creates atmospheric plasmas in different pure gases (argon, helium, nitrogen) or gas mixtures (e.g. air), over a wide range of powers (300−3000 W) and flow-rates (0.5−13 L min^{-1}), producing very hot fluxes of plasma species (electron temperatures around 20000 K and gas temperatures between 2000−6000 K).

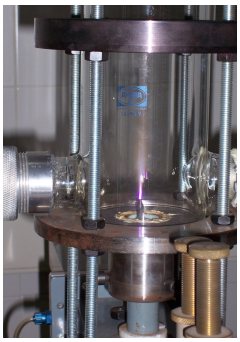

Figure 20.1 - Plasma reactor operated by the AIT.

We have started the development of a hydrodynamic model for the gas-plasma flowing system, yielding the distribution of mass density, pressure and (axial and radial) velocities, for a constant 1000 K gas temperature profile. The model solves the Navier-Stokes equations, which are discretized onto two-dimensional staggered cell-centered grids, by using a finite volume method based on surface integrals. The equations are solved using an algorithm SIMPLE, subject to the following boundary conditions: (i) symmetry conditions at reactor axis; no-slip conditions and flow conservation conditions for the velocity at reactor walls; (iii) imposition of the input gas flow at the nozzle's tip; (iv) continuity condition for the velocity and closure condition for the pressure at the gas output opening. We have considered a 0.5mm nozzle's radius and an output-to-input surface ratio of 100. Simulations were carried out in helium at atmospheric pressure, for input gas flows in the range 1000-10000 sccm.

Simulation results captured the main features with the gas flow distribution (Figure 20.2), namely: (i) for a low input gas flow the neutral particles spread radially as they move towards the output, yielding a smooth recirculation of gas inside the reactor; (ii) for a high input gas flow the radial spread is considerably reduced, whereas a strong interaction with the upper wall modifies the recirculation pattern.

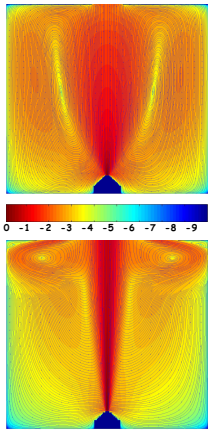

Figure 20.2 - Distribution of the gas velocity (normalized to its maximum) inside the AIT-reactor system, for the following input gas flows (in sccm): 1000 (top), 10000 (down).

[1]Activities performed in the frame of the Contract of Associated Laboratory, out of the Contract of Association EURATOM/IST, by CFP staff of the "Grupo de Electrónica e Descargas em Gases".
[2]Work supported by FCT (BPD/26420/2005) and Spanish MEC (Project CTQ2005-04974/PPQ), performed in collaboration with M.C. Quintero and A. Rodero, Departamento de Física, Universidad de Córdoba, Spain.
[3]AIT, Spanish patents P200201328 and P200302980.

20.3. MICRO-PLASMA REACTORS[4]

We have continued the study of atmospheric pressure micro-plasmas, created by electric discharges in very small geometries (100's μm) without glow to arc transition, in view of developing portable devices for flue gas treatment, biological decontamination or detection of heavy metal gaseous traces, in ambient air or aerosols.

20.3.1. Micro-Cathode Sustained Discharge (MCSD)[5]

We have started the systematic study of this device, which uses a micro-hollow cathode discharge (MHCD), running in oxygen and rare gas/oxygen mixtures at high power densities (up to 100 kW cm^{-3}), to generate a downstream plasma (MCSD) with intense fluxes of $O_2(a^1\Delta)$ metastables and oxidative radicals (O, OH, O_3). MHCDs are created by applying a voltage between two closely spaced hollow electrodes separated by a thin dielectric layer. The MCSD is created between the MHCD cathode and a third positively-biased electrode, placed at a distance of some cm's (Figure 20.3).

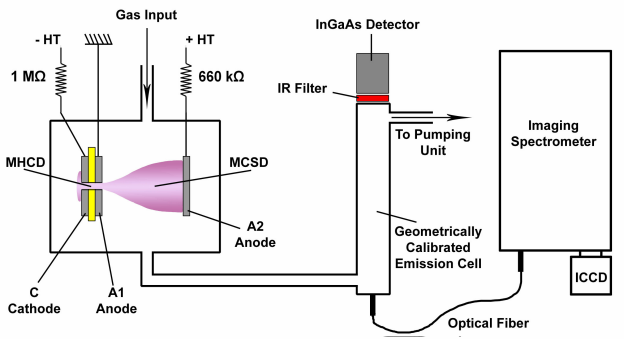

Figure 20.3 - Schematics of the MHCD-MCSD experimental setup.

We have characterized the MHCD-MCSD interaction using the current-voltage discharge response. The conditions for discharge ignition were established, as a function of the discharge voltage, pressure, flux, and composition. We have concluded that (i) the MCSD is a cold (<400 K) and low E/N (~15 Td) discharge region (similar to a positive column), which contrasts with the MHCD region characterized by very intense fields; (ii) the MHCD-MCSD mode transition is highly dependent on the presence of O_2 and discharge features are strongly influenced by the presence of (air and NO) impurities; (iii) the MHCD operating mode plays an important role on the MCSD ignition (in particular, it is possible to ignite the MCSD in a self-pulsed regime when the MHCD operates in the same regime, see Figure 20.4); (iv) the MCSD symmetry is highly affected by discharge flows above 100 sccm. We have also measured the gas temperature and the population of metastable $O_2(a^1\Delta)$, by using optical emission spectroscopy. We have started to develop a collisional-radiative model for oxygen plasmas, by setting up a very complete reaction scheme that accounts for the presence of positive ions O^+, O_2^+, O_3^+ and O_4^+, negative ions O^-, O_2^-, O_3^- and O_4^-, atoms $O(^3P)$, $O(^1D)$ and $O(^1S)$, vibrationally excited ground-state molecules $O_2(X^1,v=0–4)$, electronically excited molecules $O_2(a^1\Delta_g)$, $O_2(b^1\Sigma_g^+)$ and $O_2(C^3\Delta_u, A^3\Sigma_u^+, c^1\Sigma_u^-)$, and ozone O_3.

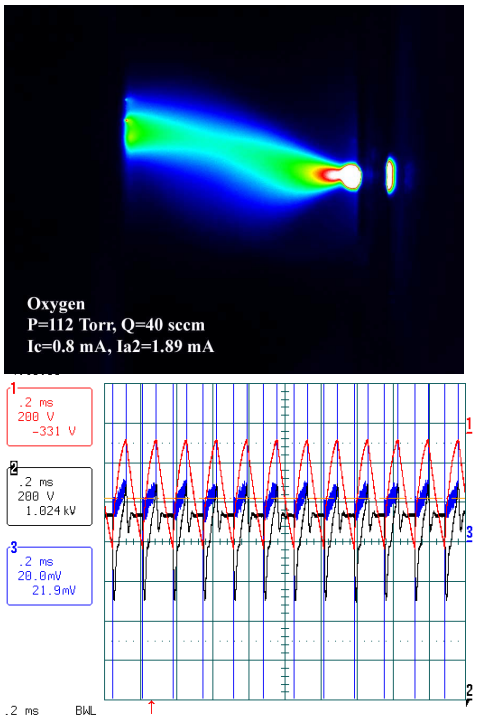

Figure 20.4 - MHCD-MCSD operating in a self-pulsed regime at 112 Torr pressure.

20.3.2. Microwave Micro-Plasma (MWMP)[6]

We have initiated the study of an innovative plasma source for the production of atmospheric pressure micro-plasmas, in view of environmental applications. The device produces high-density (>10^{15} cm^{-3}), low-power (~10 W) plasmas in ambient air or in controlled environments (argon, xenon, nitrogen, oxygen, …), within the 100-300 μm end-gap of a microwave (2.45 GHz) strip-line, by using a continuous wave excitation (thus guaranteeing a steady-state discharge regime). We concluded the design and build of version-trial and version-1 with this device, which have successfully overcome the following problems: (i) discharge auto-ignition; (ii) microwave shielding; (iii) optimization of power coupling; (iv) docking of diagnostic systems.

[4]Work performed in collaboration with V. Puech and C. Boisset-Laporte, Laboratoire de Physique des Gaz et des Plasmas, Orsay, and L. Pitchford, Laboratoire Plasmas et Conversion d'Énergie, Toulouse, France.
[5]Work performed in the frame of the PhD thesis of J. Santos Sousa and supported by FCT (SFRH/BD/28668/2006).
[6]Work performed in the frame of the PhD thesis of J. Gregório and supported by FCT (SFRH/29294/2006) and by Acordo Cooperação Científica e Técnica (GRICES / CNRS), 2006 –2008.

The MWMPs produced with this source in ambient air (Figure 20.5) were characterized by spatially-resolved emission spectroscopy measurements. By analyzing the nitrogen molecular spectra we have obtained vibrational temperatures in the range 4200-5000 K and rotational temperatures (hence gas temperatures) between 600 and 1800 K. The latter are maximum in the gap center and increase with the coupled power. We have also studied the device operation from the point of view of its electromagnetic coupling, with and without plasma, by measuring the reflected power. The optimum operating conditions were defined for a 50 µm gap and a 50 W input power, corresponding to a 60 mm length for the line transmission. These results agreed with simulation predictions obtained from commercial software (CST Microwave Studio™). This analysis was the starting point for the design of version-2 with the device, which will allow plasma ignition in a controlled atmosphere of argon and/or nitrogen.

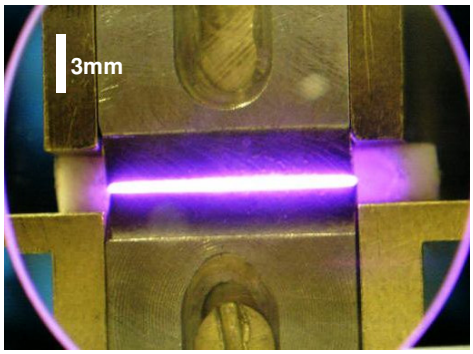

Figure 20.5 - Close-up over the MWMP produced in air at atmospheric pressure.

Finally, we have started the development of a two-dimensional stationary fluid code that solves the charged particle and the electron mean energy transport equations (for argon as a test gas), together with Poisson's equation for the space-charge field and Maxwell's equations for the electromagnetic excitation field.

20.4. CAPACITIVELY COUPLED PLASMA REACTORS[7]

The study of low-pressure capacitively coupled radio-frequency (CCRF) discharges, produced within cylindrical parallel-plate reactors (~6 cm radius and ~3-5 cm height), was continued in hydrogen and initiated in nitrogen (see Figure 20.6).

The focus was on the kinetic description of the plasma reactivity and the analysis of its influence upon charged particle dynamics. These studies used a hybrid calculation code, coupling a two-dimensional time-dependent fluid model (that solves the charged particle and the electron mean energy transport equations together with Poisson's equation), the two-term homogeneous electron Boltzmann equation (yielding the electron energy distribution function in the presence of inelastic and superelastic collisional events, involving both electronically and vibrationally excited states), and quasi-homogeneous collisional-radiative models for the populations of the main excited species considered.

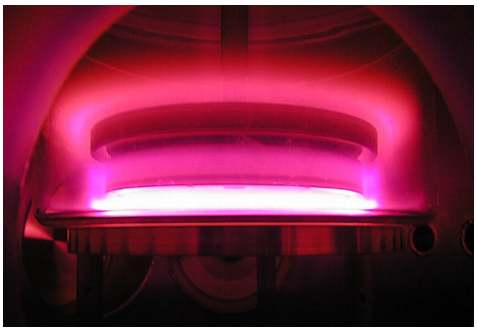

Figure 20.6 - Close-up over the plasma chamber with a CCRF reactor, running a discharge in N_2.

Hydrogen CCRF discharges are routinely used in plasma assisted material processing applications, and particularly in the plasma enhanced chemical vapor deposition of hydrogenated microcrystalline silicon (µ-Si:H) thin films, from a precursor mixture of SiH_4-H_2, under high dilution conditions for silane. The increasing demand for higher throughput, larger processing areas, improved uniformity and film quality in the semiconductor industry justifies the investment in the characterization (both theoretical and experimental) of these discharges, in view of their optimization. Therefore, we have carried out a systematic characterization of CCRF hydrogen discharges produced over a wide range of applied voltages (50-600 V), frequencies (13.56-40.68 MHz), and pressures (0.2-1 Torr). Simulations have accounted for the presence of positive ions H^+, H_2^+, and H_3^+, negative ions H^-, electronically excited atoms H(n=1s,2s,2p,3–5), and vibrationally excited ground-state molecules H_2 ($X^1\Sigma_{g+}$,v=0–14).

A good quantitative agreement was found between simulations and experiment for the coupled electrical power and the plasma potential. The model underestimates the values of the electron density, the self-bias potential, and the H(n=1) atom density with respect to measurements, but agrees with experiment when predicting that all these parameters increase with either the applied voltage, the frequency or the pressure, thus confirming that the production of atomic species proceeds mainly via electron collisions. The dissociation degree was about 10^{-3} for the work conditions considered. The quality

[7]Work performed in collaboration with J. Jolly, École Polytechnique, Palaiseau, and G. Cernogora, Service d'Aéronomie, Vérrières, France.

of simulations for the density of H atoms (Figure 20.7) was strongly related to the use of a wall recombination probability for this species that was experimentally measured, thus accounting for surface modification with discharge operating conditions. Results evidenced the key role played by the atomic wall recombination mechanism in plasma description.

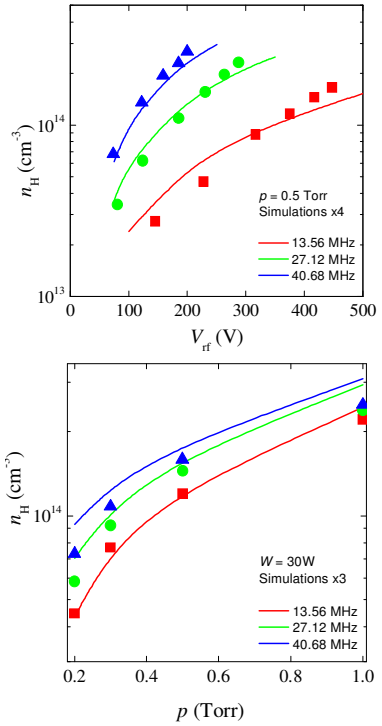

Figure 20.7 - Calculated H atom density for a CCRF discharge, as a function of the applied voltage (top) and pressure (down).

The study of CCRF discharges in nitrogen / methane mixtures (for CH_4 concentrations up to 2%) can be used to simulate the atmosphere of Titan, at laboratory scale. In the past, these discharges have already been successfully used to produce, in gas phase, dust particles analogues to Titan's aerosols-*tholins*. Therefore, we have started the study of CCRF discharges (13.56 MHz) produced in pure nitrogen, at 0.1-2 Torr pressures and 10-50 W coupled powers. Simulations have considered the presence of positive ions N_2^+ and N_4^+, vibrationally excited ground-state molecules $N_2(X^1\Sigma_{g+}$,v=0–45), and 7 electronically excited states of the N_2 molecule, accounting for the production of electrons via associative ionization mechanisms involving the N_2(A) and N_2(a') metastables. First results reveal that the 2D profile of the electron density exhibits an unexpected torsion effect (Figure 20.8), due to the spatial asymmetry in the profiles of the metastable species.

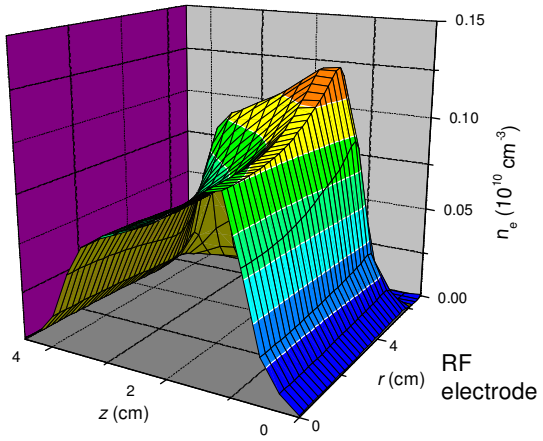

Figure 20.8 - Time-average spatial profile of the electron density for the CCRF discharge, at 250V applied voltage and 0.4Torr pressure.

20.5. INDUCTIVELY COUPLED PLASMA REACTOR[8]

We have pursued the modeling of a radio-frequency (13.56 MHz) inductively coupled plasma (ICP) reactor[9], used as an ion source for ion milling applications or the oxidation of thin films. Usually, the ICP-reactor operates in Ar and Ar/O_2 mixtures at very low pressure (~ 0.1 mTorr) and high plasma densities (~ 10^{11}-10^{12} cm^{-3}), under the action of a static magnetic field of ~ 400-800 Gauss, to ensure both a high creation rate of species and a reduced contamination. The discharge is produced by applying a rf-current of ~ 1 A to a 6-turn planar coil (52.5 mm radius), near the dielectric window (Figure 20.9) of a cylindrical metallic chamber (97.5 mm radius and 100 mm height). Ion extraction is achieved through a set of metal grids, which can be polarized yielding a maximum voltage drop of 1 kV.

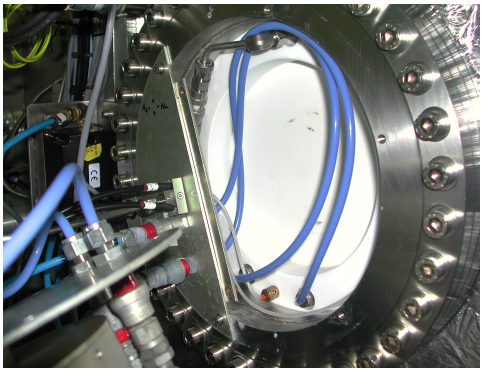

Figure 20.9 - Dielectric window of the ICP-reactor with the ion beam system.

[8]Work performed in the frame of the MsC thesis of J. Cruz, in collaboration with S. Cardoso and P. Freitas, Instituto de Engenharia de Sistemas e Computadores - Microsistemas e Nanotecnologias (INESC-MN), Lisbon, Portugal.
[9]Nordiko-3000 reactor at INESC-MN.

The two-dimensional model includes an electromagnetic module (that solves Maxwell's equations, given the applied current and the plasma-induced current density), and a hybrid calculation code including a stationary fluid module (that solves the charged particle and the electron mean energy transport equations together with Poisson's equation, given the electromagnetic field distribution), and the two-term homogeneous electron Boltzmann equation (yielding the electron energy distribution function, and thus all the corresponding transport parameters and rate coefficients).

Boundary conditions for the electromagnetic module include an analytical expression for the electric field profile, produced by a distribution of circular current rings (including the contribution of both the plasma and the rf antenna) at the dielectric window. The fluid module considers flux boundary conditions at the reactor walls for both particle and mean energy, accounting for a partial transparency at the extraction grids. After discretization, the electromagnetic equations are solved using a Gauss-Seidel method (with alternate column- and row-wise iterations), whereas the transport equations are solved using a time relaxation algorithm with an ADI method. This preliminary model version was solved for argon neglecting the presence of the static magnetic field, but considering a gas pressure of 500 mTorr as to ensure plasma confinement. Simulations for 0.8-1.5 A rf-currents, considering a single grounded grid with 50% transparency, yielded coupled powers of 27-95 W and an ion extraction current of 5 mA (Figure 20.10).

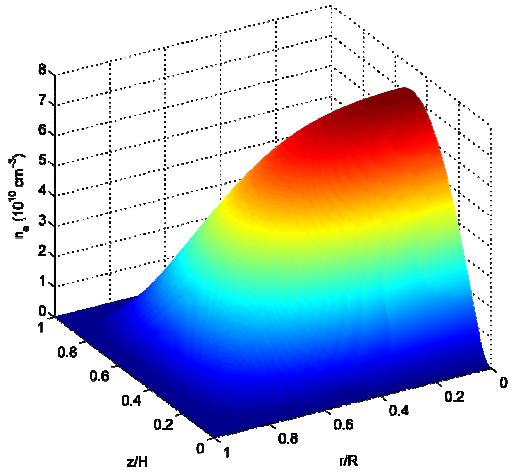

Figure 20.10 - Time-average spatial profile of the electron density in the ICP-reactor, at 1.5A rf-current and 0.5Torr pressure.

20.6. SURFACE-WAVE PLASMA REACTORS[10]

Nitrogen and nitrogen-mixture plasmas are increasingly used for plasma-assisted processing applications, such as the modification and functionalization of materials like polyethylene terephthalate (PET), low-density polyethylene (LDPE), nanotubes, polymer surfaces used in the biomedical field in view of improving their biocompatibility, and for the deposition of N_2 containing functional groups in textiles, among others. In these applications the dissociating and ionizing properties of these plasmas are used to produce large fluxes of radicals with a high chemical reactivity, at ambient temperature and low pressure (< 1 Torr). By combining the reactivity of nitrogen plasmas with the versatility of surface-wave driven discharges (2.45 GHz) we obtain a formidable engineering tool for the tailoring of materials. We have started to adapt and update a simulation code for the description of such discharges, with cylindrical geometry, by coupling a homogeneous kinetic model for N_2 (including the rate balance equations for 45 vibrationally excited levels of the ground-state molecule and 10 electronically excited atomic and molecular species) with a one-dimensional hybrid calculation code including a stationary fluid module (that solves the charged particle and the electron mean energy transport equations, together with Poisson's equation for the space-charge field and Maxwell's equations for the TM_{00} surface-wave mode) and the two-term homogeneous electron Boltzmann equation (to self-consistently calculated the electron transport parameters and rate coefficients).

[10]Work performed in collaboration with J. Cotrino, Instituto de Ciencias de Materiales de Sevilla, Spain.

21. PLASMA AND ELECTROMAGNETIC PROPULSION[1]

C.M. Ferreira (Head), M.J. Pinheiro (Principal Investigator), A.A. Martins.

21.1. INTRODUCTION

The research work in this field covered the following topics:

- Plasma propulsion;
- Electromagnetic propulsion;
- Research on fundamental problems of plasma physics;
- Analytical glow discharge optical emission spectroscopy.

21.2. PLASMA PROPULSION

There has been a growing interest in the field of plasma aerodynamics related to its outstanding importance in active flow control, overriding the use of mechanical flaps. The plasma created above a blunt body was shown to modify the laminar-turbulent transition inside the boundary layer, to induce or reduce the fluid separation, reducing drag, allowing sonic boom minimization schemes and avoiding unwanted vibrations or noise[2]. To achieve a better understanding of the mechanism responsible for the boundary layer control and propulsions of neutrals we developed (and are still improving) in our laboratory a self-consistent two-dimensional model of the temporal and spatial development of the OAUGDP$^{TM.}$.

The plasma actuator simulation domain is a 2D Cartesian geometry with total length L_x=4 mm, along the Ox-axis, and height L_y=4 mm. It consists of conductive copper strips (with negligible thickness) of 1 mm width, separated by a 0.065 cm thick dielectric with 3 mm width and relative permitivitty $\tilde{\varepsilon}_r$ Figure 21.1 shows a schematics of the device. The capacity of the reactor is given by the conventional formula $C=\varepsilon_0\varepsilon_r/d$. The working gas is an "air-like" mixture of a fixed fraction of nitrogen ($[N_2]/N=0.78$) and oxygen ($[O_2]/N=0.22$), as is normally present at sea level at p=1 atm. The electron homogeneous Boltzmann equation is solved with the two-term expansion in spherical harmonics, using the cross sections set of excitations by electron impact taken from Siglo Data Base. Rates coefficients and transport parameters are so obtained. The chemistry included in the model is the most relevant at atmospheric pressure, and it considers the following species: N_4^+, N_2^+, O_2^+, O_2^- and electrons. The reactions included in the present kinetic model are given in Ref[3]. Figure 21.2 shows the evolution, along a full period, of the calculated electric current, applied voltage, gas voltage and memory voltage.

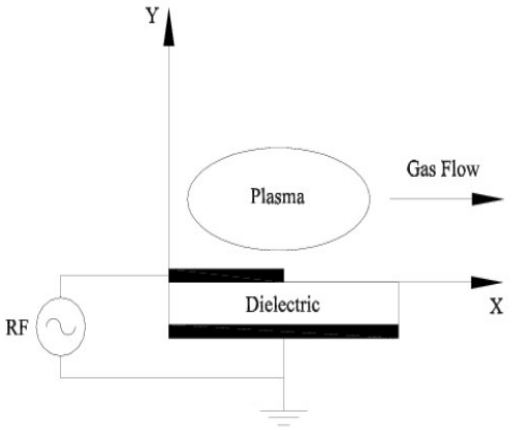

Figure 21.1 - Schematics of the device OAUGDP^{TM}.

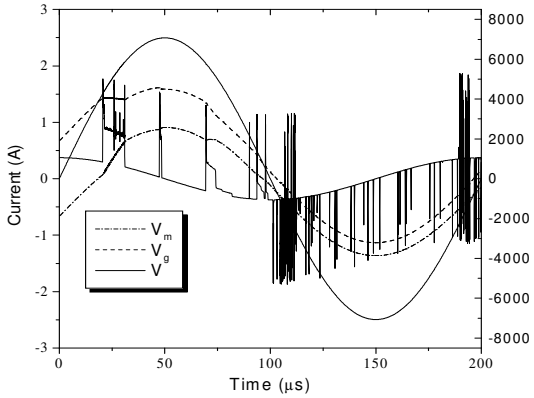

Figure 21.2 - Electric current, applied voltage, gas voltage and memory voltage as a function of time, at V_{rms}=5 kV, f =5 kHz and for a 3 mm dielectric width. Solid curve, current; dotted curve, V_m; dashed-dot curve, V_g; dashed curve, V.

With the assumed conditions at about 740 Volts electron avalanches develop, replenishing the volume above the surface with charged particles. Hence, the charged particles flowing to the dielectric surface start accumulating on the surface, building-up an electric field that prevents the occurrence of a high current, and therefore quenching the discharge development at an early stage. Figure 21.3 shows the electric field profile at a given

[1]Activities performed in the frame of the Contract of Associated Laboratory, out of the Contract of Association EURATOM/IST, by CFP staff of the "Grupo de Electrónica e Descargas em Gases".

[2]Enloe CL, McLaughlin TE, VanDyken RD, Kachner KD, Jumper EJ, and Corke TC, AIAA Journal 42(3), 589 (2004).
[3]Pinheiro MJ, Plasma Process Polym. 3, 135 (2006).

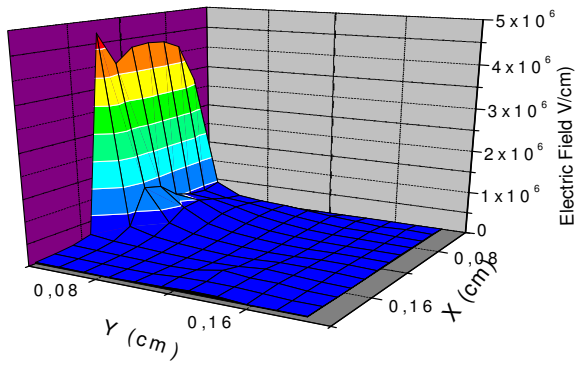

Figure 21.3 - Electric field distribution in the X-Y plane, at a given time during the first-half cycle, for the conditions of Figure 21.2.

time above the anode. Note the peak at the interface of the dielectric with the electrode. Figure 21.4 portrays the arrival of electrons at the anode at t = 6 μs. The body forces are calculate using $\vec{F} = e(n_i - n_e)\vec{E}$ and are given in Figure 21.5. They strongly depend on the number of streamers occurring during both cycles, but there is a general tendency for asymmetry, being more negative during the second half-cycle. This explains why the gas speed tends to invert between both half-cycles, one feature which reduces the performance of this device in what gas speed is concerned.

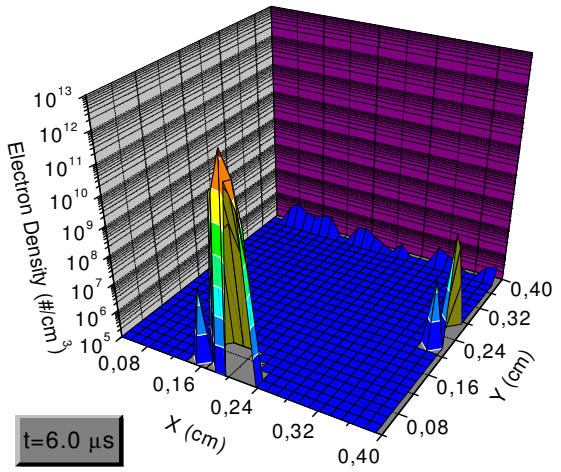

Figure 21.4 - Electron density at t=6 μs, for the conditions of Figure 21.2. This event portrays the arrival of electrons to the positive electrode.

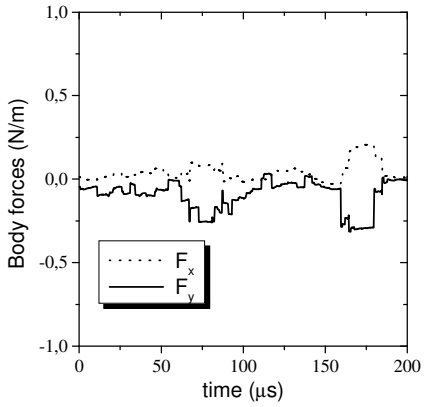

Figure 21.5 - Body forces in vs. time, showing the x-component (responsible for the neutral gas acceleration) and the y-component (responsible for the boundary layer control). Same conditions as in Figure 21.2.

21.3. ELECTROMAGNETIC PROPULSION

There is a growing interest in academia and industry on electromagnetic thrusters as a source of propulsion and energy. This quest might revolutionize space exploration and energetic in the near-future. This is the reason why, in parallel to our research in conventional atmospheric plasmas, we develop some effort to research along this direction, starting by clarifying some methodological difficulties related to the fundamental set of Maxwell's equations. These include a modification and clarification of Faraday's law of induction in vacuum, using the procedure described in[4], which embeds the Lorentz force into the formulation. The result is in complete agreement with the actual set of Maxwell's equations for bodies at rest, the only novel feature is the introduction of a new kind of electromotive force. Examining the problem of a moving circuit with this procedure, it is shown that a new force of induction should act on a circuit moving through an inhomogeneous vector potential field. This overlooked induction force is related to the Aharonov-Bohm effect, but can also be related to the classical electromagnetic field when an external magnetic field is acting on the system. Technological issues are being studied by us, needing an experimental approach in the near-future.

Along other line of research[5], the inertia property of matter is discussed in terms of a type of induction law related to the extended charged particle's own vector potential. Our approach is based on the Lagrangian formalism of canonical momentum. By writing Newton's second law in terms of the vector potential a development in terms of retarded potentials is obtained, which allows for an intuitive physical interpretation of its main terms.

[4]Pinheiro MJ, Physics Essays 20(2) to appear (2007).
[5]Martins AA and Pinheiro MJ, AIP Conf. Proc. 880, 1189 (2007).
[6]Pinheiro MJ, Space Technology International Forum (STAIF-2007), oral report, Albuquerque NM, USA, February 2007.
[7]Fermi E, Nuovo Cimento 25, 159 (1923).

This framework provides a clear physical insight on the physics of inertia. It is shown that the electron mass has a complete electromagnetic origin and the covariant equation obtained contributes to clarify the "4/3 mass paradox". This understanding broadens the possibility to manipulate inertial mass and suggests some mechanisms for possible applications of electromagnetic propulsion and the development of advanced space propulsion physics. Those findings enabled us to suggest the electromagnetic origin of inertia and mass[6]. Similar conclusion was sustained by E. Fermi[7], although he arrives to the same conclusion through a different approach.

21.4. RESEARCH ON FUNDAMENTAL PROBLEMS OF PLASMA PHYSICS

Plasma-wall interactions play a major role in plasma physics. Its complexity, however, continue to elude us when the aim is the complete description of a magnetized non-isothermal plasma transport, in a conducting vessel. Initially, the origin of the anomalous diffusion was assumed to be due to the turbulence of small-scale instabilities. Rather than attempting to solve this complex problem, our work proposes another possible ("circuital") mechanism for wall current drain, which considers the effect of the magnetic field flux "cutting" particles trajectories[8]. This model is expected to be valid in the regime where the cyclotron frequency Ω_c is much larger than the collision frequency ν_c.

We obtained an analytical expression for the anomalous diffusion coefficient. Figure 21.6 compares two numerical results to our theoretical prediction (the unit 1 Hx = 10^{-27} T m^3 is used for the *B/N* ratio). The data was obtained via Monte Carlo simulations of electron transport in crossed electric and magnetic fields[9], while the theoretical prediction was given by our analytical equation. Full agreement with the numerical calculations is not obtained, because (i) we have neglected effects related to time variations of the electromagnetic field, and (ii) we assumed that the plasma is collisionless. This explains the large discrepancy for the diffusion coefficient above 1000 Hx, when the very important effect of collisions randomizes individual trajectories, and our approach is no longer valid.

We have reviewed different models of the electric field reversal in glow discharges, including our "dielectric-like model"[10]. The field inversion occurs at the interface between the plasma sheath and the beginning of the negative glow. Fundamental properties relate to field inversion phenomena in the frame of a dielectric model. A simple analytical dependence is obtained for the axial location of the field reversal, in terms of macroscopic parameters. In addition, we have obtained the magnitude of the minimum electric field inside the trap, the trapping well length, and the trapping time of the slow electrons into the well. We have emphasized the description of the dielectric behavior, thus not contemplating plasma chemistry and plasma-surface interactions. The analytical results obtained can be useful for hybrid fluid-particle models, since simple criteria can be applied to accurately remove electrons from simulations.

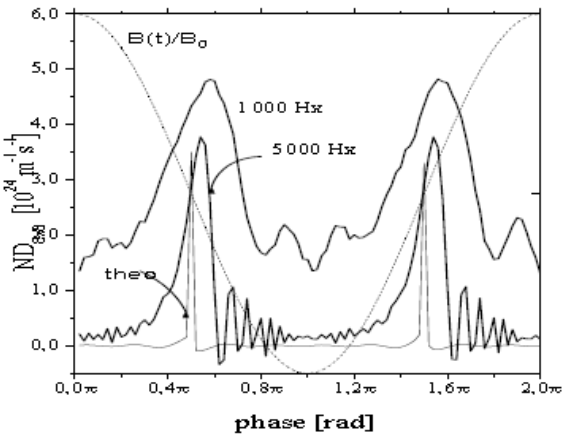

Figure 21.6 - The diffusion coefficient as a function of phase in a sinusoidal electromagnetic field. The two numerical results (at 5000 Hx and 1000 Hx) were obtained with Monte Carlo simulations of electron transport in an argon plasma, subject to crossed electric and magnetic fields. The theoretical prediction ('theo') is given by our analytical equation. The dashed line indicates the amplitude of the external magnetic field. Other parameters used for these data are as follows: f=100 MHz; $\Omega c \approx$ 1010 Hz; kT/e=5.4 eV; p=1 Torr, Tg=300 K.

21.5. ANALYTICAL GLOW DISCHARGE OPTICAL EMISSION SPECTROSCOPY[11]

Glow discharge optical emission spectroscopy is a widely used method for quantitative analysis of materials composition. The method makes possible to investigate metals, polymers, glasses and ceramics. This work aimed to determine the effect of molecular gases on analytical glow discharges[12].

[8]Pinheiro MJ, J. Phys. Conf. Ser. 71, 102002 (2007) and references therein.
[9]Raspopovic ZM, Dujko S, Makabe T, and Petrovic Z Lj, Plasma Sources Sci. Technol. 14, 293 (2005).
[10]Pinheiro MJ, Gas Discharges-Fundamentals and Applications, (J. Amorim Filho ed.), Research SignPost, Trivandrum, India, 2007.
[11]Work performed in the frame of project "Electron kinetics in gas mixtures used for Analytical Glow Discharge Optical Emission Spectroscopy" (GRICES/ITCP), in collaboration with the Research Institute for Solid State Physics and Optics, Hungary and the Instituto Tecnológico Nuclear, Portugal.
[12]Pinhão N, Pinheiro MJ, and Donko Z, 60th GEC, Arlington, Virginia, USA, October 2007.

22. PUBLICATIONS, LABORATORIAL PROTOTYPES, PRIZES AND AWARDS

22.1. MAGNETIC FUSION

22.1.1. Publications in Books

- Varandas C, *"Perspectivas das tecnologias nucleares para a produção de energia",* Energia e desenvolvimento sustentável, edição da Associação de Amizade Portugal/EUA, 127, 2007.

- Varandas C and F Serra *"Nuclear fusion: an energy for the future",* in 'A portrait of state-of-the art research at the Technical University of Lisbon, 163, Springer, Netherlands, 2007.

22.1.2. Publications in refereed scientific journals (publications in ISI)

- Angioni C, R Dux, E Fable, AG Peeters and the ASDEX Upgrade Team, *"Non-adiabatic passing electron response and outward impurity convection in gyrokinetic calculations of impurity transport in ASDEX Upgrade plasmas",* Plasma Physics and Controlled Fusion, 49, 12, 2027, 2007.

- Angioni C, H Weisen, OJWF Kardaun, M Maslov, A Zabolotsky, C Fuchs, L Garzotti, C Giroud, B. Kurzan, P Mantica, AG Peeters, J Stober and the ASDEX Upgrade Team and EFDA-JET contributor, *"Scaling of density peaking in H-mode plasmas based on a combined database of AUG and JET observations",* Nuclear Fusion, 47, 9, 1326, 2007.

- Asp E, J Weiland, X Garbet, V Parail, P Strand and JET EFDA contributers, *"Critical gradient response of the Weiland model"*, Plasma Physics and Controlled Fusion, 49, 8, 1221, 2007.

- Behn R, A Alfier, S Yu Medvedev, Ge Zhuang, R Pasqualotto, P Nielsen, Y Martin and the TCV Team, *"Edge profiles of electron temperature and density during ELMy H-mode in ohmically heated TCV plasmas"*, Nuclear Fusion 49, 8, 1289, 2007.

- Bizarro JPS, X Litaudon, TJJ Tala, and JET EFDA contributors, *"Controlling the internal transport barrier oscillations in high performance tokamak plasmas with a dominant fraction of bootstrap current"*, Nuclear Fusion (Letters Section) 48, L41-L45, 2007.

- Bizarro JPS, *"On the behavior of the continuous-time spectrogram for arbitrarily narrow windows",* IEEE Transactions on Signal Processing 55, 1793-1802, 4335, 2007.

- Buttery RJ, A Loarte, PJ Lomas, P Mantica, DC MacDonald, S Saarelma, R Sartori, G Saibena and JET EFDA contributers, *"Progress towards an integrated solution for the ITER baseline scenario based on high current and highly shaped plasma operation at JET",* Plasma Physics and Controlled Fusion, 49, 5A, A59, 2007.

- Camenen Y, A Pochelon, R Behn, A Bottino, A Bortolon, S Coda, A Karpushov, O Sauter, G Zhuang and the TCV Team, *"Impact of plasma triangularity and collisionality on electron heat transport in TCV L-mode plasmas",* Nuclear Fusion, 47, 7, 510, 2007.

- Cannas B, A Fanni, P Sonato, MK Zedda and JET-EFDA contributors, *"A prediction tool for real-time application in the disruption protection system at JET",* Nuclear Fusion, 47, 11, 1559, 2007.

- Chapman IT, SD Pinches, JP Graves, RJ Akers, LC Appel, RV Budny, S Coda, NJ Conway, M de Bock, L-G Eriksson, RJ Hastie, TC Hender, GTA Huysmans, T Johnson, HR Koslowski, A Krämer-Flecken, M Lennholm, Y Liang, S Saarelma, SE Sharapov, I Voitsekhovitch and the MAST and TEXTOR Teams and JET EFDA Contributors, *"The physics of sawtooth stabilization"*, Plasma Physics and Controlled Fusion, 49, B12, B385, 2007.

- Chapman IT, TC Hender, and JET EFDA Contributors, *"Perturbation of tokamak magnetic surfaces by applied toroidally asymmetric magnetic fields"*, Nuclear Fusion, 47, 11, L36, 2007.

- Coda S, E Asp, E Fable, TP Goodman, O Sauter, VS Udintsev, R Behn, MA Henderson, A Marinoni, GP Turri, C Zucca and the TCV Team, *"The physics of electron internal transport barriers in the TCV tokamak",* Nuclear Fusion, 47, 7, 714, 2007.

- Coelho R, E Lazzaro, *"Effect of sheared equilibrium plasma rotation on the classical tearing mode in a cylindrical geometry",* Physics of Plasmas, 14, 1, 12101, 2007.

- Coelho R, *"Nonlinear growth of marginally unstable tearing modes"*, Physics of Plasmas, 14, 052302, 2007.

- Colas L, A Ekedahl, M Goniche, JP Gunn, B Nold, Y Corre, V Bobkov, R Dux, F Braun, J-M Noterdaeme, M-L Mayoral, S Heuraux, E Faudot, J Ongena and ASDEX Upgrade and JET-EFDA contributors, *"Understanding the spatial structure of RF-induced SOL modifications",* Plasma Physics and Controlled Fusion, 49, 12B, B35, 2007.

- Donné AJH, AE Costley, R Barnsley, H Bindslev, R Boivin, G Conway, R Fisher, R Giannella, H Hartfuss, MG von Hellermann, E Hodgson, LC Ingesson, K Itami, D Johnson, Y Kawano, T Kondoh, A Krasilnikov, Y Kusama, A Litnovsky, P Lotte, P Nielsen, T Nishitani, F Orsitto, BJ Peterson, G Razdobarin, J Sanchez, M Sasao, T Sugie, G Vayakis, V Voitsenya, K Vukolov, C Walker, K Young and the ITPA Topical Group on Diagnostics, *"Diagnostics",* Nuclear Fusion, 47, 6, S337, 2007.

- Duval BP, A Bortolon, A Karpushov, RA Pitts, A Pochelon, A Scarabosio and the TCV Team, *"Bulk plasma rotation in the TCV tokamak in the absence of external momentum input",* Plasma Physics and Controlled Fusion, 49, 12B, B195, 2007.

- Eich T, P Andrew, A Herrmann W Fundamenski, A Loarte, RA Pitts and JET EFDA contributers, *"ELM resolved energy distribution studies in the JET MKII Gas-Box divertor using infra-red",* Plasma Physics and Controlled Fusion, 49, 5, 573, 2007.

- Eriksson A, H Nordman, P Strand, J Weiland, T Tala, E Asp, G Corrigan, C Giroud, M de Greef, I Jenkins, HCM Knoops, P Mantica, KM Rantamäki, PC de Vries, K-D Zastrow and JET EFDA Contributors, *"Predictive simulations of toroidal momentum transport at JET",* Plasma Physics and Controlled Fusion, 49, 11, 1931, 2007.

- Frigione D, L Garzotti, CD Challis, M De Baar, P De Vries, M Brix, X Garbet, N Hawkes, A Thyagaraja, L Zabeo and JET EFDA Contributors, *"Pellet injection and high density ITB formation in JET advanced plasmas",* Nuclear Fusion, 47, 2, 74, 2007.

- Fundamenski W, OE Garcia, V Naulin, RA Pitts, AH Nielsen, J Juul Rasmussen, J Horacek, JP Graves and JET EFDA Contributors, *"Dissipative processes in interchange driven scrape-off layer turbulence",* Nuclear Fusion, 47, 5, 417, 2007.

- Garcia-Muñoz M, P Martin, H-U Fahrbach, M Gobbin, S Günter, M Maraschek, L Marrelli, H Zohm and the ASDEX Upgrade Team, *"NTM induced fast ion losses in ASDEX Upgrade",* Nuclear Fusion, 47, 7, L10, 2007.

- Giroud C, R Barnsley, P Buratti, IH Coffey, M von Hellermann, C Jupén, KD Lawson, A Meigs, M O'Mullane, AD Whiteford, K-D Zastrow and JET EFDA Contributors, *"Method for experimental determination of Z dependence of impurity transport on JET",* Nuclear Fusion, 47, 4, 313, 2007.

- Gorelenkov NN, HL Berk, NA Crocker, ED Fredrickson, S Kaye, S Kubota, H Park, W Peebles, SA Sabbagh, SE Sharapov, D Stutmat, K Tritz, FM Levinton, H Yuh and the NSTX Team and JET EFDA Contributors, *"Predictions and observations of global beta-induced Alfvén – acoustic modes in JET and NSTX",* Plasma Physics and Controlled Fusion, 49, 12B, B371, 2007.

- Graça S, GD Conway, P Lauber, M Maraschek, D Borba, S Günter, L Cupido, K Sassenberg, F Serra, ME Manso, the CFN reflectometry group and the ASDEX Upgrade Team, *"Localization of MHD and fast particle modes using reflectometry in ASDEX Upgrade",* Plasma Physics and Controlled Fusion, 49, 11, 1849, 2007.

- Gruber O and the ASDEX Upgrade Team, *"Overview of ASDEX Upgrade results",* Nuclear Fusion, 47, 10, S622, 2007.

- Günter S, G Conway, S daGraça, H-U Fahrbach, C Forest, M Garcia Muñoz, T Hauff, J Hobirk, V Igochine, F Jenko, K Lackner, P Lauber, P McCarthy, M Maraschek, P Martin, E Poli, K Sassenberg, E Strumberger, G Tardini, E Wolfrum, H Zohm and ASDEX Upgrade Team, *"Interaction of energetic particles with large and small scale instabilities",* Nuclear Fusion, 47, 8 920, 2007.

- Hacquin S, SE Sharapov, B Alper, CD Challis, A Fonseca, E Mazzucato, A Meigs, L Meneses, I Nunes, SD Pinches and the JET EFDA Contributors, *"Localized X-mode reflectometry measurements of Alfvén eigenmodes on the JET tokamak",* Plasma Physics and Controlled Fusion, 49, 9, 1371, 2007.

- Hacquin S, A Fonseca, L Meneses, A Murari, M Walsh and the JET EFDA Contributors, *"The 3D study of X-mode reflectometry for density profile measurements on the JET tokamak",* Plasma Physics and Controlled Fusion, 49, 10, 1627, 2007.

- Igochine V, O Dumbrajs, H Zohm, A Flaws and the ASDEX Upgrade Team, *"Stochastic sawtooth reconnection in ASDEX Upgrade",* Nuclear Fusion, 47, 1, 23, 2007.

- Klimanov I, A Fasoli, TP Goodman and the TCV Team, *"Generation of suprathermal electrons during sawtooth crashes in a tokamak plasma",* Plasma Physics and Controlled Fusion, 49, 3, L1, 2007.

- Kocsis G, S Kalvin, PT Lang, M Maraschek, J Neuhauser, W Schneider, T Szepesi and the ASDEX Upgrade Team, *"Spatio-temporal investigations on the triggering of pellet induced ELMs",* Nuclear Fusion, 47, 9, 1166, 2007.

- Kurzan B, LD Horton, H Murmann, J Neuhauser, W Suttrop and the ASDEX Upgrade Team, *"Thomson scattering analysis of large scale fluctuations in the ASDEX Upgrade edge",* Plasma Physics and Controlled Fusion, 49, 6, 825, 2007.

- Lang, PT B Alper, R Buttery, K Gal, J Hobirk, J Neuhauser, M Stamp, and the JET EFDA Contributors, *"ELM triggering by local pellet perturbations in type-I ELMy H-mode plasma at JET",* Nuclear Fusion, 47, 8, 754, 2007.

- Liang Y, HR Koslowski, PR Thomas, E Nardon, S Jachmich, B Alper, P Andrew, Y Andrew, G Arnoux, Y Baranov, M Bécoulet, M Beurskens, T Biewer, M Bigi, K Crombe, E De La Luna, P de Vries, T Eich, HG Esser, W Fundamenski, S Gerasimov, C Giroud, MP Gryaznevich, D Harting, N Hawkes, S Hotchin, D Howell, A Huber, M Jakubowski, V Kiptily, A Kreter, L Moreira, V Parail, SD Pinches, E Rachlew, O Schmitz, O Zimmermann and JET-EFDA Contributors, *"Active control of type-I edge localized modes on JET",* Plasma Physics and Controlled Fusion, 49, B12, B581, 2007.

- Lima R, R Vilela Mendes, *"Fluctuations and control in the Vlasov-Poisson equation",* Physics Letters, A 368, 87, 2007.

- Litaudon X, JPS Bizarro, CD Challis, F Crisanti, PC de Vries, P Lomas, FG Rimini, TJJ Tala, R Akers, Y Andrew, G Arnoux, JF Artaud, Yu F Baranov, M Beurskens, M Brix, R Ceasario, E de La Luna, W Fundamenski, C Giroud, NC Hawkes, A Huber, E Joffrin, RA Pitts, E Rachlew, SDA Reyes-Cortes, S Sharapov, O Zimmermann, and the JET EFDA contributors, *"Prospects for steady-state scenarios on JET",* Nuclear Fusion 47, 1285-1292, 2007.

- Litaudon X, G Arnoux, M Beurskens, S Brezinsek, CD Challis, F Crisanti, PC De Vries, C Giroud, RA Pitts, FG Rimini, Y Andrew, M Ariola, Yu F Baranov, M Brix, P Buratti, R Cesario, Y Corre, E De La Luna, W Fundamenski, E Giovannozzi, MP Gryaznevich, NC Hawkes, J Hobirk, A Huber, S Jachmich, E Joffrin, HR Koslowski, Y Liang, Th Loarer, P Lomas, T Luce, J Mailloux, GF Matthews, D Mazon, K McCormick, D Moreau, V Pericoli, V Philipps, E Rachlew, SDA Reyes-Cortes, G Saibene, SE Sharapov, I Voitsekovitch, L Zabeo, O Zimmermann, KD Zastrow and the JET-EFDA Contributors, *"Development of steady-state scenarios compatible with ITER-like wall conditions",* Plasma Physics and Controlled Fusion, 49, B12, B529, 2007.

- Loarer T, C Brosset, J Bucalossi, P Coad, G Esser, J Hogan, J Likonen, M Mayer, Ph Morgan, V Philipps, V Rohde, J Roth, M Rubel, E Tsitrone, A Widdowson and the JET EFDA contributors, *"Gas balance and fuel retention in fusion devices",* Nuclear Fusion 47, 9, 1112, 2007.

- Lönnroth J-S, V Parail, V Hynönen, T Johnson, T Kiviniemi, N Oyama, M Beurskens, D Howell, G Saibene, P de Vries, T Hatae, Y Kamada, S Konovalov, A Loarte, K Shinohara, K Tobita, H Urano and JET EFDA contributers, *"Effecs of ripple-induced ion thermal transport on H-mode plasma performance",* Plasma Physics and Controlled Fusion, 49, 3, 273, 2007.

- Lunt T, C Silva, H Fernandes, C Hidalgo, MA Pedrosa, P Duarte, H Figueiredo and T Pereira, *"Edge plasma pressure measurements using a mechanical force sensor on the tokamak ISTTOK",* Plasma Physics and Controlled Fusion, 49, 11, 1783, 2007.

- Madeira TI, P Amorim, BP Duval, CAF Varandas, *"Time resolved measurements by the pulse height analysis soft x-ray diagnostic on TCV",* Review of Scientific Instruments, 78, 8, 086108, 2007.

- Maier H, T Hirai, M Rubel, R Neu, Ph Mertens, H Greuner, Ch Hopf, GF Matthews, O Neubauer, G Piazza, E Gauthier, J Likonen, R Mitteau, G Maddaluno, B Riccardi, V Philipps, C Ruset, CP Lungu, I Uydenhouwen and JET EFDA Contributors *"Tungsten and beryllium armour development for the JET ITER-Like wall project",* Nuclear Fusion 47, 3, 196, 2007.

- Mayer M, V Rohde, G Ramos, E Vainonen-Ahlgren, J Likonen, A Herrmann, R Neu and the ASDEX Upgrade Team, *"The deuterium inventory in ASDEX Upgrade",* Nuclear Fusion, 47, 11, 1607, 2007.

- Mendes RV, F Cipriano, *"A stochastic representation for the Poisson-Vlasov equation",* Communications in Nonlinear Science and Numerical Simulation 13, 221-226, 2007.

- Nedzelskiy IS, C Silva, H Figueiredo, H Fernandes, and CAF Varandas, *"Compact retarding field energy analyzer for the tokamak ISTTOK boundary plasma",* Review of Scientific Instruments, 77, 10E729, 2007.

- Nedzelskiy IS, C Silva, H Fernandes, P Duarte and CAF Varandas, *"Compact cantilever force probe for plasma pressure measurements",* Review of Scientific Instruments, 78, 123505, 2007.

- Neto A, JB Lister, H Fernandes, I Yonekawa, CAF Varandas, *"The appropriateness of XML for diagnostic description",* Fusion Engineering and Design, 82, 5, 1321, 2007.

- Neto A, H Fernandes, D Alves, D Valcarcel, BB Carvalho, J Ferreira, J Veja, M Hron, *"A standard data access layer for fusion devices R&D programs",* Fusion Engineering and Design, 82, 5, 1315, 2007.

- Neto A, H Fernandes, A Duarte, BB Carvalho, J Sousa, DF Valcarcel, M Hron, CAF Varandas, *"FireSignal-data acquisition and control system software",* Fusion Engineering and Design, 82, 5, 1359, 2007.

- Neu R, M Balden, V Bobkov, R Dux, O Gruber, A Herrmann, A Kallenbach, M Kaufmann, CF Maggi, H Maier, HW Müller, T Pütterich, R Pugno, V Rohde, ACC Sips, J Stober, W Suttrop, C Angioni, CV Atanasiu, W Becker, K Behler, K Behringer, A Bergmann, T Bertoncelli, R Bilato, A Bottino, M Brambilla, F Braun, A Buhler, A Chankin, G Conway, DP Coster, P de Marné, S Dietrich, K Dimova, R Drube, T Eich, K Engelhardt, H-U Fahrbach, U Fantz, L Fattorini, J Fink, R Fischer, A Flaws, P Franzen, JC Fuchs, K Gál, M Garcia Muñoz, M Gemisic-Adamov, L Giannone, S Gori, S da Graça, H Greuner, A Gude, S Günter, G Haas, J Harhausen, B Heinemann, N Hicks, J Hobirk, D Holtum, C Hopf, L Horton, M Huart, V Igochine, S Kálvin, O Kardaun, M Kick, G Kocsis, H Kollotzek, C Konz, K Krieger, T Kurki-Suonio, B Kurzan, K Lackner, PT Lang, P Lauber, M Laux, J Likonen, L Liu, A Lohs, K Mank, A Manini, ME Manso, M Maraschek, P Martin, Y Martin, M Mayer, P McCarthy, K McCormick, H Meister, F Meo, P Merkel, R Merkel, V Mertens, F Merz, H Meyer, M Mlynek, F Monaco, H Murmann, G Neu, J Neuhauser, B Nold, J-M Noterdaeme, G Pautasso, G Pereverzev, E Poli, M Püschel, G Raupp, M Reich, B Reiter, T Ribeiro, R Riedl, J Roth, M Rott, F Ryter, W Sandmann, J Santos, K Sassenberg, A Scarabosio, G Schall, J Schirmer, A Schmid, W Schneider, G Schramm, R Schrittwieser, W Schustereder, J Schweinzer, S Schweizer, B Scott, U Seidel, F Serra, M Sertoli, A Sigalov, A Silva, E Speth, A Stäbler, KH Steuer, E Strumberger, G Tardini, C Tichmann, W Treutterer, C Tröster, L Urso, E Vainonen-Ahlgren, P Varela, L Vermare, D Wagner, M Wischmeier, E Wolfrum, E Würsching, D Yadikin, Q Yu, D Zasche, T Zehetbauer, M Zilker and H Zohm, *"Plasma wall interaction and its implication in an all*

tungsten divertor tokamak", Plasma Physics and Controlled Fusion, 49, 12B, B59, 2007.

- Paley JI, S Coda and the TCV Team**,** *"Real time control of the plasma current and elongation in tokamaks using ECRH actuators",* Plasma Physics Controlled Fusion 49, 10, 1735, 2007.

- Pautasso G, CJ Fuchs, O Gruber, CF Maggi, M Maraschek, T Pütterich, V Rohde, C Wittmann, E Wolfrum, P Cierpka, M Beck and the ASDEX Upgrade Team**,** *"Plasma shut-down with fast impurity puff on ASDEX Upgrade",* Nuclear Fusion 47, 8, 900, 2007.

- Pedrosa MA, BA Carreras, C Hidalgo, C Silva, M Hron, L García, J A Alonso, I Calvo, J L de Pablos and J Stöckel**,** *"Sheared flows and turbulence in fusion plasmas",* Plasma Physics Controlled Fusion 49, 12B, B303, 2007.

- Peeters AG, C Angioni, ACC Sips and the ASDEX Upgrade Team**,** *"On the extrapolation to ITER of discharges in present tokamaks",* Nuclear Fusion 47, 9, 1341, 2007.

- Pitts RA, P Andrew, G Arnoux, T Eich, W Fundamenski, A Huber, C Silva, D Tskhakaya and JET EFDA Contributors, *"ELM transport in the JET scrape-off layer",* Nuclear Fusion 47, 1437–1448, 2007.

- Pochelon A, A Mueck, L Curchod, Y Camenen, S Coda, BP Duval, TP Goodman, I Klimanov, HP Laqua, Y Martin, J-M Moret, L Porte, A Sushkov, VS Udintsev, F Volpe and the TCV Team, *"Electron Bernstein wave heating of over-dense H-mode plasmas in the TCV tokamak via O-X-B double mode conversion",* Nuclear Fusion 47, 11, 1552, 2007.

- Portafaix C, P Bibet, JH Belo, et al., *"Thermal behavior of the LHCD launchers in Tore Supra",* Fusion Eng. Design, vol. 82, Issues 5-14, 658-661, 2007

- Rodrigues P and JPS Bizarro, *"Tokamak equilibria with toroidal-current reversal in the plasma core consistent with experimental data",* Physical Review Letters 99, 125001, 1-4, 2007.

- Saibene G, N Oyama, J Lönnroth, Y Andrew, E de la Luna, C Giroud, GTA Huysmans, Y Kamada, MAH Kempenaars, A Loarte, D Mc Donald, MMF Nave, A Meigs, V Parail, R Sartori, S Sharapov, J Stober, T Suzuki, M Takechi, K Toi, H Urano, *"The H-mode pedestal, ELMs and TF ripple effects in JT-60U/JET dimensionless identity experiments",* Nuclear Fusion 47, 8, 969, 2007.

- Sánchez J, et al, *"Overview of TJ-II experiments",* Nuclear Fusion 47 (2007) S677-S685.

- Schirmer J, GD Conway, E Holzhauer, W Suttrop, H Zohm and the ASDEX Upgrade Team, *"Radial correlation length measurements on ASDEX Upgrade using correlation Doppler reflectometry",* Plasma Physics and Controlled Fusion, 49, 7, 1019, 2007.

- Schmid K, T Schwarz-Selinger, W Jacob, R Dux and the ASDEX Upgrade Team, *"The implications of high-Z first-wall materials on noble gas wall recycling",* Nuclear Fusion, 47, 8, 984, 2007.

- Sips ACC, G Tardini, CB Forest, O Gruber, PJ Mc Carthy, A Gude, LD Horton, V Igochine, O Kardaun, CF Maggi, M Maraschek, V Mertens, R Neu, AG Peeters, GV Pereverzev, A Stäbler, J Stober, W Suttrop and the ASDEX Upgrade Team, *"The performance of improved H-modes at ASDEX Upgrade and projection to ITER",* Nuclear Fusion, 47, 11, 1485, 2007.

- Stober J, ACC Sips, C Angioni, CB Forest, O Gruber, J Hobirk, LD Horton, CF Maggi, M Maraschek, P Martin, PJ McCarthy, V Mertens, Y-S Na, M Reich, A Stäbler, G Tardini, H Zohm and the ASDEX Upgrade Team*"The role of the current profile in the improved H-mode scenario in ASDEX Upgrade",* Nuclear Fusion 47, 8, 728, 2007.

- Tala T, K Crombé, PC de Vries, J Ferreira, P Mantica, AG Peeters, Y Andrew, R Budny, G Corrigan, A Eriksson, X Garbet, C Giroud, M-D Hua, H Nordman, V Naulin, MFF Nave, V Parail, K Rantamäki, BD Scott, P Strand, G Tardini, A Thyagaraja, J Weiland, K-D Zastrow and JET-EFDA Contributers*, "Toroidal and poloidal momentum transport studies in tokamaks",* Plasma Physics and Controlled Fusion, 49, 12B, B291, 2007.

- Tardini G, J Hobirk, VG Igochine, CF Maggi, P Martin, D McCune, AG Peeters, ACC Sips, A Stäbler, J Stober and the ASDEX Upgrade Team*, "Thermal ions dilution and ITG suppression in ASDEX Upgrade ion ITBs",* Nuclear Fusion, 47, 4, 280, 2007.

- Tsalas M, A Herrmann, A Kallenbach, HW Müller, J Neuhauser, V. Rohde, N. Tsois, M. Wischmeier and the ASDEX Upgrade Team, *"Divertor plasma flow near the lower x-point in ASDEX Upgrade",* Plasma Physics and Controlled Fusion, 49, 6, 857, 2007.

- Valovic M, L Garzotti, I Voitsekhovitch, M Beurskens, X Garbet, C Giroud, D Keeling and JET EFDA Contributors *"On the correlation between density profile and particle flux in H-mode tokamak plasmas and the implication for ITER",* Nuclear Fusion 47, 3, 196, 2007.

- Vermare L, F Ryter, C Angioni, AG Peeters, J Stober, R Bilato, LD Horton, B Kurzan, CF Maggi, H Meister, J Schirmer, G Tardini and the ASDEX Upgrade Team*"Study of the β dependence of confinement and heat transport in ASDEX Upgrade",* Nuclear Fusion 47, 5, 490, 2007.

- Zaitsev FS, A Gondhalekar, TJ Johnson, SE Sharapov, DS Testa, II Kurbet and JET EFDA contributors *"Suprathermal deuterium ions produced by nuclear elastic scattering of ICRH driven He^3ions in JET plasmas",* Plasma Physics Controlled Fusion 49, 11, 1747, 2007.

- Zohm H, G Gantenbein, F Leuterer, M Maraschek, E Poli, L Urso and the ASDEX Upgrade Team, *"Control of NTMs by*

ECCD on ASDEX Upgrade in view of ITER application", Plasma Physics Controlled Fusion 49, 12B, B341, 2007.

22.1.3. Invited Talks in Conferences

Seminar on Fusion Diagnostics, Universidade de São Paulo, Instituto de Física, Brasil, March 2007

Manso M, *"Contribution of CFN to the reflectometry diagnostics for ITER"*.

Chaos, Complexity and Transport: Theory and Applications, Marseille, June 2007

- Vilela Mendes R, *"Stochastic representations and localized numerical codes"*.

EFDA Fusion Programme Workshop, Garching, 18-20 July, 2007

- Gonçalves B, CAF Varandas, J Sousa, H Fernandes, BB Carvalho and CFN Control and Data Acquisition Group, *"Perspectives for technical development of Control Systems and Instrumentation"*.

10th Workshop on Electric Fields Structures and Relaxation in Edge Plasmas, Warsaw, July 2007

- Lang PT, Lackner K, Fattorini L, Kallenbach A, Maraschek M, Neuhauser J, Suttrop W and the ASDEX Upgrade Team *"Investigation of pellet triggered MHD events in ASDEX Upgrade"*.

12th European Fusion Theory Conference, Madrid, 24-27 September 2007

- Ribeiro T, *"Edge turbulence simulations: self consistent MHD equilibrium and the X-point singularity"*.

International Conference on Burning Plasma Diagnostics, Villa Monastero, Varenna, Italy, 24-28 September 2007

- Manso M, *"Advances on real time reflectometry for plasma position control on ITER"*.

10th IAEA Technical Meeting on Energetic Particles in Magnetic Confinement Systems, 8-10 October 2007, Kloster Seeon, Germany

- Pinches SD, N Arcis, HL Berk, DN Borba, I Chapman, A Fasoli, S Hacquin, V Kiptily, A Klein, F Nabais, Nazikian, M Reich, SE Sharapov, D testa and JET EFDA contributors, "*Fast Ion Driven Instabilities in JET"*

17th Technical Meeting on Research Using Small Fusion Devices, Lisbon, 22-24 October 2007

- Silva C, H Fernandes, CAF Varandas, D Alves, P Balan, BB Carvalho, I Carvalho, P Carvalho, PA Carvalho, R Coelho, JB Correia, A Duarte, P Duarte, J Ferreira, H Figueiredo, J Figueiredo, J Fortunato, R Galvão, R Gomes, B Gonçalves, C Hidalgo, C Ionita, O Lielausis, V Livramento, T Lunt, A Klyukin, I Nedzelskij, A Neto, T Pereira, E Platacis, V Plyusnin, R Schrittwieser, A Sharakovski, I Tale, D Valcárcel, *"Overview of recent ISTTOK results"*.

International Conference on Stochastic Analysis and Applications, Hammamet, Tunisia, November 2007

- Vilela Mendes R, *"Stochastic solutions of nonlinear partial differential equations"*.

22.1.4. Oral Contributions

3rd Int. Conf. on the Frontiers of Plasma Physics and Technology, 5-9 March 2007, Bangkok, Thailand

- Gonçalves B, CAF Varandas, J Sousa, H Fernandes, AP Rodrigues, BB Carvalho and CFN Control and Data Acquisition Group, *"Advanced Real-Time Control Systems for Magnetically confined fusion plasmas"*.

ITER Plasma Position Reflectometry Meeting, 2-3 April, Cadarache, France

- Silva A, *"Electronics location"*.

2nd TFH Ringberg Meeting – 16-19 April 2007, Ringberg, Germany

- Ekedahl A, K Rantamaki, M Goniche, J Mailloux, V Petrzilka, Y Baranov, J Hobirk, F imbeaux, P Jacquet, E Joffrin, K Kirov, MFF Nave, I Nunes, F Piccolo A Sirinelli, K-D Zastrow and JET-EFDA Contributors, *" LH current drive efficiency variation during gas puffing and LH current profile control in Hybrid scenario plasmas"*

- Eriksson LG, T. Hellsten*, M.F.F.Nave, J. Brzozowski, K. Holmstrom, K.D. Zastrow, "Plasma Rotation with little or no external momentum injection"*

- Nave MFF, L.G. Eriksson, T. Hellsten, K.D. Zastrow, B. Alper, T. Johnson, K. Crombe, Y. Andrew, *"Rotation analysis of discharges with low momentum input. Implications for future experiments"*.

- Rantamaki K, A. Ekedahl, M Goniche, J Mailloux, V Petrzilka, G. Granucci, B. Alper, G. Arnoux, Y Baranov, G. Corrigan, L.Delpech, K. Erents, N. Hawkes, J Hobirk, E. Joffrin, K Kirov, T. Loarer, MFF Nave, I Nunes, J. Ongena, F Piccolo, E. Rachlew, C. Silva, M. Stamp, K-D Zastrow and JET-EFDA Contributors*, " LH wave coupling and SOL charachterisation at ITER-like distances at JET"*

15th Real Time Conference, IEEE NPSS, Fermilab, Batavia, Illinois, USA, April 29 - May 4, 2007

- Rodrigues AP, N Cruz, B Santos, CAF Varandas, J-M Moret, J Berrino, BP Duval, *"TCV Advanced Plasma Control System Software Architecture and Preliminary Results"*.

8th International Reflectometry Workshop, 2-4 May, Saint-Petersburg, Russia

- Graça S, GD Conway P Lauber, M Maraschek, D Borba, S Günter, L Cupido, K Sassenberg, F Serra, ME Manso, the CFN reflectometry group and the ASDEX Upgrade Team, *"Localization of MHD and fast particle modes using reflectometry in ASDEX Upgrade"*.

- Santos J, ME Manso, CFN Reflectometry team and ASDEX Upgrade Team, *"Ongoing work towards real-time reflectometry density profile measurements on ASDEX Upgrade"*.

- Silva F da, S Heuraux, E Gusakov, M Manso and A Surkov, *"Evaluation of the forward scattering contribution to the Doppler signal using a FDTD code"*.

17th Topical Conference RF Power in Plasmas, Clearwater, Florida, USA, May 7-9 2007

- Eriksson L-G, T. Hellsten, MFF. Nave, J. Brzozowski, K. Holmström, T. Johnson, J. Ongena, K.-D. Zastrow, JET-EFDA Contributors *"Toroidal rotation in RF heated JET plasmas"*

- Mantsinen MJ, B Alper, C Angioni, R Buttery, S Coda, L-G Eriksson, JP Graves, T Hellsten, D Howell, LC Ingesson, T Johnson, V Kiptily, M Lennholm, M-L Mayoral, A Mueck, F Nabais, F Nave, J-M. Noterdaeme, J Ongena, O Sauter, SE Sharapov e E Westerhof, "*Modification of sawtooth oscillations with ICRF waves in the JET tokamak*".

- Ongena J, A Ekedahl, L-G Eriksson, J Mailloux, ML Mayoral, K Rantamaki, D Van Eester, Yu Baranov, C Chalis, L Colas, F Durodié, G Ericsson, Ph Jacquet, I Jenkins , T Johnson, M Goniche, G Granucci, C Hellesen, T Hellsten, J Kallne, K Holmstrom, A Krasilnikov, E Lerche, I Monakhov, M Nave et al, "*Overview of recent results in heating and current drive in JET*".

- Rantamaki K, A Ekedahl, M Goniche, J Mailloux, V Petrzilka, G Granucci, B Alper, G Arnoux, Y Baranov, L Delpech, K Erents, N Hawkes, J Obirk, E Joffrin, K Kirov, T Loarer, F Nave, I Nunes, J Ongena, V Parail, F Piccolo, E Rachlew, C Silva and JET EFDA contributors, *"LH wave coupling over ITER-like distances at JET"*.

Workshop on "Dimensão Internacional do Programa Nacional de Energia na AIE (OCDE)", INETI, Lisbon, May 2007

- Serra F and Varandas C *"Energia de Fusão na Agência Internacional de Energia"*.

- Varandas C and Serra F *"Acordos Internacionais no âmbito da Fusão Nuclear"*.

ITER Plasma Position Reflectometry Meeting, 4-5 June, Milan, Italy

- Silva A, *"Combiner and decombiner"*.

6th IAEA TM on Control, Data Acquisition and Remote Participation for Fusion Research, Inuyama, 4-8 June 2007

- Sousa J, *"Control and data acquisition sub-systems for fusion experiments"*.

10th Workshop on Electric Fields Structures and Relaxation in Edge Plasmas, Warsaw, July 2007

- Silva C, P Duarte, H Fernandes, H Figueiredo and P Balan, *"Poloidal structure of the ISTTOK edge fluctuations"*.

US-EU-JPN RF Heating Technology Workshop, Heidelberg, 10-12 September 2007

- Hoang GT, F Kazarian, B Beaumont, YX Wan, A Bécoulet, J Belo, G Berger-By, J Bizarro, J Decker, A Ekedahl, M Goniche, D Guilhem, J Jacquinot, X Litaudon, R Magne, J Mailloux, F De Marco, F Mirizzi, JM Noterdaeme, V Pericoli-Ridolfini, Y Peysson, F Rimini, M Schneider, A Tuccillo, PK Sharma, JG Kwak, P Bonoli, S Milora, R Parker and D Rasmussen, *"A Day-1 LHCD system on ITER"*.

TF-ITM General Meeting – 17-20 September 2007, Garching, Germany

- Nave MFF, M. Brix, B.Alper,C.Boswell, S. Gerasimov, S. Hacquin, N.Hawkes, J. E. de la Luna, D.Borba, C. Challis, R. Galvão[1], E. Joffrin, J. Mailloux, S. Sharapov, P.Smeulders and EFDA-JET contributors *"On the use of mhd analysis for validation of q-profiles in JET plasmas "*

International Workshop on Burning Plasma Diagnostics, Villa Monastero, Varenna, Italy, 24-28 September 2007

- Kiptily VG, D Borba, FE Cecil, M Cecconello, D Darrow, V Goloborod'ko, K Hill, T Johnson, A Murari, F Nabais, SD Pinches, M Reich, SE Sharapov, V Yavorskij, IN Chugunov, DB Gin, G Gorini, AE Shevelev, DB Syme and V Zoita, "*Fast ion JET diagnostics: confinement and losses*".

ITER Plasma Position Reflectometry Meeting, 1-2 October, Madrid, Spain

- Silva A, *"Electromagnetic study of the 90º waveguide bend"*

10th IAEA Technical Meeting on Energetic Particles in Magnetic Confinement Systems, 8-10 October 2007, Kloster Seeon, Germany

- Plyusnin VV, MF Johnson, B Alper, J Mlynar and JET EFDA contributors, *"Critical issues addressed to runaway electron generation expected at major disruptions in reactor-scale tokamaks"*.

Reflectometry Simulation Meeting, Garching, Germany, 29–30 October 2007.

- Silva F, *Overview of CFN's reflectometry simulation code-2D FDTD fullwave code*.

ITER Plasma Position Reflectometry Meeting, October 2007, Madrid, Spain

- Heuraux S, F Silva, *"Characterization of the turbulence in fusion plasma by reflectometry"*.

17th Technical Meeting on Research Using Small Fusion Devices, Lisbon, 22-24 October 2007

- Carvalho BB, *"Real-time diagnostics for control on small tokamaks"*.

- Gomes RB, H Fernandes, C Silva, A Sarakovskis, T Pereira, J Figueiredo, B Carvalho, A Soares, P Duarte, C Varandas, O Lielausis, A Klyukin, E Platacis and I Tale, *"Interaction of a liquid Gallium jet with ISTTOK edge plasmas"*.

- Livramento V, JB Correia, D Nunes, PA Carvalho, H Fernandes, C Silva, K Hanada, N Shohoji, E Osawa, *"Novel approach to plasma facing materials in nuclear fusion reactors"*.

- Nedzelskiy IS, A Malaquias, Yu Tashchev, C Silva, H Figueiredo, B Goncalves, H Fernandes, CAF Varandas, *"Development of a multichannel time-of-flight technique for plasma potential profile measurements by heavy ion beam diagnostic on the tokamak ISTTOK"*.

Arcus – 3rd France-Russia Seminar, Metz, 7-9 November, 2007
Heuraux S and F da Silva, *2D Full-wave simulations on the GAP5 ITER plasma position reflectometer*

Greifswald-Garching Theory Meeting, Sellin, Alemanha, 19-23 November, 2007

- Ribeiro T, *"Turbulence simulations near the X-point with self-consistent equilibrium".*

22.1.5. Poster Contributions

8th International Reflectometry Workshop, 2-4 May, Saint-Petersburg, Russia

- Fattorini L, E Strumberger, LD Horton, W Schneider, J Santos, the CFN reflectometry team and the ASDEX Upgrade team, *"Magnetic ripple effects on density profiles measurements at ASDEX Upgrade".*

16th International Stellarator/Heliotron Workshop, Toki, Japan 2007

- Guimarãis L, T Estrada, E Ascasíbar, ME Manso, L Cupido, T Happel, E Blanco, R Jiménez-Gómez, MA Pedrosa, C Hidalgo, I Pastor, A López-Fráguas and the TJ-II team, *"Parametric dependence of the perpendicular velocity shear layer formation in TJ-II plasmas".*

17th Topical Conference RF Power in Plasmas, Clearwater, Florida, USA, May 7-9 2007

- Cesario R, C Castaldo, A Fonseca, P Smeulders, G Calabrã, "*Lower hybrid current drive and low magnetic shear at large radii in transport barriers at high betaN of JET (Joint European Torus)".*

- Kazarian F, B Beaumont, A Beunas, D Guilhem, J Achard, JH Belo, G Berger-By, B Bertrand, E Bertrand, L Delpech, S Dutheil-Hertout, C Goletto, P Mollard, M Prou, K Vulliez, *"Status of the Tore Supra CIMES Project",* In AIP Conference Proceedings, vol. 933, pp.245-248 (2007).

6th IAEA Technical Meeting on Control, Data Acquisition, and Remote Participation for Fusion Research, 4-8 June 2007, Inuyama, Japan

- Castro R, J Veja, A Portas, DR López, S Balme, JM Theis, P Lebourg, H Fernandes, A Neto, A Duarte, F Oliveira, F Reis, K Purahoo, K Thomsen, W Schiller, J Kadlecsik, *"PAPI based federation as a test-bed for a common security infrastructure in EFDA sites".*

- Cruz N, AP Rodrigues, B Santos, CAF Varandas, BP Duval, J-M Moret, J Berrino, Y Martin, X Llobet, *"The Integration of the New Advanced Digital Plasma Control System in TCV".*
- Duarte AS, JH Santos, H Fernandes, A Neto, T Pereira and CAF Varandas, *"FireCalc: An XML-based framework for distributed data analysis".*

- Figueiredo, ACA, JS Ferreira, R Coelho, D Alves, *"A signal processing tool to compute and visualize the Choi–Williams distribution and the Hilbert–Huang transform of nonstationary signals in fusion research".*

- Neto A, J Sousa, B Carvalho, H Fernandes, RC Pereira, AM Fernandes, C Varandas, G Gorini, M Tardocchi, D Gin, A Shevelev and K. Kneupner, *"The control and data acquisition software for the gamma-ray spectroscopy ATCA sub-systems of the JET-EP2 enhancements".*

- Pereira RC, J Sousa, AM Fernandes, F Patrício, B Carvalho, A Neto, CAF Varandas, G Gorini, M Tardocchi, D Gin, A Shevelev *"ATCA Data Acquisition System for Gamma Rays Spectroscopy ".*

- Valcárcel DF, BB Carvalho, IS Carvalho, H Fernandes, AS Duarte, P Duarte, C Silva, R Coelho, J Sousa, CAF Varandas, *"Real-Time Plasma Position Control on the ISTTOK Tokamak".*

34th EPS conference on Controlled Fusion and Plasma Physics, Warsaw, Poland, 2-6 July 2007

- Alonso JA, Andrew P, Neto A, Pablos JL, Cal E., Fernandes H, Gafert J, Heesterman P, Hidalgo C, Kocsis G, Manzanares A, Murari A, Petravich G, Rios L, Silva C, Thomasand PD and JET EFDA contributors, *"Fast visible camera installation and operation in JET"*

- Belo P, V Parail, G Corrigan, W Fundamenski, C Giroud, J Spence, and JET EFDA contributors, *"Numerical simulations of recycling impurity screening on JET".*

- Budny, RV, E Mazzucato, J Candy, RE Waltz, R Bravenec, A Fonseca, and the TFTR and EFDA-JET teams, *"Gyrokinetic simulations of electron density fluctuations and comparisons with measurement".*

- Carvalho, PA et al., *"Plasma-erosion of Cu-nanodiamond and W-nanodiamond composites".*

- Figueiredo ACA, A Fonseca, L Meneses, S Hacquin, J Fessey, E Mazzucato, and JET EFDA contributors; *"Recent results of radial correlation reflectometry in JET".*

- Fonseca A, B Alper, R Budny, L Cupido, J Fessey, A Figueiredo, S Hacquin, ME Manso, E Mazzucato, L Meneses, A Sirinelli, M Walsh, and JET EFDA Contributors; *"Radial correlation reflectometry measurements on the JET tokamak".*

- Gomes RB, H Fernandes, C Silva, A Sarakovskis, T Pereira, J Figueiredo, B Carvalho, A Soares, C Varandas, O Lielausis, A Klyukin, E Platacis and I Tale, *"Interaction of a liquid Gallium jet with ISTTOK edge plasmas"*, ECA Vol.31F, P-1.033 (2007).

- Graça S, GD Conway P Lauber, M Maraschek, D Borba, S Günter, L Cupido, K Sassenberg, F Serra, ME Manso, the CFN reflectometry group and the ASDEX Upgrade Team, *"Studies of fast particle modes in ASDEX Upgrade using reflectometry and comparison with theoretical prediction".*

- Mazzitelli G, ML Apicella, V Pericoli Ridolfini, A Alekseyev, G Apruzzese, W Bin, P Buratti, R Cesario, S Cipiccia, G Calabrò, R De Angelis, L Gabellieri, F Gandini, E Giovannozzi, R Gomes, G Granucci, B Esposito, H Kroegler, I Lyublinski, M Marinucci, C Mazzotta, A Romano, O Tudisco, A Vertkov, FTU Team, ECRH Team,

"Experiments on FTU with a liquid lithium limiter", ECA Vol.31F, O-2.001 (2007).

- Nabais F, D Borba, M Garcia-Muñoz, T Johnson, V Kiptily, M Reich, MFF Nave, SD Pinches, P Sandquist and S Sharapov, *"Redistribution of ICRH Fast Ions in the Presence of Fishbones and Alfvén Eigenmodes"*.

- Nave MFF, LG Eriksson, T Hellsten, K-D Zastrow, B Alper, Y Andrew, R Barnsley, J Brzozowski, K Crombé, A Czarnecka, M von Hellermann, J Ongena and JET EFDA contributors, *"Toroidal Rotation in Ohmic and RF heated Plasmas"*.

- Petrzilka V, J Maillou, M Goniche, K Rantamäki, G Corrigan, V Parail, P Belo, A Ekedahl, K Erents, P Jacquet, K Kirov, J Ongena, J Spence and JET EFDA contributors, *"Near LH Grill Density Variations as a Function of Gas Puff and LH power"*.

- Ribeiro T, B Scott and F Serra, *"Self consistent MHD equilibrium in turbulence simulations"*.

- Sandquist P, SE Sharapov, M Lisak, T Johnson and F Nabais, "*Fast ion anisotropy drive for bi-directional tornado modes on JET*".

- Udintsev VS, E Asp, O Sauter, H Shidara, F Turco, G Turri, S Coda, G Falchetto, TP Goodman, X Llobet, TI Madeira, Ph Marmillod, H Weisen, "*Control of the oscillatrory regime by local current perturbation in ECCD plasmas on TCV"*

Società Italiana di Fisica, Pisa (Italy), 18th September 2007

- Cesario R, C Castaldo, A Fonseca, V Parail, P Smeulders, M Beurskens, *"Esperimenti di barriera interna di trasporto in plasmi ad alta triangolariti del JET (Joint European Torus) con impiego di lower hybrid current drive (LHCD)"*.

International Workshop on Burning Plasma Diagnostics, Villa Monastero, Varenna, Italy, 24-28 September 2007

- Coelho R, D Alves and JET EFDA contributors, *"Real-time magnetic field pitch angle estimation with a motional stark effect diagnostic using Kalman filtering"*.

- Madeira TI, P Amorim, BP Duval, CAF Varandas, *"High throughput pulse height analysis diagnostic for hot burning plasmas"*

11th IAEA Technical Meeting on H-mode Physics and Transport Barriers, Tsukuba, Japan, 26th September 2007

- McDonald DC, C Giroud, L Laborde, C Petty, B Alper, M Brix, R Buttery, E de la Luna, A Fonseca, N Hawkes, J Hobirk, D Howell, S Jachmich, E Joffrin, R Koslowski, H Leggate, I Nunes, C Perez Von Thun, I Voitsekhovitch, and JET EFDA contributors, *Collisionality and beta dependence of confinement in JET ELMy H-modes.*

10th IAEA Technical Meeting on Energetic Particles in Magnetic Confinement Systems, 8-10 October 2007, Kloster Seeon, Germany

- Pinches SD, N Arcis, HL Berk, DN Borba, I Chapman, A Fasoli, S Hacquin, A Klein, F Nabais, M Reich, SE Sharapov, D Testa, V Kiptily, "*Fast Ion Driven Instabilities in JET*".

- Plyusnin VV, B Alper, E de La Luna and JET EFDA contributors, *"Analysis of non-thermal features of electron cyclotron emission measured during ELMs in JET"*.

International Conference on Research and Applications of Plasmas, 16-19 October 2007

- Carvalho PJ, H Thomsen, S Gori, U Toussaint, J Geiger, A Weller, R Coelho and H Fernandes, *"Comparison of fast tomographic methods for application on the Soft X-Ray Tomography System on Wendelstein 7-X Stellarator"*.

17th Technical Meeting on Research Using Small Fusion Devices, Lisbon, 22-24 October 2007

- Alonso MP, JH Severo, FO Borges, JI Elizondo, LA Berni, M Machida, CAF Varandas, RMO Galvão, *"Multipoint Thomson scattering diagnostic for the TCABR tokamak with centimeter spatial resolution"*.

- Carvalho PJ, H Thomsen, S Gori, U Toussaint, A Weller, R Coelho, A Neto, T Pereira, C Silva and H Fernandes, *"Fast tomographic methods on the tokamak ISTTOK"*.

- Coelho R, D Alves and C Silva, *"Time scale analysis of ISTTOK probe data"*.

- Duarte AS, J Santos, H Fernandes, A Neto, T Pereira, CAF Varandas, *"FireCalc: an XML-based Framework for Distributed Data Analysis"*.

- Figueiredo J, RB Gomes, H Fernandes, A Sharakovski, *"Plasma Spectroscopy in ISTTOK"*.

- Lunt T, C Silva, H Fernandes, C Hidalgo, MA Pedrosa, P Duarte, H Figueiredo and T Pereira, *"Edge plasma pressure measurements using a mechanical force sensor on the tokamak ISTTOK"*.

- Severo JHF, Nascimento IC, Kuznetov Yu K, Tsypin VS, Elfimov AG, Galvão RMO, Alonso MP, Ruchko LF, Machida M, Ribeiro C, Usuriaga OC, Bellintani, V Jr Germano, TM, Sanada, EK Elizondo, JI Fagundes, AN, de Sá WP, and Tendler M, *"Temporal evolution of plasma rotation measurement in tokamaks using an optical monochromator and two photomultipliers as detector"*.

- Valcárcel DF, IS Carvalho, BB Carvalho, H Fernandes, C Silva, P Duarte, A Duarte, PJ Carvalho e T Pereira, *"Validation of ISTTOK Plasma Position Controller"*.

ASDEX Upgrade Seminar, 22-25 October 2007, Kloster Seeon, Germany

- Conway GD, C Tröster, S da Graça, ASDEX Upgrade & CFN Teams, *"Pedestal fluctuations and GAMs"*.

- Maraschek M, M Garcia Muñoz, S da Graça, S Günter, V Igochine, P Lauber, P Martin, P Piovesan, K Sassenberg, H Zohm, ASDEX Upgrade Team, *"Experimentalists view on fast particle driven mode"*.

Arcus – 3rd France-Russia Seminar, Metz, 7-9 November, 2007

- Heuraux S, E Gusakov, A Yu Popov, M Schubert, F da Silva, T Gerbaud, *"The reflectometry as a multi-function diagnostic to characterize turbulence of fusion plasmas"*.

- Schubert M, S Heuraux, E Gusakov, A Popov, T Gerbaud, F da Silva, *"On the absolute value of the density fluctuation measured by reflectometry"*.

49th Annual Meeting of the Division of Plasma Physics, Orlando - Florida, USA, 12-16 November 2007

- Budny RV, E Mazzucato, A Fonseca, R Bravenec, J Candy, RE Waltz, TFTR Team, EFDA-JET Collaboration, *"Gyrokinetic simulations of electron density fluctuations and comparisons with measurement"*.

- Fonseca A, B Alper, R Budny, L Cupido, J Fessey, A Figueiredo, S Hacquin, ME Manso, E Mazzucato, L Meneses, A Sirinelli, M Walsh, and JET EFDA Contributors, *"Radial correlation reflectometry measurements on the JET tokamak"*.

9th Brazilian Meeting on Plasma Physics 25-28 November, São Pedro, SP, Brazil, 2007

- Berni LA, MP Alonso , JH Severo, FO Borges, JI Elizondo, M Machida, CAF Varandas, RMO Galvão, *"Design of a Multipoint Thomson Scattering Diagnostic for the TCABR Tokamak"*.

- Berni LA, E del Bosco, MP Alonso, *"10-Channel Thomson Scattering Diagnostic for the ETE Tokamak"*.

- Severo JHF, Bellintani V Jr, Kuznetov, Yu K, Nascimento IC, Tsypin VS, Guimarães-Filho Z O, Caldas IL, Elfimov A G, Galvão RMO, Alonso MP, Ruchko LF, Machida M, Ribeiro C, Usuriaga OC, Flores DAM, Germano TM, Sanada EK, Elizondo JI, Fagundes AN, and Sá de WP, *"Spectroscopy study of the MHD activity"*.

22.1.6. Other publications

- Belo JH, and Dominique Guilhem, *"Assessing the likelihood of arcing from brazing deficiencies in the C4 launcher by studying the electric fields inside its waveguides"*, DRFC-CEA report (2007)

- Belo JH, and Dominique Guilhem, *"Gauging how (small) changes in the position and depth of a single passive waveguide on the C4 LH launcher (could) affect the main parameters of its radiated spectrum"*, DRFC-CEA report (April 2007)

- Cupido L, M. Manso, *"Proposal for a Profile Reflectometry System on JET"*, internal report CFN/IST, August 2007.

- Cupido L, M. Manso, L. Meneses, A. Silva, P. Varela, *"Upgrade of the KG8a Sweeping Reflectometer to a Multi-Band System"*, internal report CFN/IST, November 2007.

- Cupido L, *"Tecnologia de varrimento de HTOs com Sincronização de Fase/Frequência para aplicação em Reflectometria de Banda Larga"*, internal report CFN/IST, August 2007.

- Cupido L, "Status of technology for millimeter and sub-millimeter wave Reflectometry, ECE and ECA Diagnostics", internal report CFN/IST, March 2007.

- Cupido L, *Reflectometria de Banda Larga em Tokamaks de grande Dimensão (ITER e JET) – limitações das tecnologias actuais,* internal report CFN/IST, February 2007.

- H&CD working group, LHCD Sub-group, contributors to the proposal, *"A 'day1' LHCD system on ITER"*, February 2007

- Santos J, M. Manso *"Proposal for a real time electron density profile measurement diagnostic for ASDEX Upgrade"*, internal report CFN/IST, June 2007.

- Silva A, Zajac J, Manso M, *"Design of reflectometry system for the Compass-D tokamak"*, internal report CFN/IST, December 2007.

- Varela P, M. Manso *"Support to ITER Diagnostic Design, ITER Task: Plasma Position Reflectometry"*, Contract: EFDA 03.1118, Final Report, Association EURATOM/IST, March 2007.

22.1.7. Projects/Funding awarded in 2007

- *"Data Acquisition System for Compass-D"*.

- *"Diagnostic Design for ITER - Plasma Position Reflectometer"*, EFDA Contract Nº 06-1449.

- *"Microwave Diagnostics Engineering in preparation for ITER"* EURATOM Fusion Training Scheme – EFDA Contract Nº 042961.

- *"JET Experimental Campaigns C18-C19"*, JW7-O-IST-30A.

- *"JET Gamma Ray Spectrometer"*, JW7-OEP-IST-31.

- *"JET Plasma Control Upgrade"*, JW5-TA-EP2-PCV-02**.**

- *"Integration of Transport and MHD Codes at JET"*, EFDA-30/4.6

- *"Reequipment of the CFN Microwave Laboratory"*, Fundação para a Ciência e Tecnologia.

22.1.8. Laboratorial prototypes

- Mechanical plasma pressure sensor based on two pendulums whose heads are exposed to plasma, while the deflection is measured by high sensitivity semi-conductor strain gauges (Plasma Phys. Control. Fusion 49, 1783, 2007).

- Compact cantilever probe for plasma pressure measurements (Rev. Sci. Instrum. 034702, 2007).
- Water cooled PC Cluster (Internal report 1/2007).
- Eurocard Generic Microcontroller.
- Multi-channel amplifier for the tomography diagnostic.
- Bolometer tomography diagnostic based on 3 linear 10-pixel detectors (17th IAEA TM on RUSFD, Oct. 2007).
- High gain photodiode sensor for the ISTTOK spectrometer.
- Full active bridge for the mechanical plasma pressure diagnostic.
- A digital controlled high voltage (1.5kV) power supply for PMT's.
- Development of a real-time controller for the plasma position (17th IAEA TM on RUSFD, Oct. 2007).
- Fast rise-time digitally controlled power supplies for the ISTTOK plasma control system.
- A five-channel retarding field energy analyzer for edge ion temperature measurements on TJ-II.
- Bibet Ph., D Guilhem, JH Belo, et al, Prototype of the C4 PAM LH launcher module.
- Bibet Ph., D Guilhem, JH Belo, et al, Prototype of the TE_{10}-TE_{30} mode converter for the PAM-C4 LH launcher.
- Control and data acquisition Group, *EPN-PCI,* fast timing and event management board for the PCI bus.
- Control and data acquisition Group, *PMC-PCIe,* 32-bit PMC interface card which provides one x1 PCIe fiber optical channel.
- Control and data acquisition Group, *ATCA-CONTROLLER-PCIe,* ATCA double width blade compliant with the PCIe and ATX standards.
- Control and data acquisition Group, *ATCA-MIMO-ISOL,* the card provides 32 analog input channels (digitizer/transient recorder) and 8 analog output channels (waveform generator).
- Control and data acquisition Group, *SR-TR-ATCA,* ATCA board with eight acquisition channels per modul with dData transfer rate of up to 800 Mbyte/s over x4 PCI Express to the host processor.
- Control and data acquisition Group, *Test-Bench System of the JET RTP Phase 2 (JW3-TA-EP-RTP-01),* the test-Bench system provides analogue and ATM stimulus signals to a real time control systems under test.
- Control and data acquisition Group, *Data Acquisition for the Gamma Ray diagnostics (JET-DNG)*, this system provides a modern data acquisition for the JET neutron camera.
- Control and data acquisition Group, *Real-time DSP-based control system for ISTTOK plasma position,* this system acquires a set of 12 pick-up coils measuring the poloidal field from the plasma.

22.1.9. Numerical codes

- Cross-spectrum analysis of the data from the Mirnov coils and determination of the poloidal/toroidal mode numbers.
- Coherency analysis of cross diagnostic data (Mirnov, Heavy ion beam, X-ray Tomography) for fluctuation analysis in time/spatial content.
- Kalman filtering approach to the real-time amplitude estimation of spectral harmonics involved in the magnetic field pitch angle determination using Motional Stark Effect diagnostic in JET.
- Development of a SCAD – a cooperative software for shared tokamak operation.
- Development of remote data access tools.
- FusionTalk – Video Conference Web based tool.
- FireCalc – Remote procedure invocation for job scripting submissions under general software (MatLab, IDL, SciLab Mathematica and others).
- Tomographic reconstruction of the ISTTOK plasma emissivity.
- Nave MFF, Sawtooth models in JETTO.
- Nave MFF, ELM models in JETTO.
- Ribeiro TT, Scott B, "SOL and self-consistent MHD equilibrium (including an X-point) in the 3-D gyrofluid turbulence model GEM".
- Goniche M, O. Izacard, D. Voyer, J.H.Belo, Codes SWAN and ALOHA for the coupling of LH.
- Silva F, S. Heuraux, M. Manso, "Full wave 2D code using Finite Difference Techniques in the Time Domain (FDTD), with an unidirectional transparent source (UTS)".

22.1.10. Organization of conferences and workshops

- Nave MFF, (member of the Scientific Program Committee), 5th International Conference on the Physics of Dusty Plasmas, Azores, Portugal, May 2008
- Silva C, chairman of the 17th IAEA Technical Meeting on Research Using Small Fusion Devices, Lisbon, October 2007.

- Varandas C, chairman of the RUSFD, Lisbon, October 2007.

- Varandas C and Serra F, members of the LOC of the 8th IEA International Workshop on Beryllium Technology, ITN, Lisbon, December 2007.

22.1.11. Participation in scientific committees of conferences and workshops

- Silva C, Workshop on Electric Fields, Turbulence and Self-Organisation in Magnetised Plasmas.

22.1.12. Ph.D thesis completed in 2007

- Silva, A, "*The ASDEX Upgrade broadband microwave reflectometry system*", Universidade Técnica de Lisboa

- Silva, F, *"Finite-difference time-domain simulation of reflectometry in fusion plasmas",* Universidade Técnica de Lisboa

22.1.13. Other activities

- Bizarro JP, Co-author of the LITE (Lower-Hybrid and Ion-Cyclotron Technology) proposal on RF enginnering within the EFDA Goal Oriented Training Programme, a collaboration among the Associatons Euratom-IST, Euratom-CEA, Euratom-ENEA, Euratom-IPP and Euratom-Belgian State.

- Cupido L, Consultant of the United States – DOE (Department of Energy) for the evaluation of scientific proposals for public (US) funding.

- Manso M, Coordination of the project on "Microwave Diagnostics Engineering in preparation for ITER" of the EURATOM Fusion Training Scheme

- Manso M, Jury member (rapporteur) – Thèse d´habilitation à diriger des recherches de Dr. Fréderic Clairet, March 2007, Université de Marseille, France.

- Ribeiro TT, Participation in the "EFDA Task Force on Integrated Tokamak Modelling" within the turbulence project (IMP4), and in the European DEISA project in collaboration with the Max-Planck-Gesellschaft Computer Centre (RZG).

- Silva F, Invited expert at the 1st European Reflectometry Simulation Code Meeting, Garching, Germany, 29–30 October 2007.

- Varandas CAF and EFDA Public Information Group, "Interview to Carlos Varandas", Fusion News Newsletter, Vol. 1, 8, March 2007.

- Organization of the ISTTOK Joint Experiment in collaboration with the IAEA with the participation of 24 scientists from 13 countries.

22.1.14. Collaborations

- Associación Euratom/CIEMAT, Madrid (Estrada T, Hidalgo C).
- Association EURATOM/HAS, Hungary.
- Association EURATOM/ENEA, CNR – Milan, Italy (Lazzaro, E, Simonetto).
- CRPP, Lausanne (Duval B, Moret JM)
- CSU EFDA JET, United Kingdom (Morlock C).
- Departamento Engenharia Electrotécnica Computadores, IST, Portugal (Silva FM and Nunes F)
- DRFC/CEA Cadarache, France (Clairet F, Goniche M, Guilhem G, Litaudon X, Sabot R).
- ERM/KMS, Belgium (Ongena J).
- EURATOM/University of Latvia, Institute of Solid State Physics, Riga, Latvia.
- Humboldt-Universitat zu Berlin, Germany.
- IEPPG, Institute for Ion Physics and Applied Experimental Physics, Association EURATOM/ÖAW, University of Innsbruck, Innsbruck, Austria.
- INETI, Departamento de Materiais e Tecnologias de Produção, Estrada do Paço do Lumiar, Lisboa, Portugal.
- Institut Ioffe, Saint Petersbourg, Russian Federation (Gusakov E).
- Institute of Plasma Physics, IPP.CR, Prague, Czech Republic (Zajac J, Pavlo P).
- Instituto de Telecomunicações, IST (Fernandes C).
- Laboratório de Física de Plasmas, Universidade de São Paulo, Brasil (Elfimov A, Galvão R).
- Laboratoire de Physique des Millieux Ionisés et Applications da Université Henri Poincaré, Nancy, França (Heuraux S).
- Max Planck Institut fuer Plasma Physik, Greifswald, Germany (Hirsh M).
- Max-Planck Institut fuer Plasmasphysik, Garching, Germany (Behler K, Conway G, Coster D, Lang P, Maraschek M, Scott B, Zohm H).
- UKAEA Culham, United Kingdom (Parail V, Sharapov S, Walsh M).
- Université des Marseille, France (Briolle F, Gendrih P).
- VTT, Finland (Tala T).

22.2. TECHNOLOGIES OF PLASMAS AND LASERS

22.2.1. Publications in refereed scientific journals (publications in ISI)

- Ali S, Moslem WM, Shukla PK and Kourakis I, "*Fully nonlinear ion-sound waves in a dense Fermi magnetoplasma"*, Physics Letters A, 366 (6): 606-610 Jul 9 2007.

- Ali S and Shukla PK, "*Streaming instability in quantum dusty plasmas"*, European Physical Journal D, 41 (2): 319-324 Feb 2007.

- Álvarez R and Alves LL, "*Two-dimensional electromagnetic model of a microwave plasma reactor operated by an axial injection torch"*, Journal Applied Physics 101: 103303 1–6 May 2007.

- Alves LL, "*Fluid modelling of the positive column of direct-current glow discharges",* Plasma Sources Science and Technology 16: 557–569 June 2007 Paper originally presented at the European Summer School 'Low Temperature Plasma Physics: Basics and Applications' and 'Master Class: Biotechnical and Medical Applications' (Bad Honnef, Germany, 26 September–8 October 2004).

- Bertolami O, Boehmer, CG Harko T and Lobo FSN, "*Extra force in f(R) modified theories of gravity",* Physical Review D75: 104016 2007

- Bertolami O and Carvalho C, "*Spontaneous symmetry breaking in the bulk as a localization mechanism of fields on the brane",* Physical Review D76: 104048 2007

- Bertolami O and Paramos J, "*A Mission to test the Pioneer anomaly: Estimating the main systematic effects",* International Journal Modern Physics D16: 1611-1623 2007

- Bertolami O, Pedro, FG and Delliou ML, "*Dark Energy-Dark Matter Interaction and the Violation of the Equivalence Principle from the Abell Cluster",* Physics Letters B654: 165-169 2007

- Bhowmika C, Misrab AP and Shukla PK, "*Oblique modulation of electron-acoustic waves in a Fermi electron-ion plasma",* Physics of Plasmas, 14 (12): Art. No. 122107 Dec 2007

- Bingham R, Silva LO, Mendonca JT, Shukla PK, Mori WB and Serbeto A, "*Plasma wakes driven by neutrinos, photons and electron beams",* International Journal of Modern Physics B 21 (3-4): 343-350 Feb 2007

- Dias FM and Popov Tsv, "*EEDF probe measurements: differentiation methods, noise, and error",* J. Physics: Conference Series 63: 012005 (16pp) 2007

- Diaz AM, Garcia OE, Diaz JP, Exposito FJ, Utrillas MP, Martinez-Lozano JA, Alados-Arboledas L, Olmo FJ, Lorente J, Cachorro V, Horvath H, Labajo A, Sorribas M, Vilaplana JM, Silva AM, Elias T, Pujadas M, Rodrigues JA and Gonzalez JA, "*Aerosol radiative forcing efficiency in the UV region over southeastern Mediterranean: VELETA2002 campaign",* Journal of Geophysical Research-Atmospheres, 112 (D6): Art. No. D06213 Mar 31 2007

- Eloy M, Guerreiro A, Mendonça JT and Bingham, R, "*Hamiltonian formulation of direct laser acceleration in vacuum",* Journal of Plasma Physics, 73: 635-647 Part 5 Oct 2007

- Figueira G, Wemans J, Pires H, Lopes NC and Cardoso L, "*Single adjuster deformable mirror with four contact points for simultaneous correction of astigmatism and defocus",* Optics Express 15: 5664-5673 2007

- Gargaté L, Bingham R, Fonseca RA, and Silva LO, "*dHybrid: A massively parallel code for hybrid simulations of space plasmas",* Computer Physics Communications 176 (6): 419-425 Mar 15 2007

- Guerra V, "*Analytical model of heterogeneous atomic recombination on silicalike surfaces",* IEEE Transactions on Plasma Science 35: 1397–1412 2007

- Guerra V, Sá PA and Loureiro J, "*Nitrogen pink afterglow: the mystery continues",* Journal of Physics Conference Series 63: 012007 2007

- Guerra V and de Abreu R, *Comment on: "From classical to modern ether-drift experiments: the narrow window for a preferred frame"* [Phys. Lett. A 333 (2004) 355], Physics Letters A 361: 509–512 2007

- Guerreiro A, Eloy M, Mendonca JT and Bingham R, "*Dipolar radiation from spinning dust grains coupled to an electromagnetic wave",* Journal of Plasma Physics, 73: 555-563 Part 4 Aug 2007

- Krasheninnikov SI, Shevchenko VI and Shukla PK, "*Spinning of a charged dust particle in a magnetized plasma",* Physics Letters A, 361 (1-2): 133-135 Jan 22, 2007

- Kutasi K, Pintassilgo CD, Loureiro J and Coelho PJ, "*Active species in a large volume N_2-O_2 post-discharge reactor",* Journal of Physics D: Applied Physics 40: 1990–2001 2007

- Kutasi K and Loureiro J, "*Role of the wall reactor material on the species density distributions in an N_2-O_2 post-discharge for plasma sterilization",* Journal of Physics D: Applied Physics 40: 5612–5623 2007

- Lancaster KL, Green JS, Hey DS, Akli KU, Davies JR, Clarke RJ, Freeman RR, Habara H, Key MH, Kodama R, Krushelnick K, Murphy CD, Nakatsutsumi M, Simpson P, Stephens R, Stoeckl C, Yabuuchi T, Zepf M and Norreys PA, "*Measurements of Energy Transport Patterns in Solid Density Laser Plasma Interactions at Intensities of 5 x 10^{20} W cm^{-2}",* Physical Review Letters 98 (12): Art. No. 125002 Mar 23 2007

- Lino da Silva M, Guerra V and Loureiro J, "*State-resolved dissociation rates for extremely nonequilibrium atmospheric entries",* Journal of Thermophysics and Heat Transfer 21(1): 40–49 2007

- Lino da Silva M, Guerra V and Loureiro J, *Nonequilibrium dissociation processes in hyperbolic atmospheric entries,* Journal of Thermophysics and Heat Transfer 21(2): 303–310 2007

- Lino da Silva M, Guerra V and Loureiro J, *"Two-temperature models for nitrogen dissociation",* Chemical Physics 342: 275–287 2007

- Lino da Silva M, "*An adaptive line-by-line-statistical model for fast and accurate spectral simulations in low-pressure plasmas",* Journal of Quantitative Spectroscopy and radiative Transfer, 108(1): 106–125 2007

- Lu W, Tzoufras M, Tsung FS, Joshi C, Mori WB, Vieira J, Fonseca RA and Silva LO, "*Generating Multi GeV electron bunches using single stage laser wake field acceleration in a 3D nonlinear blowout regime",* Physical Review Special Topics-Accelerators and Beams 10 (6): Art. No. 061301 Jun 2007

- Marques LSA, Jolly J and Alves LL, *"Electrical characterization of capacitively-coupled radio-frequency discharges in hydrogen",* Plasma Process & Polymers 4: S937–S941 2007

- Marques L, Fernandes AC, Vaz F and Ramos MMD, "*Influence of oxygen addition on the structural and elastic properties of TiC thin films",* Plasma Process & Polymers 4: S195 2007

- Marques L, Jolly J and Alves LL, "*Capacitively coupled radio-frequency hydrogen discharges: The role of kinetics",* Journal Applied Physics 102: 063305 1–14 Sep 2007

- Martins AA and Pinheiro MJ, "*The connection between inertial forces and the vector potential",* American Institute of Physics Conference Proceedings 880: 1189–1200 (2007)

- Mendonca, JT, "*Axion excitation by intense laser fields",* European Physica Letters, 79 (2): Art. No. 21001 2007

- Mendonca JT and Shukla PK, "*Excitation of ion-acoustic perturbations by incoherent kinetic Alfven waves in plasmas",* Physics of Plasmas, 14 (12): Art. No. 122304 Dec 2007

- Mendonca JT, Silva LO and Bingham R, "*Reflection of an electron beam by a photon mirror",* Journal of Plasma Physics 73: 627-634 Part 5 Oct 2007

- Moslem WM, Kourakis I, Shukla PK and Schlickeiser R, "*Nonlinear excitations in electron-positron-ion plasmas in accretion disks of active galactic nuclei",* Physics of Plasmas, 14 (10): Art. No. 102901 Oct 2007

- Moslem WM, Kourakis I and Shukla PK, "*Finite amplitude envelope solitons in a pair-ion plasma",* Physics of Plasmas, 14 (10): Art. No. 109902 Oct 2007

- Moslem WM, Shukla PK, Ali S and Schlickeiser R, "*Quantum dust-acoustic double layers",* Physics of Plasmas, 14 (4): Art. No. 042107 Apr 2007

- Peano F, Coppa G, Peinetti F, Mulas R and Silva LO, "*Ergodic model for the expansion of spherical nanoplasmas",* Physical Review E 75 (6): Art. No. 066403 Part 2 Jun 2007

- Peano F, Martins JL, Fonseca Ra, Silva LO, Coppa G, Peinetti F and Mulas R, "*Dynamics and control of the expansion of finite-size plasmas produced in ultraintense laser-matter interactions",* Physics of Plasmas 14 (5): Art. No. 056704 May 2007

- Pinheiro MJ, "*Anomalous Diffusion at Edge and Core of a Magnetized Cold Plasma",* Journal of Physics D: Conference Series 71: 102002–012014 2007

- Pinheiro MJ, "*Do Maxwell's equations need revision? - A methodological note",* Physics Essays 20(2) 2007 [Los Alamos ArXives:physics/0511103]

- Pinheiro MJ, "*Electron trapping by electric field reversal in Glow Discharges, in Gas Discharges -Fundamentals and Applications"* (J de Amorim Filho ed.), Research SignPost, Trivandrum, India 2007

- Pintassilgo CD, Kutasi K and Loureiro J, "*Modelling of a low-pressure N_2-O_2 discharge and post-discharge reactor for plasma sterilization",* Plasma Sources Science and Technology 16: S115–S122 2007

- Pintassilgo CD, Jaoul C, Loureiro J, Belmonte T and Czerwiec T, "*Kinetic modelling of a N_2 flowing microwave discharge with CH_4 addition in the post-discharge for nitrocarburising treatments",* Journal of Physics D: Applied Physics 40: 3620–3632 2007

- Resendes DP, Mota S, Mendonca JT, Sanders B, Encarnacao J and del Amo JG, "*Laser propulsion for ground launch",* Journal of Propulsion and Power 23 (1): 73-80 Jan-Feb 2007

- Ricard A, Henriques J, Cousty S, Villerger S and Amorin J, "*Determination of N, H and O–atom in N_2–H_2 and in N_2–H_2 gas mixtures by optical actinometry in flowing microwave discharges and NO titration in post–discharges",* Plasma Process & Polymers 4: S965–S968 2007

- Rus B, Mocek T, Kozlova M, Polan J, Homer P, Stupka M, Tallents GJ, Edwards MH, Mistry P, Whittaker DS, Booth N, Zhai Z, Pert GJ, Dunn J, Nelson AJ, Foord ME, Shepherd R, Rozmus W, Baldis HA, Fajardo M, De Lazzari D, Zeitoun P, Jamelot G, Klisnick A, Ros D, Cassou K, Kazamias S, Bercego H, Danson C, Hawkes S, Juha L, Hajkova V, Chalupsky J, Feldhaus J, Wabnitz H, Nejdl J, Kuba J, Davidkova M and Stisova V, "*Development and applications of multimillijoule soft X-ray lasers",* Journal of Modern Optics, 54:16, 2571 - 2583 (2007)

- Santos JE, Silva LO and Bingham R, "*White-light parametric instabilities in plasmas",* Physical Review Letters 98 (23): Art. No. 235001 Jun 8 2007

- Shukla PK, *"Generation and dynamics of plasma blobs in partially ionized tokamak scrape-off-layer",* Physics Letters A, 371 (5-6): 453-456 Nov 26 2007

- Shukla PK, *"Purely growing electromagnetic mode driven by ion-temperature anisotropy in a collisional plasma",* Physics Letters A, 370 (3-4): 316-318 Oct 22 2007

- Shukla PK, "*Extraordinary electromagnetic waves in a warm dense magnetoplasma",* Physics Letters A, 369 (4): 312-314 Sep 24 2007

- Shukla PK, Coppi B and Eliasson B, "*Electron parallel velocity and temperature gradient driven electrostatic fluctuations in nonuniform magnetoplasmas",* Physics of Plasmas, 14 (1): Art. No. 014504 Jan 2007

- Shukla N, Moslem WM and Shukla, PK, "*Instability of electromagnetic waves in a self-gravitating rotating magnetized dusty plasma with opposite polarity grains",* Physics of Plasmas, 14 (5): Art. No. 053702 May 2007

- Shukla N and Shukla PK, "*Generation of magnetic field fluctuations in relativistic electron-positron magnetoplasmas",* Physics Letters A 362 (2-3): 221-224 Feb 26 2007

- Shukla N and Shukla PK, "*A new purely growing instability in a strongly magnetized nonuniform pair plasma",* Physics Letters A, 367 (1-2): 120-122 Jul 16 2007

- Shukla N, Shukla PK, Liu CS and Morfill GE, "*Generation of magnetic fields in a positive-negative dusty plasma",* Journal of Plasma Physics, 73: 141-144 Part 2 Apr 2007

- Shukla N, Shukla PK and Morfill GE, "*Amplification of magnetic fields by polaritonic flows in quantum pair plasmas",* Journal of Plasma Physics, 73: 289-293 Part 3 Jun 2007

- Shukla PK, Shukla N and Stenflo L, "*Enhanced electromagnetic emission from plasmas containing positive dust grains and electrons",* Physics Letters A, 365 (1-2): 131-134 May 21 2007

- Shukla PK, Shukla N and Stenflo L, "*Kinetic modulational instability of broadband dispersive Alfven waves in plasmas",* Journal of Plasma Physics, 73: 153-157 Part 2 Apr 2007

- Shukla PK and Stenflo L, "*Nonlinear interactions between upper-hybrid and Alfven modes in a magnetized plasma containing charged dust impurities",* Journal of Plasma Physics, 73: 3-8 Part 1 Feb 2007

- Siebold M, Hornung M, Bock S, Hein J, Kaluza MC, Wemans J and Uecker R, "*Broad-band regenerative laser amplification in ytterbium-doped calcium fluoride ($Yb:CaF_2$)",* Applied Physics B 84: 543-547 2007

- Tatarova E, Dias FM, Ferreira CM and Puac N, "*Spectroscopic Determination of H, He and H2 Temperatures Profiles in a Large-Scale Microwave Plasma Source",* Journal Applied Physics 101: 063306 2007

- Tatarova E, Dias FM, Puac N and Ferreira CM, "*Hydrogen Balmer Line Broadening in a Microwave Plasma Source",* Plasma Sources Science and Technology 16: S52–S56 2007

- Tatarova E, Guerra V, Henriques J and Ferreira CM, "*Nitrogen Dissociation in Low-Pressure Microwave Plasmas",* J. Physics: Conference Series 71: 012010 2007

- Tatarova E, Dias FM, Felizardo E, Henriques J, Ferreira CM and Gordiets B, "*Microwave plasma torches driven by surface waves",* Plasma Sources Science and Technology (printed version on the net) 2008

- Trines R, Bingham R, Dunlop MW, Vaivads A, Davies JA, Mendonca JT, Silva LO and Shukla PK, "*Spontaneous generation of self-organized solitary wave structures at earth's magnetopause",* Physical Review Letters 99 (20): Art. No. 205006 Nov 16 2007

- Tzoufras M, Ren C, Tsung FS, Tonge JW, Mori WB, Fiore M, Fonseca RA, and Silva LO, "*Stability of arbitrary electron velocity distribution functions to electromagnetic modes",* Physics of Plasmas 14 (6): Art. No. 062108 Jun 2007

- Vieira J, Fonseca RA, Silva LO, Lu W, Tzoufras M, Tsung FS and Mori WB, "*Sheet crossing and wave breaking in the laser wakefield accelerator",* International Journal of Modern Physics B 21 (3-4): 439-446 Feb 2007

22.2.2. Invited Talks in Conferences

- Bertolami O, *"Searching for the nature of dark energy and dark matter",* VI Workshop Nova Física no Espaço, Campos do Jordão, São Paulo, Brazil, February 2007

- Bertolami O, *"The Pioneer Explorer Collaboration: Second Team Meeting at ISSI",* International Space Science Institute, Bern, Switzerland, February 2007

- Bertolami O, *"From Quantum to Cosmos",* Space-based research in fundamental physics and quantum technologies, Bremen, Germany, June 2007

- Bertolami O, *Encuentros Relativistas Españoles - Spanish Relativity Meeting,* Puerto de La Cruz, Tenerife, Spain, September 2007

- Bertolami O, *Scientific and Fundamental Aspects of the Galileo Programme,* Cité de l'Espace, Toulouse, France, October 2007

- Davies JR, *"The Effect of Magnetic Field on Electron Beam Propagation in Plasmas",* 5th Direct Drive and Fast Ignition Workshop, Madrid, Spain, April 2007

- Davies JR, Fajardo M and Rus B, *"Magnetic Field Driven Filamentation in Laser Ablation of Solids",* Theory of Short Pulse Petawatt Laser Plasma Interaction - Laserlab Europe Workshop, Darmstadt, Germany, October 2007

- Guerra V, *"Vibration-to-Electronic energy transfers in the nitrogen afterglow"*, Workshop on Streamers, sprites, leaders, lightning: from micro- to macroscales, Leiden, The Netherlands, October 2007

- Guerra V, *"Special Relativity as a simple geometry problem",* Sixth Int. Workshop on Applied Category Theory, Graph-operad-logic, Special Relativity, Dynamics and Electromagnetics, Ixtapa, Mexico, February 2007

- Lopes NC, Bendoyro RA, Berardo J, Dias JM, Figueira G, Fiúza F, Fonseca RA, Lemos N, Marti M, Martins J, Martins SF, Onofrei RI, Peano F, Vieira JM and Silva LO, *"Research on laser-plasma accelerators at GoLP-IST-Lisbon",* Laser and plasma accelerators workshop 2007, Angra do Heroismo, Ilha Terceira, Açores, Portugal, July 2007

- Páramos J, *Scientific and Fundamental Aspects of the Galileo Programme,* Cité de l'Espace, Toulouse, France, October 2007

- Peano F, Vieira J, Fonseca RA, Silva LO and Bingham R, *"Direct acceleration of muons with variable-frequency lasers",* Topical workshop on The Neutrino Factory and Muon Collider, the physics and the R&D programmes, The Cosener's House, Abingdon, Oxfordshire, UK, October 2007

- Silva LO, *"Control of the explosions of nanoplasmas",* Dream Beams Symposium, Max Planck Institute for Quantum Optics, Munich, Germany, February 2007

- Silva LO, *"White light parametric instabilities in plasmas" and "Expansions/explosions of nanoplasmas",* Invited Lecturer at the Summer College on Plasma Physics, International Center for Theoretical Physics, Trieste, Italy, August 2007

- Tatarova E, *"Microwave discharges in molecular gases driven by surface waves",* 28th ICPIG (International Conference on Phenomena in Ionized Gases), Prague, Czech Republic, July 2007, Book of Abstracts, p.179

- Tatarova E, *"Hydrogen Balmer Lines Broadening in Microwave Plasma Sources",* 60th GEC (Annual Gaseous Electronics Conference), Arlington, Virginia, USA, October 2007

- Vieira J, Peano F, Fonseca RA, Fiuza F, Martins JL, Silva LO, Huang C, Tsung F and Mori WB, *"One-to-one kinetic simulations of intense laser-matter interactions",* Laserlab Europe Workshop, Darmstadt, Germany, October 2007

22.2.3. Oral Contributions

Alpha-X Workshop, Lisbon, Portugal, October 2007

- Fiúza F, Martins SF, Fonseca RA and Silva LO, *"Novel effects in ionization fronts"*

- Gallacher JG, Jaroszynski DA, Lemos N, Dias JM, Sun J, and Issac RC, *"Relativistic Plasma Mirrors"*

- Lemos N, Dias JM, Onofrei RI, Lopes NC, Figueira G, Fiuza F, Silva LO, Gallacher JG, Issac RC and Jaroszynski DA, *"Formation of Plasma Channels by ultra-short laser pulses in gas jets"*

- Lopes NC and Fajardo M, *"Path to laser-plasma based seeded FEL"*

- Vieira J, Fiuza F, Fonseca RA, Martins SF, Silva LO, Huang C, Tsung FS and Mori WB, *"One-to-one full scale kinetic modeling of the LWFA"*

60th Annual Gaseous Electronics Conference, Arlington, Virginia, USA, October 2007

- Guerra V, Lino da Silva M, Gocić S and Loureiro J, *"An improved description of the vibrational energy transfers in nitrogen discharges",* Bulletin American Physical Society 52: 12 Oct 2007

- Henriques J, Tatarova E, Felizardo E, Dias FM and Ferreira CM, *"Microwave Plasma Torches Driven by Surface Waves",* Bulletin American Physical Society 52: 15 Oct 2007

49th APS Annual Meeting of the Division of Plasma Physics, Orlando, Florida, USA, November 2007

- Silva LO, *"White light parametric instabilities"*

Conference on Lasers and Electro-Optics (CLEO-EUROPE), Munich, Germany, June 2007

- Cardoso L, Figueira G, Pires H and Wemans J, *"Experimental results on ultra-broadband OPCPA"*

- Wemans J, Siebold M, Figueira G, Lopes N, Cardoso L, Hein J and Diaz F, *"Ytterbium-based regenerative amplification at 1053 nm"*

CLF High Power Laser Science Christmas Meeting, Abingdon, December 2007

- Valente J, Onofrei R, Fiuza F, Davies JR, Ma T and Beg FN *"XUV imaging as a diagnostic for fast electron transport: statistical analysis"*

34th EPS Conference on Plasma Physics, Warsaw, Poland, July 2007

- Fiore M, Marti M, Fonseca RA and Silva LO, *"Enhancement of the filamentation instability due to collisions"*

- Peano F, Silva LO and Coppa G, *"Dimensional collapse in Coulomb explosions"*

Frontiers in Low Temperature Plasma Diagnostics VII, Beverly, UK, April 2007

- Dias FM, *"Combined multi-harmonic - numerical, adaptive differentiation: analysis of the noise level influence on speed improvement"*

Laser and Plasma Accelerators Workshop 2007, Azores, Portugal, July 2007

- Gallacher JG, Lemos N, Sun J, Dias JM, Issac RC, Fonseca RA, Silva LO, Lopes NC, Mendonça JT and Jaroszynski DA, *"Optical pulse tailoring using THz pulses"*

- Najmudin Z, Bellei C, Bingham R, Bourgeois N, Brunetti E, Clarke RJ, Collier J, Dangor AE, Divall EJ, Fiúza F, Fonseca RA, Foster PS, Gallagher J, Gonsalves AJ, Gopal A, Hooker CJ, Hooker SM, Heathcote R, Jaroszynski DA, Kaluza MC, Kamperidis C, Kneip S, Karsch S, Krushelnick K, Lancaster KL, Langley AJ, Lopes N, Mangles S, Marsh K, Marquès JR, Maksimshuk A, Mendonça JT, Murphy C, Mori WB, Nazarov W, Nagel SR, Nilson P, Norreys PA, Ta Phuoc K, Reed SA, Reitsma A, Rowlands-Rees TP, Schreiber J, Silva LO, Thomas A, Trines R, Vieira J, Viskup R and Willingale L, *"Plasma based particle acceleration experiments at Imperial College"*

- Peano F, Vieira J, Fonseca RA and Silva LO, *"Numerical analysis of the electron injection with colliding pulses in laser-wakefield accelerators"*

- Peano F, Vieira J, Fonseca RA, Silva LO, Coppa G and Mulas R, *"Direct acceleration of ions with counterpropagating lasers"*

- Vieira J, Fiúza F and Silva LO, *"Self-Steepening of intense laser pulses in plasmas"*

- Vieira J, Fonseca RA, Silva LO, Huang C, Lu W, Tzoufras M, Tsung F, Mori WB, Cooley J and Antonsen T, *"Simulations of Laser Wake Field Acceleration in channels using QuickPIC"*

Space Technology International Forum, Albuquerque, NM, USA, February 2007

- Martins AA and Pinheiro MJ, "The connection between Inertial Forces and the Vector Potential"

22.2.4. Poster Contributions

Advanced Solid-State Photonics, Vancouver, Canada, January 2007

- Siebold M, Jochmann A, Hornung M, Bock S, Hein J, Kaluza MC, Podleska S, Boedefeld R, Uecker R, Wehrhan O, Roeser F and Wemans J, *"Characterization of Ytterbium-doped CaF2 for broadband regenerative pulse amplification"*

American Geophysical Union Fall Meeting, San Francisco, California, USA, December 2007

- Gargaté L, Bingham R, Fonseca RA, Bamford R and Silva LO, *"Hybrid simulations of energetic ion interaction with mini magnetospheres"*

- Bamford R, Bingham R, Gibson KA, Thornton A, Bradford J, Hapgood M, Gargate L, Silva LO, Norberg C, Todd T, Wilson H and Stamper R, *"Initial experimental results of a laboratory mini-magnetosphere for astronaut protection"*

38th AIAA Plasmadynamics and Lasers Conference in conjunction with the 16th International Conference on MHD Energy Conversion, Miami, Florida, USA xxx 2007

- Bauville G, Lacour B, Magne L, Puech V, Santos Sousa J, Bœuf JP, Hagelaar G, Munoz-Serrano E, Pitchford LC, Sadeghi N and Touzeau N, *"Experimental and Theoretical Study of Singlet Delta Oxygen Production in Microcathode Sustained Discharges"*, AIAA Paper 2007-4025

49th APS Annual Meeting of the Division of Plasma Physics, Orlando, Florida, USA, November 2007

- Fiúza F, Fonseca RA and Silva LO, *"Phase-matched even-harmonics generation in relativistic ionization fronts"*

- Fonseca RA, Gargaté L, Martins SF, Peano F, Vieira J, Silva LO and Mori WB, *"Detailed numerical modeling of electron injection in the Laser Wakefield Accelerator: Particle Tracking Diagnostics in PIC codes"*

- Gargaté L, Bamford R, Bingham R, Fonseca RA and Silva LO, *"Hybrid Simulations of Mini Magnetospheres in the Laboratory"*

- Lu W, Tzoufras M, Huang C, Tsung FS, Mori WB, Vieira J, Fonseca RA Silva LO, Cooley J and Antonsen Jr T, *"Design and Simulation of a single 100 GeV stage in LWFA"*

- Martins SF, Fonseca RA, Mori WB and Silva LO, *"Numerical study of ultra-relativistic electromagnetic filamentation in boosted frames"*

- Martins JL, Peano F, Gargaté L, Fonseca R and Silva LO, *"Interaction of intense lasers with nanostructured plasmas"*

- Peano F, Vieira J, Fonseca RA, Silva LO, Coppa G and Mulas R, *"Direct ion acceleration with variable-frequency lasers"*

- Silva LO, Bingham R, Brandao B and Santos JP, *"Transverse modulation instability of white light in plasmas"*

- Trines R, Murphy C, Bingham R, Lancaster K, Chekhlov O, Norreys P, Mendonca JT, Silva L, Mangles S, Kamperidis C, Thomas A, Krushelnick K and Najmudin Z, *"Photon acceleration and modulational instability during wakefield excitation using long laser pulses"*

- Tzoufras M, Lu W, Huang C, Tsung FS, Mori WB, Vieira J, Fonseca RA and Silva LO, *"Beam loading of the blowout-regime of laser/plasma wakefield acceleration"*

- Vieira J, Fiúza F and Silva LO, *"Self-steepening of intense laser pulses in plasmas"*

60th Annual Gaseous Electronics Conference, Arlington, Virginia, USA, October 2007

- Álvarez R, Marques L and Alves LL, *"2D Electromagnetic and hydrodynamic models of a microwave plasma torch"*, Bulletin American Physical Society 52: 27 Oct 2007

- Gregório J, Synek P, Alves LL, Boisse-Laporte C, Leprince P, Leroy O and Teulé-Gay L, *"Study of a 2.45 GHz microwave micro-plasma in air"*, Bulletin American Physical Society 52: 22 Oct 2007

- Guerra V, *"Study of the influence of collisions between physisorbed atoms on the surface recombination probability"*, Bulletin American Physical Society 52: 46 Oct 2007

- Isola L, Gómez BJ, Feugeas JN and Guerra V, *"Dependence of the emission intensities with the flow in pulsed N_2 dc discharges"*, Bulletin American Physical Society 52: 38 Oct 2007

- Pinhão N, Pinheiro MJ and Donko Z, "Effect of H2 and N2 impurities in Argon on the kinetics of electrons", Bulletin American Physical Society 52: Oct 2007

- Pitchford LC, Makasheva K, Callegari Th, Boeuf JP, Santos Sousa J and Puech V, *"Study of the transition between MicroHollow Cathode Discharge and MicroCathode Sustained Discharge in a 3-electrode system"*, Bulletin American Physical Society 52: Oct 2007

- Tatarova E, Dias FM, Gordiets B and Ferreira CM, *"Hydrogen Balmer-Line Broadening in a Water Vapor Microwave Plasma Source"*, Bulletin American Physical Society 52: 38 Oct 2007

AstroGPU 2007 — Workshop on General Purpose Computation on Graphics Processing Units in Astronomy and Astrophysics, IAS, Princeton, USA, November 2007

- Abreu P, Pereira JM and Silva LO, *"A distributed memory GPU implementation of the Boris particle pusher algorithm"*

CLF High Power Laser Science Christmas Meeting, Abingdon, December 2007

- Davies JR, Fiuza F, Silva L, Honrubia JJ, Norreys PA, Robinson APL and Sherlock M, *"Integrated Numerical Modelling for the Design of Laser - Plasma Experiments"*

E-MRS Spring Meeting, Strasbourg, France 2007

- Marques L and Carvalho S, *"Ab initio study of structural and elastic properties of (Ti,Si,Al)N thin films"*

2nd European Planetary Science Congress, Postdam, Germany August 2007

- Pintassilgo CD and Loureiro J, *"Numerical study of Titan's atmosphere using a N_2-CH_4 post-discharge"*

34th EPS Conference on Plasma Physics, Warsaw, Poland, July 2007

- Dias FM and Popov Tsv K, *"Data Processing of Electrical Probe Data Measured in TOKAMAKs",* ECA 31F, P-5.080
- Fiúza F, Fonseca RA and Silva LO, *"Generation of relativistic even-harmonics in uniform underdense plasmas";* proceeding paper at http://www.eps2007.ifpilm.waw.pl/pdf/P4_013.pdf.
- Gargaté L, Bingham R, Fonseca RA and Silva LO, "Massively parallel simulations of coronal mass ejections"
- Marti M, Peano F, Fiore M, Fonseca RA and Silva LO, *"Collisional algorithm for relativistic PIC codes"*
- Martins JL, Peano F, Fonseca R and Silva LO, *"Relativistic harmonic generation in clusters"* proceeding paper at http://epsppd.epfl.ch/Warsaw/pdf/P4_014.pdf.
- Peano F, Silva LO and Coppa G, *"Dimensional collapse in Coulomb explosions"*
- Popov Tsv K, Ivanova P, Stöckel J, Dejarnac R and Dias FM, *"EEDF Measurements in the CASTOR Tokamak Using the First Derivative Langmuir Probe Method",* ECA 31F, P-5.104
- Shukla N, Shukla P, Fonseca RA, Sorasio G and Silva LO, *"Generation of magnetic field fluctuations in relativistic electron–positron magnetoplasmas"*
- Silva LO, Santos JP and Bingham R, *"Filamentation of intense broadband radiation in plasmas"*
- Sorasio G, Fonseca RA and Silva LO, *"Laser-plasma interaction with thin targets proton acceleration above 300 MeV"*
- Tonge J, Tzoufras M, Tsung FS, Mori WB, Ren C, Marti M and Silva LO, *"Fast ignition with ultra-high intensity lasers"*
- Vieira J, Fonseca RA, Silva LO, Lu W, Tzoufras M, Tsung FS and Mori WB, *"Self guided propagation of intense laser pulses in the blowout regime"*

4th European Space Weather Week, Brussels, Belgium, November 2007

- Bamford R, Bingham R, Thornton A, Gibson KA, Gargate L, Bradford J, Fonseca RA, Silva LO, Mendonça JT, Hapgood M, Norberg C, Todd T, Wilson H and Stamper R, *"Raise shields, Scotty: initial experimental results of a laboratory mini-magnetosphere for astronaut protection"*

12th European Summer School on Low Temperature Plasma Physics: Basics and Applications, Bad Honnef, Germany, October 2007

- Gregório J, Synek P, Alves LL, Boisse-Laporte C, Leprince P, Leroy O and Teulé-Gay L, *"Study of a 2.45 GHz microwave micro-plasma in air"*
- Pitchford LC, Makasheva K, Callegari Th, Boeuf JP, Santos Sousa J and Puech V, *"Study of the transition between MicroHollow Cathode Discharge and MicroCathode Sustained Discharge in a 3-electrode system"*

Hasylab Users Meeting, January 2007

- Timneanu N, Abreu E et al., *"Coulomb induced acceleration of protons with FLASH and prospects of nuclear fusion"*

Ibergrid — 1st Iberian Grid Infrastructure Conference, Santiago de Compostela, Spain, May 2007

- Abreu P, Pereira JM and Silva LO, *"Exposing stream processors as Grid services: a GPGPU example"*

16th International Colloquium on Plasma Processes, Toulouse, France, June 2007

- Álvarez R and Alves LL, *"Electromagnetic characterization of a microwave-driven mini-plasma reactor operated by an axial injection torch"*, p.112 (Société Française du Vide ed.)
- Lallement L, Cardinaud C, Rhallabi A and Alves LL, *"Electrical properties and transport phenomena in Inductive Coupled Plasma discharges: experimental and simulation approaches",* p.124 (Société Française du Vide ed.)

20th International Conference on the Numerical Simulation of Plasmas, Austin, Texas, USA, October 2007

- Fonseca RA, Marti M, Martins SF, Silva LO, Tonge J, Tsung F and Mori WB, *"OSIRIS 2.0: an integrated framework for parallel PIC simulations"*
- Gargaté L, Bingham R, Fonseca R, Silva LO and Bamford R, *"dHybrid: a massively parallel kinetic ion fluid electron code for space plasma simulations"*

28th International Conference on Phenomena in Ionized Gases, Prague, Czech Republic, July 2007

- Álvarez R, Marques L and Alves LL, *"Two-dimensional modelling of a microwave plasma reactor operated by an axial injection torch",* CD-Proceed. and Book of Abstracts, p. 45 (J. Schmidt, M. Simek, S. Pekárek, V. Prukner, eds.)
- Cruz J, Gregório J, Cardoso S, Freitas PP and Alves LL, *"Modelling of a radio-frequency ICP-reactor with an ion beam system",* CD-Proceed. and Book of Abstracts, p. 45 (J. Schmidt, M. Simek, S. Pekárek, V. Prukner, eds.)
- Felizardo E, Henriques J, Tatarova E, Dias FM and Ferreira CM, *"Surface wave driven microwave plasma torch",* 5P09-47 (J. Schmidt, M. Simek, S. Pekárek, V. Prukner, eds.)
- Gordiets B, Tatarova E, Henriques J, Felizardo E, Dias FM, Pinheiro M, Ganachev I and Ferreira CM, *"Microwave Air Plasma Torch",* 5P09-42 (J. Schmidt, M. Simek, S. Pekárek, V. Prukner, eds.)

- Guerra V, *"Calculation of heterogeneous recombination probabilities from a dynamical Monte Carlo scheme: fluctuations and averaging",* CD-Proceed. and Book of Abstracts, p. 26 (J. Schmidt, M. Simek, S. Pekárek, V. Prukner, eds.)

- Henriques J, Tatarova E and Ferreira CM, *"Modelling of a large-scale N_2-Ar microwave plasma source",* 5P09-44 (J. Schmidt, M. Simek, S. Pekárek, V. Prukner, eds.)

- Henriques J, Felizardo E, Tatarova E and Ferreira CM, *"Atmospheric N_2-Ar wave driven discharge",* 5P09-46 (J. Schmidt, M. Simek, S. Pekárek, V. Prukner, eds.)

- Kutasi K, Pintassilgo CD and Loureiro J, "Optimization of N2-O2 post-discharges for plasma sterilization by *modeling",* CD-Proceed. and Book of Abstracts, p. 1330 (J. Schmidt, M. Simek, S. Pekárek, V. Prukner, eds.)

- Lino da Silva M, Guerra V and Loureiro J, *"A two-temperature N_2 dissociation model derived from state-resolved rates",* CD-Proceed. and Book of Abstracts, p. 107 (J. Schmidt, M. Simek, S. Pekárek, V. Prukner, eds.)

- Martins AA and Pinheiro MJ, *"Plasma discharges at atmospheric pressure for boundary layer separation control and neutral flow propulsion"* (J. Schmidt, M. Simek, S. Pekárek, V. Prukner, eds.)

- Mrázková M, Vašina P, Pintassilgo CD, Kudrle V, Guerra V and Tálský A, *"Evolution of nitrogen atom density in the nitrogen post-discharge with oxygen admixture",* CD-Proceed. and Book of Abstracts, p. 199 (J. Schmidt, M. Simek, S. Pekárek, V. Prukner, eds.)

- Pintassilgo CD, Alcouffe G, Cernogora G and Loureiro J, *"Electron transport parameters and rate coefficients for the modeling of a RF discharge in N_2-CH_4",* CD-Proceed. and Book of Abstracts, p. 476 (J. Schmidt, M. Simek, S. Pekárek, V. Prukner, eds.)

- Tatarova E, Dias FM, Gordiets B and Ferreira CM, *"A spectroscopic investigation of a water-vapor microwave plasma source",* 5P09-41 (J. Schmidt, M. Simek, S. Pekárek, V. Prukner, eds.)

18th International Symposium on Plasma Chemistry, Kyoto, Japan, August 2007

- Kutasi K, Loureiro J and Pintassilgo CD, *"Effects of the wall material on the species density distributions in a large volume N_2-O_2 post-discharge reactor",* p. 88 (Tachibana K, Takai O, Ono K, Shirafuji T, eds.)

- Pinheiro MJ, *"Edge and core mechanism for anomalous diffusion in a magnetized cold plasma"* (Tachibana K, Takai O, Ono K, Shirafuji T, eds.)

Laser and Plasma Accelerators Workshop 2007, Azores, Portugal, July 2007

- Bendoyro RA, Onofrei RI, Lopes NC, Figueira G, Silva LO, *"Plasma channels for electron accelerators using high-voltage discharges on structured gas cells"*

- Dias JM, Lemos N, Onofrei RI, Lopes NC, Figueira G, Fiuza F, Silva LO, Gallacher JG, Issac RC and Jaroszynski DA, *"Formation of plasma channels by ultra-short laser pulses in gas jets "*

- Fiúza F, Fonseca RA and Silva LO, *"Phase-matched even-harmonics generation in relativistic ionization fronts"*

NanoSmat, Alvor, Portugal 2007

- Shein K, Marques LSA, Carvalho S, Rebouta L and Vaz F, *"Structural Properties of Metastable Ti1-xSi$_x$N$_y$ Thin Films"*

New Trends in Physics 2007, Brno, Czech Republic, November 2007

- Soural I, Guerra V and Krčma F, *"Numeric modeling of nitrogen ground state kinetics under post-discharge conditions"*, p. 237

Summer College on Plasma Physics, The Abdus Salam International Center for Theoretical Physics, Trieste, Italy, July-August 2007

- Shukla N, Shukla P, Sorasio G, Fonseca RA and Silva LO, *"Generation of magnetic field fluctuations in relativistic electron–positron magnetoplasmas"*

16th Symposium on Applications of Plasma Processes, Podbanské, Slovakia, January 2007

- Vašina P, Mrázková M, Pintassilgo CD, Guerra V, Kudrle V and Tálský A, *"Increase in nitrogen dissociation degree due to oxygen admixture to nitrogen post-discharge"*, p.275

Terahertz Photonics in Photonics Asia Conferences 2007, Beijing, China, 2007

- Sun JH, Gallacher G, Lemos N, Issac R, Dias JM, Huand ZX and Jaroszynski DA, *"High energy Terahertz pulse emission from GaAs illuminated by a femtosecond laser"*, Proc. SPIE, Vol. 6840 68401B, 20

Workshop on Radio-frequency Discharges, Drumcondra, Dublin, Ireland, June 2007

- Marques LSA, Jolly J and Alves LL, *"Capacitively-coupled radio-frequency hydrogen discharges: the role of kinetics"*

22.2.5. Other Publications

- Amiranoff F, Aguer P, Atzeni S, Azechi H, Bagnoud V, Balcou P, Badziak J, Batani D, Bellei C, Besnard D, Bingham B, Breil J, Borghesi M, Borneis S, Caruso A, Chanteloup JC, Clarke RJ, Collier JL, Davies JR, Dufour J-P, Dunne M, Estraillier P, Evans RG, Fajardo M, Fedosejevs R, Figueria G, Fils J, Feugeas JL, Galimberti M, Gauthier J-C , Giulietti A, Gizzi L, Gregori G, Gus'kov S, Hallo L, Hernandez-Gomez C, Hoffman D, Honrubia J, Jacquemot S, Key M, Kingham R, Koenig M, Kovacs F, Krushelnic K, Labaune C, Lancaster K, Leblanc C, Maire PH, Martin W, McEvoy A, McKenna P, Mendonça T, Meyer-ter-Vehn J, Mima K, Morou G, Moustaizis S, Najmudin Z, Nickles P, Neely D, Norreys P, Olazabal M, Offenberger A, Papadogianis N, Perlado J M, Ramirez J, Ramis R, Rhee Y, Ribeyre X, Robinson A, Rohlena K, Rose S, Roth M, Rouyer C, Rulliere C, Rus B, Sandner W, Schiavi A, Schurtz G, Sergeev A, Sherlock M, Silva L, Smith R, Sorasio G, Strangio C, Takabe H, Tatarakis M, Tikhonchuk V, Tolley

M, Vaselli M, Velarde P, Winstone T, Witte K, Wolowski J, Woolsey N, Wyborn B, Zepf M, Zhang J, HiPER Technical Background and Conceptual Design Report 2007

- Bastos C, Bertolami O, Dias NC, Prata JN, "*Deformation quantization of noncommutative quantum mechanics and dissipation, 3rd International Workshop DICE2006: Quantum Mechanics between Decoherence and Determinism: New Aspects from Particle Physics to Cosmology",* Castello di Piombino, Tuscany, Italy, 11-15 Sep 2006, J.Phys.Conf.Ser.67: 012058,2007, e-Print: hep-th/0612239

- Bertolami O, Carvalho C, Brane Lorentz Symmetry from Lorentz Breaking in the Bulk, 3rd International Workshop DICE2006: "*Quantum Mechanics between Decoherence and Determinism: New Aspects from Particle Physics to Cosmology",* Castello di Piombino, Tuscany, Italy, 11-15 Sep 2006, J.Phys.Conf.Ser.67: 012009, 2007, e-Print: gr-qc/0612129

- Delliou M Le, Bertolami O, Pedro FG, "*Dark Energy-Dark Matter Interaction from the Abell Cluster A586 and violation of the Equivalence Principle"*, 13th International Symposium on Particles, Strings and Cosmology (PASCOS 07), London, England, 2-7 Jul 2007, in AIP Conf.Proc.957: 421-424,2007, e-Print: arXiv:0709.2505 [astro-ph]

- Green JS, Evans RG, Heathcote Lancaster KL, Norreys PA, Bellei C, Najmudin Z, Ovchinnikov VM, Freeman RR, VanWoerkom LR, Akli KU, Key MH, MacKinnon AJ, McPhee A, Waugh J, Woolsey NC, Beg FN, King JA, Ma T, Habara H, Tanaka KA, Tanimoto T, Azechi H, Takeda K, Stephens R, Nilson P, Theobald W, Lopes NC, Onofrei R, Davies JR, Markey K, Zepf M, "*The effect of laser intensity on fast electron beam divergence in solid density plasmas"*, Central Laser Facility Annual Report 2006-2007 21 2007

- Nakatsutsumi M, Nakamura H, Habara H, Kodama R, Davies JR, Green JS, Heathcote R, Lancaster KL, Norreys PA, Krushelnick K, Clark D, Highbarger K, Weber RL, Freeman RR, VanWoerkom LR, Akli KU, Hey DS, Key MH, Macphee A, Mackinonn AJ, Gregory CD, Woolsey NC, Ma T, Wei MS, Chen SN, Beg FN, Tampo M, Stephens R, Jaanimagi P, Storm M, Theobald W, "*Isochoric heating of solid targets to ten million Kelvin by PetaWatt laser pulses"*, Central Laser Facility Annual Report 2006-2007 44 2007

22.2.6. Prizes and Awards

- Abreu E, First Prize for Graduates, Technical University of Lisbon (UTL), Lisbon (Portugal), December 2007.

- Bertolami O, Prémio Universidade Técnica de Lisboa/Santander Totta for scientific excellence in Biophysics and Physics.

- Fiúza F, First Prize for Graduates, Technical University of Lisbon (UTL), Lisbon (Portugal), December 2007.

- Fiúza F, PPCF Student Poster Prize, 34th EPS Conference on Plasma Physics, Warsaw (Poland), July 2007 (http://www.iop.org/EJ/news/-topic=1241).

- Gargaté L, 5th Oscar Buneman Award, Animation Category, Austin, Texas (USA), October 2007.

- Martins SF, Prémio Gulbenkian de Estímulo à Investigação 2007, Cosmology/Astrophysics scientific area, Lisbon (Portugal), November 2007.

22.2.7. Patents

- Figueira G, "*Device for aberration correction in optical systems",* March 2007.

- Fiúza F and Silva LO, *"Aparelho e método para a geração de harmónicas pares de radiação electromagnética em frentes de ionização"*, PT 103762 (pending).

- Peano F, Vieira J and Silva LO, *"Aparelho e método para a aceleração de iões no vácuo baseado em lasers de frequência variável"*, PT 103709 (granted).

22.2.8. Laboratorial Prototypes

- Dias FM, Henriques J, Felizardo E and Tatarova E, "*Microwave plasma source at atmospheric pressure"*.

- Dias FM, Felizardo E and Tatarova E, "*Microwave plasma source for UV and visible spectral diagnostics"*.

- Dias FM, Felizardo E and Tatarova E, "*Microwave plasma sterilizer"*.
- Figueira G, "*Single-adjuster, four-actuator deformable mirror for correction of astigmatism and defocus in a high power laser"*.

- Lemos N, Berardo J, Lopes N and and Dias JM, "*Single-beam Interferometer and Shadowgrather"*

- Lopes NC and Bendoyro RA, *"Shockline based magnetic pulse compressor for high-voltage pulses"*.

22.2.9. Numerical codes

- Alvarez R and Alves LL, *"Two-dimensional electromagnetic model for a microwave cavity excited by a coaxial antenna"*.

- Alvarez R, Marques, LSA and Alves LL, *"Two-dimensional hydrodynamic model for the transport of a neutral gas in high-flow regime"*.

- Alves LL, *"Homogenous kinetic model for a nitrogen plasma"*.

- Marques LSA, C. Pintassilgo and Alves LL, "*Two-dimensional, time-dependent fluid model for the transport of charged particle within capacitively coupled radio-frequency discharges in hydrogen and nitrogen"*.

- Pinheiro MJ, "*Self-consistent two-dimensional model of the temporal and spatial development of the One Atmosphere Uniform Glow Discharge Plasma (OAUGDP^{TM}), called EHD code (CODEHD)"*.

22.2.10. Organization of Conferences and Workshops

- Mendonca JT (Chairman), 5th International Conference on the Physics of Dusty Plasmas, Azores, Portugal, May 2008
- Silva LO (chairman of the Local Organizing Committee), Fonseca RA, Dias JM, Lopes N, Lemos N, Bendoyrro R, Onofrei R, Peano F, Vieira J, Martins SF and Fíuza F, Laser and Plasma Accelerators Workshop 2007, Azores, Portugal, 9-13 July 2007 (http://cfp.ist.utl.pt/lpaw07)
- Silva LO (member of the Local Organizing Committee), XVII International Symposium on Gas Flow and Chemical Lasers & High Power Lasers 2008, Lisbon, Portugal, September 2008
- Silva LO (Chairman), Alpha-X Workshop, Lisbon, Portugal, October 2007

22.2.11. Participation in scientific committees of conferences and workshops

- Dias FM (member of the International Scientific Committee), International Workshop and Summer School on Plasma Physics (IW&SSPP), Bulgaria
- Fajardo M (member of the Programme Committee), 35th European Physical Society Conference on Plasma Physics, Creete, Greece, July 2008 (in Beam Plasmas Inertial Fusion panel)
- Fajardo M (Programme Committee Member), RPHDM2008
- Fonseca RA (Working Group Coordinator), Laser and Plasma Accelerators Workshop 2007, Azores, Portugal, July 2007
- Guerra V (member of the International Scientific Committee), Summer School and International Symposium on Physics of Ionized Gases (SPIG)
- Guerra V (member of the International Scientific Committee), Europhysics Conference on Atomic and Molecular Physics of Ionised Gases (ESCAMPIG)
- Silva LO (member of the Programme Committee), 35th European Physical Society Conference on Plasma Physics, Creete, Greece, July 2008 (in Basic Plasmas, Astro and Space)
- Silva LO (Chairman, member of the International Scientific Committee), 5th International Conference on the Physics of Dusty Plasmas, Azores, Portugal, May 2008

22.2.12. Board of Scientific Journals

- Alves LL, European Physical Journal – Applied Physics (EDP Sciences, ed.), Associated Editor (Section "Plasmas discharges and processes")
- Fonseca RA, IEEE Transactions on Plasma Science, Guest Editor for the Special Issue on Laser and Plasma Accelerators (August 2008)
- Mendonça JT, Plasma Physics and Controlled Fusion, member of Editorial Board

22.2.13. Projects/Funding Awarded in 2007

- Alves LL, Sistema inovador de micro-ondas para a produção de mini-plasmas à pressão atmosférica, Cooperação Científica e Técnica Luso-Francesa (GRICES / CNRS), January 2007 – December 2008
- Fajardo M, Plasma-based Free Electron Lasers, FCT, PTDC/FIS/71709/2006, June 2007 – May 2010
- Fonseca RA, Grid Computing in Plasma Physics and Nuclear Fusion, FCT, GRID/GRI/81800/2006, January 2008 – December 2009
- Lino da Silva M, CFD validation in CO2 environment, Fluid Gravity Eng./European Space Agency Aurora Contract 19677, September 2007 – January 2008
- Lopes NC, Science and technology of laser-plasma accelerators, FCT, POCI/FP/81925/2007, July 2007
- Silva LO, "Harnessing the power of ultra intense lasers in plasmas for ultra fast science", FCT, PTDC/FIS/66823/2006, October 2007 – September 2010
- Silva LO, NVIDIA Professor Partnership Program, NVIDIA (Nasdaq: NVDA), December 2007

22.2.14. Awarded Fellowships

- FCT Post-doctorate fellowship for Dr. Tayyab Imran (supervisor: Gonçalo Figueira), September 2007.
- FCT Post-doctorate fellowship for Dr. Fabio Peano (supervisor: Luis O. Silva), May 2007.
- FCT PhD Fellowship for Eng. Samuel Martins (supervisor: Luis O. Silva), September 2007.
- FCT PhD Fellowship for Eng. Frederico Fiuza (supervisor: Luis O. Silva), September 2007.
- FCT PhD Fellowship for Eng. Joana Martins (supervisor: Luis O. Silva), September 2007.
- FCT PhD Fellowship for Eng Rodolfo Bendoyro (supervisor: Nelson Lopes), September 2007.

22.2.15. Ph.D thesis completed in 2007

- Letout S, *"Couplage onde de surface-plasma en présence de résonances, dans une décharge micro-onde à basse pression",* Universidade Técnica de Lisboa (Portugal) and Université de Paris XI (France): co-tutorial Thesis, September 2007, Supervisors: Alves LL (IST); C. Boisse-Laporte (UPS).
- Puac N, *"Development, diagnostics and applications of microwave and radiofrequency plasma reactors, Institute of Physics"*, Belgrade (Serbia), April 2007, Supervisor: Tatarova E.

22.2.16. MSc thesis completed in 2007

- Abreu E, Coulomb *"Acceleration of Protons with a Free-Electron Laser: Prospects for Nuclear Fusion"*, Instituto

Superior Técnico, MSc Thesis in Physics Engineering, July 2007, Supervisors: M. Fajardo (IST); N. Timneanu (Upsala).

- Baptista I, *"Aberrações oculars associadas ao uso de lentes de contacto hidrofílicas mensais"*, Instituto Superior Técnico, MSc Thesis in Biomedical Engineering, November 2007, Supervisor: JM Dias.

- Cruz J, *"Estudo de um reactor de acoplamento indutivo com um sistema de feixe iónico: Modelização e caracterização experimental"*, Instituto Superior Técnico, MSc Thesis in Physics Engineering, November 2007, Supervisors: LL Alves and S Cardoso.

- Felizardo E, *"Plasma a Pressão Atmosférica Mantido por Ondas de Superfície"*, Instituto Superior Técnico, MSc Thesis in Physics Engineering, November 2007, Supervisors: E Tatarova and FM Dias.

- Fiúza F, *"Tunability and control of intense laser sources in plasmas"*, Instituto Superior Técnico, MSc Thesis in Physics Engineering, July 2007, Supervisor: LO Silva.

- Lemos N, Characterization of ionization fronts by interferometric diagnostics, Instituto Superior Técnico, MSc Thesis in Physics Engineering, September 2007, Supervisor: JM Dias.

- Martins JL, Ultraintense Ultrashort Laser-Cluster Interactions, Instituto Superior Técnico, MSc Thesis in Physics Engineering, July 2007, Supervisor: LO Silva.

- Viola F, Wavefront reconstruction and simulation of visual acuity to study the impact of optical aberrations after eye surgeries, Instituto Superior Técnico, MSc Thesis in Biomedical Engineering, July 2007, Supervisor: JM Dias.

22.2.17. Outreach Activities

- Figueira G is the Assistant Editor of the new editorial team of "Gazeta de Física", the official journal of the Portuguese Physical Society

- Figueira G made a poster representing the activities of IPFN for a one-day exhibition on the activities of Portuguese research laboratories at Pavilhão do Conhecimento, April 2007
- Pinheiro MJ was in the jury of the 19th "Annual space design competition" (addressed to high school students from New Mexico), held during the Space Technology Applications International Forum in 2007. This event was sponsored by the Institute for Space and Nuclear Power Studies of the University of New Mexico. The subject of the 2007 space design competition was "Lunar Resort".

- Pinheiro MJ was invited to give a talk at the Department of Physics of the Eduardo Mondlane University, Maputo, Mozambique

22.2.18. Other Activities

- Martins SF, responsible for the "Update Physics", a monthly epp magazine with relevant papers published in important scientific journals, description and principle take-aways of conferences attended by epp members, developments on internal software infra-structures, and main achievements at epp

- Silva LO, Chairman of Selection Committee of the John Dawson PhD Thesis Prize on Laser and Plasma Accelerators 2007.

- Silva LO, President-elected of the "Rede Nacional de Computação Avançada", Portugal.

22.2.19. Courses

- Alves LL, *"Electron Kinetics in Atomic and Molecular Plasmas"* (2.5h lecture) and *"Fluid Modeling of DC Discharge Plasmas"* (1.5h lecture), 12th European Summer School Low Temperature Plasma Physics: Basics and Applications, Bad Honnef, Germany, October 2006

22.2.20. Consulting

- Alves LL, Programme National en Nanosciences et Nanotechnologies (PNANO), consultant on Plasma modelling and simulation for material treatment, Agence National de la Recherche (ANR), France

22.2.21. Popular accounts of research

- Gargaté L, live interview in the TV news "Jornal 2", October 24 2007 (http://cfp.ist.utl.pt/golp/epp/movies/LuisGargate.avi)

- Gargaté L in the article "Atmosfera artificial dá prémio nos EUA a investigador do IST", Diário de Noticias, October 24 2007.

- Silva LO, participation in Luís Osório's radio show "Rádio Clube Português de Luís Osório", June 23 2007.

- Silva LO, biographical TV Show on LO Silva "Geração Cientista", first played in RTP 2, January 2007 (http://cfp.ist.utl.pt/golp/epp/los/livepage.apple.com).

- The IST Cluster on the news in "Parceiros de sucesso", Expresso Emprego, May 19 2007 (http://cfp.ist.utl.pt/golp/epp/mediadocs/ExpressoISTCluster.pdf).

- Silva LO, in the article "Computadores de Gigante", Exame Informática, June 2007 (http://cfp.ist.utl.pt/golp/epp/mediadocs/ExameInfISTCluster.pdf).

22.2.22. Conferences Attended in 2007

- Guerra V, Sixth International Workshop Applied Category Theory, Graph-operad-logic, Special Relativity, Dynamics and Electromagnetics, Ixtapa, Mexico, February 2007.

- Dias FM, FLTPD VII (Frontiers in Low Temperature Plasma Diagnostics VII), Beverly, UK, April 2007.

- Marques LSA, E-MRS Spring Meeting, Strasbourg, France 2007.

- Abreu P, Ibergrid — 1st Iberian Grid Infrastructure Conference, Santiago de Compostela, Spain, May 2007.
- Cardoso L, Figueira G, Wemans J, Conference on Lasers and Electro-Optics (CLEO-EUROPE), Munich, Germany, June 2007.
- Abreu E, SLAC Ultra-Fast X-ray Summer School, SLAC, June 2007.
- Fajardo M, Workshop - New and emerging sources of intense beams of particles and short-wavelength radiation, Lund, June 2007.
- Marques LSA, Workshop on Radio-frequency Discharges, Drumcondra, Dublin, Ireland, June 2007.
- Alves LL, 16th CIP (International Colloquium on Plasma Processes), Toulouse, France, June 2007.
- Álvarez R, Alves LL, Cruz J, Felizardo E, Guerra V, Henriques J, Kutasi K, Lino da Silva M, Martins AA, Pinheiro MJ, Pintassilgo CD and Tatarova E, 28th ICPIG (International Conference on Phenomena in Ionized Gases), Prague, Czech Republic, July 2007.
- Marques LSA, NanoSmat, Alvor, Portugal 2007.
- Dias FM, Fiore M, Fiúza F, Fonseca RA, Marti M, Martins JL, Peano F and Silva LO, 34th EPS Conference on Plasma Physics, Warsaw, Poland, July 2007.
- Dias JM , Lemos N, Bendoyro RA, Lopes NC, Onofrei RI, Fiúza F, Fonseca RA, Martins SF, Peano F, Silva LO and J. Veiria, Laser and Plasma Accelerators Workshop 2007, Azores, Portugal, July 2007.
- Shukla N, Summer College on Plasma Physics, The Abdus Salam International Center for Theoretical Physics, Trieste, Italy, July-August 2007.
- Kutasi K and Pinheiro MJ, 18th ISPC (International Symposium on Plasma Chemistry), Kyoto, Japan, August 2007.
- Álvarez R, Gregório J, Guerra V, Henriques J, Santos Sousa J and Tatarova E, 60th GEC (Annual Gaseous Electronics Conference), Arlington, Virginia, USA, October 2007.
- Alves LL, Gregório J and Santos Sousa J, 12th European Summer School on Low Temperature Plasma Physics: Basics and Applications, Bad Honnef, Germany, October 2007.
- Guerra V, Workshop on Streamers, sprites, leaders, lightning: from micro- to macroscales, Leiden, The Netherlands, October 2007.
- Brandão B, Fiúza F, Fonseca RA, Martins JL, Martins SF, Peano F, Shukla N, Silva LO and Vieira J, Alpha-X Workshop, Lisbon, Portugal, October 2007.
- Gargaté L and Martins SF, 20th International Conference on the Numerical Simulation of Plasmas, Austin, Texas, USA, October 2007.
- Fiúza F, Martins JL, Martins SF, Silva LO and Vieira J, 49th APS Annual Meeting of the Division of Plasma Physics, Orlando, Florida, USA, November 2007.
- Abreu P, AstroGPU 2007 — Workshop on General Purpose Computation on Graphics Processing Units in Astronomy and Astrophysics, IAS, Princeton, USA, November 2007.
- Gargaté L, 4th European Space Weather Week, Brussels, Belgium, November 2007.
- Gargaté L, American Geophysical Union Fall Meeting, San Francisco, California, USA, December 2007.

22.2.23. Collaborations

- Gómez BJ, Instituto de Física Rosario, Argentina
- De Amorim Silva J, Instituto Tecnológico de Aeronáutica, São José dos Campos, Brazil
- Benova E, Sofia University, Sofia, Bulgaria
- Moisan M, Departement de Physique, Université de Montréal, Montréal (Québec), Canada
- Krčma F, Brno University of Technology, Brno, Czech Republic
- Vašina P, Masaryk University, Brno, Czech Republic
- Belmonte T, Laboratoire de Science et Génie des Surfaces, Ecole des Mines, Nancy, France
- Boisse-Laporte C, Puech V, Laboratoire de Physique des Gaz et des Plasmas, Orsay, France
- Cernogora G, Service d' Aéronomie, Verrières le Buisson, France
- Chikhaoui A, Université de Provence, Marseille, France
- Dudeck M, Université Paris VI, Paris, France
- Glinec Y, Laboratoire D'Optique Apliquée, École Polytechnique, France
- Jolly J, Laboratoire de Physique et Technologie des Plasmas, École Polytechnique, Palaiseau, France
- Malka V, Laboratoire D'Optique Apliquée, École Polytechnique, France
- Pitchford L, Ricard A, Laboratoire Plasmas et Conversion d'Énergie, Toulouse, France
- Rhallabi A, Lallement L, Institut de Matériaux Jean Rouxel de Nantes, Nantes, France
- Sadeghi N, Laboratoire de Spectrométrie Physique, Université Joseph Fourier, Grenoble, France
- Vacher D, Université Blaise Pascal, Paris, France
- Donkó Z, Hartmann P, Research Institute for Solid State Physics and Optics, Hungary
- Atzeni S, Dipartimento di Energetica, Università di Roma «La Sapienza» and CNISM, Italy
- Capitelli M, Esposito F, Bari University, Bari, Italy
- Coppa G, Politecnico di Torino, Italy
- Ganachev I, Shibaura Mechatronics Corp., Japan
- Nakatsutsumi M, Graduate School of Engineering, Osaka University, Japan
- Giordano D, Marraffa L, European Space Agency, ESTEC, The Netherlands

- Kroesen G, Wijtvlet R, Van der Mullen J, Eindhoven University of Technology, Eindhoven, The Netherlands
- Liang D, Faculdade Ciências e Tecnologia, Universidade Nova Lisboa, Portugal
- Freitas P, Cardoso S, Instituto de Engenharia Sistemas e Computadores – Microsistemas e Nanotecnologias, Lisboa, Portugal
- Pinhão N, Instituto Tecnológico e Nuclear, Portugal
- Gordiets B, Lebedev Physical Institute, Russian Academy of Sciences, Moscow, Russia
- Yu. Starikovski A, Moscow Institute of Physics and Technology, Russia
- Cotrino J, Lopez-Santos C, Instituto de Ciencias de Materiales de Sevilla, Sevilla, Spain
- Diaz F, University of Tarragona Rovira i Virgili, Spain
- Honrubia JJ, GIFI, Universidad Politecnica, Madrid, Spain
- Quintero MC, Rodero A, Departamento de Física, Universidad de Córdoba, Córdoba, Spain
- Roso L, University of Salamanca, Spain
- Goktas H, Canakkale Onsekiz Mart University, Canakkale, Turkey
- Bamford R, Bingham R, Norreys PA, Rutherford Appleton Laboratory, United Kingdom
- Jaroszynski DA, University of Strathclyde, Glasgow, United Kingdom
- Beg FN, Department of Mechanical and Aerospace Engineering, University of California San Diego, USA
- Drake P, University of Michigan, USA
- Katsouleas T, University of Southern California, USA
- Mori WB, University of California Los Angeles, USA
- TUIXS project, as coordinator (LOA, CEA, ULund, UUppsala, UPM, PALS), see www.tuixs.org
- ELI-PP project, as WorkPackage leader (30 European Institutions), see www.eli-laser.eu